Mechanisms of Peripheral Sensitization in Inflammatory Knee Pain

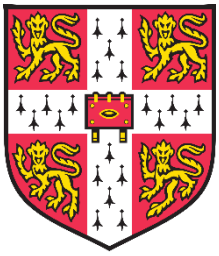

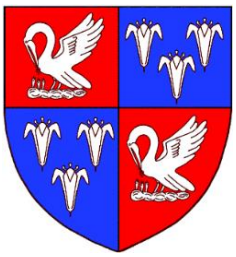

Dissertation submitted for the degree of Doctor of Philosophy

Sampurna Chakrabarti

Department of Pharmacology

Corpus Christi College, University of Cambridge

December, 2019

I. Preface

This thesis is the result of my own work and includes nothing which is the outcome of work done in collaboration except as declared in the Preface and specified in the text. All work presented was carried out at the Department of Pharmacology, University of Cambridge between October 2016 and November 2019. Some pilot data were obtained at the European Molecular Biology Laboratory, Rome, Italy. All other collaborations are detailed in the thesis, and the findings that resulted from such collaborations qualified by the pronoun "we" where appropriate.

It is not substantially the same as any that I have submitted, or, is being concurrently submitted for a degree or diploma or other qualification at the University of Cambridge or any other University or similar institution except as declared in the Preface and specified in the text. I further state that no substantial part of my dissertation has already been submitted, or, is being concurrently submitted for any such degree, diploma or other qualification at the University of Cambridge or any other University or similar institution except as declared in the Preface and specified in the text. This thesis also adheres to the word limit of 60,000 not including the references.

Part of the work has been published (or is in pre-print) as follows:

Chakrabarti, S., Jadon, D.R., Bulmer, D.C., Smith, E.St.J., 2019a. Human osteoarthritic synovial fluid increases excitability of mouse dorsal root ganglion sensory neurons: an in-vitro translational model to study arthritic pain. Rheumatology. https://doi.org/10.1093/rheumatology/kez331

Chakrabarti, S., Pattison, L.A., Bhebhe, C.N., Callejo, G., Bulmer, D.C., Smith, E.St.J., 2019b. Sensitization of knee-innervating sensory neurons by tumor necrosis factor-α activated fibroblast-like synoviocytes: an in vitro, co-culture model of inflammatory pain. bioRxiv 791251. https://doi.org/10.1101/791251

Chakrabarti, S., Pattison, L.A., Singhal, K., Hockley, J.R.F., Callejo, G., Smith, E.St.J., 2018. Acute inflammation sensitizes knee-innervating sensory neurons and decreases mouse digging behavior in a TRPV1-dependent manner. Neuropharmacology 143, 49–62. https://doi.org/10.1016/j.neuropharm.2018.09.014

II. Acknowledgements

This thesis would not have been possible without the kindness and support of my mentors, friends and family.

Firstly, massive thanks to Dr Ewan St. John Smith for being the role model supervisor – I truly appreciated the independence of driving multiple projects all the while being supported by his wonderfully prompt intellect. The Smith Lab and later the Smith/Bulmer Lab was also a friendly environment where I formed bonds that I hope will continue beyond this PhD: I was very happy to be the "little grasshopper" to the wise Dr Gerard Callejo, enjoyed the long chats during digging experiments with Luke Pattison and sitting next to the (soon-to-be Dr) Toni Taylor. I would also like to thank my key collaborators Drs Deepak Jadon, David Bulmer, Paul Heppenstall and Frances Henson, each of whom has helped me to grow as a scientist.

Beyond collaborators and the lab, my village consisted of incredible friends Young Mi Kwon, Sarianna Tuovinen and Dewi Safitri all of whom were my constant support throughout the last three years. As has been true since 2012, the primary node of this emotional support system was my partner-in-crime Suman Ghosh – our adventures across Europe were something I looked forward/backward to after every rough week in the lab.

I was lucky to have been born in a family of academics who empathized with the very unique toils of academic life. I would like to thank my mother, Prof Sampa Chakrabarti (who was more worried about me finishing this thesis than I was) for being the first one to show me that research is fun and my father, Dipankar Chakrabarti, for his support and encouragement in all the diverse topics that I pursued since undergraduate.

Furthermore, I am grateful to the Gates Cambridge Trust for generously funding my PhD, during which I had the opportunity to spend a few memorable months in Rome, Italy, thanks to the Department of Pharmacology fieldwork fund, Cambridge Philosophical Society Research fund and Corpus Christi research fund. Additionally, thanks to the Society for Neuroscience and the Wellcome Genome Center for their financial support which helped me to present my work at the Neuroscience Annual meeting 2018 (San Diego, USA) and the Chronic Pain conference 2019 (Hinxton, UK).

Finally, I am indebted to my mentees and everyone else who contributed in making this PhD a fulfilling experience. I am grateful to have had the chance to stand on the shoulder of giants.

III. Abbreviations

2-AG = 2-arachidonoylglycerol	AA = Adjuvant -Ainduced arthritis
AAV= Adeno-associated virus	ACLT = Anterior cruciate ligament transection
ACT = Acceptance and commitment therapy	AHP = Afterhyperpolarization
AEA = Anandamide	AMPA = α-amino-3-hydroxy-5-methyl-4-isoxazolepropionic acid
AIA = Antigen-induced arthritis	AS = Ankylosing spondylitis
AP = Action potential	BCE = Before common era
ASIC = Acid-sensing ion channel	C21 = Compound 21
BLC = B lymphocyte chemoattractant	CBT = Cognitive and behavioral therapy
Cav = Voltage-gated Ca^{2+} channel	CDH-11 = Cadherin-11
CD = Cluster of differentiation	CE = Commen era
CFA = Complete Freund's adjuvant	CGRP = Calcitonin gene-related peptide
CIA = Collagen-induced arthritis	CNS = Central nervous system
COX = Cyclooxygenase	CRP = C-reactive protein
DALY = Disability adjusted life years	DMM = Destabilization of medial meniscus
DNA = Deoxyribonucleic acid	DREADD = Designer receptors exclusively activated by designer drugs
DRG = Dorsal root ganglion	ECS = Extracellular solution
EMBL = European Molecular Biology Laboratory	ESR = Erythrocyte sedimentation rate
EULAR = European League Against Rheumatism	FB = Fast Blue
FLS = Fibroblast-like synoviocytes	GABA = γ-amino butyric acid
GBD = Global burden of disease	GCSF = Granulocyte colony stimulating factor
GECI = Genetically encoded calcium indicator	GEVI = Genetically encoded voltage indicator
GluCl = Glutamate-gated chloride channel	GM-CSF = Granulocyte-macrophage colony stimulating factor
GPCR = G protein-coupled receptors	HA = Hyaluronic acid

HCN = Hyperpolarization activated cyclic nucleotide gated ion channel	HPD = Half peak duration
HSV = Herpes simplex virus	IASP = International Association for the Study of Pain
IFN = Interferon	IL = Interleukin
IP3 = Inositol 1,4,5-trisphosphate receptors	iPSC = Induced pluripotent stem cells
I-TAC = interferon inducible T-cell apha chemoattractant protein	KC = Keratinocyte chemoattractant
Kv = Voltage-gated K^+ channel	L = Lumbar
LIX = Lipopolysaccharide induced chemokine	LMIC = Low to middle economic countries
LPS = Lipopolysaccharide	MCP = Monocyte chemoattractant protein
MCSF = Macrophage colony stimulating factor	MIA = Monoiodoacetate-induced arthritis
MIG = Monokine-induced by gamma interferon	MIP = Macrophage inflammatory protein
MMP = Matrix metalloprotease	MS = Mass spectrometry
NA = Not applicable	Nav = Voltage-gated Na^+ channel
NGF = Nerve growth factor	NMDA= N-methyl-D-aspartate
NO = Nitric oxide	NSAID = Non-steroidal anti-inflammatory drugs
OA = Osteoarthritis	P = Passage
PAD = Primary afferent depolarization	PAG = Periaqueductal grey
PAM = Pressure application measurement	PBS = Phosphate buffered saline
PFA = Paraformaldehyde	PG = Prostaglandin
PGIA = Proteoglycan induced arthritis	PKC = Protein kinase C
PNS = Peripheral nervous system	q/PCR = Quantitative polymerase chain reaction
RA = Rheumatoid arthritis	RANTES = Regulated on activation, normal T cell expressed and secreted
RhF = Rheumatoid factor	RMP = Resting membrane potential

RNA = Ribonucleic acid	RT = Reverse transcriptase
S = Sustained current	SCID = Severe combined immunodeficiency
SDF = Stromal cell derived factor	SF = Synovial fluid
TCA = T cell activation gene	TDAG8 = T cell death associated gene
TECK = Thymus expressed chemokine	TGF = Transforming growth factor
THIP = 4,5,6,7-tetrahydroisoxazolo[5,4-c]pyridin-3-ol hydrochloride	TIMP = Tissue inhibitor of metalloproteinase
TNF = Tumor necrosis factor	TrkA = Tropomyosin receptor kinase A
TRP = Transient receptor potential	TS = Transient + sustained current
VAS = Visual analog score	

IV. Summary

Arthritis affects millions of people and costs billions to the global economy with painful, inflamed joints being the major clinical symptoms. Knee joints are innervated by the distal ends of dorsal root ganglion (DRG) neurons and hyperexcitability of knee-innervating DRG neurons (knee neurons), through a process called peripheral sensitization, underlies arthritic knee pain. My research goal was to elucidate the mechanisms of knee neuron peripheral sensitization by developing and utilizing several *in vitro* and *in vivo* disease models.

Since experimental animal models of arthritis do not fully recapitulate the human disease, I developed a novel, *in vitro* translational model of arthritic pain by incubating mouse knee neurons with human synovial fluid obtained from osteoarthritic patients. Results from this disease model provide proof-of-concept that synovial fluid is a key modulator of arthritic pain. In order to reconcile the behavioral and neural correlates of arthritic pain, I utilized the mouse model of complete Freund's adjuvant (CFA)-induced knee inflammation to establish digging behavior as an ethologically relevant spontaneous pain measure. I observed that digging is reduced after knee inflammation and that it occurs concomitant with an increase in knee neuron excitability. After inflammation, knee neurons also showed increased expression of the nociceptive ion channel transient receptor potential vanilloid 1 (TRPV1), possibly mediated by nerve growth factor, and systemic administration of a TRPV1 antagonist normalized digging behavior in mice.

Interactions between non-neuronal cells and neurons are critical in peripheral sensitization and I examined the role of fibroblast-like synoviocytes (FLS, non-neuronal joint cell) in mediating knee neuron hyperexcitability by establishing a mouse FLS/DRG neuron co-culture system. A pro-inflammatory phenotype was produced in FLS after stimulation with tumor necrosis factor-α (TNF-α a cytokine that is upregulated in CFA mouse models, TNF-FLS); and in co-culture with TNF-FLS or their secreted mediators knee neurons became hyperexcitable and showed altered TRP channel function.

These results suggest that specifically controlling the excitability of knee neurons could provide pain relief in arthritis, one possibility for achieving such control is to deliver excitatory or inhibitory genes via adeno-associated virus (AAV). However, delivering genes into DRG neurons by injection of AAVs into the peripheral organs has had limited success due to the large distances

involved. Here I show that the newly engineered serotype, AAV-PHP.S, can deliver functional excitatory (G_q) and inhibitory (G_i) designer receptors activated by designer drugs (DREADDs) into knee neurons to bi-directionally control excitability *in vitro* and that G_i- DREADD activation *in vivo* can reverse a knee inflammation-induced decrease in digging behavior.

Findings from this thesis highlight multiple ways to identify drivers of inflammatory knee pain and open the door for peripheral organ targeted gene therapy to alleviate arthritic pain.

V. Table of contents

VI. List of figures

VII. List of Tables

Chapter 1. Introduction

1.1. Pain

At the outset of this work, the definition of pain as stated by the International Association for the Study of Pain (IASP) was "an unpleasant sensory and emotional experience associated with actual or potential tissue damage, or described in terms of such damage." In 2019, a global taskforce has proposed an updated definition which states that pain is "an aversive sensory and emotional experience typically caused by, or resembling that caused by, actual or potential tissue injury." At a glance, these two definitions express pain in strikingly similar ways, emphasizing its interacting emotional and physiological states. However, the updated version highlights the aversive nature of pain, which under non-diseased states functions to protect an individual from damaging stimuli. However, persistent pain, as encountered during musculoskeletal disorders like arthritis, serves no protective function and arises due to direct tissue injury or through an inflammatory response to tissue injury. In arthritis, pain typically originates in the joint (referred to as arthritic pain in this thesis) and, in stark contrast to cutaneous pain, is often constantly present at some level with spontaneous, unprovoked increased sensations; episodic flares can also occur (Walsh and McWilliams, 2014). Since arthritis patients either experience constant or intermittent pain (with no obvious trigger), it severely restricts their ability to plan for advance activities which leads to reduced quality of life. In this thesis, mechanisms of arthritic pain were investigated using a variety of *in vitro* and *in vivo* pre-clinical models. An important distinction between clinical and pre-clinical studies is that pre-clinical models can largely only measure the sensory response to harmful stimuli (termed as nociception) devoid of the emotional aspects. However, for the purposes of simplicity, nociception and pain have been used interchangeably throughout the thesis.

1.2. Arthritis

"Arthritis" is derived from the Greek words "arthros" meaning joint and "itis" meaning inflammation. One crucial feature that the etymology of arthritis excludes is the concept of pain, although arthritis is a broad term encompassing musculoskeletal disorders in which chronic pain is the leading cause of morbidity (Neogi, 2013). There are 100s of different forms of arthritis with over 10 broad subgroups (Blumberg et al., 1964), however, clearly defined classification criteria are lacking. In 1936, an article notes "desirable as it maybe, it is often impossible neatly to define

and classify clinical syndromes the origin of which is unknown." (Archer, 1936). 83 years on, the search for the cause and mechanism of arthritic conditions in still ongoing. Classification of arthritis forms is further complicated by the inherent subjectivity involved in clinical assessment and pattern recognition of pain and radiographic images. Nevertheless, evidence from ancient documents suggest that medical practitioners around the world were aware of the major forms of arthritis, such as rheumatoid arthritis (RA) and osteoarthritis (OA), along with their stages of disease progression and painful nature. Therefore, investigating the history of arthritic pain can shed light on epidemiology and inform current research on disease mechanism. Table 1-1 lists the notable events in the history of arthritis and pain research that are relevant to this thesis.

1.3. History of arthritis

Studying the history of a disease relies heavily on the state of excavated human remains, which often comprise of eroded bones making diagnoses of arthritis difficult. The ancient Egyptian civilization provides a unique advantage in this regard because of their custom of mummification, as well as extensive documentation of medical conditions in texts and illustrations. Correspondingly, the first recorded evidence of arthritis has been found in medical papyri dating from 4000-1000 BCE which described OA, spondyloarthropathy and reactive arthritis (Kwiecinski, 2014; Rothschild et al., 1999). Importantly, a papyrus describing reactive arthritis mentions joint inflammation and pain caused by walking, suggesting that the symptoms of the disease are largely unchanged in modern times (Kwiecinski, 2014). With regard to epidemiology, computerized tomography scanning of 52 mummies (with a mean age of 38.1 years) revealed that 48% of them had spinal OA, while only 2% and 8% had hip and knee OA respectively (Fritsch et al., 2015). This distribution of the affected joint(s) is in stark contrast to the modern world where OA of the large joints (knee and hip) is predominant. One possible explanation is that mummification was a costly process and hence carried out only for people in the higher socio-economic strata of ancient Egypt, who led a sedentary lifestyle. In agreement with this hypothesis, another paleopathological study on skeletal remains in Deir-el-Medina in Egypt found ~30% occurrence of knee and hip OA in working class males who had to hike to work and hence likely experienced more wear and tear of joints (Austin, 2017).

At a similar point in antiquity (1000 BCE), the Indian medico-religious text Atharvaveda details the etiology of arthritis as having acute pain arising from the "feet, legs, buttocks, thighs, back

bone, neck joints and head" which can "cripple" one's life (Sharma and Arora, 1973). Later, around 100 CE, two physicians (Charaka and Susruta) of ancient India wrote two books (Charaka and Susruta Samhitas) that consolidated the medical knowledge of that time where arthritis was described in more detail. In particular, Charaka states that arthritis causes stiffness and aching pain in bones and joints, limping, lameness, atrophy of joints and insomnia (Sharma and Arora, 1973). Furthermore, Charaka alludes to the fact that arthritis is a systemic disease that starts in the joints and then spreads throughout the body through a mystical bodily fluid called "vata", thus suggesting that RA might have been present in ancient India (Sturrock et al., 1977). In terms of therapeutics, he recommended a poultice made of a variety of everyday kitchen items such as cooked rice, barley and wine (Sharma and Arora, 1973). Amongst these ingredients was gum-guggul, a resin derived from the guggul tree (Burseraceae family), which contains a large number of steroids including the cis and trans-4,17(20)-pregnadiene-3,16-dione as active ingredients and has shown some efficacy in arthritic conditions in modern times (Kunnumakkara et al., 2018).

Although an ancient civilization with history of excellence in therapeutics, arthritis in ancient China is not well-documented, possibly because dissection was forbidden at that time and the subject of anatomy did not exist (Luesink, 2019). Nevertheless, the oldest medical text of China, The Yellow Emperor's Inner Classic Plain questions (written around 476-221 BCE), describes a "painful obstruction of the bone" that causes stiffness and edema of the joint with pain that becomes worse with changing temperature (Hua and O'Brien, 2010). This description, combined with the supposed effectiveness of the Chinese traditional medicine technique of acupuncture (Tang et al., 2018) in arthritic diseases, suggest that arthritis did exist in ancient China. Indeed, analysis of human skeletal remains from Yinxu (the last capital of the Late Shang dynasty, 1250-1046 BCE) shows frequent presence of OA especially in males, compared to females, likely because of gendered division of physical labor (Zhang et al., 2017).

In the global west, paleopathological evidence places the first skeletal remains that had signs of arthritis between 3000-1000 BCE, such remains being found in Alabama and Kentucky in the United States and Sweden in Europe. Skeletal remains with arthritis dating between 1000-1 BCE have also been found in Denmark, England and Ohio (Entezami et al., 2011). In terms of descriptive accounts, Hippocrates (~300 BCE) described arthritis as a "mischief" that spreads from feet to hands, through the knee and hip joints, possibly after observing an RA patient (Short, 1974).

Following on from Hippocrates, Aretaeus of Cappadocia, Abu Bakr Mohammad Ibn Zakariya Razi of Iran (Changizi Ashtiyani et al., 2012) and Soranus of Ephesus also described polyarthritis that causes intense pain and joint deformity (Short, 1974). Interestingly, Roman Emperor Claudius's physician Scribonius Largus (~40 CE) described a chronic polyarthritis which he treated by administering a shock of static electricity to the patient's feet using torpedo fish, presumably in an attempt to modulate neuronal activity to suppress pain (Kellaway, 1946). Most evidence of arthritis from the Middle Ages comes from physicians of the Byzantine Emperors, 14/86 of whom had some form of arthritis (Lascaratos, 1995). There are very few other documented descriptions of arthritis from the Middle Ages, however a clay sculpture recovered from the classic Velacruz period in Mexico shows Heberden's node, a bony protrusion that causes joint stiffness in arthritis (Alarcó-Segovia, 1976).

During the Renaissance, major evidence for the existence of arthritis can be seen in artworks, however uncertainties remain as to whether these were artistic choices or true rendition of the model's rheumatic conditions (Hinojosa-Azaola and Alcocer-Varela, 2014). Nevertheless, some paintings such as Hieronymus Bosch's (1450-1516) "The Procession of the Cripples" and Quinten Metsys' (1465-1530) "A Grotesque Old Woman" clearly show arthritic patients and the names of the paintings suggest that the reproduced disease conditions were intentional (Dequeker et al., 2001). Later in the Baroque period, Caravaggio's "The Sleeping Cupid" (1608) shows signs of juvenile idiopathic arthritis, Rubens' "The Three Graces" (1640) depicts limbs with deformities consistent with benign familial hypermobility syndrome (also corroborated by this letters) while the post-impressionist maestro Vincent Van Gogh's portrait of Augustine Roulin (1888) shows hand arthritis (Dequeker, 2006, 2001; Weinberger, 1998).

The medical literature is relatively less loquacious during the 1600-1800s, although "The English Hippocrates" Thomas Sydenham talks about the chronic, episodic nature of arthritis and that it torments the patients throughout their ("miserable") lives (Sydenham and Swan, 1742). In 1800, the first full medical description of RA was published in the doctoral thesis of Augustin-Jacob Landre-Beauvais (France) where he made several key observations that still hold, such as arthritis being a disease that predominantly affects females and also a systemic disease producing severe joint immobility that persists after pain has disappeared (Short, 1974). In 1859, Sir Alfred Baring Garrod (England) introduced the term "rheumatoid arthritis" for this disease in the medical

literature while his son Sir Archibald Edward Garrod published “A Treatise on Rheumatism and Rheumatoid Arthritis” later in 1890 (Garrod, 1890).

The history of arthritis demonstrates the enormous impact that arthritis and arthritic pain had on the lives of ancient people, and the next section will demonstrate how it continues to take its toll on patients’ lives and society.

Table 1-1: Notable events in the fields of arthritis and pain that are relevant to this thesis.

Approximate year	**Event**
Pre-history	Evidence of arthritic pain in dinosaurs
4000-1000 BCE	Evidence of arthritis in Egypt, India, China, United States and Northern Europe
1000 BCE-100 CE	Chinese medical text, Hippocrates (Greece) and Atharvaveda and Charaka Samhita (India), describes a variety of symptoms for arthritis
350 BCE	Herophilus (Greece) describes nerves
16th century	Arthritis depicted in art, Descartes describes pain as a circuit from the periphery to the brain
1667	Robert Hooke publishes Micrographia, hence beginning of investigation *in vitro*
1791	Galvani demonstrates electrical activation of nerves and muscles
1800	Augustin-Jacob Landre-Beauvais (France) gives first full medical description of rheumatoid arthritis
1849	von Helmholtz measures speed of nerve impulses in frog
1859	Sir Alfred Baring Garrod introduces the term "rheumatoid arthritis"
1889	Ramon y Cajal describes individual neurons in the nervous system
1896	von Frey describes pain spots
1897	Aspirin is developed
1906	Sherrington describes nociception
1939	Hodgkin and Huxley publish first action potential recording
1956	Levi Montalcini isolates nerve growth factor, Pearson describes a rodent model of arthritis
1965	Melzak and Wall describe the gate control theory of pain (where innocuous input can override noxious stimuli through interneurons in the spinal cord)
1980	Ca^{2+} indicators developed by Roger Tsien
1984	Neher and Sakmann develop patch clamp technique
1998	Anti-tumor necrosis factor-α developed for RA treatment
2000	Sequencing of the human genome
2008	Chemogenetics is developed
2015	Single cell transcriptomics gains popularity in pain field
2017	South Korea approves first gene therapy for arthritis
2019	IASP proposes new definition of pain and opioid crisis continues in the United States

1.4. Impact of arthritic pain

As has been known since antiquity, musculoskeletal conditions span many forms of arthritis. Amongst them, a study on the Global Burden of Disease (GBD) specifically emphasizes the burden of hip and knee OA and RA, along with back and neck pain, and gout (Blyth et al., 2019). Epidemiology of the affected population determines the burden of any disease. Correspondingly, the Centers for Disease Control and Prevention estimates that ~55 million people in the United States live with some form of arthritis and that it affects women more than men (26% of adult women vs. 19 % of adult men. Moreover, statistics predict a further rise to 78 million people living with some form of arthritis in the United States by the year 2040 (Centers for Disease Control and Prevention, 2015). Knee and hip OA are the most commonly diagnosed forms of arthritis that drastically reduce the quality of human life and can cost up to 1% of the gross national product (Leardini et al., 2004; Murphy et al., 2008, 2010). In Europe, around 40 million people are affected by OA and a study with around 4000 respondents from France, Germany, United Kingdom, Italy and Spain found that 55-74 years old obese patients formed the majority of this group with ~20% also reporting pain-related depression (Kingsbury et al., 2014). In this study only 30% reported satisfaction with their disease management. An additional 2.3 million people are living with RA in Europe with the annual direct and indirect cost for disease management amounting to over €45 billion (Lundkvist et al., 2008). Furthermore, a study with ~45,000 participants from low to middle economic countries (LMICs, China, Ghana, Mexico, India, the Russian Federation and South Africa) shows that the incidence rate of men with arthritis is higher than their higher income counterparts, while the incidence rate in women is similar to higher income countries in all LMICs except for Russia (where it was higher) (Brennan-Olsen et al., 2017). This higher incidence rate of arthritis in LMICS is possibly because these countries are more reliant on manual labor, which is supported by the correlation found between lower educational levels and arthritis (Brennan-Olsen et al., 2017).

The principle reasons for the disease burden of arthritis are pain and restricted mobility, factors that result in musculoskeletal disorders being the most important contributors to the years lived with disability and accounting for 6.7 % of the total global disability-adjusted life years (DALY) (Blyth et al., 2019; Vos et al., 2012). The age standardized DALY rates were higher for females

and the elderly (Safiri et al., 2019). The main cause of this alarming incidence of arthritis globally is the skewed age structure and increasing longevity of the population (Briggs et al., 2016), such that 2018 was the first year in recorded history in which people older than 65 years of age outnumbered 5 year olds (United Nations, 2019). Beyond socioeconomic costs and disability indexes, chronic pain is associated with several psychological comorbidities, such as anxiety and depression (Burston et al., 2019; McWilliams et al., 2004), which decrease the quality of life of patients, although the definition of quality of life remains complex and subjective (Malm et al., 2017). Nevertheless, in a study where health-related quality of life was assessed using self-reported 12-item Short Form version 2 questionnaires, a significant decrease in this measure was seen in OA and RA patients compared to demographically matched controls (Heimans et al., 2013; Kingsbury et al., 2014). The impact of arthritis on the lives of individuals, and wider socioeconomic burden, are more profound in LMICs because access to pain managing therapies are sub-optimal (Bond, 2011), along with limited flexibility in working hours, the combination of which could compound chronic pain conditions and poverty. Indeed, according to the World Health Organization (WHO) 5-33% of primary care patients in LMICs experience chronic pain on a daily basis with co-morbid anxiety and depression (Gureje et al., 1998).

Finally, the incidence of arthritis and chronic pain (Berkley, 1997; Srikanth et al., 2005; van Vollenhoven, 2009) is higher in females although the underlying causal factors are controversial and/or unknown (Mogil, 2012). Although there is some evidence of sex-specificity in pain mechanisms, the biology of this is often shrouded by experiential and socio-cultural differences in pain experience. Investigating whether sex differences exist for sensitivity to pain is complicated given the prominent hormonal cycle in women along with the fact that it is currently unclear whether estrogen is pre or anti-nociceptive (Mogil, 2012). Therefore, studying the epidemiology of sex differences in arthritis is critical to the development of pain medication and should be explored more carefully in pre-clinical models of arthritis.

1.5. Management of arthritic pain

An important consideration for pain management is accurate assessment of pain by clinicians. Although both patients and physicians report that pain management is their highest priority goal in arthritis management (Gibofsky, 2012), evidence from vignette studies suggests that health care

professionals underestimate the pain level of patients, especially that of females (Samulowitz et al., 2018). Therefore, in 2018 the multi-disciplinary European League Against Rheumatism (EULAR) task-force published a set of approaches for pain management in inflammatory arthritis and OA where validation of patients' pain experience was greatly emphasized, as this promotes trust and subsequently better compliance with any treatment plan (Geenen et al., 2018).

The two major ways pain manifests are hyperalgesia (in which a moderately painful stimulus is perceived to be more painful) and allodynia (in which a previously non-painful stimulus causes pain). Pain is commonly assessed and measured in arthritis using a variety of questionnaires, such as: Arthritis impact measurement scales, European quality of life-5 dimensions, visual analog scale, McGill pain questionnaire and West Haven-Yale multidimensional pain inventory (Walsh and McWilliams, 2014). The most commonly used adjectives that patients use to qualify their pain are: aching, sharp, burning, tiring, sickening and shooting, which are characteristic of joint/deep tissue pain. However, the major challenge of assessing and treating arthritic pain is that pain intensity poorly correlates with radiographic assessment of disease activity and inflammation, such that pain persists even without inflammation (Bedson and Croft, 2008; Salaffi et al., 2018). Therefore, pain management is a complex issue spanning biological, psychological and social domains with limited options for joint pain specific analgesia. The following paragraphs summarize commonly used treatment options in arthritic pain (reviewed in (Majeed et al., 2018; Walsh and McWilliams, 2014)).

1.5.1. Non-pharmacological methods

EULAR recommends health professions to explore non-pharmacological measures before and/or in combination with pharmacotherapy or surgery (Geenen et al., 2018). Exercise is the most well studied non-pharmacological measure that has demonstrable positive effects. When performed in moderation, aerobic training, Tai chi, strength training and aquatic exercise are beneficial for pain management and increasing function of arthritic patients (Bennell and Hinman, 2011). As an added benefit, exercise also helps in weight management, thus reducing the risk of obesity which is one of the strongest modifiable risks for arthritis (Messier et al., 2013). However, long distance running (> 20 miles per week) can increase the risk for OA (Cheng et al., 2000). The mechanistic basis of exercise-induced analgesia is thought to be mediated by higher levels of circulating endorphins

and inhibition of spinal nociceptive reflexes; although more basic science research is needed to develop a complete understanding (Sluka et al., 2018).

Psychological interventions such as cognitive behavioral therapy (CBT), mindfulness training and acceptance and commitment therapy (ACT) have also been explored for arthritic pain since pain catastrophizing, anxiety and depression are associated with chronic pain (Burston et al., 2019; Edwards et al., 2010). CBT seeks to change unhelpful beliefs about pain while encouraging productive coping strategies and has been shown to improve function and pain severity, albeit with a small effect size (Zautra et al., 2008). On the contrary, ACT and mindfulness seek to prevent adverse consequences without changing beliefs and have also shown small reductions in pain intensity (Edwards et al., 2010).

1.5.2. Pharmacological methods: Analgesics

Conventionally and frequently used pharmacological therapies in arthritic pain are nonsteroidal anti-inflammatory drugs (NSAIDs) and acetaminophen (paracetamol). NSAIDs provide analgesia by both peripheral and central mechanisms (Atzeni et al., 2018). In the periphery, the majority of NSAID efficacy is mediated by inhibition of cyclooxygenase enzymes and thus reduction of prostaglandin (PG) and thromboxane synthesis, in addition to decreasing sensitization by stimulating the nitric oxide (NO)/cGMP/K^+ channel pathway. Central mechanisms proposed for NSAID analgesia are increased endorphin levels in the plasma and inhibition of N-methyl-D-aspartate (NMDA) receptor-mediated hyperalgesia by the NO/cGMP pathway.

The (in)famous NSAID, aspirin, acetylates COX in an irreversible and non-competitive manner, which prevents production of PGs because COX is essential for the transformation of arachidonic acid to PGH_2 (Flower, 2003). As aspirin gained popularity as a pain medication, two side effects were observed – increase in the risk for gastrointestinal and cranial bleeding and reduction in the risk of cardiovascular events (Meek et al., 2010). At a low dose of aspirin, the cardiovascular protection predominated and hence could be prescribed (Lin et al., 2014). The reasons for these side effects became clearer after the discovery of the two isoforms of COX – COX-1 (constitutively present in several tissues) and COX-2 (inducible in inflammation) (Fu et al., 1990). By inhibiting COX-1, aspirin acted as an anti-coagulant (by preventing thromboxane production by platelets, a critical factor for inducing platelet aggregation and vasoconstriction) that decreased the risk of stroke but increased gastrointestinal bleeding. However, the endothelial cells in the

gastrointestinal system are able to rapidly re-synthesize COX-1 and therefore, at low doses, aspirin-induced gastric bleeding has low incidence (Jaffe and Weksler, 1979)

Based upon the knowledge of two different COX isoforms, several other classes of NSAIDs were developed with varying degree of COX-1 and COX-2 specificity. Diclofenac, for example, is four times more selective for COX-2 and is effective in controlling arthritic pain (Atzeni et al., 2018). COX-2 specific NSAIDs, such as celecoxib and etoricoxib, have also been developed by addition of a rigid side chain that binds to COX-2's side pocket, but cannot access the much narrower side pocket of COX-1. However, problems with NSAID-induced analgesia still persist after long term use. For example, although COX-2 selective NSAIDs do not cause gastrointestinal ulcers, some of them can increase the risk of cardiovascular toxicity after long term use (Vonkeman et al., 2006), although a 2016 clinical trial found that celecoxib has a similar associated cardiovascular risk compared to the non-selective NSAIDs, naproxen and ibuprofen (Nissen et al., 2016). Additionally, various studies show that both topical and oral NSAIDs have similar (small to medium effect size) effectivity for pain reduction in arthritis with topical application being the safer option (Kienzler et al., 2010).

Acetaminophen or paracetamol is another first line of therapy for arthritic pain and is often prescribed to patients that have co-morbid peptic ulcers or salicylate sensitization and hence cannot be prescribed NSAIDs. However, the mechanisms of action of acetaminophen are less well understood and include stimulation of descending serotonergic neuronal pathways, inhibition of L-arginine/NO pathway and stimulation of endocannabinoid system (Jozwiak-Bebenista and Nowak, 2014). There is also evidence that metabolism products of acetaminophen are involved in the analgesic effects observed (Andersson et al., 2011). Overall, acetaminophen seems to be less effective in pain reduction when compared to NSAIDs (Chou et al., 2011).

Patients who are unresponsive to NSAIDs and paracetamol are generally prescribed synthetic opioids which harness the endogenous opioid system in the body for pain management. The three major opioid receptors the δ, μ and κ receptors. along with the comparatively recently discovered opioid-like receptor (Przewłocki and Przewłocka, 2001). The expression of these receptors is widespread in the central (periaqueductal grey, locus coerelus, raphe nuclei) and peripheral nervous system and immune cells (Chuang et al., 1995; Wittert et al., 1996). Opioid mediated analgesia occurs primarily through the reward/reinforcement mechanisms of the central nervous

system (CNS), mediated through the mesolimbic pathway. Exogenous opioids that are often prescribed for chronic pain (for e.g., morphine, codeine, oxycodone) alter the endogenous opioid system primarily in the reinforcement pathway and lead to changes in gene expression in the brain (Crofford, 2010). Additionally, opioids also produce analgesia by spinal mechanisms including inhibition of somatostatin-positive interneurons that gate mechanosensory input and by erasure of the spinal memory of pain that contributes to central sensitization (reviewed in (Corder et al., 2018)).

One of the major adverse effects of opioid therapy is opioid induced hyperalgesia, which is mediated by sensitization of central pathways, where opioids paradoxically exacerbate pain in patients. Multiple central sensitization pathways have been suggested for this phenomenon including it being NMDA-mediated, protein kinase C (PKC) mediated, repeated G_i protein activation mediated (Araldi et al., 2015), arising from dysregulation of endogenous opioid peptides and through pro-inflammatory phenotype trigger of immune cells in the spinal cord (reviewed in (Crofford, 2010)).

Although, opioids have demonstrable analgesic effects during short term use, effectivity (in terms of pain intensity and functional outcome) of chronic opioid therapy, like those prescribed to arthritic patients, remains uncertain (Von Korff, 2013; Webster et al., 2007). Additionally, opioids prescribed for chronic pain severely increase the risk for misuse and addiction which has led to the opioid crisis in the United States: in 2006 approximately 250,000 people visited medical emergency departments in the United States due to opioid related adverse effects with around 13,800 deaths between 1999 and 2006 (Becker et al., 2008; Woodcock, 2009). Therefore, evidence warrants a more cautious approach to opioid prescription for pain management.

In addition to these major classes, other analgesics currently in use for arthritic pain are duloxetine (a centrally acting serotonin-norepinephrine reuptake inhibitor) (Abou-Raya et al., 2012) and capsaicin (naturally occurring compound found in hot chili peppers) (Guedes et al., 2018). The endocannabinoid system has also been explored for pain relief in arthritic pain. The cannabinoid receptors, CB1 and CB2, are expressed in the synovial tissues, peripheral nervous system (PNS) and CNS (O'Brien and McDougall, 2018; Sarzi-Puttini et al., 2019) and in addition, synovial fluid from OA and RA patients (but not from healthy people) contains endogenous cannabinoids, anandamide (AEA) and 2-arachidonoylglycerol (2-AG), suggesting a possible pain ameliorating

role of cannabinoids (Richardson et al., 2008). However, a clinical trial of OA patients with PF-04457845 (an inhibitor of fatty acid amide hydrolase which breaks down AEA) did not produce analgesia (Huggins et al., 2012). By contrast, the cannabis extract, nabiximol, was effective in improving pain and movement in RA with mild side effects, such as dizziness (Blake et al., 2005). However, it still remains for systematic randomized clinical trials to be conducted to ascertain the true potential of cannabis products for arthritic pain.

1.5.3. Pharmacological methods: Joint modifying drugs

Several joint-modifying drugs are also available that control pain on a short-term or long-term basis. Methotrexate, sulfasalazine and leflunomide are conventionally used disease modifying drugs in RA that suppress inflammation and control pain in some patients which can be maintained over months (Walsh and McWilliams, 2014). Methotrexate is an inhibitor of dihydrofolate reductase which confers its anti-proliferative effect on residing joint cells and controls inflammation. Additionally, methotrexate also increases extracellular adenosine that can inhibit secretion of pro-inflammatory interleukins (IL) in immune cells (Cutolo et al., 2001). Another commonly prescribed joint modifying drug, sulfasalazine also inhibits inflammation through dysregulation of the PG system as well as through other mechanisms (Smedegård and Björk, 1995). Lastly, leflunomide is an inhibitor of dihydroorotate dehydrogenase that prevents de novo synthesis of pyrimidines, which restricts the rapid proliferation of lymphocytes (e.g., B cell, T cell) because they require significant amounts of pyrimidines for proliferation (Breedveld and Dayer, 2000).

On a short term basis (6 months) a combination of glucosamine and chondroitin provide pain relief by increasing proteoglycan synthesis in the articular cartilage (Hochberg et al., 2016). Additionally, intra-articular steroid injections can also provide moderate efficacy for pain relief for up to two weeks. Hyaluronic acid (HA) is the principal component of synovial fluid which can be directly injected into the joint and acts as a lubricant and shock absorber, as well as by inhibiting the nociceptive ion channel, transient receptor potential vanilloid 1 (TRPV1) (Gupta et al., 2019). However, the efficacy of HA in arthritic pain is not well established. Like HA, platelet-rich plasma containing growth factors important in tissue repair can be injected directly to reduce pain and improve functionality in arthritic pain (Cole et al., 2017).

1.5.4. Pharmacological method: Biologics

In recent years, several biological agents have also been explored for pain management in arthritis. In RA, anti-tumor necrosis factor-α (TNF-α) (e.g. adalimumab) (Keystone et al., 2004), anti-IL-6 (e.g. tocilizumab) (Scott, 2017) and anti-CD20 (B cell antigen, e.g. rituximab) (Mok, 2013) antibodies have demonstrated reduced joint pain by reducing inflammation and decreasing peripheral and central sensitization. There is also evidence suggesting that the rapid effect of TNF-α-blockers in RA is due to their modulation of descending nociceptive inputs that are important for emotional processing of pain (Rech et al., 2013). In OA, anti-nerve growth factor (NGF) antibodies are promising candidates for pain management. NGF is a pro-inflammatory mediator and tanezumab, a monoclonal anti-NGF antibody shows efficacy in treating OA pain. Specifically, in the treatment of knee and hip OA, tanezumab showed greater improvement of pain scores when compared to NSAIDs (Schnitzer et al., 2015). Consequently in 2019, this drug has successfully completed a Phase III clinical trial for OA pain (Schnitzer et al., 2019), but it is not yet in clinical use. This is primarily because concerns remain over its safety since rapidly progressive joint necrosis, paresthesia and dysthesia have been reported as its major side effects (Birbara et al., 2018). Additionally, an anti-granulocyte-macrophage colony stimulating factor antibody is currently being investigated for the treatment of arthritic pain (Cook and Hamilton, 2018).

1.5.5. Gene therapy

Gene therapy is the most recently developed therapeutic option that holds great potential for targeted therapy in arthritis. The major hurdle to treatment with biologics (Section 1.5.4) is that they have difficulty in entering joints from the systemic circulation and, when introduced intra-articularly, are rapidly removed from the joints by diffusing into the sub-synovial capillaries. Delivery of cDNA that encodes these biologics, with or without viral packaging, can offer benefits, thus highlighting the advantage of gene therapy. In a major breakthrough in 2017, the first gene therapy for arthritis, Invossa, was approved in South Korea, with multiple others in clinical trials around the world at present (Evans et al., 2018). Invossa is an allogeneic cell-mediated gene therapy in which chondrocytes from patients are harvested and transduced with a retrovirus carrying the anti-inflammatory, transforming growth factor β (TGF-β), after irradiation to avoid

malignancies, and finally injected into a patient's joints (Evans et al., 2017). A similar strategy has also been investigated to deliver IL-1 receptor antagonist to control inflammation (Wehling et al., 2009). However, the major disadvantage of allogenic strategies is that they require multiple steps (successful cell harvesting – from the same or another patient – expansion and then transplantation), thus increasing cost and chances of malignancy; in addition retrovirus tools are themselves pathogenic (Hacein-Bey-Abina et al., 2008).

Viral delivery using vectors of very low pathogenicity such as adeno-associated viruses (AAV) is perhaps a better choice in the clinic. An exciting clinical trial using AAVs is currently underway in the Netherlands in which the anti-inflammatory cargo, interferon β (IFN- β), is under an inducible promoter that responds to the inflammatory mediator, nuclear factor-κB (NF- κB) (Clinical trial # NCT02727764, (U.S. National library of medicine, 2019)). This strategy, if successful, will mean that the anti-inflammatory IFN- β will be secreted only when an inflammatory environment is encountered, thus minimizing the side-effects. A Phase I clinical trial with an AAV encoding IL-1 receptor antagonist is also underway in the United States, with results expected in 2022 (Clinical trial # NCT02790723, (U.S. National library of medicine, 2019)).

Although the next 5 years will provide critical insights about the success of AAV-mediated gene therapy in arthritis, most of these efforts discussed above are geared towards immune cell pathologies and not targeted for pain relief. For gene therapies to specifically control pain, it is necessary for delivery directly into the site of injury (Goins et al., 2012). For example, NP2, A herpes simplex virus-mediated enkephalin gene therapy, showed promising results in a Phase I clinical trial when injected into pain-inducing metastatic tumors (Fink et al., 2011); the outcome of the Phase II trial is pending. One reason for the lack of pain specific gene therapy in arthritis is that arthritic pain is mediated through the cell bodies of pain-sensing nerves present in the dorsal root ganglia (DRG) and conventional AAV serotypes do not have sufficient transduction capabilities to infect DRG when injected into the knee (Chan et al., 2017). Chapter 6 of this thesis identifies a newly engineered AAV serotype that can help break through this barrier.

Overall, discussion about therapeutics in arthritis suggests that although several pain managing options are available (administered on their own or in combination), the efficacy of these is overall inadequate, coupled with often dubious safety profiles when drugs are used chronically. To combat

these problems, advancement of basic science research is required in the pain fields for proper pain management in arthritis.

1.5.6. Surgery

Since a large proportion of arthritis patients are unresponsive to currently available pharmacological treatments, orthopedic surgery has also been used to control progression and pain in arthritis. Arthroscopic procedures such as debridement of the joint and lavage has had limited success. Furthermore, in RA, patients who undergo arthroscopic synovectomy (removal of the synovial lining), while attaining pain relief, show recurrence of synovitis and radiographic progression of the disease (Chalmers et al., 2011). In knee OA, osteotomy is performed to realign joints because of joint misalignment frequently occurs, however, although no extensive meta-analysis is available, total knee arthroplasty seems to produce better results for pain relief when compared to osteotomy (Katz et al., 2010). Overall, total joint replacement is the most commonly used surgical technique for controlling arthritis pain (Katz et al., 2010) and total knee replacement can provide pain relief and functional improvement in the majority of patients undergoing such surgery (Ethgen et al., 2004). The patient population (~30 %) that report no significant improvement often have worse pre-operative biopsychosocial conditions, while 1-5 % of patients die or have serious complications during and after surgery (Judge et al., 2012).

1.6. *In vivo* experimental models of arthritis to study pain

The basic understanding of pain mechanisms, identification of drug targets and subsequent development of therapeutics all rely heavily on experimental models. This has led to the establishment of multiple *in vivo* and *in vitro* inflammatory pain models to resemble the arthritic pain observed in humans, each of which has its unique strengths and weaknesses. The two main strategies used for developing arthritic pain models are modulating the joint environment by administering an irritant or by trauma that leads to either acute or chronic development of pain (induced models) and utilizing animals that spontaneously develop arthritis.

Acute and chronic inflammatory pain can be studied in various organs, such as skin, muscle and gut, and has been extensively reviewed (Boyce-Rustay et al., 2010; Gregory et al., 2013; Muley et

al., 2016). The following discussion will focus on models of joint pain (reviewed in (Muley et al., 2016; Schinnerling et al., 2019) because of their relevance to arthritis and the work in this thesis.

1.6.1. Inflammation-focused models

Amongst the induced animal models of arthritis, perhaps the most commonly studied is injection of adjuvants. A single injection of complete Freund's adjuvant (CFA, an oil emulsion of heat killed mycobacterium) intra-dermally at the base of tail (Pearson, 1956) or repeatedly into the joints (Gauldie et al., 2004) causes poly-articular inflammation and chronic pain along with structural deformation of joints due to the release of pro-inflammatory mediators into the joint environment. As opposed to this chronic model, a single injection of CFA into one or multiple joints can also cause localized inflammation that models acute inflammatory pain (Fernandes et al., 2016) (See also Chapter 4 for more details). Besides CFA, other adjuvants like avridine and pristine also give rise to adjuvant-induced arthritis (AA) and these models resemble human RA, with milder cartilage damage than observed in the human disease (Schinnerling et al., 2019). In order to overcome this problem, the collagen-induced arthritis (CIA) model was developed in which type II collagen, in combination with CFA, is injected into the base of the tail (Brand et al., 2007). An autoimmune response is triggered that leads to symmetrical joint inflammation, prominent synovitis and cartilage damage. However, unlike AA models, CIA takes a long time to develop (about a month) which is quickly (10-14 days) followed by remission (Mauri et al., 1996). Additionally, multiple mouse strains (including the commonly used C57BL/6 strain upon which most transgenic mice are generated) are resistant to CIA (Brand et al., 2007) which has led to the generation of the collagen-antibody-induced arthritis model (Khachigian, 2006). Collagen based models engage only a subset of Th cells that are involved in human RA, therefore the relevance of Th cells in arthritis can be studied differentially using the proteoglycan-induced arthritis (PGIA) (Glant et al., 1987). For example, immunization with CFA or dimethyldioctadecyl-ammonium bromide before proteoglycan injection engages Th17 or Th1 cells respectively (Stoop et al., 2013). However, like CIA, PGIA is also dependent on the genetic strain of mice.

Another induced inflammatory model that is not dependent on the genetic background of mice is antigen-induced arthritis (AIA), commonly induced by intra-articular injection of methylated bovine serum albumin, and transfer of serum antibodies against endogenous type II collagenase, proteoglycan or glucose-6-phosphate isomerase (Brackertz et al., 1977). These models are mostly

utilized to study the rapid onset, effector phase of the disease involving immune complex formation on joint tissues and inflammatory mediator release but not prolonged enough to study the destructive arthritis. Another acute model of joint inflammatory pain is injection of kaolin-carrageenan into the joint, which has a rapid onset (1-3-hour) of inflammation and is maintained for about a week (Rees et al., 1995).

Besides induced arthritis models, spontaneous models of inflammatory arthritis also exist. The K/BxN mice are one of the most commonly used examples which were produced by crossing KRN mice (expressing transgenic T cell receptor for bovine pancreas ribonuclease) with autoimmune prone non-obese diabetic mice (Christensen et al., 2016). K/BxN mice spontaneously develop severe arthritis and transfer of their serum IgG induces robust arthritis in healthy mice. Another commonly used mechanism by which arthritis develops spontaneously is by mutation in a specific gene or by over-expression of a pro-inflammatory gene. In SKG mice, arthritis develops after zymosan administration or microbial stimulation due to a missense mutation in the T cell receptor signaling adaptor molecule resulting in an aberrant immune response (Yoshitomi et al., 2005). In addition, transgenic mice constitutively expressing human TNF-α or IL-1α also develop spontaneous arthritis (Keffer et al., 1991; Niki et al., 2001). These models are suitable for understanding contributions of a specific pathway in arthritis.

1.6.2. Degeneration-focused models

Specialized models for OA also exist where degeneration of joints is emphasized although inflammation is also observed in these models, as is the case in human OA. Experimentally, OA can be induced either by injection of chemical substances, such as mono-sodium iodoacetate (MIA), or by surgically destabilizing the joint. Among chemical-induction models, MIA acts by inhibiting glyceraldehyde-3-phosphate dehydrogenase, which leads to the death of chondrocytes and has proven useful for understanding OA pain (Combe et al., 2004). Destabilization of the joint can be achieved surgically by anterior cruciate ligament transection (ACLT) (Fu et al., 2012), meniscectomy (Bove et al., 2006) and medial meniscal destabilization (DMM) (Malfait et al., 2010). These models are induced by trauma making them the models of choice for understanding immediate response to trauma and then the chronic stages of arthritis that develops later on. However, given the invasive nature of induction they might not be useful to study the early stages of OA development (Malfait et al., 2013). Given these challenges, several non-invasive, but

traumatic injury-induced models of OA have emerged. The commonly used models of this category are intra-articular tibial plateau fracture (Furman et al., 2007), cyclic articular cartilage tibial compression (Melville et al., 2015), ACL rupture (Gilbert et al., 2018), and tibial compression overload (Christiansen et al., 2012). The common mechanism of induction in these models is that the experimenter loads the joint with varying force to cause a fracture (Kuyinu et al., 2016).

Spontaneous OA animal models are more common in larger animals (discussed in Section 1.10), nevertheless transgenic mice like STR/ort (Kyostio-Moore et al., 2011) and Col9a1$^{-/-}$ (Hu et al., 2006) mice have been studied as spontaneous mouse models of OA to elucidate the roles of chondrocyte metabolism and collagen type IX alpha 1 respectively.

1.6.3. Criticism of rodent models

A common criticism for all models of experimental arthritis is that they do not model the human disease and hence several therapeutics that show efficacy in rodents fail to translate to humans. One reason for this discrepancy is that most of the models make use of the rodent immune system which differs significantly from the human immune system in the domains of B and T cell signaling pathways, composition of leukocyte subsets and responses to cytokines (Schinnerling et al., 2019). These differences also mean that the pain pathologies studied do not fully reflect human joint pain, thus hindering development of arthritis specific analgesics. Some emerging humanized mouse models of arthritis have tried to combat this problem. The first strategy for these humanized models is to utilize transgenic mice that lack a specific endogenous mouse gene to be replaced by its human counterpart. For example, transgenic mice with human leukocyte antigen class II alleles or human type II collagenase develop severe arthritis which might resemble the human disease more closely (Malmström et al., 1997; Taneja and David, 2010). However, even though some pathways are humanized in these mice, the disease pathology is still driven by the murine immune system. Human/mouse chimeras offer a possibility where a functional part of the human disease (in the form of tissues or cells) can be grafted on to severe combined immunodeficient mice (SCID). These types of models have been in use in the cancer field for quite some time, however, their potential application in arthritis is beginning to be acknowledged (Wege, 2018). For example, synovial tissue from RA patients transplanted into the joints of SCID mice causes RA-like inflammation, cartilage infiltration and even destruction of co-transplanted normal human synovial

tissue (Geiler et al., 1994). Other relatively simpler transplantations involve transfer of human RA fibroblast-like synoviocytes (FLS) and peripheral blood or synovium derived mononuclear cells to study cell specific disease pathologies (Müller-Ladner et al., 1996; Tighe et al., 1990). Although, laboratories need to be cognizant of cross species toxicity, models like this offer exciting possibilities to study arthritic pain.

1.7. Behavioral measures of pain

Although several experimental models of arthritis exist, basic science efforts have focused on understanding the disease progression at the level of the joint, rather than the pain aspect of the disease. Arthritic pain in the above mentioned models can be studied behaviorally by measuring several outcomes *in vivo* (reviewed in (Deuis et al., 2017; Gregory et al., 2013; Malfait et al., 2013)) or at a cellular level *in vitro*. The two main categories of behavioral pain measures are evoked-pain measures and spontaneous pain measures. Evoked behaviors measure the reaction of an animal to mechanical or thermal stimuli; however, it is controversial whether these reflexive behaviors reflect true "pain". In contrast, non-reflexive measures might be better models to recapitulate the human experience of persistent, ongoing pain that decreases the quality of life, although it is to be noted that, by definition, pain is anthropomorphic and hence we can only comment about "pain-like" states in animal models. A summary figure of in vivo arthritic pain models and measures of behavioral outcomes are presented in Figure 1-1.

1.7.1. Reflexive assays

Evoked pain in response to mechanical stimuli can be assessed using manual or automated von Frey or Randall-Selitto tests. In von Frey tests, a monofilament is typically applied (manually or electronically) to the plantar surface of the hind paw until it bends and nocifensive behaviors (for example, paw withdrawal, paw shaking) of the rodents are recorded (Chaplan et al., 1994). In Randall-Selitto tests, a handheld device is used to apply mechanical force until paw withdrawal/vocalization occurs (Randall, 1957). Along similar lines, heat-evoked pain can be tested based on latency to withdraw by using the tail-flick test (time taken for the tail of a rodent to flick upon application of heat) (D'Amour and Smith, 1941), hot/cold plate test (Allchorne et al., 2005; Woolfe and MacDonald, 1944) (time taken to observe nocifensive behavior while on a

hot/cold plate) or Hargreaves test (Hargreaves et al., 1988) (time taken to withdraw from a heat source). The actual temperature at which the mice show pain-like behavior can be recorded using a thermal probe test (Deuis and Vetter, 2016) or a thermal preference test (Touska et al., 2016) (shows temperature preference of rodents in a plate with temperature gradient). Additionally, the acetone evaporation test (Carlton et al., 1994) (application of acetone to cool skin surfaces) and cold plantar assay (Brenner et al., 2012) (application of dry/wet ice underneath the paw) are used to measure cold pain. However, these mechanical and thermal tests assess pain at the paw, and not at the joint level, thus indicating secondary hyperalgesia/allodynia (i.e., away from the primary point of tissue injury). To circumvent this problem, a pressure application measurement (PAM) device was designed to evoke mechanical pain at the joints, although no such devices exist to evoke thermal pain. For measurements using PAM, the experimenter wears a calibrated force sensor on their thumb and the PAM device is pressed against the joint to elicit withdrawal (Malfait et al., 2013). A less sophisticated version of this method, is to record animal vocalization in response to noxious stimulation of the joint (Calvino et al., 1996).

Although evoked pain behavioral measures are reflexive and direct joint stimulation are difficult to achieve, these are amongst the simplest tests that can be conducted on animal models. Therefore, high speed videography and machine learning technologies have been combined recently in an attempt to segregate movement features during an evoked response that characterize innocuous reflexive quality and that which are of noxious quality (Abdus-Saboor et al., 2019). Applicability of this "mouse pain scale" remains to be seen in models of arthritic pain as more laboratories adopt high speed videography.

1.7.2. Non-reflexive assays

In addition to the challenges of evoked pain measures described above, these also lack clinical translatability because of their reliance on hyperexcitable states rather than on spontaneous pain states that accompany chronic pain in human patients (Mogil, 2009). Therefore, to overcome these challenges, non-reflexive measures of pain are gaining popularity among researchers. The two types of non-reflexive pain commonly in use are spontaneous behavioral measures and operant behavioral measures.

Gait analysis is a clinically relevant, spontaneous pain test which involves observing animal movements to identify nocifensive behaviors either in their home cages or in novel environments.

The simplest experimental design for gait analysis is dipping mouse paws in ink and allowing them to walk in straight line to quantify paw area and stride length (Sugimoto and Kawakami, 2019). This technique has also been automated in a Catwalk apparatus where a camera records animal movement on a moving or immobile platform thus allowing extraction of more features relevant to mobility (Ferland et al., 2011). Another gait analysis feature of relevance to assessment of arthritis in humans is weight bearing of paws, which can be tested in either static or dynamic weight bearing apparatuses. In static weight bearing, differential weight bearing capabilities of each hindlimb is compared, by training animals to stand on two limbs (Schött et al., 1994). This test is, however, only suitable for testing mono-arthritis and even so, mice often lean on the side of the test apparatus, which distributes their body weight. In order to overcome these shortcomings, dynamic weight bearing apparatus (Krug et al., 2019) was developed in which mice can move relatively freely in a box lined with piezoelectric material. In this box, weight bearing of both front and hind paws can be measured along with duration of immobility. Although effective in understanding some aspects of pain perception, there is the possibility that gait changes mostly reflect variation in biomechanics of the joint which are not reversible by analgesics (Malfait et al., 2013; Shepherd and Mohapatra, 2018). On the other hand, rodents might also hide gait changes to avoid predation in the wild (Malfait et al., 2013).

Activity based pain tests are another class of spontaneous pain measure that are relatively harder to implement, but might be more clinically relevant since chronic and acute pain patients show severe reduction in general everyday activities, and thus reduction in their general feeling of well-being (Sections 1.1, 1.4). In rodents, quality of life can be assessed by recording their feeding, grooming and social interactions over long periods of time (Gregory et al., 2013). However, a study that recorded these behaviors for 16 days in neuropathic (spared nerve injury and chronic constriction injury) and inflammatory (intra-plantar CFA) pain models found very little change in these daily life activities that persisted beyond two weeks (Urban et al., 2011). The authors concluded that their result highlights the failure of animal models to emulate the human disease. Alternatively, it is possible that the measured behaviors are essential for the survival of the animals and hence more optional activities that rodents perform in a natural environment are needed to assess well-being in these species. Indeed burrowing (Jirkof, 2014), marble burying and digging behaviors (Deacon, 2006a) have been put forth as natural rodent behaviors that can be utilized to assess pain that is linked to a reduced feeling of well-being. Chapter 4 and Chapter 6 in this thesis

further establish digging as a measurable spontaneous pain behavior in mice relevant to arthritic pain. The mouse grimace scale, where facial expression of rodents can be scored for pain level, is another activity based measure used to measure pain in rodents in a manner similar way to how pain is assessed in non-verbal humans and has been utilized in non-rodents such as horses and rabbits (Dalla Costa et al., 2014; Hampshire and Robertson, 2015; Langford et al., 2010).

Operant behavior pain assays take advantage of the learning abilities of rodents to determine their avoidance of a specific noxious stimuli. An important distinction between these tests and evoked pain assays is that these tests measure aversive behavior in response to a particular noxious stimulus. For example, the thermal escape test (a two chamber apparatus where animals can escape to the "safe" chamber) and the conditioned place preference/avoidance test (animals are pre-conditioned to a pain stimulus and the preference for that chamber is measured on test days without noxious stimulation) are examples of such operant pain behavioral assays (Johansen et al., 2001; Mauderli et al., 2000).

In addition to *in vivo* behavioral studies, a holistic study of pain mechanisms requires concomitant *in vitro* analysis. The following paragraphs will discuss various *in vitro* models and assessment techniques utilized to study general and joint-specific nociception.

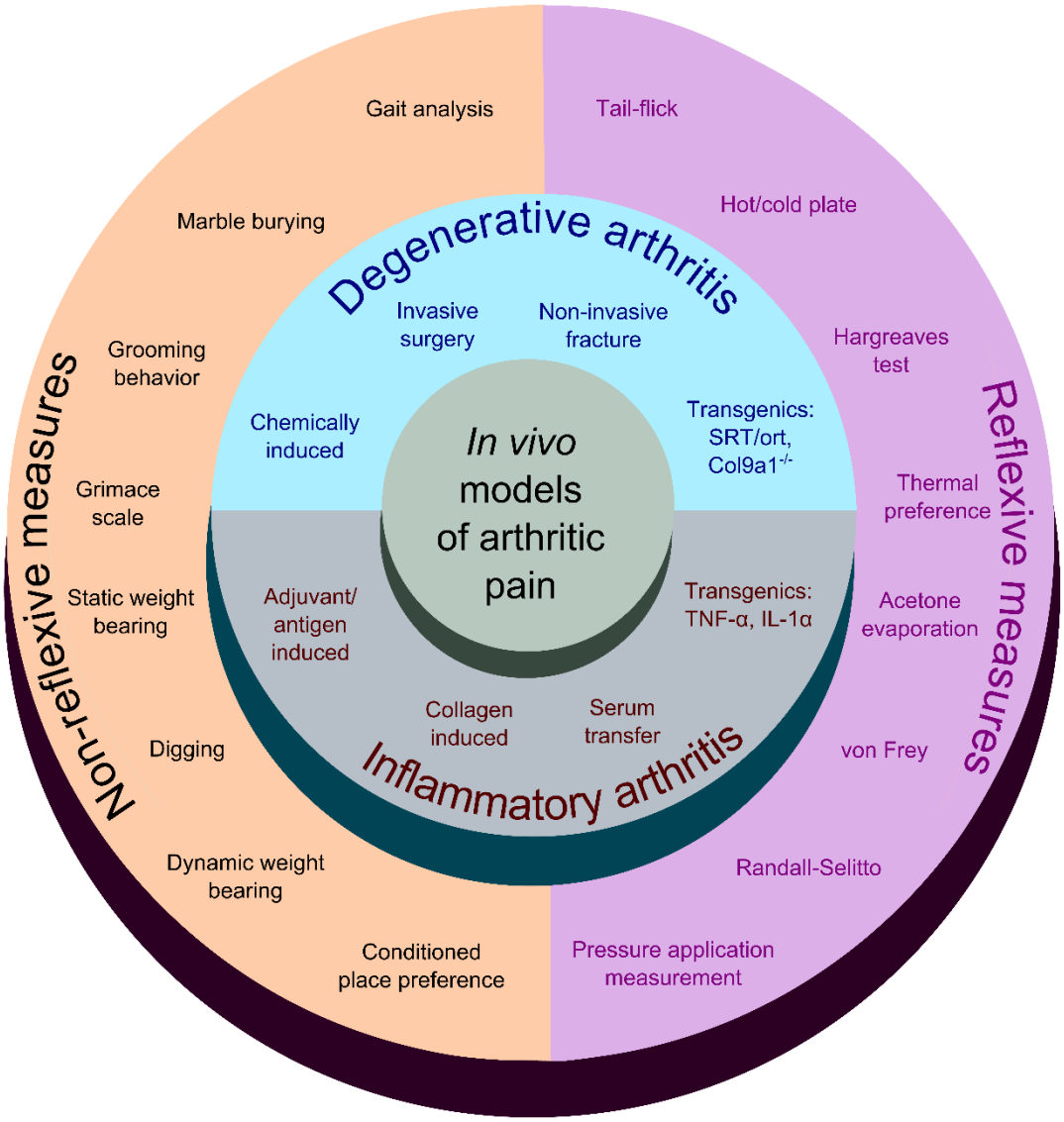

Figure 1-1: *In vivo* models and behavioral measures of arthritic pain.

Pictorial representation of the *in vivo* models and their behavioral assessments described in Sections 1.6, 1.7.

1.8. *In vitro* models to study arthritic pain

To see a World in a Grain of Sand

And a Heaven in a Wild Flower

Hold Infinity in the palm of your hand

And Eternity in an hour

- William Blake, Auguries of Innocence

The rationale for developing *in vitro* models of inflammatory pain is based on the philosophy of reductionism (Kaiser, 2011), so that a complex disease like arthritis can be studied at the cellular and molecular level, away from confounding systemic effects. Even so, *in vitro* models must still show some manifestation of the *in vivo* phenotype of interest so as to facilitate discovery of drug targets and understanding of disease mechanisms. Consequently, multiple *in vitro* models of pain and assays to test these models have been developed. The major strategy utilized in these models is to harvest a variety of tissues from animal models of arthritis described above or from human pathological samples. The following paragraphs discuss these *in vitro* models, emphasizing those tissues of importance in this thesis and also summarized in Figure 1-2.

1.8.1. DRG

Each DRG contains cell bodies of primary sensory neurons that innervate the periphery, apart from the head and neck that are innervated by sensory neurons arising from the trigeminal ganglia. Somatosensory information from the periphery is first processed by the primary sensory neuron, which then communicates the information to the CNS, and hence DRG neurons act as the gatekeeper between PNS and CNS (St. John Smith, 2018). DRG neurons are pseudo-unipolar with one branch extending to the peripheral organ and another branch synapsing with neurons in the dorsal horn of the spinal cord. In addition to these neurons being the first to respond to noxious stimuli in the periphery, they can easily be dissected from small animals, which makes DRG neurons an important *in vitro* model for studying the mechanisms of pain. Experimentally, DRG neurons have been studied *in vivo, ex vivo* and *in vitro,* with acutely dissociated neuronal cultures from control and diseased rodents *in vitro* being the most commonly used setup in recent years

(Melli and Höke, 2009); although mouse DRG neuron cell lines are also available, these are typically less physiologically relevant (Doran et al., 2015). The first action potential (AP) recordings from rodent DRG neurons were conducted electrophysiologically *in vivo* in terminally anesthetized rats using sharp electrodes. This technique enabled both morphological and functional characterization of mechanoreceptors based on their conduction velocity and site of innervation, as well as to record changes in these sensory neurons when an inflammatory agent was injected at the distal site (Harper and Lawson, 1985; Ritter and Mendell, 1992). However, this system is technically challenging since a laminectomy has to be performed on a live animal before recordings can be conducted; additionally, not all DRG neurons can be accessed while recording. By contrast, DRGs can be seeded as explants to performed experiments in a more controlled manner than *in vivo* (Gong et al., 2016). In explant cultures, the *in vivo* morphology of DRGs and associated non-neuronal Schwann cells and macrophages is retained, features that are lost when using dissociated cultures (Melli and Höke, 2009). Since DRG explants grow nerve processes, the interaction between DRG axons and other cells/inflammatory mediators can be studied in this system using Campenot chambers (Campenot, 1977). Although acutely dissociated DRG neuron cultures *in vitro* do not allow study of axons, they offer the unparalleled advantage of characterizing individual neuronal cell bodies, which have been shown to have largely similar properties to their terminals (Harper, 1991). Furthermore, acute DRG neuron cultures have emerged to be robust *in vitro* models of pain since they reflect the hypothesized neuronal basis of pain in experimental animal models, such as changes in nociceptive gene expression and excitability. For example, in a rat AIA-induced ankle inflammation model , whole cell patch clamp recordings from *in vitro* acutely cultured DRG neurons revealed increased excitability of joint neurons, which was consistent with the joint inflammation and mechanical hyperalgesia observed behaviorally in the affected limb (Qu and Caterina, 2016). Precise mechanisms of an inflammatory mediator's effect on sensory neurons can also be elucidated in these cultures (Segond von Banchet et al., 2005). In addition to the reasons described above, acutely cultured DRG neurons allow for whole-cell patch clamp recording of individual retrograde-labelled neurons from a peripheral organ, which is not possible in a more intact preparation.

Although there is a substantial body of literature on the expression profile of nociceptive genes and neuronal excitability of DRG neurons in arthritic pain, limited information is available on how pain pathologies affect joint-innervating DRG neurons. Given the high level of heterogeneity of

lumbar DRG neurons (Usoskin et al., 2015) and availability of retrograde tracers that can be used to identify neurons innervating specific targets (Puigdellívol-Sánchez et al., 1998), important experiments would be to conduct experiments on joint-innervating neurons in health and disease to identify joint specific disease mechanisms.

Given the utility of DRG neurons in studying pain, efforts have been made to characterize human DRG neurons derived from pain pathologies, although not yet in the field of arthritis (Haberberger et al., 2019). Comparative analysis of human and rodent DRG neurons might provide important insights to bridge the translational gap in pain research. Indeed, recent advances have shown important differences between human and rodent DRG neurons. Compared to rodents, human DRG are larger and contain more neurons, and although the identity of ion channels and other proteins in human DRG neurons is largely similar to that of rodents, differences have been found in the expression level and function. For example, in human DRG neurons, the voltage-gated sodium channel (Na_V) 1.8 blocker A-803467 was found to be much less potent in blocking Na^+ currents, compared to in rat DRG neurons, suggesting that Na_V blockers that show efficacy in rodents might not translate to the clinic for pain relief in humans (Zhang, et al., 2017).

Although acquiring and using human DRG neurons is becoming more common and inexpensive, this might not be a suitable system to study arthritic pain. This is because arthritis has a high incidence rate in the population and hence a lower likelihood of obtaining "control" human DRGs. An alternate strategy is to utilize reprogramed human induced pluripotent stem cell (iPSCs) from somatic cells to derive sensory neurons *in vitro* (Wainger et al., 2015). Recent advancements in iPSC technologies have achieved ~80% similarity of gene expression between iPSCS-derived neurons and human DRGs and thus there is the potential to significantly impact the field of pain research (Young et al., 2014). The power of this method and indeed the effectivity of DRG neurons as a pain model has been shown in 2019 in an elegant study in which blood samples from three members of a family with inherited erythromelalgia was used to derive iPSCs (Mis et al., 2019). Sensory neurons were then differentiated from these iPSCs and electrophysiological recordings were performed using multi-electrode array and whole cell patch clamp to show that both excitability and resting membrane potential (RMP) of the differentiated neurons correlated with pain scores. Furthermore, the authors found using whole genome sequencing that the voltage-gated K^+ channel (K_V) 7.2, was responsible for setting the RMP and hence pain. This technology has

potential in the field of arthritic pain since FLS derived iPSCs have been generated that can be differentiated into osteoblasts (Lee et al., 2014), but as of yet, no study has developed such iPSC-derived sensory neurons.

1.8.2. Non-neuronal tissues

The previous section emphasized the importance of DRG neuron hyperexcitability in chronic pain conditions like arthritis. Hyperexcitability is often mediated by neuronal exposure to a nocifensive environment, which is produced by non-neuronal cells, thus investigating non-neuronal cells is also important for the understanding of arthritic pain. The on-going pathology of both RA and OA are registered as tissue damage in the body which leads to triggering of innate immune responses and recruitment of a variety of cells through damage associated molecular patterns (Sokolove and Lepus, 2013). The non-neuronal cells of primary interest to this study are FLS, which are thought to be one of the key effectors of arthritis (Bartok and Firestein, 2010). Indeed one of the mechanisms of action of the disease modifying anti-rheumatic drug methotrexate is reducing FLS proliferation (Lories et al., 2003) and a reduction in the number of FLS means a reduction in the levels of inflammatory mediators that they secrete, which are key to driving arthritic pain (Sokolove and Lepus, 2013).

In vitro studies on FLS have mostly focused on gene expression and protein assessment of factors released into the culture medium to show that cytokine stimulated or human arthritis-derived FLS show upregulated pro-inflammatory genes and cytokine release (Hong et al., 2018; Jones et al., 2016; Kawashima et al., 2013). This result has been replicated in some rodent models of arthritis such as K/BxN (Hardy et al., 2013) and AIA (von Banchet et al., 2007), however before the findings reported in this thesis (Chapter 5) it was unknown whether FLS derived from acute CFA-induced inflammatory models also retain their inflammatory state. Some attempts have also been made to perform whole cell patch clamp on FLS that has identified the presence of various K^+ and Ca^{+2} channels (Clark et al., 2017), although these results need to be verified in human-derived FLS and the effect of inflammation on these channels investigated.

In addition to FLS, T cell, B cell, macrophages and chondrocytes have also been studied to understand their role in inflammatory pathways in arthritis. In brief, investigation of T cells has identified a range of distinct subtypes based on their cytokine secretion profile (Raphael et al.,

2015). B cells on the other hand have been shown to inhibit osteoblast formation in RA, mediated by cytokine CCL3 and TNF-α (Sun et al., 2018). In OA, the ability of chondrocytes to bear load has been elucidated *in vitro* by embedding them in an agarose matrix and then compressing in a bioreactor, which showed that increase in load leads to cell proliferation (Johnson et al., 2016). These non-neuronal cells have also been studied in co-culture with each other to reveal interdependent aspects of disease pathology. For example, it was found that IL-21 producing T cell mediated joint destruction occurs because these cells stimulate FLS to secrete matrix metalloproteases, which in turn contribute to joint destruction (Lebre et al., 2017).

A handful of studies have also attempted to study non-neuronal cells in combination with DRG neurons to understand the inflammation-pain axis (Massier et al., 2015; von Banchet et al., 2007). For example, in neuron-macrophage co-cultures, lipopolysaccharide (LPS)/IFN-γ stimulated macrophages were able to increase calcitonin gene related peptide (CGRP) release from DRG neurons in both direct (cells cultured together) and indirect (neurons only come into contact with macrophage-derived soluble mediators) co-cultures suggesting neuronal activation ((Massier et al., 2015) also see Chapter 5 for details on FLS/neuron co-cultures). The field of co-culture has recently received a boost with the development of microfluidics techniques (Vysokov et al., 2019), which can be useful to study arthritic pain *in vitro*. Notably, the above mentioned studies on 2D co-cultures might be less physiologically relevant compared to 3D co-culture models which mimic spatial arrangement of different cell types *in vitro*. Multiple methods for 3D neuronal co-cultures have been described (using polymeric materials as scaffold) to study nerve generation biology (reviewed in (Ayala-Caminero et al., 2017)). Adopting these strategies to study arthritic pain might provide physiologically relevant information about cell-to-cell communication. However, implementing 3D models was not suitable for this thesis because the complex interaction between cells in such setup do not allow for accurate whole cell eletrophysiological recordings.

Finally, an exciting study has recently shown that glial cells in the skin can themselves sense noxious stimuli (Abdo et al., 2019), thus opening up a new line of investigation for non-neuronal contributions to pain.

1.9. *In vitro* assays to understand pain mechanisms

Since the underlying motivation of *in vitro* analysis is to better understand cellular and molecular pathways, multiple assays have also been developed to enable thorough assessment of expression and function of cells associated in arthritic pain mechanism. These assays can be largely divided into three categories, assays that seek to understand: 1) gene expression changes, 2) protein expression changes, and 3) functional changes. It is important to make distinction amongst these categories to understand disease mechanisms since their interactions are often ambiguous.

1.9.1. Gene expression

Gene expression studies enable assessment of the contribution of genes to a particular pathology and are typically conducted by comparing differential expression patterns in diseased and control tissues. One of the first gene expression assays to be developed that is still popular today, was the quantitative polymerase chain reaction (qPCR). In this technique, a specific region of the DNA is amplified and the amount of starting material can be quantified by measuring the fluorescence emitted from the fluophore attached to the primers (San Segundo-Val and Sanz-Lozano, 2016). qPCR has helped identify key genes that are upregulated in the synovium in the MIA model of joint pain, hence providing useful insights into disease mechanisms in OA (Dawes et al., 2013). Although PCR based techniques are easy and fast to conduct, their primary drawback is that they are of low-throughput and do not allow for unbiased probing of differential gene expression. By contrast, microarray-based transcriptomics allow for low cost, high throughput studies for a limited set of genes using the principle of hybridization of cDNA with oligonucleotides (Starobova et al., 2018). Application of microarray analysis to RNA extracted from joints of spontaneous RA mouse models has identified that lymphocyte chemotaxis is an important disease mechanism (Fujikado et al., 2006). This result was further validated using Northern blot, a technique where denatured RNA is loaded in an agarose gel and separated by electrophoresis to assess gene expression (Eberwine and Sugimoto, 2001).

The field of gene expression studies has been revolutionized in recent years with the advent of whole transcriptome analysis either from tissues or single cells that allow for unbiased analysis of differential gene expression. The focus of transcriptomics in pain research has been DRG neurons and large databases have been generated to compare between different species and between painful and healthy conditions (Megat et al., 2019; North et al., 2019; Ray et al., 2018). Additionally, single cell transcriptomics has been instrumental in arthritis and pain research by identifying

clusters of sensory neurons (Hockley et al., 2019; Hu et al., 2016; Usoskin et al., 2015) and synovial fibroblasts (Croft et al., 2019; Ji et al., 2019).

1.9.2. Protein expression

Although gene expression analysis provides insights into disease mechanisms, gene expression does not always correlate to protein expression and functionality. This is largely because of post-translational modifications which have been found in multiple ion channels, including nociceptive channels, such as TRPV1 and Na_Vs (Hall et al., 2018; Laedermann et al., 2015). Therefore, several assays that measure protein expression have been developed. A widely used antibody based, semi-quantitative technique for measuring protein expression is immunohistochemistry which is regularly used in the pain field (Cregger et al., 2006). Two dimensional electrophoresis is another semi-quantitative method that involves electrophoresis, staining, fixing and densitometry. (Greenbaum et al., 2003). More quantitative methods have also been developed, the simplest of which is the enzyme linked immunosorbent assay where the antibody-conjugated enzyme activity is monitored to measure protein expression (Engvall, 1980).

Mass spectrometry (MS) is a more sophisticated way of quantifying proteins in a sample and has become popular in pain research in recent years (reviewed in (Wood et al., 2018b)). In this technique protein extracts from tissues are cleaved into short peptides and separated by chromatography before being analyzed in a mass spectrometer. Using MS on DRG protein extracts from pre-clinical murine models has provided useful insights in chronic pain (Rouwette et al., 2016); and proteomic analysis of synovial fluid taken from arthritis patients has identified key proteins involved in the disease mechanism (Balakrishnan et al., 2014).

The data rich era of proteomics and transcriptomics highlights the need for bioinformatics in pain research, so that data collected from different labs can be collated and common pathways for disease mechanisms identified (Jamieson et al., 2014; Platzer et al., 2019).

1.9.3. Functional assays: Electrophysiology and voltage imaging

Although transcriptomics and proteomics can help identify promising targets for pain research, functional tests are essential for assessing their actual contribution to the disease. The two commonly used functional assays in pain research are measuring potential changes across the cell membrane voltage and intracellular Ca^{2+} measurement.

Measurement of voltage changes across nerve fibers began with the seminal work of Hodgkin and Huxley where they recorded intra-cellular APs in squid giant axons using electrodes (Hodgkin and Huxley, 1939). Their work also led the way for the groundbreaking development of whole cell patch clamp techniques by Neher and Sakmann, where a cell could be held at any command voltage, to record currents and voltage either across a whole cell or single ion channels. Multiple conformations of the patch clamp technique allow for recording the activity of ion channels when stimuli is applied to the outside (whole cell recording and outside out patch) or inside (inside out patch) of the cell membrane (Sakmann and Neher, 1984), achieved by appropriate maneuvering of the electrode. Electrophysiological techniques have provided many fundamental insights about inflammatory pain such that an increase in the excitability of DRG neurons occurs after an inflammatory insult in cats (Xu et al., 2000), rats (von Banchet et al., 2000), guinea pig (Djouhri and Lawson, 1999) and mice (Belkouch et al., 2014). Correspondingly, *in vivo* recordings from rat joint afferents have shown increased excitability after PGE_2-induced inflammation (Grubb et al., 1991). Furthermore, single channel recordings have verified the sensitization of mechanosensitive ion channels in OA (He et al., 2017).

Although patch clamp is a very precise way of understanding ion channel function, it has low throughput, is labor intensive and requires substantial expertise of the experimenter. To increase the throughput of this assay multi-electrode arrays have been used that can simultaneously record from multiple neurons (Mis et al., 2019). In order to bypass the manual expertise, automated micropipette based platforms have been developed that capture and seal cells in suspension and can produce results at a higher throughput (reviewed in (Annecchino and Schultz, 2018)). Several ion channels important in pain pathologies have been studied using this technique including Na_Vs, hyperpolarization activated cyclic nucleotide gated (HCN), voltage-gated Ca^{2+} channels (Ca_Vs) and γ-amino butyric acid receptors (GABA) (Ji and Neugebauer, 2011; Payne et al., 2015; Swensen et al., 2012; Vasilyev et al., 2009). Therefore, although further validation and cost optimization is necessary, automated patch clamp platforms might speed up drug discovery in the future.

The advantage of patch clamp is that it provides direct access to neurons, however it is also a disadvantage because direct contact on the neuron, even in perforated patch clamp technique where the aim is to minimize disruption of neuronal function, can change membrane properties. Therefore, an ideal experiment would be to image changes in neuronal voltage in a high throughput

manner (reviewed in (Bando et al., 2019a)). This can be achieved by loading voltage sensitive dyes into neurons and measuring the membrane potential especially in large neurons *in vitro*. *In vivo*, single cell resolution is difficult to achieve with voltage sensitive dyes and hence genetically encoded voltage indicators (GEVIs) have been developed. Technically this can be achieved by three different ways: coupling the voltage sensor to a fluorescent protein (e.g., ArcLight (Bando et al., 2019b)), using rhodopsin to act as both a voltage sensor and reporter (e.g., VARNAM (Kannan et al., 2018)) and lastly by using chemicals that activate GEVIs (e.g., HAPI-Nile (Sundukova et al., 2019)). However, imaging voltage in neurons is not without challenges with the most important ones being thinness of the membrane which demands high sensitivity chromophores, difficulty in specifically targeting the plasma membrane and photo-damage of the plasma membrane (Bando et al., 2019a).

1.9.4. Functional assays: Ca^{2+} imaging

Although electrophysiology is considered to be the gold standard for recording neuronal activity, it is technically demanding, often requiring direct contact with cells (and thus invasive). Imaging intracellular Ca^{2+} can provide indirect measurement for AP firing in neurons, as well as activation of cells (both neuronal and non-neuronal) by algogens. In addition, Ca^{2+} signals in the nucleus can regulate gene transcription and an increase in intracellular Ca^{2+} can release neurotransmitter that has both short- and long-term effects (Berridge et al., 2003; Lyons and West, 2011). Therefore, quantifying the intracellular [Ca^{2+}] offers distinct advantages to understanding pain mechanisms. The two major breakthroughs that allowed imaging and quantification of Ca^{2+} signals in cells were development of fluorescent Ca^{2+} indicators, such as fura-2 and fluo-3, and the development of genetically encoded Ca^{2+} indicators (GECIs), both from the laboratory of Roger Tsien (Miyazawa et al., 1998; Tsien, 1980). The principle underlying fluorescent Ca^{2+} indicators is that these dyes undergo large increases in fluorescence (or spectral shifts) depending upon the amount Ca^{2+} bound and can be either non-ratiometric (excited by one wavelength of light) or ratiometric (can be excited by more than one wavelength of light, e.g. fura-2, or have a dual emissions peak, e.g. indo-1). For example, the commonly used non-ratiometric fluophore for imaging neurons, fluo-4, can be efficiently loaded into cells in salt form or acetoxymethyl ester form, has an absorbance wavelength of 488 nm and has low Ca^{2+} binding affinity thus making it suitable for imaging a broad range of cells using microscopes equipped with standard fluorescein filter sets (Gee et al.,

2000). In comparison, a ratiometric Ca^{2+} indicator like fura-2 allows for more precise quantitative measurements and comparison of Ca^{2+} signals because it is excited at 350 and/or 380 nm thus allowing for ratioing of the signals. Specifically, the dye is excited at 380 nm in the Ca^{2+} free form (resting fluorescent signal) and at 350 nm in the Ca^{2+} bound form both of which emits at 500 nm. Dividing these two emitted fluorescence gives an accurate measure of Ca^{2+} concentration and cancels out the effects of differential dye loading and photobleaching between experiments (Paredes et al., 2008).

A large number of cells can be imaged at the same time using this technique and it has provided useful insights into pain signaling mechanisms. For example, DRG neurons have been profiled based on their intracellular Ca^{2+} response to a multitude of algogens in order to functionally distinguish between the different neuronal subtypes (Teichert et al., 2012). Furthermore, Ca^{2+} imaging of FLS has revealed the link between an increase in intracellular Ca^{2+} via acid-sensing ion channel 3 (ASIC3) and cell death, a pathway that might be important in understanding arthritic pain (Gong et al., 2014).

To enable *in vivo* Ca^{2+} imaging, GECIs have also been developed, with the GCaMP family being the current GECI of choice for neuroscientists (Anderson et al., 2018). This technique has been used to visualize some fundamental somatosensory pathways, such as identification of unmyelinated sensory fibers expressing the GPCR, MRGPRB4, that detect massage-like stroking of hairy skin (Vrontou et al., 2013). It has also ignited debates about the long-held view regarding polymodality of nociceptors with one study validating polymodality with *in vivo* Ca^{2+} (Chisholm et al., 2018) and another study challenging it (Emery et al., 2016). A possible explanation for this disparity is that the pain community is currently unsure about the best ways to stimulate nociceptors for *in vivo* imaging, as well as to accurately apply statistical tools to large scale data. Importantly for the field of arthritis, *in vivo* imaging of GCaMP3 transgenic mice with DMM has shown that an increased number of DRG neurons respond to noxious mechanical stimuli following injury, thus directly relating pain behavior to neuronal function (Miller et al., 2017).

However, the major disadvantage of Ca^{2+} imaging is that it is an indirect measure of AP firing and the increase in intracellular Ca^{2+} can be mediated via ion channels such as, TRP channels, Ca_Vs, NMDA receptors, α-amino-3-hydroxy-5-methyl-4-isoxazolepropionic acid (AMPA) receptors, and/or through Ca^{2+} release from internal stores through inositol 1,4,5-trisphosphate receptors

(IP3Rs) and ryanodine receptors (reviewed in (Grienberger and Konnerth, 2012; Taylor et al., 1999)). Therefore, efforts have been made to simultaneously perform Ca^{2+} imaging and patch clamp on DRG neurons (Hayar et al., 2008).

1.9.5. *In vivo* to *in vitro* and back

The reductionist goal of *in vitro* experiments is to identify cellular and molecular pathways in a controlled environment that does not suffer from the systemic ambiguity associated with a whole organism. However, understanding the complexity of a disease that involves multiple cell types requires a combination of behavioral and cellular knowledge, hence recent efforts have focused on providing *in vitro* resolution in more intact systems. For example, a semi-intact preparation has been developed where the circuitry from the periphery (skin) through DRG to spinal cord is intact and recordings can be conducted at multiple sites of this set-up (Hachisuka et al., 2016). Recently it has also been possible to perform single DRG neuron Ca^{2+} imaging in awake, moving animals that has shown that neuronal activity is higher in these animals compared to *in vivo* imaging from anesthetized animals (Chen et al., 2019).

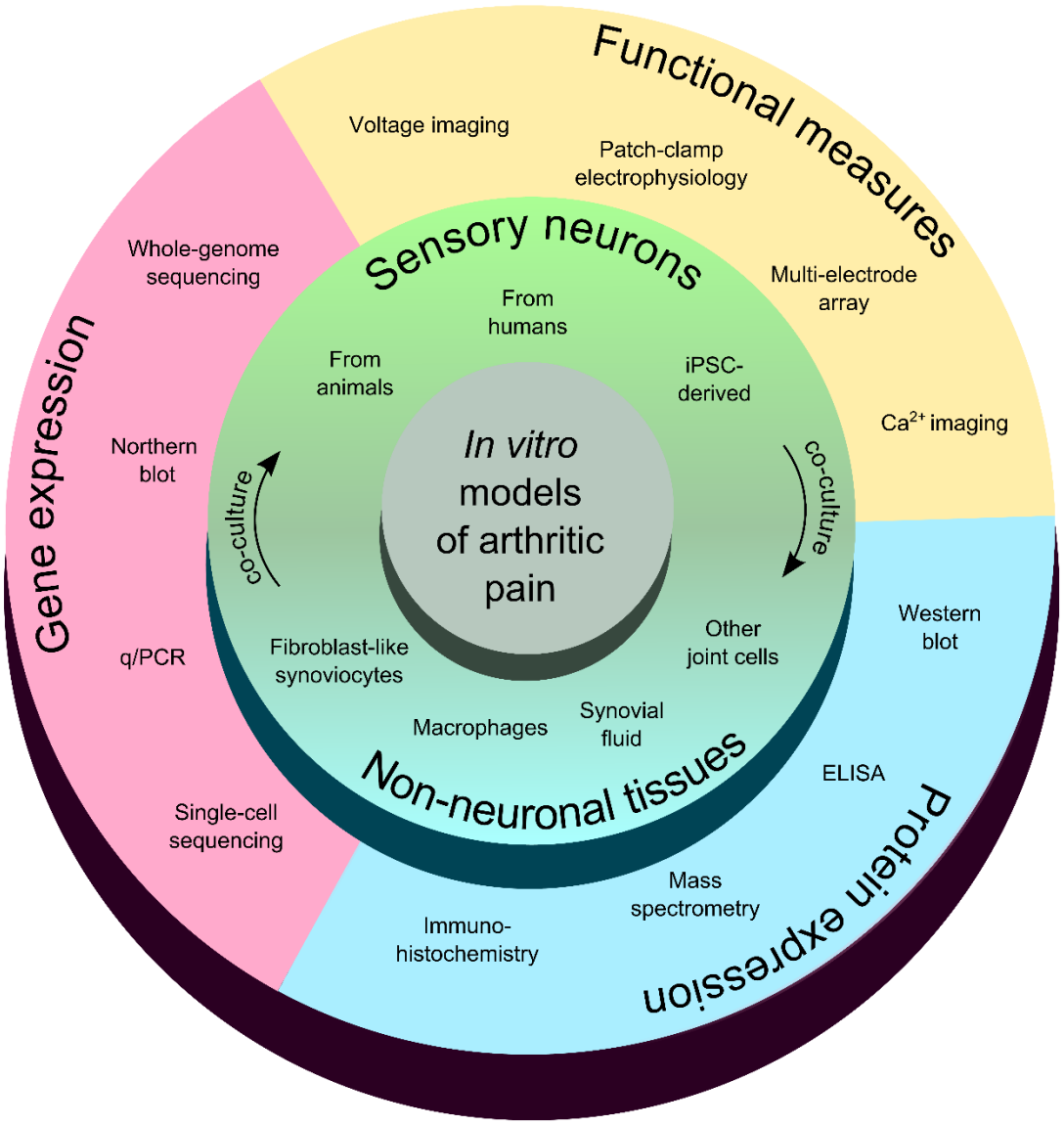

Figure 1-2: *In vitro* models to study and assess mechanisms of arthritic pain.
Pictorial representation of the *in vitro* models and their assessment techniques described in Sections 1.8, 1.9

1.10. Non-rodent animal models of arthritis

The above discussion on animal models of arthritic pain centered around rodent experimental models since that is the focus of this thesis (although I have been involved with functional characterization of DRG neurons in an ovine knee injury model, but is not within the purview of this thesis) , however significant anatomical and biomechanical differences between the joints of rodents and humans exists and hence understanding of arthritic pain can benefit from the study of larger animals (Gregory et al., 2012; Malfait et al., 2013). For example, in addition to large joint structures in dogs, the cartilage thickness of their joints are also similar to humans (Shepherd and Seedhom, 1999). Additionally, therapies (such as, arthroscopic procedures and surgery) and diagnostics (MRI and radiography) can be conducted in accordance with standard human clinical practices in large animals (Boileau et al., 2008; D'Anjou et al., 2008). The non-rodent animals currently used for arthritis research are rabbits, sheep, goats, dogs and horses. Most experimental models discussed in Section 1.6, including injection of CFA, collagenase, menisectomy and ACLT, can be conducted on these animals and their behavioral outcome measured using altered static or dynamic weight bearing (Malfait et al., 2013). Additionally, a number of large animals (e.g., horses and dogs), including dinosaurs in the pre-historic era (Anné et al., 2016), spontaneously develop/ed arthritis which helps in the investigation of natural progression of the disease (Gregory et al., 2013). Importantly, arthritic pain and disability in dogs and horses are a significant veterinary burden and thus it warrants studying of disease mechanisms in these species on their own merit. Unfortunately, however, very few studies have looked into cellular basis of pain in large animals possibly because DRG neurons are harder to access in these species. Recently, Ca^{2+} imaging has been conducted on acutely cultured primary canine DRG neurons which show that these can respond to algogens (Ganchingco et al., 2019). Furthermore, transcriptomics analysis of sheep, goat and pig DRG neurons have identified several important pain pathways (Deng et al., 2018; Sandercock et al., 2019). Nevertheless, further work is needed to understand peripheral mechanisms of sensitization in larger animals which can be correlated to histology and behavior for better translation into the clinic and/or veterinary practices.

1.11. Mechanisms of arthritic pain in the periphery

The disease progression of arthritis is marked by changes in non-neuronal/immune cells, which cause inflammation in the joint environment and aberrant communication between these non-neuronal cells and neurons at the site of the disease cause pain. Although differences exist between arthritic conditions, i.e., OA pain is considered to be more degenerative in nature (French et al., 2017), whereas RA is perceived as more inflammatory (Walsh and McWilliams, 2014), recent evidence has clearly shown that inflammation plays an important role in OA pain (Goldring and Otero, 2011). Therefore, the focus of this thesis is inflammatory pain with an emphasis on its effect on nerves, the current understanding of which the following paragraphs will summarize in the context of arthritis (Figure 1-3, further reviewed in (McDougall, 2006; Salaffi et al., 2018; Syx et al., 2018)).

1.11.1. The joint

Although inflammatory pain has been studied for a long time, inflammation and pain do not always occur together, such that arthritic patients and pre-clinical animal models can have pain without overt inflammation (Agalave et al., 2014; Nieto et al., 2015). These observations suggest that pain and inflammation can be disjointed events and that sub-clinical inflammation also contributes to pain. Therefore, understanding the interactions between non-neuronal cells, their secreted mediators and nerves is important to further the understanding of arthritic pain. Triggering of an RA joint (which can be caused by tissue injury or auto-antigens) leads to cross reactivity with other cells in the joint which activates the body's innate immune response. One of the major effects of the innate immune response is to trigger T cells to be polarized into Th1 and Th2 cells. The Th1 cells exert pro-inflammatory effects by secreting numerous cytokines and other inflammatory mediators including TNFs and IFNs, thereby activating monocytes, macrophages and synoviocytes (Smolen and Steiner, 2003). In response to these cytokines, non-neuronal cells show abnormal proliferation, release cytokines of their own which, combined with activated genes, are responsible for chronic inflammatory response (Bottini and Firestein, 2013). The cellular cascades in OA joints are less well defined and hence OA is often termed as failure of the joint as an organ, which includes degeneration of articular cartilage and ligaments, hypertrophy of the joint capsule, osteophyte formation, and variable degrees of synovial inflammation (Loeser et al., 2012) that

triggers innate immunity. These arthritis-related dysregulations in the joint environment directly affects functioning of joint innervating nerves, which is hypothesized to cause pain.

1.11.2. Peripheral sensitization

As is true for most joints, knee joints are richly innervated by sympathetic and sensory nerves, such that the former terminate near the blood vessels and regulate blood flow in the joints and the latter transduces polymodal (chemo, thermo, mechano) innocuous (non-painful warmth, cooling, light touch) and noxious information (Samuel, 1952). The diversity of stimuli detected by the peripheral nerve endings is also reflected in their functional, genetic and morphological diversity (Wood et al., 2018a). For example, large diameter myelinated nerve fibers transduce proprioceptive information which helps in location (static) and motion sensing (dynamic) of the joints (Erlanger and Gasser, 1937). Although some myelinated nerves (Aδ and Aβ fibers) are involved in pain sensing, a large proportion of nociceptive nerves are unmyelinated (C-fibers) free endings (Erlanger and Gasser, 1937). Since these nociceptors are tuned to detect painful conditions, they typically have a high threshold of activation. In cats and rats ~80% of knee innervating nerves are nociceptors (Hildebrand et al., 1991; Langford, 1983) and in the DMM mouse model of OA there is increased nociceptive innervation of the medial synovium and subchondral bones compared to healthy mice (Obeidat et al., 2019). Similarly in humans, a large proportion of articular branches of the tibial nerve that innervate the knee are unmyelinated C-fibers (Hines et al., 1996). These nociceptors can detect painful stimuli when exposed to the arthritic joint which, as a result of dysregulated intracellular pathways (e.g., the janus kinase/signal transducer and activator of transcription pathway (Fernandes et al., 2016)), contains increased pro-inflammatory and decreased anti-inflammatory mediators.

Joint-innervating nerves, as well as their cell bodies in the DRG, detect noxious agents and transmit pain stimuli using a variety of strategies (which can occur exclusive to each other or in combination). Inflammatory mediators can directly activate joint nociceptors to fire action potentials. This inflammatory milieu can also unmask previously silent nociceptors to transmit extra information and the threshold of nociceptor action potential firing can decrease in response to inflammation by a process called peripheral sensitization. Peripheral sensitization can occur due to changes in sensitivity/expression of ion channels either involved in transduction of mechanical (Lechner and Lewin, 2009) or chemical stimuli, or in action potential generation (Staunton et al.,

2013). The direct behavioral consequence of these pain generating mechanisms is allodynia and/or hyperalgesia. Although evidence of all the three nociceptive mechanisms has been shown with individual pro-inflammatory mediators (reviewed in (Miller et al., 2009)) at the outset of this work there were no reports showing the overall nociceptive effect of the inflammatory milieu from the joint.

The role of peripheral sensitization has been particularly highlighted in arthritic pain in recent years and a multitude of factors have been implicated as causative agents. The major evidence for peripheral sensitization in arthritic pain is as follows: 1) local administration of analgesics relieves arthritic pain (Creamer et al., 1996), 2) peripherally restricted anti-NGF antibody administration relieves OA pain (Schnitzer et al., 2019) and 3) total joint replacement can provide pain relief in OA (Neogi, 2013). The known chemical classes that contribute to sensitization through modulation of ion channels are cytokines (e.g. TNFs, ILs), eicosanoids (e.g. PGs derived from arachidonic acids) and endocannabinoids (e.g. a high concentration of anandamide). Additionally, inflammatory neuropeptides typically released from nerves can also cause neurogenic inflammation and peripheral sensitization. For example, when substance P is locally administered into the knee joint, afferents become sensitized to mechanical stimuli (Heppelmann and Pawlak, 1997). Spinal application of CGRP also increases the firing rate of spinal, wide dynamic range neurons that receive input from knee joint afferents (Neugebauer et al., 1996).

1.11.3. Voltage-gated ion channels

Given that AP firing is an important neuronal correlate of pain, voltage-gated ion channels are actively being investigated as potential targets for ameliorating arthritic pain. Na_Vs are a major pain target of this ion channel family that depolarize neurons and are essential for AP firing (Bennett et al., 2019). Inflammatory pain is known to upregulate Na_V channel expression and function in DRG neurons. For example, after injection of carrageenan into the rat hind paw, tetrodotoxin-resistant Na_V current density is increased along with elevation in $Na_V1.3$, $Na_V1.7$ and $Na_V1.8$ gene expression, only the latter being resistant to tetrodotoxin (Black et al., 2004). More relevant to joint pain, CFA-induced inflammation of the temporomandibular joint increases excitability of nociceptors via increased function of slowly inactivating TTX-resistant Na_Vs (Flake and Gold, 2005), $Na_V1.8$ blockers can reverse MIA-induced increased joint afferent firing (Schuelert and McDougall, 2012) and a non-specific Na_V channel blocker can reverse mechanical

hyperalgesia in CFA-induced ankle inflammatory rat model (Laird et al., 2001). However, one of the major barriers to translating Na_V blockers into the clinic is the potential for disrupting broader physiological function and hence the search is on for novel post-translational modulators (e.g. CRMP2 (Dustrude et al., 2016)) of Na_V binding proteins. K_Vs are another family of voltage-gated ion channels, which regulate repolarization of APs that has been investigated as targets for treating inflammatory pain. For example, the K_V7.x family is activated by bradykinin, which is an important inflammatory mediator in arthritis (Peiris et al., 2017). HCN is another voltage dependent ion channel family (selective for Na^+ and K^+) being actively investigated for inflammatory and other pain (Emery et al., 2011; Tsantoulas et al., 2017). Although not well-explored for pain relief in arthritis, the analgesic gabapentin binds to the $\alpha_2\delta_1$ sub-unit of Ca_Vs and reduces acute inflammation evoked articular afferent mechanosensitivity (Hanesch et al., 2000).

1.11.4. TRP channels

TRPs are another large family of Ca^{2+} permeable ion channels that has been explored as targets for controlling arthritic pain, TRPV1 (heat sensor) and TRPA1 (cold sensor) being the two most prominent members (Galindo et al., 2018). TRPV1 fibers are located in the human OA synovium and 12-hydroxy-eicosatetranoic acid (12-HETE, an endogenous ligand of TRPV1) has been found to be upregulated in the knee joint of MIA-induced OA rats, and a TRPV1 antagonist was able to reverse joint afferent sensitization and weight bearing in these rats (Kelly et al., 2015). However, evidence suggests that TRPV1 antagonists might only be effective in the acute phases of OA and not effective for MIA-induced chronic pain in rats (Haywood et al., 2018). This might be because inflammatory pain is more prominent in the first phase of OA. In support of this hypothesis, $TRPV1^{-/-}$ mice display reduced pain-related behavior in a CFA-induced inflammatory arthritic model. (Barton et al., 2006). By contrast, other studies found no change in guarding behavior and place preference after administration of TRPV1 antagonists in experimental arthritis models (Ängeby Möller et al., 2015; Okun et al., 2012). Additionally, some studies showed increased TRPV1 expression in DRG neurons after inflammation (Amaya et al., 2003; Ji et al., 2002), while others did not (Bär et al., 2004). It has also been suggested that TRPV1 positive neurons can be sub-divided based on whether they express surface carbohydrates that bind to isolectin B4. This plant lectin is thought to be the marker for a group of non-peptidergic, small diameter C-fiber sensory neurons (Molliver et al., 1995; Stucky and Lewin, 1999), although some studies have

shown overlap between isolectin B4 and neuropeptide expression (Wang et al., 1994). Regardless, it has been shown that increase in TRPV1 function following CFA-induced inflammation is more pronounced in the isolectin B4 positive population compared to the isolectin B4 negative population, thus suggesting targeting of isolectin B4 positive neurons can be beneficial for inflammatory pain (Stucky, 2007). Knee-innervating DRG neurons have not been categorized into isolectin B4 negative and positive populations in this thesis in order to have a larger sample size.

Literature on TRPA1's involvement in arthritic pain is similarly ambiguous. In CFA- and MIA-induced models of knee arthritis, TRPA1 antagonists were able to normalize weight bearing and mechanical hyperalgesia (Fernandes et al., 2016, 2011), while another study saw no effect on conditioned place preference after TRPA1 antagonist administration in a MIA-induced knee arthritis model (Okun et al., 2012). However, before the findings in this thesis, the functions of TRPV1 and TRPA1 have not been explored in knee-innervating DRG neurons after inflammation, which might provide more joint nerve specific information. These results also highlight that different behavioral measures test different modalities of pain and many prominent drug targets are unable to reverse all pain-like behaviors. Furthermore, TRP channels are also found in non-neuronal cells therefore suggesting that these are also important in neuron/non-neuronal communications. For example, evidence of functional TRPV1, TRPA1 and other members of the TRP channels like TRPV4 and TRPCs has been found in FLS (Itoh et al., 2009; Kochukov et al., 2009, 2006; Xu et al., 2008). Efforts are also underway to test the suitability of TRPM3 as an arthritic pain target (Ciurtin et al., 2010; Vriens et al., 2011).

1.11.5. Other ion channels and G-protein coupled receptors

In addition to the voltage-gated ion channels and the TRP family, purinergic ion channels and ASICs might also be involved in arthritic pain. Several members of the purinergic ion channel family P2X have been identified in the cartilage (Varani et al., 2008), and PGE_2 treatment enhances P2X3 mediated currents in DRG neurons (Wang et al., 2007). Expression of ASIC3 is upregulated in carrageenan-induced inflammation of mouse knee joint (Ikeuchi et al., 2009) and ASIC function is increased by inflammatory mediators in sensory neurons (Deval et al., 2008; Marra et al., 2016; Smith et al., 2007), suggesting they might be a good target for arthritic pain. However, other studies have reported that mice lacking ASICs were not protected from CFA-induced inflammatory pain (Staniland and McMahon, 2009).

G protein-coupled receptors (GPCRs) are also important in arthritic pain since inflammatory mediator driven modulation of ion channels (described above) often happens through these receptors (Neumann et al., 2014). For example, bradykinin has been shown to sensitize TRPV1 ion channels through phospholipase C and PKC suggesting that G_q protein coupled mechanisms modulate TRPV1 function (Cesare and McNaughton, 1996; Chuang et al., 2001). GPCRs can also affect sensory neurons through G protein independent mechanisms. For example, it was recently shown that proteases released during inflammatory conditions lead to endocytosis of protease activated receptor 2, which through endosomal signaling, cause hyperexcitability of nociceptors (Jimenez-Vargas et al., 2018). Furthermore, close proximity of $GABA_B$ receptors with TRPV1 ion channels inhibits inflammatory pain (Hanack et al., 2015) implicating the various roles of GPCRs in modulation of pain signaling.

1.12. Central sensitization in arthritic pain

From the periphery, APs from joint nociceptors are transmitted into the dorsal horn of the spinal cord where they synapse with the spinal neurons. Peripheral sensitization of nociceptors thus can lead to central sensitization (hyperexcitability in the CNS) in chronic pain conditions and this effect might be longer lasting from deep tissue nociceptors (Wall and Woolf, 1984). The following paragraph gives a very brief overview of central sensitization mechanisms because this phenomenon has not been explored in this thesis, but has recently been reviewed elsewhere (Harte et al., 2018; Wood et al., 2019b; Woolf, 2011).

The three major mechanisms of central sensitization are 1) glutamatergic neurotransmission mediated (summation of sub-threshold excitatory post-synaptic currents from acute pain leads to AP firing in higher order neurons), 2) loss of tonic inhibitory controls (due to disinhibition of GABA and glycinergic pathways) and 3) glia-mediated (Basbaum et al., 2009; Old et al., 2015). The glia-mediated mechanism relies on inflammatory mediators since elevated levels of IL-1β were detected in the cerebrospinal fluid of RA patients (Lampa et al., 2012). The cytokine fractalkine (shown to be upregulated in protein isolated from human OA synovium (Gowler et al., 2019)) might also play a role in central sensitization since its receptor CX3CR1 is upregulated in spinal microglia following neuropathic pain in rats (Lindia et al., 2005). Indeed, it has been shown that the microglial protease cathepsin S exerts pro-nociceptive effects in the CNS by cleaving neuronal fractalkine (Clark et al., 2009). Furthermore, in a CIA model of RA in rats, cathepsin S

inhibitor and fractalkine neutralizing antibody was able to normalize mechanical hypersensitivity (Clark et al., 2012). Advancement in neuroimaging has also revealed brain networks involved in processing of arthritic pain. Specifically OA patients show disruption of resting state default mode network and a decrease in grey matter volume in the thalamus, as well as involvement of periaqueductal gray region (PAG, part of the descending pain modulation system) (Gwilym et al., 2010, 2009). Importantly, imaging of the PAG, nucleus cuneiformis and rostral ventromedial medulla provided evidence that OA patients with neuropathic pain (as opposed to nerve injury pain) have poorer outcome post-arthroplasty, thus suggesting that neuroimaging can be an useful tool to stratify patients (Soni et al., 2019).

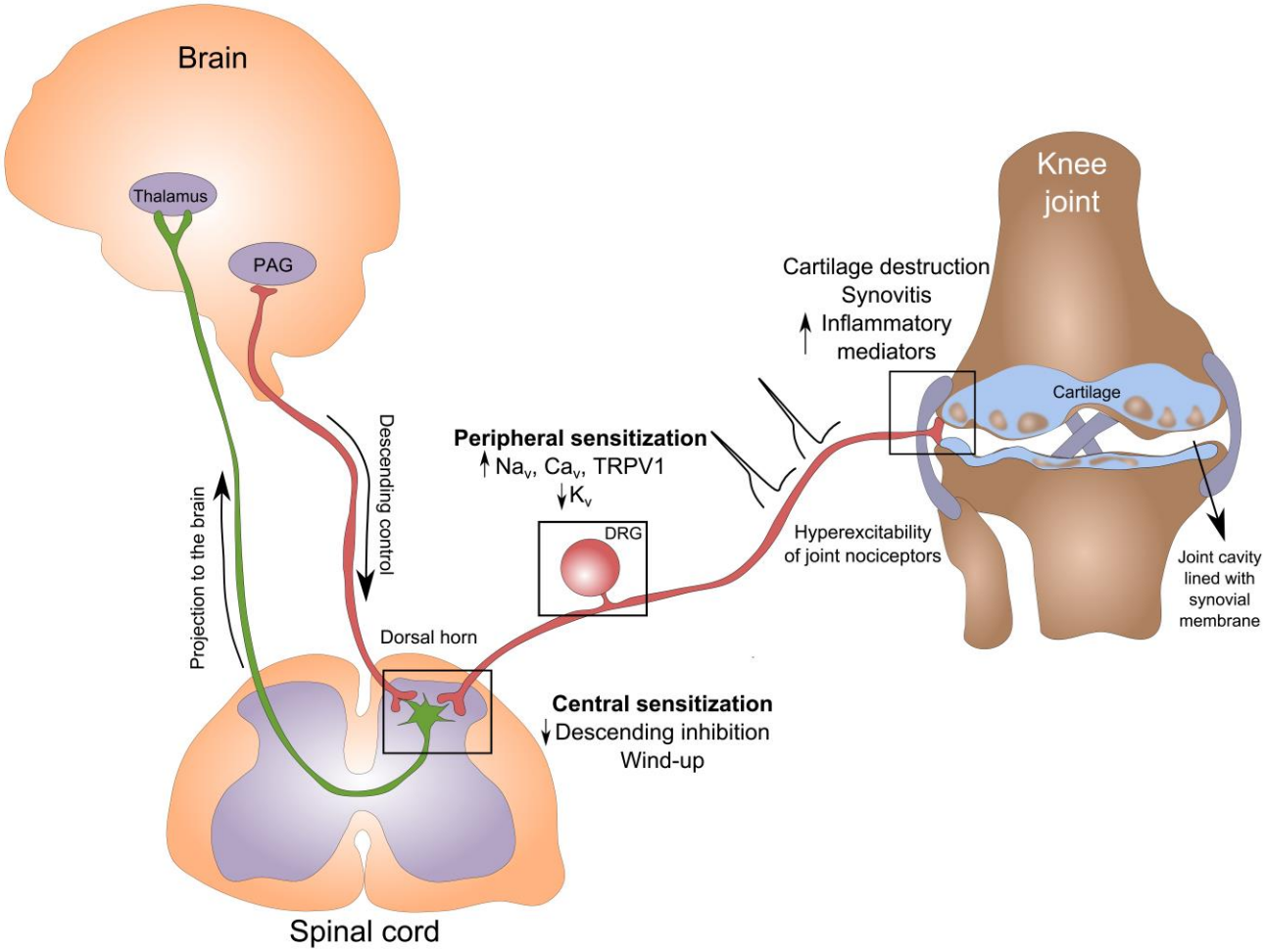

Figure 1-3: Mechanisms of arthritic pain.
Broad summary diagram highlighting the major mechanisms and structures involved in transmitting and processing of pain from the knee joint to the brain in humans.

1.13. Aims and objective of the thesis

Based on the discussions above, my overarching hypothesis was that knee-innervating DRG neurons are sensitized by multiple arthritis-related stimuli and therefore controlling the excitability of these neurons will be a novel therapeutic option. In order to test this hypothesis, I asked the following questions:

1) Can clinical samples from human arthritis patients be used in combination with mouse tissue to create a translatable, *in vitro* model of arthritic pain?
2) Does the acute CFA-induced knee inflammation model sensitize knee neurons and therefore cause changes in spontaneous pain behavior?
3) Does communication exist between knee neurons and non-neuronal FLS that is relevant to arthritic pain?
4) Can an AAV serotype be identified that can specifically deliver functional genes from the periphery (knee joint) to the DRG neurons to control neuronal excitability?

Chapter 2. Materials and Methods

2.1. Animals

All animal research conducted in the UK was regulated under the Animals (Scientific Procedures) Act 1986 Amendment Regulations 2012 following ethical review by the University of Cambridge Animal Welfare and Ethical Review Body.

2.1.1. Mice:

Adult (6-15 week old) male and female C57/Bl6J mice (Envigo) were used in this study. Most experiments only used female mice because being female increases the risk for arthritis (Berkley, 1997; Srikanth et al., 2005; van Vollenhoven, 2009). The mice were normally housed in standard (49 x 10 x 12 cm) cages with wire lids in groups of up to five in a temperature controlled room (21 °C). The mice were on a 12-hour light/dark cycle and had food and water available *ad libitum*. All procedures on mice carried out at the University of Cambridge were conducted under Project Licences 70/7705 and P7EBFC1B1 granted to Dr Ewan St. John Smith and by individuals who had a UK Home Office Personal License.

Pilot experiments with viral retrograde tracers Chapter 6 were conducted on mice housed in the Neurobiology and Epigenetics Unit of European Molecular Biology Laboratories (EMBL), Rome as per the guidelines of the Italian Legislature, Articles 9, 27. Jan 1992, no 116. All experiments were performed under the license of the Italian Ministry of Health.

2.2. Human synovial fluid samples

The human-aspect of the study was performed in collaboration with Dr Deepak Jadon (Department of Medicine, University of Cambridge) with ethical approval from London City and East Regional Ethics Committee (17/LO/0714), Cambridge University Hospitals NHSFT Research and Development Department approvals, informed written consent was obtained from participants, and in accordance with the Declaration of Helsinki.

Unselected consecutive patients with a rheumatologist-made diagnosis of osteoarthritis (OA), based upon symptoms, laboratory tests, and radiographic and/or magnetic resonance imaging, attending a University Hospital joint injection clinic for symptomatic knee OA management were

approached to participate in the study. With informed consent, an anatomically-guided knee joint synovial fluid (SF) aspiration was performed using a 16-gauge needle and syringe. Subsequently, methylprednisolone and lidocaine were injected into the knee joint as per clinical need. Patients were asked to score their knee pain using a 0-100 mm visual analogue scale (VAS). SF samples thus obtained were transported from the clinic on dry ice, passed through a 70 µm filter for acellularization and stored at -80 °C until use. Research nurse Jolanta Mil assisted with the procurement of samples. SF from post-mortem, healthy donors (Ctrl-SF) were purchased from BioIVT (n = 1) and Articular Engineering LLC (n = 2). Donor details are listed in Table 2-1. SF samples were applied to neurons after diluting in a 1:10 ratio to prevent osmotic stress (extracellular solution, 316 ± 5.9 mOsm, n = 7 vs. 1:10 Ctrl-SF, 324.3 ± 1.2 mOsm, n = 3 vs. 1:10 OA-SF, 317.4 ± 12.4 mOsm, n = 4, $F(2,11) = 0.2$, $p = 0.8$, ANOVA).

Table 2-1 Synovial fluid donor details.

ESR: Erythrocyte Sedimentation Rate, CRP: C-Reactive protein, RhF: Rheumatoid factor, AS: ankylosing spondylitis, OA: osteoarthritis, RA: rheumatoid arthritis, VAS: visual analog scale, NA: not applicable.

ID	Age (years), Sex	Diagnosis	Year of OA diagnosis	ESR (mm/hr)	CRP (mg/l)	RhF	Current medication	Pain Score (0-100 mm VAS)
1	77, Male	OA, AS	2016	2	4	Not available	Adalimumab, Aspirin, Atorvastatin, Cetirizine, Diltiazem, Glyceryl trinitrate, Isosorbide, Morphine sulphate, Lansoprazole, Nicorandil, Prednisolone, Tamsulosin	60
2	72, Female	OA, RA	2004	13	4	Positive	Adalimumab, Colecalciferol, Adcal-D3, Methotrexate, Paracetamol, Prednisolone	100
3	71, Female	OA	2008	12	6	Positive	Doxazosin, Glucosamine, Indapamide, Irbesartan, Levothyroxine, Omeprazole, Paracetamol, Vitamin B	80
4	68, Female	OA, RA	1980	52	67	Not available	Folic Acid, Methotrexate, Omeprazole, Paracetamol, Sulfasalazine	70
5	59, Female	No joint disease	NA	NA	NA	NA	NA	NA
6	70, Male	No joint disease	NA	NA	NA	NA	NA	NA
7	54, Male	No joint disease	NA	NA	NA	NA	NA	NA

2.3. Adeno-associated virus production

Adeno-associated virus (AAV) production was conducted in the lab of Dr Paul Heppenstall at EMBL in Monterotondo, Rome, with protocols adapted from those published (Challis et al., 2019). Ten 150 mm dishes of HEK293 cells were triple transfected with plasmids of AAV-PHP.S, helper (Agilent, 240071), and the appropriate cargo (Table 2-2) in a 1:4:1 ratio with PEI reagent (1:3, Sigma). Three days after transfection, cells and media were collected, after dislodging from the surface of the dish with 1% Triton X-100 (Sigma). This mixture was then centrifuged at 3700 g at 4 °C to remove debris and then concentrated by ultrafiltration using Vivaflow 200 (Sartorius). The purified AAV particles were collected after running the viral concentrate through an iodixanol column (Opti-Prep density gradient medium, Alere Technologies) by ultracentrifugation (Beckmann, L8-70M) at 44400xg for 2-hours at 18 °C) followed by filtration using a 100 kDa filter to further concentrate the sample and for buffer exchange. Viral titers (vg/ml) were measured by probing for WPRE regions (forward: GGCTGTTGGGCACTGACAAT, reverse: CCGAAGGGACGTAGCAGAAG) using SyBR green qPCR of linearized virus particles as described previously (Challis et al., 2019) using a StepOnePlus Real Time PCR system, following the manufacturer's guidelines on settings (Applied Biosystems). Virus used for the pilot experiments reported in Chapter 6 was produced by members of the Heppenstall lab and the Genetic and Viral facility at EMBL.

Table 2-2 List of plasmids used in AAV production.

Plasmids	Addgene #	Acknowledgement
pAAV-hSyn-hM4D(Gi)-mCherry	50475	Bryan Roth
pAAV-hSyn-hM3D(Gq)-mCherry	50474	Bryan Roth
pUCmini-iCAP-PHP.S	103006	Viviana Gradinaru

2.4. Knee injections

Unless otherwise stated, all intra-articular injections into the knee joint were performed through the patellar tendon under ketamine (100 mg/kg) and xylazine (10 mg/kg) anesthesia, administered intra-peritoneally (i.p.).

2.4.1. Retrograde tracer – fast blue:

To label knee-innervating DRG neurons, 1.5 µl of the retrograde tracer, Fast Blue (FB, 2 % in 0.9 % saline; Polysciences) was injected into the knee.

2.4.2. Retrograde tracer – AAV:

Initial experiments with viral retrograde tracers were conducted in EMBL, Rome. Viruses (Table 2-3) were injected intra-articularly (2-10 µl, depending on titer values) either on their own bilaterally or co-injected with FB unilaterally.

2.4.3. Complete Freund's adjuvant:

To induce joint inflammation, 7.5 µl CFA (10 mg/ml, Chondrex) was injected unilaterally into the knee of mice; when prior retrograde tracer injection had occurred, CFA injection was made according to the experimental designs of the studies conducted. To quantify inflammation, knee width was measured with digital Vernier's calipers before and 24-hours after CFA injection.

Table 2-3 List of viruses injected.

Studies where the respective viral serotypes were utilized are noted in reference column.

Virus	Reference	Co-injections
AAV1/2-Cre-EGFP	(Hauck et al., 2003)	No
AAV2-Cre-EGFP	(Lee et al., 2016)	No
AAV2-retro-Cre-EGFP	(Tervo et al., 2016)	No
AAV9- CAG-DIO-EYFP	(Jackson et al., 2016)	No
AAV-PHP.S-CAG-DIO-EYFP	(Challis et al., 2019)	No
AAV-PHP.S-CAG-dTomato	Addgene virus #59462 (Edward Boyden Lab)	With FB
AAV-PHP.S-hSyn-hM4d(G_i)-mCherry	(Challis et al., 2019)	No
AAV-PHP.S-hSyn-hM3d(G_q)-mCherry	(Challis et al., 2019)	No

2.5. Digging behavior testing

The testing apparatus was a standard mouse cage filled with Aspen midi 8/20 wood chip bedding (LBS Biotechnology) that was tamped down to ~ 4cm. The mice were tested individually in the testing apparatus for 3 minutes without food and water (to limit distractions). The experiments were conducted by one male and one female experimenter between 12:00 and 15:00 on weekdays. Before any digging behavior test was conducted, mice were habituated in the procedure room in their home cages for 30 min. All test digs were video recorded; the digging duration was measured by the experimenters (Luke Pattison, Sampurna Chakrabarti), who were blinded (by Ewan St. John Smith) to the conditions, independently from the video recordings. An average of these measurements was reported since the individual experimenter scores had a Pearson correlation R^2 = 0.93. Digging duration was defined as the time spent actively displacing bedding materials with paws. The number of visible burrows in test cages was also counted.

2.5.1. Experimental design for testing the impact of CFA-induced inflammation:

For training on the digging paradigm, mice were allowed to dig twice with a 30 min interval in between, 2 days before FB or CFA injections. Then they were tested once 24-hours pre- and post-FB and CFA injections.

2.5.2. Experimental design for testing the effect of A-425619, a TRPV1 antagonist:

Mice were trained as described above and then tested the day before intra-articular CFA/saline (Pre-CFA/ Pre-Saline) injections twice with a 30 min interval in between. Both CFA and saline (Control) groups were tested again 24-hours after the injections; after which all the mice were injected intra-peritoneally with the TRPV1 antagonist, A-425619 (100 µmol/kg, Tocris) made up in 10% DMSO and 34% 2-hydroxylpropyl β-cyclodextrin (Sigma) in dH_2O (Hillery et al., 2011). Digging behavior was measured again 30 min after the antagonist administration since the drug shows maximal anti-nociceptive effect after 30 min (Hillery et al., 2011). Previously, A-425619 showed transient hyperthermia in rats (Mills et al., 2008), but this was not measured in the present study. At the time of measuring the digging duration from videos, the experimenters were blinded to the testing conditions.

2.5.3. Experimental design for testing chemogenetic modulation

The following groups were tested in this study; dynamic weight bearing and rotarod behavioral measures are described in subsequent sections:

1. **Compound 21 (C21) controls:** Mice with no knee injections (i.e. no virus/DREADD) were tested on digging, rotarod and dynamic weight bearing 20 min before and after C21 (2 mg/kg diluted in sterile saline from a stock of 100 mM in ethanol, i.p., Tocris) injection.

2. **Activation of G_q-DREADD:** Three-four weeks after intra-articular administration of virus, mice were tested on digging, rotarod and dynamic weight bearing 20 min before and after vehicle (1:100 ethanol in sterile saline) or C21 injections.

3. **Activation of G_i-DREADD:** Three-four weeks after intra-articular administration of virus, mice were tested on digging, rotarod and dynamic weight bearing (pre-CFA). CFA was injected into the knee joints the next day to induce inflammation. 24-hours after that, the above-mentioned behavioral tests were conducted 20 min before (post-CFA) and after (post-C21) vehicle or C21 injections.

2.6. Dynamic Weight Bearing

Deficit in weight bearing capacity is a characteristic measure of spontaneous inflammatory pain behavior and this was measured using a dynamic weight bearing device (Bioseb) in freely moving mice for 3 min. Animals were not trained in this device and coding was done by one experimenter, blinded to the conditions. In at least 1 min 30 s of the 3 min recording, fore- and hind paw prints were identified using the two highest confidence levels (based on correlation between manual software algorithm tracking) of the in-built software, at least 30 s of which was manually verified. Appropriate parameters of dynamic weight bearing were then extracted from the in-built software based upon the underlying hypothesis of the studies conducted.

2.7. Rotarod

Locomotor function and coordination of mice were tested using a rotarod apparatus (Ugo Basile 7650). Mice were tested on a constant speed rotarod at 7 rpm for 1 min, then in an accelerating program (7-40 rpm in 5 min) for 6 min. The same protocol was used to train mice one day before testing. Mice were removed from the rotarod after two passive rotations or when they fell from the rotarod. Mice were video recorded on test days and one experimenter blinded to the conditions coded these videos for latency(s) to passive rotation or fall.

2.8. Isolation and culture of murine primary cells

2.8.1. DRG:

Mice were killed by cervical dislocation and their spinal column was dissected to isolate lumbar (L2-L5) DRG, since these DRG innervate knee joints (da Silva Serra et al., 2016). DRG were collected in ice-cold L-15 Medium (1X) + GlutaMAX-1 (Life technologies) supplemented with 24 mM NaHCO3 which was followed by incubation in 3 ml type 1A collagenase for 15 min and 3 ml trypsin solution for 30 min at 37 °C. After removal of the enzymes using a pipette, DRG were transferred to culture media containing L-15 Medium (1X) + GlutaMAX-l, 10 % (v/v) fetal bovine serum, 24 mM $NaHCO_3$, 38 mM glucose, 2 % penicillin/streptomycin, mechanically dissociated with a 1 ml Gilson pipette and briefly centrifuged. Supernatant containing dissociated DRG neurons were collected in a fresh tube. This cycle of mechanical trituration was repeated five times, after which the cells were plated into poly-D-lysine and laminin coated glass bottomed dishes (MatTek) and kept at 37°C, 5 % CO_2 for 4, 24 or 48-hours depending upon experimental need for electrophysiological recording and Ca^{2+}-imaging. For experiments with mice following unilateral CFA knee injection, the ipsilateral and contralateral DRG were kept separate throughout the dissociation.

2.8.2. FLS:

Knee joints of mice were exposed by removing the skin, then the quadriceps muscles were resected in the middle and pulled distally to expose the patellae. Patellae were then collected in PBS by cutting through the surrounding ligaments, as described before (Futami et al., 2012), and then transferred into one well of a 24-well plate with FLS culture media containing Dulbecco's

Modified Eagle Medium F-12 Nutrient Mixture (Ham) (Life Technologies), 25% fetal bovine serum (Sigma), 2 mM glutamine (Sigma) and 100 mg/ml penicillin/streptomycin (Life Technologies). Cells took approximately 10 days to grow to 70% confluency with changing of the media every 3-4 days. For P1, FLS were trypsinized with 1% trypsin (Sigma), re-suspended in culture media and transferred into two wells of a 6-well plate. FLS from two animals were combined at P2. For subsequent passages, FLS were transferred into 60 mm dishes. Contralateral (Ctrl) and CFA-injected knees/cells were kept separate at all stages. The cells were maintained in a humidified 37 °C, 5% CO_2 incubator. For some experiments FLS were cultured until P5 from mice without any knee injections (Control). A random selection of these dishes, from three separate mice, were incubated for 48-hours in culture media with tumor necrosis factor-α (TNF-α, 10 ng/ml from a stock solution of 100 μg/ml made up in 0.2 % bovine serum albumin and sterile PBS, R&D systems) to stimulate release of inflammatory mediators as described previously (Hardy et al., 2013). For electrophysiological recordings and Ca^{2+}-imaging studies, FLS were plated on poly-D-lysine and laminin coated glass bottomed dishes and cultured for 24-hours with FLS culture media (with or without TNF-α) and the next 24-hours with DRG culture media to match co-culture studies (see below). Luke Pattison assisted with the upkeep of FLS and some Ca^{2+}-imaging experiments.

2.8.3. DRG/FLS co-culture

For co-culture studies, FLS were plated onto poly-D-lysine and laminin coated glass bottomed dishes and cultured for 24-hours with FLS culture media (with or without TNF-α). The next day medium was removed from FLS plates, then DRG neurons were isolated as described above and plated on top of the FLS. Co-culture plates were then kept in DRG culture medium for up to 24-hours for electrophysiogical recording.

2.9. Culture of cell line: Raw 264.7

Raw 264.7 cells (EACC) were cultured in media containing Dulbecco's Modified Eagle Medium F-12 Nutrient Mixture (Ham) (Life Technologies), 10% fetal bovine serum (Sigma) and 2 mM glutamine (Sigma).

2.10. Staining

2.10.1. Immunohistochemistry of whole DRG sections

Mice used for immunohistochemistry were terminally anaesthetized by sodium pentobarbital (200 mg/kg, i.p.), then transcardially perfused with PBS, followed by 4% (w/v) paraformaldehyde (PFA, in PBS, pH 7.4). L2-L5 DRGs were collected from the CFA-injected and non-injected side of FB labelled mice and fixed in 4% PFA for an hour, followed by cryo-protection with 30% (w/v) sucrose overnight at 4 °C.

For freezing, DRG were embedded in Shandon M-1 Embedding Matrix (Thermo Fisher Scientific), snap frozen by immersing in a 2-methylbutane (Honeywell International) / dry ice slurry. The frozen sections were stored at -80 °C, before being sectioned using a Leica cryostat (CM3000; Nussloch, Germany) and mounted on Superfrost Plus slides (Thermo Fisher Scientific), which were kept at -20 °C until staining. For staining, slides were washed thoroughly with PBS-tween twice and blocked with 0.2 % (v/v) Triton X-100, 5 % (v/v) donkey serum, 1 % (v/v) bovine serum albumin in PBS (antibody diluent) for 1 hour at room temperature. These were then incubated overnight at 4 °C with primary antibodies. The next day, primary antibodies were washed off three times with PBS-tween and incubated for 2-hours at room temperature (20-22 °C) in corresponding secondary antibodies diluted to 1:1000 in PBS. See Table 2-4 for a list of antibodies used. Slides were thoroughly washed again in PBS-tween, mounted and imaged with an Olympus BX51 microscope (Tokyo, Japan) and QImaging camera (Surrey, Canada). Exposure levels and digital contrast enhancements were uniformly applied to all slides and negative controls of primary antibodies did not show staining with either secondary antibodies.

Contributions: Experiments reported in Chapter 4 were conducted by Kaajal Singhal, as a Part II research project on the Medical and Veterinary Sciences Tripos (University of Cambridge) under my supervision. Some immunohistochemistry experiments reported in Chapter 6 were performed by Rebecca Rickman.

2.10.2. Immunostaining of FLS

FLS were plated overnight in wells of a 24-well plate, fixed with Zamboni's fixative (Stefanini et al., 1967) for 10 min, permeabilized with 0.05 % TritonX-100 and blocked with antibody diluent (0.2% (v/v) Triton X-100, 5% (v/v) donkey serum and 1% (v/v) bovine serum albumin in PBS)

for 30 min. The cells were then incubated overnight at 4 °C in 1:100 (in antibody diluent) anti-cadherin-11 antibody (CDH-11, rabbit polyclonal, Thermo Fisher, 71-7600). Cells were washed three times with PBS-tween and incubated in the conjugated secondary antibody, anti-rabbit Alexa-568 (1:1000 in PBS, Thermo Fisher, A10042) for 1-hour at room temperature (21 °C). The secondary antibody was washed off three times with PBS-tween and the cells were incubated in the nuclear dye DAPI (1:1000 in PBS, Sigma, D9452) for 10 min. Cells were further washed with PBS-tween once and imaged in PBS using an EVOS FLoid Cell Imaging Station (Thermo Fisher) at 598 nm (for CDH-11) and 350 nm (for DAPI) wavelength of light. Cells without primary antibody did not show fluorescence.

2.10.3. DRG/FLS co-culture live stain

To visualize neuron/FLS co-culture, live cell imaging was performed. FLS were plated on MatTek dishes with 1:1000 (diluted in FLS culture medium) CellTracker Deep Red Dye (Thermo Fisher, C34565) and incubated for 24-hours in a humidified 37 °C, 5% CO_2 incubator. Dissociated DRG neurons (see above) were incubated in CellTracker Green Dye (1: 1000 diluted in DRG culture media, Thermo Fisher, C7025) for 15 min at room temperature (21 °C), centrifuged (16000 g, 3 min, 5415R, Eppendorf) and re-suspended in fresh medium. The FLS dishes were then washed twice with PBS and the neuronal suspension was plated on top of the FLS monolayer and incubated overnight in the incubator. The co-culture dishes were washed with PBS and imaged the following day using an Olympus BX51 microscope and QImaging camera at 650 nm (for deep red dye) and 488 nm (for green dye) wavelength of light.

2.10.4. Data analysis

Qualitative analysis was carried out for FLS staining, whereas whole DRG sections were analyzed using a semi-quantitative method (https://github.com/amapruns/Immunohistochemistry_Analysis). Briefly, one to three stained sections were chosen for analysis from both experimental and control conditions from each DRG level investigated of each mouse. Each neuron of interest was manually marked as region of interest in the ImageJ software and its mean gray value (intensity) was measured. Another normal distribution was constructed for cells with the minimum mean gray value in each image analyzed.

A neuron was scored positive for a stain if it had an intensity value greater than average normalized minimum grey value across all sections + 2 times the standard deviation.

Table 2-4 List of antibodies used for whole DRG immunohistochemistry.

Trpv1 = transient receptor potential vanilloid 1, TrkA = tropomyosin receptor kinase A

Antibody	Dilution	Description and Reference
Anti-TRPV1, rabbit polyclonal	1:1000	Primary antibody, Abcam ab31895
Anti-TrkA, goat polyclonal	1:1000	Primary antibody, R & D Systems, AF1056
Anti-TRPV1, guinea pig polyclonal	1:500	Primary antibody, Alomone AGP-118
Alexa-488, anti-guinea pig	1:500	Secondary antibody, Jackson ImmunoResearch 706-545-148
Alexa 488, anti-rabbit	1:1000	Secondary antibody, Invitrogen A21206
Alexa 568, anti-goat	1:1000	Secondary antibody, Invitrogen, A11057

2.11. RNA extraction and RT-q/PCR

For all conditions, RNA was extracted from two 60 mm dishes (Thermo Fisher) of FLS (various passages) and from one T-25 flask (Greiner Bio-one) of Raw 264.7 cells at P3 using the RNeasy Mini Kit (Qiagen). 500 ng of the extracted RNA was used to synthesize cDNA using a High Capacity cDNA RT kit (Applied Biosystems) following the manufacturer's guidelines, using a T100 Thermal Cycler (Bio-Rad). The resultant cDNA was diluted to a 1:5 ratio with nuclease free water and quantitative PCR (qPCR) was performed using a StepOnePlus Real Time PCR system, following the manufacturer's guidelines on settings (Applied Biosystems) using TaqMan probes (Thermo Fisher) (Table 2-5). The fluorescence intensity of samples was captured during the last minute of each cycle. All reactions were run in triplicate with appropriate negative controls with water containing no cDNA. FLS gene expression was also assessed by reverse-transcriptase (RT)-PCR. DreamTaq Polymerase (ThermoFisher) was used to amplify a section within the open reading frames of various genes from 5 ng template cDNA. The sequences of designed oligonucleotides (Sigma) are listed in (Table 2-5). Negative controls (using water/RNA as the template) were performed for each biological sample with a randomly selected primer pairing. PCR products were resolved on 2% agarose containing 1X GelRed Nucleic Acid Stain (Biotum) and imaged with a GeneFlash Gel Documentation System (Syngene). A randomly selected subset of reactions was repeated with 2.5 ng template cDNA to ensure reproducibility.

Table 2-5 Genes of interest analyzed in this study.

Cd = cluster of differentiation, Cdh = cadherin, Il = interleukin, Cox = cyclooxygenase, Gpr = G-protein receptor, Asic = acid sensing ion channel, Trpv1 = transient receptor potential vanilloid 1.

Gene	TaqMan Assay ID/sequence	Role
Taqman Probes		
18S	Mm03928990_g1	Housekeeping
Cd-68	Mm03047343_m1	Macrophage marker
Cdh-11	Mm00515466_m1	Intimal synovial fibroblast marker
Cd-248	Mm00547485_s1	Synovial fibroblast marker
Cd-31	Mm01242576_m1	Endothelial marker
Il-6	Mm00446190_m1	Inflammation
Il-1r1	Mm00434237_m1	Inflammation
Cox-1	Mm04225243_g1	Constitutively active gene
Cox-2	Mm03294838_g1	Inflammation
RT-PCR primers		
18S	Fwd: CCGGTACAGTGAAACTGCGA Rev: ATCTAGAGTCACCAAGCCGC Product size: 230 bp	Housekeeping
Gpr4	Fwd: ATTCAGCACCGCTCTTCCAT Rev: CAGGGCCAGACGTTTGATCT Product size: 236 bp	Proton-sensing GPCR
Gpr65	Fwd: CAACATCGGATCTTTATGCG Rev: ATGTAGGTGAAGAAAACGCT Product size: 195 bp	Proton-sensing GPCR
Gpr68	Fwd: TTCTCCCTCCTCCTCACCAG Rev: GGCTGAGTGGAGCTTGGTTA Product size: 234 bp	Proton-sensing GPCR
Gpr132	Fwd: CCACTACCTGCGTTTCACCT Rev: CCAGGAAGATGGTGACGACC	Proton-sensing GPCR

	Product size: 161 bp	
Asic1	Fwd: ACACATTCAACTCGGGCCAA Rev: TGCTCCTGGCAAGACACAAA Product size: 250 bp	Acid-sensing ion channel
Asic2	Fwd: TGCTGCCTTACTTGGTGACA Rev: CGGAGTGGTTTGGCATTGTG Product size: 194 bp	Acid-sensing ion channel
Asic3	Fwd: AGAAGGAGCTCTCAAAGGCG Rev: AGGTAACAGGTACGGTGGGA Product size: 158 bp	Acid-sensing ion channel
Asic4	Fwd: AGCGGCTAACTTATCTGCCC Rev: CAAGGGAGTCCAGTGTGTGG Product size: 234 bp	Acid-sensing ion channel
Trpv1	Fwd: GACACCATTGCTCTGCTCCT Rev: GCCTGGACATCTGCTCCATT Product size: 176 bp	Heat and proton transducing ion channel
Il6	Fwd: AGCCAGAGTCCTTCAGAGAGA Rev: TGGTCTTGGTCCTTAGCCAC Product size: 226 bp	Inflammation

2.11.1. Data analysis

For qPCR reactions, data were obtained as Ct values (the cycle number at which fluorescent signals emitted by the TaqMan probe crossed a software determined threshold value). Only Ct values below 35 were analyzed to determine ΔCt values by subtracting the Ct of *18S* ribosomal RNA from the Ct of target gene (McCall et al., 2014). ΔCt values of target genes were subtracted from average ΔCt values of their controls to calculate ΔΔCt, followed by 2^(- ΔΔCt) to calculate fold change (Livak and Schmittgen, 2001). For semi-quantitative PCR, densitometry analyses were performed using ImageJ Software (NIH) where relative expression was determined by dividing the band intensity of each gene by that of the housekeeping gene, *18S* ribosomal RNA, for each biological replicate.

2.12. Cytokine antibody array

Before RNA extraction, 2 ml of culture media from P5 Contra, Ipsi, control and TNF-FLS (48-hour) were collected and stored at -80 °C until use. Culture medium was pooled from three cultures for each of the four conditions and assayed (undiluted) for the presence of 40 inflammatory mediators using Mouse Inflammatory Antibody Array Membranes (ab133999, Abcam) according to the manufacturer's instructions. Chemiluminescence was imaged using a BioSpectrum 810 imaging system (UVP) with 3 min exposure. Location of the 40 cytokines detected by the array membranes are shown in Table 2-6.

Table 2-6 Location of cytokines detected by the mouse inflammatory antibody array membrane.

BLC = B lymphocyte chemoattractant, GCSF = granulocyte colony stimulating factor, GM-CSF = granulocyte-macrophage colony stimulating factor, IFN = interferon, IL= interleukin, I-TAC = interferon inducible T-cell alpha chemoattractant, KC = Keratinocyte chemoattractant (chemokine ligand 1), LIX = lipopolysaccharide induced chemokine, MCP = monocyte chemoattractant protein, MCSF = macrophage colony stimulating factor, MIG = monokine induced by gamma interferon, MIP = macrophage inflammatory protein, RANTES = Regulated on activation, normal T-cell expressed and secreted, SDF= stromal cell derived factor, TCA = T-cell activation gene, TECK = thymus expressed chemokine, TIMP = Tissue inhibitor of metalloproteinase, TNF(R) = tumor necrosis factor (receptor), Pos = Positive spot, Neg = negative spot.

	A	B	C	D	E	F	G	H	I	J	K	L
1	Pos	Pos	Neg	Neg	Blank	BLC	CD30 L	Eotaxin	Eotaxin-2	Fas Ligand	Fractalkine	GCSF
2	Pos	Pos	Neg	Neg	Blank	BLC	CD30 L	Eotaxin	Eotaxin-2	Fas Ligand	Fractalkine	GCSF
3	GM-CSF	IFNγ	IL-1α	IL-1β	IL-2	IL-7	IL-4	IL-6	IL-9	IL-10	IL-12 p40/p70	IL-12 p70
4	GM-CSF	IFNγ	IL-1α	IL-1β	IL-2	IL-7	IL-4	IL-6	IL-9	IL-10	IL-12 p40/p70	IL-12 p70
5	IL-13	IL-17	I-TAC	KC	Leptin	LIX	Lymphotactin	MCP-1	MCSF	MIG	MIP-1α	MIP-1γ
6	IL-13	IL-17	I-TAC	KC	Leptin	LIX	Lymphotactin	MCP-1	MCSF	MIG	MIP-1α	MIP-1γ
7	RANTES	SDF-1	TCA-3	TECK	TIMP-1	TIMP-2	TNF-α	sTNF RI	sTNF R II	Blank	Blank	Pos
8	RANTES	SDF-1	TCA-3	TECK	TIMP-1	TIMP-2	TNF-α	sTNF RI	sTNF R II	Blank	Blank	Pos

2.12.1. Data analysis

Densitometry of the spots on the Mouse Inflammatory Array Membranes was performed using ImageJ software (NIH). Briefly, the mean gray value of each spot was measured from all membranes using the same circular region of interest. The spots of interests were then background (average of all negative control spots) subtracted and normalized to the positive control spots of the reference membrane (control FLS media). Fold change was obtained by dividing normalized intensities of the membrane of interest and the control membrane, analyte-by-analyte.

2.13. Whole cell patch clamp electrophysiology

All recordings were performed using a HEKA EPC-10 amplifier (Lambrecht) and its corresponding Patchmaster software. Patch pipettes of 4-9 MΩ were pulled with a P-97 Flaming/Brown puller (Sutter Instruments) from borosilicate glass capillaries.

2.13.1. Composition of extracellular and intracellular recording solutions:

The cells were bathed in an extracellular solution (ECS) that contained (in mM). NaCl (140), KCl (4), $MgCl_2$ (1), $CaCl_2$ (2), glucose (4) and HEPES (10) adjusted to the required pH (> 6.0) with NaOH (340-360 mOsm). For solutions with pH < 6.0, MES was used instead of HEPES. The intracellular solution used in patch pipettes contained (in mM): KCl (110), NaCl (10), $MgCl_2$ (1), EGTA (1), HEPES (10), Na_2 ATP (2), Na_2 GTP (0.5) adjusted to pH 7.3 with KOH (300-310 mOsm).

2.13.2. Protocols and Data Analysis

Action potential generation in DRG neurons: APs were generated by 80 ms current injections of 150-1050 pA in 50 pA steps (Figure 2A). If an AP was generated at 150 pA, the neuron was retested with current injections of 0–1000 pA, in 50 pA steps. Threshold, amplitude, half peak duration (HPD), afterhyperpolarization (AHP) duration and AHP amplitude (Figure 4-3) were measured using Fitmaster software (HEKA) or IgorPro software (Wavemetrics) as described before (Bonin et al., 2013; Djouhri et al., 2001; Kim et al., 1998). AP amplitude is defined as the peak of the AP from the repolarized membrane potential; HPD is the AP width at half-amplitude, AHP was obtained by fitting the decay to a single exponential function and AHP amplitude was obtained by subtracting the peak voltage during AHP from the repolarized membrane potential.

Pharmacology: Solutions (Table 2-7) were made up in ECS from their respective stocks (if applicable) and applied in a random order through a gravity-driven 12 barrel perfusion system (Dittert et al., 2006) in 5 s pulses with at least a 30 s wash period (with pH 7.4) between stimuli. To test for inhibition of currents observed, the solution of interest was applied before and after 1-2 min of antagonist application. Cells that produced an inward current, larger than the baseline, and time-locked to the drug applications were counted as responders while non-responders did not evoke any currents. Current amplitude was measured in Fitmaster (HEKA) by subtracting the maximum peak response from the baseline (average of the 3 s before stimulation), which was then normalized by dividing by neuron capacitance to give current density.

2.14. Ca^{2+}-imaging

Neurons were incubated with the Ca^{2+} indicator, Fluo-4 AM (10 μM diluted in ECS from a 10 mM stock solution in DMSO, Invitrogen) for 30 min (40 min for FLS) at RT (21 °C). Culture dishes were then washed and imaged under an inverted Nikon Eclipse T*i* microscope. Fluo-4 fluorescence were excited using a 470 nm LED (Cairn Research) and captured with a camera (Zyla cSMOS, Andor) at 1 Hz with a 50 ms (250 ms for FLS) exposure time using Micro-Manager software (v1.4; NIH). Solutions were perfused through a gravity-driven 12 barrel perfusion system (Dittert et al., 2006).

2.14.1. Protocols and Data analysis:

Solutions (Table 2-7) to test for chemical sensitivity (e.g. capsaicin) were applied for 10 s after a 10 s baseline was established with ECS. Unless otherwise stated, for testing the effect of antagonists upon test solutions, the solution of interest was applied before and after 1 min of antagonist application. There was a wash out period of 4 min between drug applications and 50 mM KCl and 10 μM ionomycin were used as positive controls in experiments with neurons and FLS respectively.

Analysis was conducted by extracting mean gray values of neurons from manually drawn regions of interests (ROIs) in the ImageJ software. These values were then fed into a custom-made R-toolbox (https://github.com/amapruns/Calcium-Imaging-Analysis-with-R.git) to compute the proportion of cells responding to each drug and their corresponding magnitude. Briefly, after

subtraction of background intensities from the ROIs, the difference between 5 s of pre-compound application baseline and 2 s of peak drug response was calculated. Cells that had a peak drug response greater than baseline mean ± 5 standard deviation (threshold) were counted as "responders". Then neurons were normalized to their peak KCl and FLS to their peak ionomycin response (ΔF/Fmax); cells not crossing threshold for positive controls were excluded from the analysis. Finally, a manual quality control was performed by excluding cells that had a peak ΔF/Fmax of less than 0.001 and that did not reach peak 30 s after termination of drug application. It is to be noted that a neuron's response to KCl is not the global Fmax, nevertheless responses of neurons were normalized to KCl because it causes a substantial depolarization of neurons and I was interested in testing the depolarizing potential of algogens which directly correlates with their nociceptive potential.

Table 2-7 List of solutions used in electrophysiological recordings and Ca^{2+}-imaging.

NA = not applicable.

Solution	Working concentration	Stock concentration	Supplier	Application
pH 4-7	NA	NA	NA	Agonist of proton sensors
Capsaicin	1-10 μM	1 mM in ethanol	Sigma	TRPV1 agonist
Cinnamaldehyde	100 μM	1 M stock in ethanol	Merck	TRPA1 agonist
Menthol	100 - 250 μM	1 M stock in ethanol	Alfa Aesar	TRPM8 agonist
γ-aminobutyric acid (GABA)	100 μM	100 mM in water	Sigma	GABA agonist
Bicuculline	250 μM	100 mM in DMSO	Sigma	$GABA_A$ antagonist
4,5,6,7-tetrahydroisoxazolo[5,4-c]pyridin-3-ol hydrochloride (THIP)	100 μM	100 mM in water	Sigma	$GABA_A$-δ subunit agonist
Nifedipine	10 μM	1 M in DMSO	Sigma	Ca_v blocker
Tetrodotoxin	2 μM	1 mM in water	Alomone Labs	Na_v blocker
Ruthenium red	20 μM	1 mM in water	Sigma	TRP antagonist
Amiloride	200 μM	100 mM in DMSO	Cayman Chemical	Non-selective ASIC antagonist
APET-x2	2 μM	100 μM in water	Smartox	ASIC3 selective antagonist
YM-254890	100 nM	10 mM in DMSO	Adipogen	G_qPCR antagonist

2.15. Statistical Analysis

The number of mice to be used in each part of the study was calculated by power analysis using G*Power software and approved by the UK Home Office and the University of Cambridge Animal Welfare and Ethical Review Body. All data are presented as mean ± SEM. Student's unpaired t-tests were performed for comparison between two groups with similar distribution while the chi-sq test was performed to compare two proportions. An ANOVA followed by an appropriate post hoc test was performed for comparison of more than two groups using Graphpad Prism software. Following publication of all findings in this thesis, data will be made available in the Cambridge University Apollo Repository.

Chapter 3. Human OA synovial fluid increases excitability of mouse DRG neurons: an *in vitro*, translational model to study arthritic pain.

This chapter has been published as "Human osteoarthritic synovial fluid increases excitability of mouse dorsal root ganglion sensory neurons: an *in vitro* translational model to study arthritic pain" (Chakrabarti et al., 2019a).

Authorship contributions in the published manuscript: I designed the studies, collected and analyzed data, and wrote the manuscript. Dr Deepak R. Jadon obtained the human synovial fluid samples and revised the manuscript. Drs David C. Bulmer and Ewan St. John Smith were involved in the design of the study and writing of the manuscript.

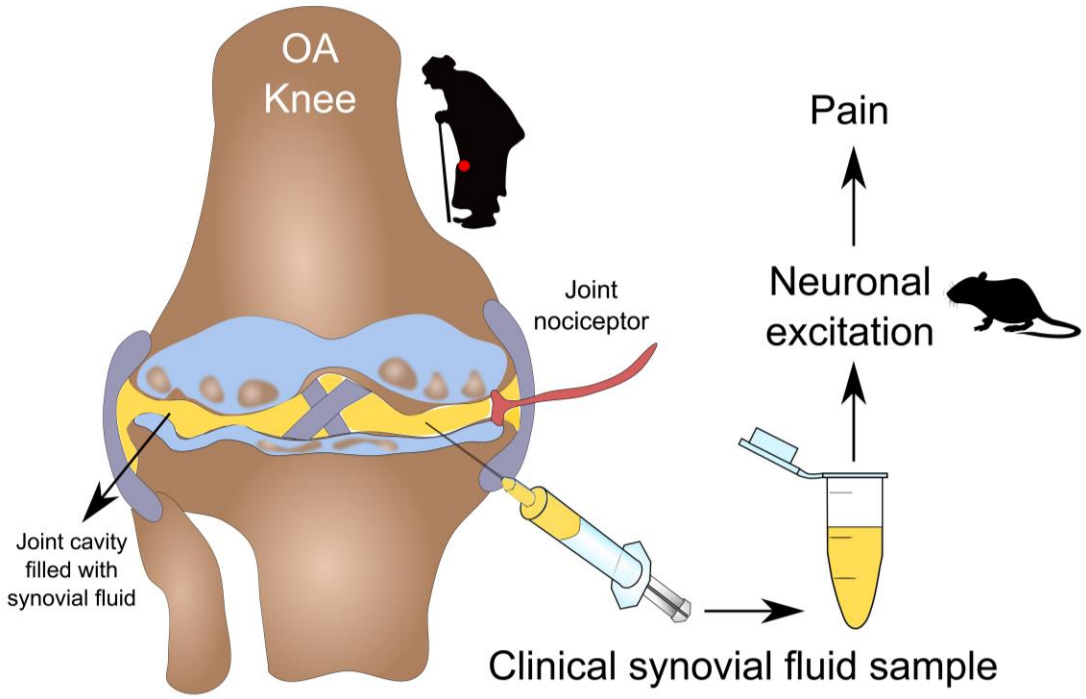

Figure 3-1: Graphical abstract for Chapter 3.

3.1.Key message

Experimental animal models of arthritis do not fully recapitulate the human disease and hence there is a need to develop models that utilize human clinical samples to bridge the translational gap between bench and bedside. I developed a novel, *in vitro* translational model to study arthritic pain by stimulating mouse dorsal root ganglion neurons with human synovial fluid obtained from OA patients and post-mortem donors with no known joint disease. Results in this chapter show that OA synovial fluid directly increases knee neuron excitability and hence drives knee pain. This chapter highlights the inflammatory phenotype of OA, provides proof-of-concept that synovial fluid is a key modulator of arthritic pain and establishes knee-innervating neurons as a distinct subset of DRG neurons that are important in arthritic pain.

3.2.Introduction

Clinicians have noted differences between the quality of cutaneous and deep tissue (e.g. joint) pain since the early 1900s, with deep tissue pain being more diffuse, dull, intermittent and "sickening" (Lewis, 1938). In his article in the British Medical Journal, Sir Thomas Lewis goes as far as to say, "the difference in the quality of pain derived from skin and from deeper structures has led me to suppose that these may be fundamentally different forms of sensation" (Lewis, 1938). Later retrograde tracing studies from the knee have also shown important differences in the cell bodies of knee-innervating neurons (knee neurons) compared to skin, such as knee neurons having increased proportions of peptidergic, TRPV1 (transient receptor potential vanilloid 1) positive and unmyelinated neurons (Cho and Valtschanoff, 2008; O'Brien et al., 1989). Furthermore, electrophysiological recordings of the medial articular nerve supplying the cat knee joint revealed a large group of high threshold or mechano-insensitive afferents that become responsive after inflammation (Schaible and Schmidt, 1985). Therefore, in this study I hypothesized that knee-innervating DRG neurons likely form a functionally distinct group with a higher firing threshold for action potential generation, and that respond to the inflammatory joint environment as encountered during arthritis.

The knee joint is of particular interest in this study because knee OA is one of the most commonly reported musculoskeletal disorders and as of 2017 (The Institute for Health Metrics and

Evaluation, 2017), musculoskeletal disorders are the principle contributing factor to the years lived with disability index of the global disease burden (Vos et al., 2012). Moreover, knee OA is one of the top ten global causes of morbidity, with pain being a predominant symptom (Neogi, 2013). Perhaps due to OA being considered a degenerative joint disorder, the focus of drug development has been on managing structural disease progression, even though pain severity only tenuously correlates with radiographic joint damage (Syx et al., 2018). Furthermore, prescribed pain management drugs, such as diclofenac, etoricoxib and opioids, show limited efficacy and are accompanied by safety concerns after long-term use (Syx et al., 2018). Overall, mechanisms driving OA pain are poorly understood and there is a significant unmet clinical need to improve pain management in OA.

OA is historically thought to be a degenerative joint disease that accompanies old age, however, a medico-evolutionary study of cadaveric knee OA found a 2.1 fold increase in its prevalence from the early to post-industrial era after controlling for increases in longevity and body mass index (Wallace et al., 2017). These data suggest knee OA may be preventable and is not simply a by-product of aging. Subsequently, the roles of synovitis and inflammation in OA-related pain have become clear, thus providing a druggable disease mechanism (Goldring and Otero, 2011). Synoviocytes produce inflammatory mediators like TNF-α, IL-6 and lysophosphatidylcholine that are detected in the SF of OA patients (Carlson et al., 2018; Gobezie et al., 2007) and in animal models of arthritis (Zhang et al., 2013). Attempts have been made to stratify arthritic patients based upon biomarkers present in SF using proteomics (Balakrishnan et al., 2014; Bhattacharjee et al., 2016), lipidomics (Kosinska et al., 2014) and metabolomics (Hugle et al., 2012) revealing the presence of multiple inflammatory mediators in diverse forms of arthritis. These inflammatory mediators stimulate the distal terminals of DRG neurons, which in turn transmit sensory information to the central nervous system. Individually, inflammatory mediators can induce neuronal hyperexcitability (Zhang et al., 2013), which likely explains the efficacy of NSAIDs like diclofenac (Deng et al., 2016) that inhibit prostaglandin production, but it is unknown whether arthritic SF directly excites mouse knee neurons.

The hyperexcitability of peripheral sensory neurons (peripheral sensitization), is clinically important (Malfait and Miller, 2016) as demonstrated by the efficacy of peripherally restricted anti-nerve growth factor antibodies in OA (Lane et al., 2010). However, mechanistic

understanding of peripheral sensitization in OA is largely restricted to animal models. For example, electrophysiological studies in the MIA model of OA in rats (Brenn et al., 2007; Segond von Banchet et al., 2005) and OA-prone Hartley guinea pig (Schuelert et al., 2011) showed that hyperexcitability of joint afferents and DRG neurons was mediated by IL-6 and IL-1β. Even though use of multiple animal models helps to improve translational value, such models cannot fully recapitulate the human disease, and thus further work is needed to bridge the gap between pre-clinical and clinical studies. One possibility is to use SF obtained following routine SF aspiration from OA patients (that is regularly used to identify biomarkers) to further study the nociceptive potential of the joint environment. Here I hypothesize that SF also plays a direct role in OA pain and describe an *in vitro*, translational model of OA-SF stimulated DRG sensory neurons that can potentially identify clinically relevant pain targets in arthritis. The specific aims of this Chapter are 1) to develop an *in vitro*, translational model of inflammatory knee pain utilizing SF from patients with painful OA and DRG neurons from mice 2) to understand whether OA-SF can directly increase excitability and 3) dysregulate TRP channel functions in knee neurons.

3.3.Methods

See Materials and Methods chapter for detailed description of SF procurement and processing (Section 2.2), mice knee injections (Section 2.4), whole cell patch clamp electrophysiology (Section 2.13) and Ca^{2+} imaging (Section 2.14) on DRG neurons. Most of the animals used in this Chapter were females since being female is a risk factor for arthritis. In the patient cohort, 5/7 were females and I did not have enough statistical power to compare the two sexes. Therefore, this study is based on predominantly female subjects and inferences about sex difference is not possible solely based on the results presented here.

3.4.Results

SF was obtained from OA patients (disease duration: 13 years (median), 5-33 years (interquartile range)) with pain score >50 mm (VAS) and from healthy donors with no known joint disease (Table 2-1).

3.4.1. Knee neurons are a distinct subset of DRG neurons.

DRG neurons are heterogeneous, displaying distinct electrophysiological subtypes (Petruska et al., 2000) and gene expression profiles that are dependent upon the site of innervation (Hockley et al., 2019). Therefore, I performed whole cell electrophysiology on fast blue labelled knee neurons (yellow arrow, n = 21, Figure 3-2A) and unlabeled neurons (white arrow, n = 22, Figure 3-2A) of similar diameters (knee, 29.4 ± 1.2 μm, unlab, 27.9 ± 1.0 μm, p = 0.4, unpaired t-test, Figure 3-2B). Knee and unlabeled neurons had a similar resting membrane potential (RMP; knee, -53.6 ± 2.0 mV, unlab, -51.9 ± 2.0 mV, p = 0.6, unpaired t-test, Figure 3-2C), but upon injection of current steps, the threshold for AP generation was higher for knee neurons when compared to the unlabeled neurons (knee, 561.9 ± 67.1 pA, unlab, 363.6 ± 68.2 pA, p = 0.04, unpaired t-test, Figure 3-2Di). By contrast, the half peak duration (HPD; knee, 1.9 ± 0.3 ms, unlab, 1.9 ± 0.3 ms, p = 0.9, unpaired t-test, Figure 3-2Dii) and afterhyperpolarization peak (AHP peak; knee, 16.6 ± 1.3 mV, unlab, 14.9 ± 1.0 mV, p = 0.3, unpaired t-test, Figure 3-2Diii) of the evoked AP were similar between the two groups. Taken together, knee neurons were less excitable than unlabeled DRG neurons and therefore I utilized knee neurons for testing excitability changes in the subsequent sections.

Since we had limited amount of SF, I tested whether knee neurons differed from the unlabeled population in terms of their sensitivity to agonists of the two TRP channels TRPV1 and TRPM8 (which are involved in arthritic pain (Galindo et al., 2018)) in order to make informed decision on designing later experiments (Results 3.4.3) of the study. A similar proportion of neurons from both groups responded to 1 μM capsaicin (TRPV1 agonist, knee, 57%, unlab, 41%), although knee neurons had a higher magnitude of peak response (knee, 9.4 ± 2.0 pA/pF, unlab, 3.2 ± 1.1 pA/pF, p = 0.03, unpaired t-test, Figure 3-2Ei, ii). 100 μM menthol (TRPM8 agonist) evoked responses of similar magnitude in 29 % of knee and 31% of unlabelled neurons (knee, 2.7 ± 1.1 pA/pF, unlab, 1.4 ± 0.5 pA/pF, p = 0.3, unpaired t-test, Figure 3-2Fi, ii).

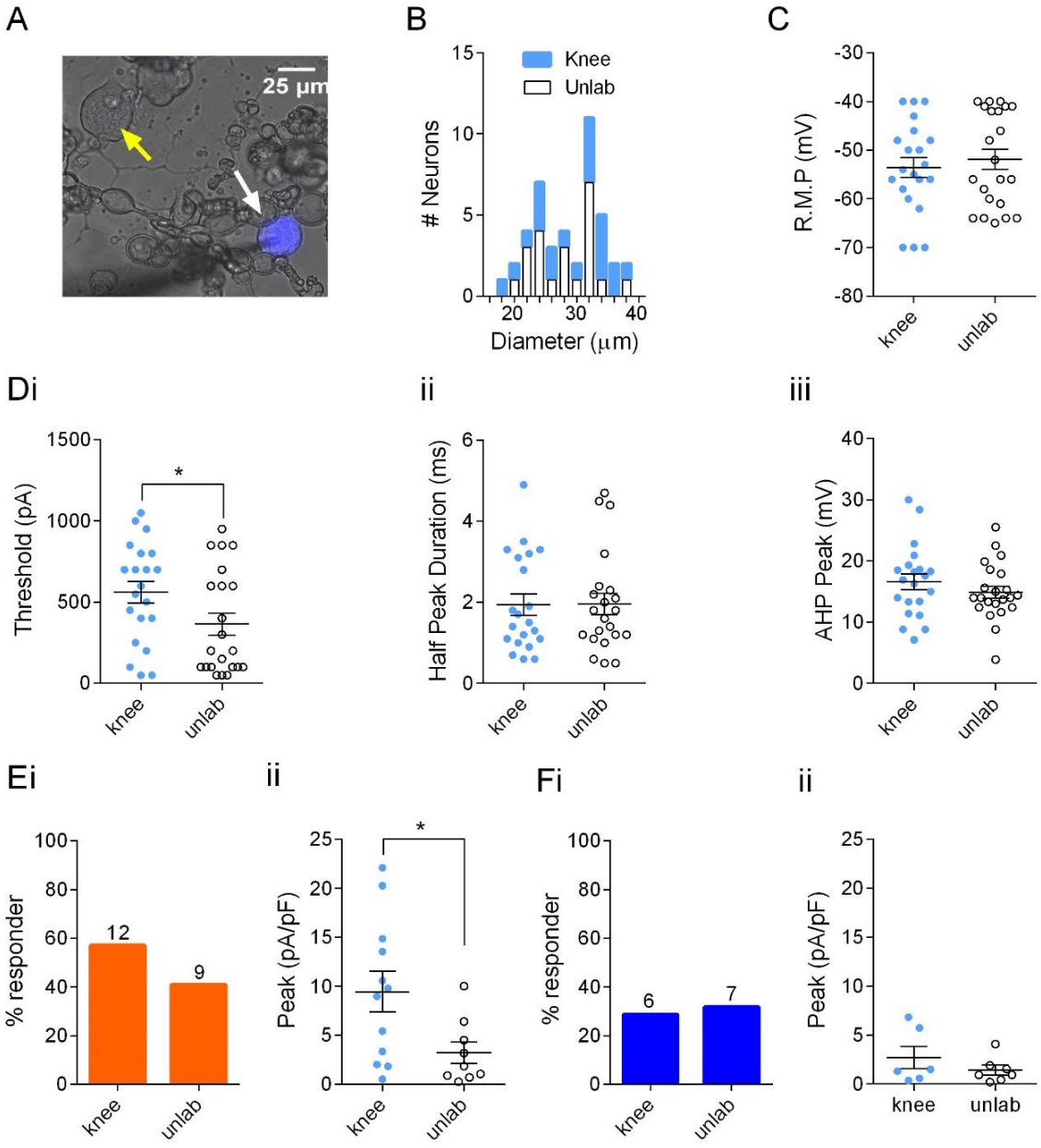

Figure 3-2: Electrophysiological comparison of knee vs. unlabeled neurons.
A) Representative image of dissociated DRG sensory neurons in culture. White arrow, a retrograde traced (Fast Blue) labelled knee neuron; yellow arrow, an unlabeled neuron and the black triangular shadow is from a patch pipette used for recording from neurons. Distribution of neuronal diameter (B), resting membrane potential (RMP, C), action potential threshold (Di) half peak duration (Dii) and afterhyperpolarisation peak amplitude (AHP Peak, Diii) from knee (light blue dots, n = 21) and unlabeled neurons (black open dots, n = 22). Bar graphs showing proportion of neurons responding to the TRP agonists and their magnitude of response, capsaicin (orange, Ei, ii) and menthol (blue, Fi, ii). Values above the bars represent numbers of neurons that responded in each condition. Data were obtained from 5 female mice. * represents $p < 0.05$, unpaired t-test. Error bars = SEM.

3.4.2. Knee neurons are hyper-excitable following overnight incubation with OA-SF.

I recorded from knee neurons incubated overnight with control media (n = 46), Ctrl-SF (n = 20) or OA-SF (n = 29) (Figure 3-3Ai,ii) to test the hypothesis that mediators present in OA-SF can excite and/or sensitize DRG neurons. OA-SF incubated knee neurons had a more depolarized RMP compared to those incubated with either control media or Ctrl-SF (Control media, -50.9 ± 1.3 mV, Ctrl-SF, -50.9 ± 1.6 mV vs. OA-SF, -43.2 ± 2.5 mV, p = 0.005, ANOVA, Figure 3-3Bi). Furthermore, the AP generation threshold also decreased by ~40% in OA-SF incubated neurons (Control media, 519.6 ± 36.5 pA, Ctrl-SF, 472.5 ± 51.2 pA vs. OA-SF, 188.5 ± 35 pA, p = 0.0003, ANOVA, Figure 3-3Bii). However, no change in HPD (Control media, 1.8 ± 0.2 ms, Ctrl-SF, 1.5 ± 0.2 ms vs. OA-SF, 2.5 ± 0.4 ms, p = 0.1, ANOVA, Figure 3-3Biii) or AHP peak (Control media, 15.4 ± 0.7 mV, Ctrl-SF, 18.0 ± 0.9 mV vs. OA-SF, 17.9 ± 0.9 mV, p = 0.02, ANOVA – no statistically significant difference after Holm-Sidak post hoc comparison between groups; Figure 3-3Biv) was observed. These results show that OA-SF increases excitability of knee neurons and thus likely contributes to knee pain through peripheral sensitization.

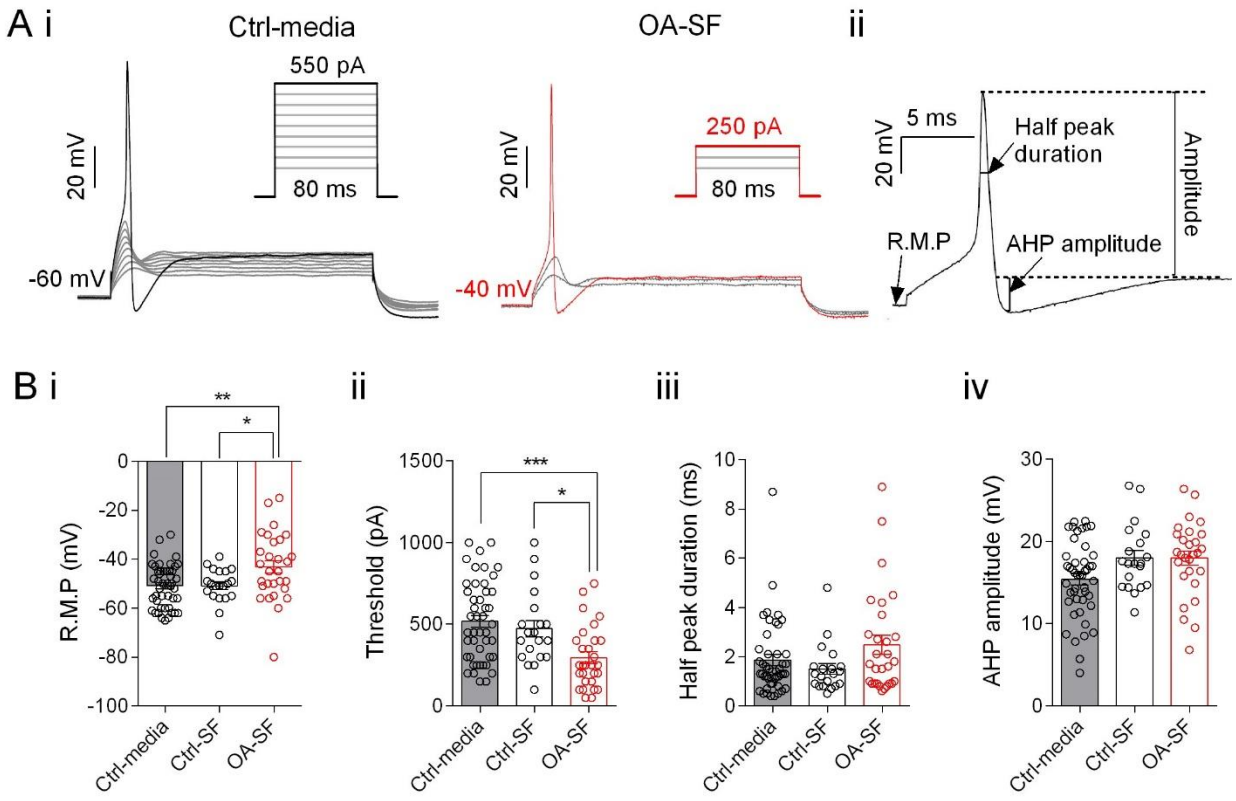

Figure 3-3: Incubation with OA-SF increases neuronal excitability.
A) Representative AP traces generated by whole cell patch clamp after incubation with Control media and OA-SF (i) and schematics of measured AP properties (ii). B) Distribution of resting membrane potential (i, RMP), AP threshold (ii), AP half peak duration (iii) and AP AHP amplitude (iv), measured from control media (black dot, grey bar, n = 46), Ctrl-SF (black dot, white bar, n = 20) and OA-SF incubated knee neurons (red dots, n = 29). Data were obtained from 3 Ctrl-SF, 4 OA-SF and 9 mice (7 females, 2 males). * represents $p < 0.05$, ** represents $p < 0.01$, *** represents $p < 0.001$, ANOVA followed by Holm-Sidak post hoc test.

3.4.3. Overnight incubation with OA-SF increases capsaicin- and menthol-evoked responses in DRG sensory neurons compared to Ctrl-SF.

Inflammatory mediators sensitize TRP channels and antagonists of TRPV1 and TRPM8 have been clinically explored for analgesia (Galindo et al., 2018). Since the proportions of capsaicin (TRPV1 agonist) and menthol (TRPM8 agonist) responsive neurons were similar in knee vs. unlabeled neurons (Figure 3-2E, F), these Ca^{2+}-imaging experiments were conducted on unidentified DRG neurons to increase sample size.

Compared to Control media, I observed a decrease in the magnitude of capsaicin-evoked responses from neurons after incubation with Ctrl-SF, whereas no such decrease was observed following incubation with OA-SF (Control media, 0.5 ± 0.03, n = 184, Ctrl-SF, 0.4 ± 0.03, n = 89, OA-SF, 0.5 ± 0.03, n = 175, p = 0.02, ANOVA, Figure 3-4Ai, ii). Hyaluronic acid (HA) is a key constituent of SF that shows dysregulation in arthritis and I observed a similar decrease in the magnitude of capsaicin-evoked responses when neurons were incubated overnight in high molecular weight HA to that observed with Ctrl-SF (Control media, 0.5 ± 0.03, n = 111, HA, 0.4 ± 0.03, n = 72, p = 0.003, unpaired t-test, Figure 3-4Aiii). Similar to capsaicin, menthol-evoked responses were also smaller in magnitude in Ctrl-SF incubated neurons when compared to Control media or OA-SF incubated neurons (Control media, 0.3 ± 0.04, n = 59, Ctrl-SF, 0.2 ± 0.02, n = 94, OA-SF, 0.4 ± 0.06, n = 24, p < 0.0001, ANOVA, Figure 3-4Bi, ii). However, neurons incubated with HA did not show a decrease in menthol-evoked response (Control media, 0.3 ± 0.04, n = 26, HA, 0.2 ± 0.06, n = 18, p = 0.7, unpaired t-test, Figure 3-4Biii).

Taken together these data suggest that OA-SF disinhibits neuronal TRP channel activity and lends support to the theory that HA present in Ctrl-SF inhibits TRPV1 channels, whereas OA-SF with low-content HA relieves TRPV1 inhibition, causing pain (Caires et al., 2015). Although the mechanism underlying TRPM8 disinhibition is likely not HA-mediated and requires further investigation, our data support the therapeutic potential of TRP channel modulators in OA.

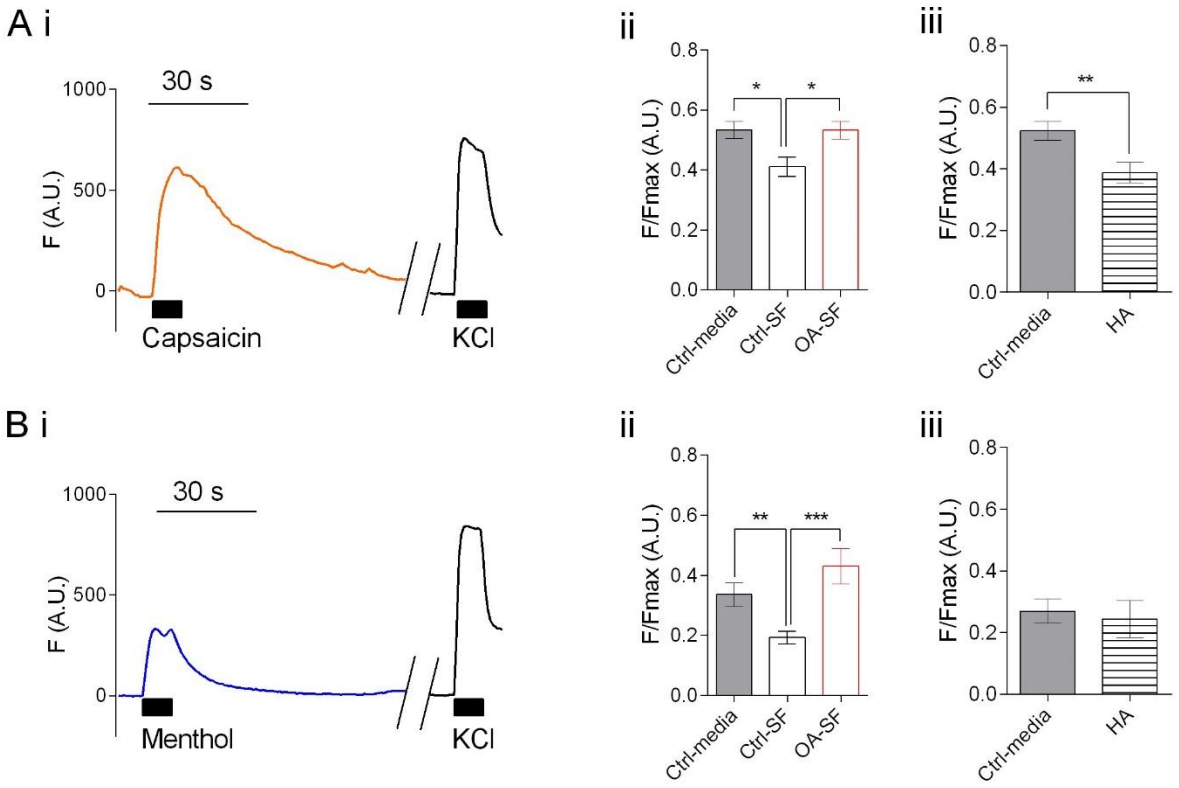

Figure 3-4: Incubation with OA-SF dysregulates TRPV1 and TRPM8 function.

Representative (Ai) capsaicin-evoked (F, fluorescence intensity, orange), menthol-evoked (Bi, blue) and KCl-evoked (Fmax, maximum fluorescence intensity, black) response obtained by Ca^{2+}-imaging , followed by bar graph of peak F/Fmax of capsaicin-responding (Aii) and menthol-responding (Bii) neurons incubated in Control-media (grey), Ctrl-SF (black border) or OA-SF (red border). Data were obtained from 3 Ctrl-SF, 3 OA-SF and 5 female mice. At least 200 neurons were imaged in each category. * represents $p < 0.05$, ** represents $p < 0.01$, *** represents $p < 0.001$, ANOVA followed by Holm-Sidak post hoc test. Error bars = SEM. Bar graph of peak F/Fmax of capsaicin-responding (Aiii) and menthol responding (Biii) neurons after incubation with Control media (grey) or 0.5 mg/ml high molecular weight hyaluronic acid (HA, hatched bar). Data were obtained from 3 female mice with at least 200 neurons in each category. ** represents $p < 0.01$, unpaired t-test. Error bars = SEM.

3.4.4. Acute application of SF increases intracellular Ca^{2+} in DRG sensory neurons.

Increased cytosolic Ca^{2+} involves multiple mechanisms and is implicated in various pain pathologies (Bourinet et al., 2014). Both Ctrl-SF and OA-SF contain mediators that can increase Ca^{2+} influx in DRG sensory neurons (Carlson et al., 2018; Gobezie et al., 2007). Accordingly, acute application of Ctrl-SF or OA-SF induced Ca^{2+} influx in similar proportion of DRG sensory neurons (Ctrl-SF, 79%, OA-SF, 81%, Figure 3-5Ai, ii).

In order to understand the basis of this Ca^{2+} influx, I tested a range of antagonists of receptors involved in arthritic pain. OA-SF-evoked, but not Ctrl-SF-evoked, Ca^{2+} influx was significantly reduced by 1 min pre-incubation with the voltage-gated Ca^{2+} channel (Ca_V) blocker, nifedipine (OA-SF, $p = 0.0003$, Ctrl-SF, $p = 0.4$, unpaired t-test, Table 3-1, Figure 3-5B), and the voltage-gated Na^+ channel (Na_V) blocker, tetrodotoxin (OA-SF, $p < 0.0001$, Ctrl-SF, $p = 0.09$, unpaired t-test, Table 3-1, Figure 3-5C), suggesting sub-threshold depolarization-mediated increase in intracellular Ca^{2+}; no spontaneous APs were observed upon acute application of OA-SF in $n = 10$ neurons, data not shown. Mediators present in SF can also release Ca^{2+} from intracellular stores by G_q protein coupled receptors (G_qPCR) (Neumann et al., 2014) and a 10 min pre-incubation with the G_q-protein inhibitor, YM-248590, significantly decreased the magnitude of Ctrl-SF ($p < 0.0001$, unpaired t-test) and OA-SF-evoked ($p = 0.0001$, unpaired t-test) Ca^{2+} response (Table 3-1, Figure 3-5D). Consistent with the idea that TRP channels are involved in normal joint homeostasis (Galindo et al., 2018), I saw a decrease ($p = 0.02$, unpaired t-test) in Ctrl-SF-evoked response (but not OA-SF evoked response ($p = 0.5$, unpaired t-test)) on application of the non-selective TRP channel blocker, ruthenium red (Table 3-1, Figure 3-5E). However, this decrease was not TRPV1 mediated because the selective TRPV1 antagonist A-425619 showed no effect (Table 3-1, Figure 3-5F). Similarly, the non-selective ASIC blocker, amiloride and the ASIC3 selective antagonist, APETx2 did not significantly suppress the OA-SF-evoked Ca^{2+} influx (Table 3-1, Figure 3-5F-G, H)).

Table 3-1: SF-evoked Ca^{2+} responses (normalized to KCl responses) before and after antagonist applications.

Statistical significance between Ctrl-SF (before) vs. Ctrl-SF (after) and between OA-SF (before) vs. OA-SF (after) were made using unpaired t-tests. * represents $p < 0.05$, *** represents $p < 0.001$, **** represents $p < 0.0001$, unpaired t-test. Error = SEM.

	Ctrl-SF (before)	Ctrl-SF (after)	df	OA-SF (before)	OA-SF (after)	df
Nifedipine	0.06 ± 0.002	0.06 ± 0.004	304	0.07 ± 0.002	0.06 ± 0.002***	466
Tetrodotoxin	0.07 ± 0.003	0.07 ± 0.003	450	0.07 ± 0.006	0.04 ± 0.002****	423
YM-248590	0.07 ± 0.003	0.05± 0.003****	428	0.09 ± 0.004	0.06 ± 0.003***	575
Ruthenium red	0.06 ± 0.002	0.05 ± 0.002*	486	0.07 ± 0.004	0.07 ± 0.004	617
A-425619	0.1 ± 0.004	0.1 ± 0.005	364	0.06 ± 0.003	0.06 ± 0.004	289
Amiloride	0.05 ± 0.003	0.06 ± 0.004	275	0.05 ± 0.002	0.05 ± 0.003	477
APETx2	0.05 ± 0.001	0.05 ± 0.001	452	0.07 ± 0.004	0.08 ± 0.005	399

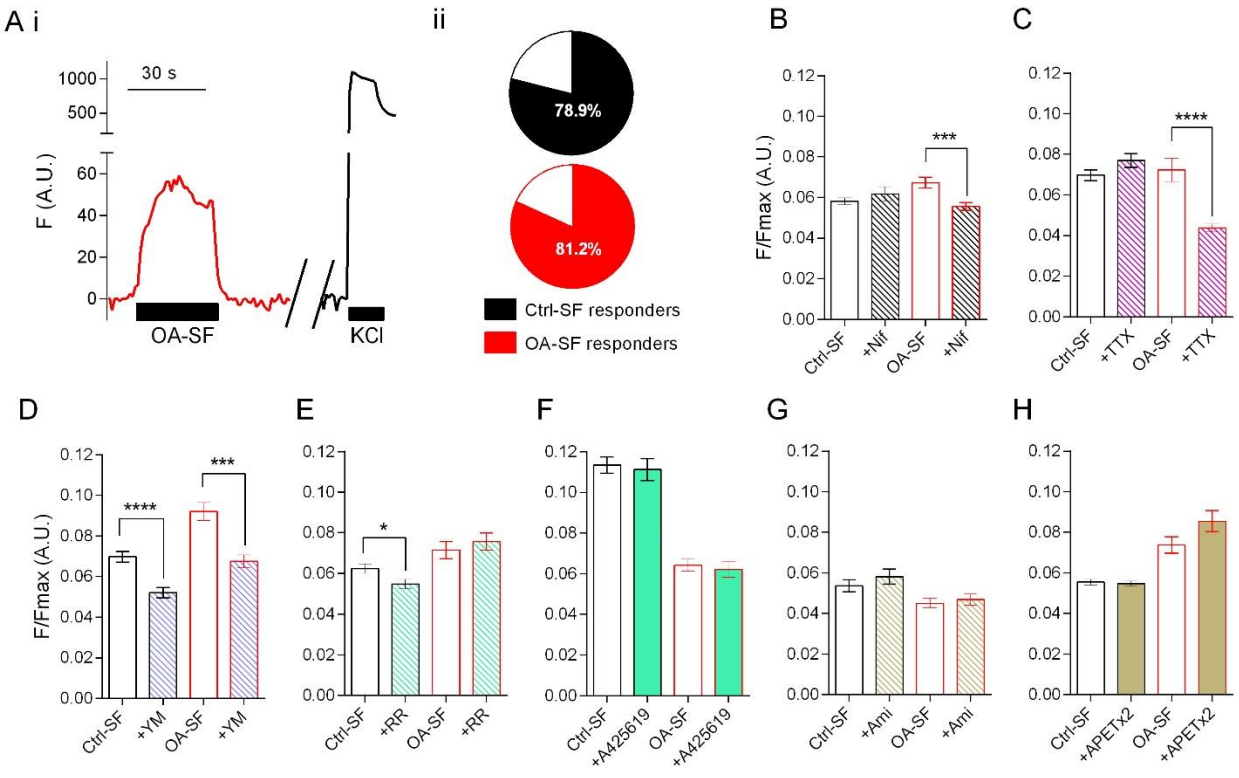

Figure 3-5: Acute application of OA-SF increases intracellular Ca^{2+}.

A) Representative response of a DRG neuron to OA-SF (red) and KCl (black) (i) and pie charts showing percentage of neurons that responded to Ctrl-SF (black) and OA-SF (red) (ii). B-G) Bar graphs showing normalised peak fluorescence intensity of neurons responding to Ctrl-SF or OA-SF before (black or red border) and after application of Ca_V blocker, nifedipine (Nif, B, black hatched), Na_V blocker tetrodotoxin (TTX, C, purple hatched), G_q inhibitor YM-245890 (YM, D, blue hatched), non-selective TRP channel blocker ruthenium red (RR, E, green hatched), selective TRPV1 antagonist A-425619 (F, green solid) non-specific ASIC blocker amiloride (Ami, G, gold hatched) and ASIC3 blocker APETx2 (H, gold solid). Data were obtained from at least 2 Ctrl-SF and OA-SF with 2 mice and each bar represents data from at least 100 neurons. * represents $p < 0.05$, *** represents $p < 0.001$, **** represents $p < 0.0001$, unpaired t-test. Error bars = SEM.

3.5.Discussion

Multiple pro- and anti-inflammatory mediators are present in OA-SF, some of which directly excite sensory neurons (Carlson et al., 2018; Zhang et al., 2013). I reasoned that overnight incubation of DRG sensory neurons with OA-SF will simulate OA joints bathed in SF and will be a suitable system to interrogate the net effect of these mediators. In this study I first describe knee neurons as a distinct class of DRG neurons based on their electrophysiological properties, then show that the net effect of OA-SF incubation is increased neuronal excitation of mouse knee neurons.

Knee joints are innervated by low and high threshold fibers (Schaible and Schmidt, 1983) as well as by mechanoinsensitive ones (Prato et al., 2017) and in this study I found that knee neurons have an increased threshold of AP firing compared to unlabeled neurons thus indicating a greater contribution of high threshold/mechanoinsensitive units to sensory afferents. The distal ends of these neurons are exposed to the knee synovium and a previous study showed upregulation of inflammatory genes, such as IL-6, COX-2, neurokinin1, 2 and neuropeptide Y, in whole DRG when they were co-cultured with biopsy punch explants from human OA synovium (Li et al., 2011). This result supports our observation that overnight incubation with OA-SF increases excitability of knee neurons and hence establishes a nociceptive arc between mediators in the joint environment and peripheral nerves. In addition to a decreased AP firing threshold, I report an increased RMP, similar to that observed in knee afferents of OA pigs (Zhang et al., 2013), which might underpin the pain-at-rest observed in OA patients (Neogi, 2013).

Additionally, our data show that overnight incubation with OA-SF disinhibits TRPV1 and TRPM8 channel activity when compared to Ctrl-SF. Contribution of TRPV1 to neuronal excitability and arthritic pain has been described before (Chakrabarti et al., 2018; Hsieh et al., 2017; Kelly et al., 2015) (also see Chapter 4 for detailed discussion) and although no TRPV1 antagonists are currently approved for clinical use in OA due to poor efficacy and detrimental side effects (Galindo et al., 2018), mavatrep (a TRPV1 antagonist) has recently shown promising results in a Phase 2 clinical trial of knee OA (Manitpisitkul et al., 2018). I also provide proof that HA can decrease TRPV1 function in DRG neurons, which suggests that the observed increase in TRPV1 function in neurons incubated in OA-SF might be HA mediated. HA is a component of the extracellular matrix, present throughout the body including in SF and has many (patho)physiological roles

(reviewed in (Gupta et al., 2019)). It is of high molecular weight with concentration ranging from 1.45 – 3.12 mg/ml in Ctrl-SF, whereas arthritic SF is of low molecular weight and low concentration (0.17 – 1.32 mg/ml) HA (Balazs et al., 1967; Dahl et al., 1985). Consequently, several HA preparations are currently used clinically as viscosupplement to relieve OA pain (Tamer Mahmoud Tamer, 2013) for which multiple mechanisms of action have been proposed (Gupta et al., 2019). Our data suggest that the low content HA in OA-SF fails to block TRPV1 channels as efficiently as Ctrl-SF, and hence supports the HA-mediated TRPV1 inhibition hypothesis (Caires et al., 2015). By contrast, the role of TRPM8 in pain is more complex with its activation showing both algesic and analgesic effects (Fernandez-Pena, 2013). Specifically in knee OA, topical application of menthol did not show greater analgesic effect than placebo (Topp et al., 2013), whereas adding menthol to the existing topical drug Celadrin improved functional performance in arthritic patients (Kraemer et al., 2001). Our data show enhanced TRPM8 function in neurons incubated in OA-SF, suggesting that TRPM8 antagonists may relieve OA pain, pending replication in larger cohorts. TRPM8/TRPM8+ve fibres are also involved in cold pain (Knowlton et al., 2010) and thus this result supports the anecdotal evidence that cold temperatures are associated with arthritic pain (Guedj and Weinberger, 1990), for which there is mixed experimental evidence (Mandl et al., 2017; Wilder et al., 2003).

Acutely, both Ctrl-SF and OA-SF produced an increase in intracellular Ca^{2+} in DRG sensory neurons, from intra- and extra-cellular sources, suggesting a regulatory role of SF on neurons. However, since only OA-SF responses were Ca_V- and (TTX-sensitive) Na_V-mediated, we postulate that inflammatory mediators that are present in OA-SF cause depolarization leading to the observed increase in excitability after overnight exposure (Malfait and Miller, 2016; Neumann et al., 2014). Additionally, based on our data, TRPs and ASICs are not acutely activated by OA-SF.

Although further work is needed to understand if and how SF from diverse forms of arthritis gives rise to DRG neuron excitability (discussed as future directions in Chapter 7), our study provides proof-of-concept that OA-SF can directly activate DRG sensory neurons to produce peripheral sensitization. The OA-SF/neuron system is simple to establish since SF aspiration is a standard procedure for patients attending routine clinic appointments. Hence our model can be used in combination with high throughput assays to bridge the gap between experimental animal models

and clinical studies and help identify clinically relevant drivers of knee pain. Finally, since this model allows for unbiased assessment of mediators present in OA-SF to excite nociceptors, it can be used before and after drug treatment in pre-clinical tests to identify mechanisms of drug action.

Although more clinically relevant, this model does not allow for correlation of behavioral and neural components of arthritic pain. Therefore, the next chapter will characterize behavioral and neural correlates in a mouse model of joint inflammation.

Chapter 4. Acute inflammation sensitizes knee-innervating sensory neurons and decreases mouse digging behavior in a TRPV1-dependent manner.

This chapter has been published as “Acute inflammation sensitizes knee-innervating sensory neurons and decreases mouse digging behavior in a TRPV1-dependent manner” (Chakrabarti et al., 2018).

Authorship contributions in the published manuscript: I designed the studies, collected and analyzed data, and wrote the manuscript. Luke A. Pattison collected and analyzed mouse behavioral data, Kaajal Singhal performed immunohistochemistry experiments and helped with analysis, Drs James R.F. Hockley and Gerard Callejo helped with animal work and writing of the manuscript. Dr Ewan St. John Smith designed experiments and wrote the manuscript.

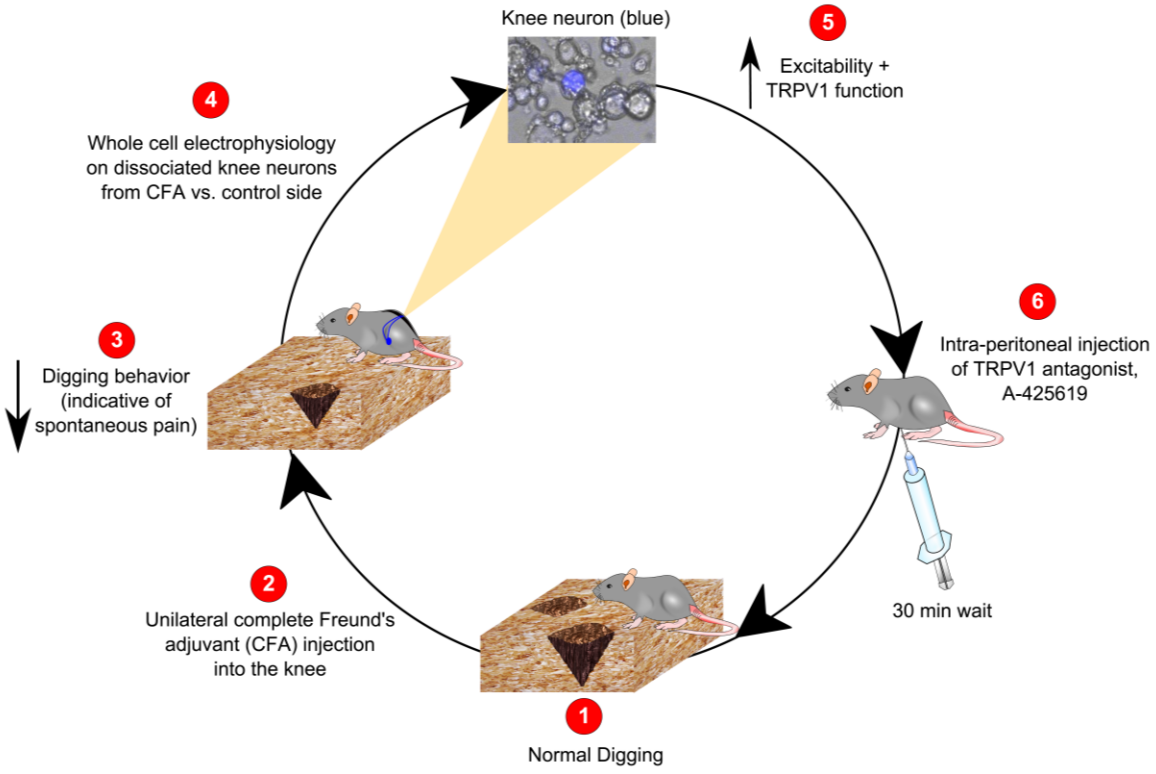

Figure 4-1: Graphical abstract for Chapter 4.

4.1. Key message

Knee inflammation is a major symptom of arthritis. In this study, complete Freund's adjuvant (CFA)-induced unilateral knee inflammation caused a decrease in mouse digging behavior concomitant with an increase in the excitability of knee-innervating dorsal root ganglion (DRG) neurons. Knee-innervating neurons also showed a nerve growth factor (NGF)-mediated increase in expression of the polymodal nociceptive ion channel TRPV1 and systemic administration of a TRPV1 antagonist normalized digging behavior in mice. This Chapter establishes digging as a measurable behavioral output for spontaneous pain and highlights the importance of TRPV1 in inflammatory arthritis.

4.2.Introduction

Inflammatory joint pain is a hallmark of multiple musculoskeletal disorders and animal models of arthritis are crucial to improve our understanding of inflammatory pain mechanisms. Since both the duration of insult (acute vs. chronic) and mechanism of injury (inflammation vs. nerve damage) produces distinct pain profiles, multiple animal models of joint pain exists (Gregory et al., 2013). The common features amongst these models are their recapitulation of some of the clinical features of human arthritis and that they produce a measurable nociceptive behavior in the model organism.

Initially utilized for triggering experimental autoimmunity in combination with other agents, CFA is a paraffin oil suspension of heat-killed *Mycobacterium tuberculosis* that causes localized inflammation within 12-hour of injection when used on its own (Billiau and Matthys, 2001). Therefore, injections of CFA either locally into paws/joints or systemically in the tail are robust and well-tested model of mono- and polyarthritis respectively. Advantages of localized inflammation to the injected joint over polyarthritis are that it causes less discomfort to animals, aids in specifically studying the affected joint and enables the non-injected joint (and neurons that supply it) to act as a control. In the unilateral model of CFA-induced knee inflammation, mice show an acute inflammatory phase lasting 7 days, which upon repeated intra-articular injections develops into a chronic inflammatory state lasting at least for 28 days (Gauldie et al., 2004). These mice also showed behavioral signs of hyperalgesia (reduced amount of pressure required to evoke limb withdrawal) and histological changes in the knee (e.g. hypertrophy of the synovial membrane and infiltration of synoviocytes into the joint space), consistent with observations made in clinical

arthritis (Gauldie et al., 2004), although with less cartilage damage than that of the human disease (Schinnerling et al., 2019). Subsequently it was shown that acute inflammation (within 24-hour of CFA injection) also produces behavioral hyperalgesia in mice (Keeble et al., 2005). Importantly, in both of the above models of monoarthritis (also confirmed by knee diameters reported in this Chapter), inflammation of the contralateral knee was not observed. Therefore, in this study the DRG neurons innervating the contralateral knee were used to compare with neurons innervating the CFA-injected knee. Furthermore, SF samples obtained from mouse knee joints 4 days after CFA injection showed elevated IL-6 levels, similar to the increase observed in human arthritic SF samples (Gobezie et al., 2007; Syx et al., 2018). Due to the similarities observed between the CFA-induced arthritis model in mice and human arthritic conditions, we reasoned that CFA-induced acute inflammation of the knee is a suitable model to investigate mechanisms of arthritic pain.

Although most rodent studies focus on evoked pain behaviors (e.g. paw withdrawal to a noxious stimulus), these are poor indicators of the spontaneous pain experienced in joint pain (Arendt-Nielsen, 2017; Schaible et al., 2002). Therefore, we studied the natural digging behavior of mice with knee inflammation and aimed to determine the underlying molecular drivers in knee-innervating DRG neurons (knee neurons) that are involved in nociception. It is important to specifically study identified knee neurons to investigate joint pain because our lab and others have shown the diversity of DRG neurons using single-cell RNA sequencing (Hockley et al., 2018; Usoskin et al., 2015; Zeisel et al., 2018), electrophysiology Chapter 3/(Chakrabarti et al., 2019a) and immunohistochemistry (da Silva Serra et al., 2016) .

During joint inflammation, protons are released as endogenous mediators and joint acidosis correlates with increased severity of inflammatory arthritis in humans (Farr et al., 1985). Moreover, acidic solutions activate and sensitize rodent nociceptors (Smith et al., 2011; Steen and Reeh, 1993). Interestingly, mice lacking the proton-gated ion channels ASIC3 and TRPV1 have reduced mechanical hyperalgesia following intra-articular CFA injection (Hsieh et al., 2017), but not following subcutaneous hind paw CFA injection, suggesting regional differences exist in nociceptive processing (Staniland and McMahon, 2009). Subsequently, using magnetic resonance spectroscopic imaging, we found no evidence of tissue acidosis following subcutaneous CFA injection (Wright et al., 2018), suggesting absence of a key stimulus for ASIC3/TRPV1 activation, and hence perhaps explaining the lack of phenotype observed in the hind paw CFA model.

However, it remains unknown how proton-gated channels contribute to knee-innervating neuron activation during acute inflammation.

Another group of ion channels involved in processing joint pain is the Transient Receptor Potential (TRP) channel family (Moore et al., 2018). Articular neurons can be activated by the TRP channel agonists capsaicin (TRPV1), cinnamaldehyde (TRPA1) and menthol (TRPM8) (Serra et al., 2016) and both $TRPV1^{-/-}$ and $TRPA1^{-/-}$ mice show reduced pain behavior in CFA models of articular nociception (Chen et al., 2009; Fernandes et al., 2016). Although not tested after CFA-induced joint inflammation, $TRPM8^{-/-}$ mice develop similar mechanical hyperalgesia to wildtype mice following CFA injection into the footpad (Caceres et al., 2017).

After their peripheral terminal activation, sensory neuron input to the spinal cord is pre-synaptically modulated by $GABA_A$ receptor signaling, the source of GABA being spinal cord interneurons (Sutherland et al., 2002). In adults, due to the high intracellular [Cl^-] in DRG neurons compared to central nervous system neurons, activation of $GABA_A$ receptors produces depolarization through Cl^- efflux (Chen et al., 2014). Furthermore, after subcutaneous CFA-induced inflammation in rat paws, the magnitude of GABA-evoked currents is increased in cutaneous DRG neurons (Zhu et al., 2012), as well as in isolated human DRG neurons incubated in an inflammatory soup (Zhang et al., 2015). However, the characteristics of GABA-evoked currents in knee-innervating neurons, and their modulation during inflammation are unknown.

Based upon the above-mentioned studies, I hypothesized that sensitization of knee-innervating neurons following CFA-induced knee inflammation underlies changes in natural behavior. Therefore, the specific aims of this Chapter are 1) to establish digging behavior as an ethologically relevant pain behavior 2) to determine if CFA-induced knee inflammation is associated with knee neuron hyperexcitability, TRP channel and GABA channel functions 3) to investigate whether time-in-culture influences excitability, TRP channel and GABA channel function of DRG neurons 4) to evaluate if systemic administration of a peripherally restricted TRPV1 blocker can reverse digging behavior deficits elicited by acute knee inflammation.

4.3.Methods

See Materials and Methods chapter for detailed description of digging behavior (Section 2.5), mouse knee injections (Section 2.4) and whole cell patch clamp electrophysiology (Section 2.13) on DRG neurons. All animals used in this Chapter were females.

4.4.Results

4.4.1 Inflammation and reduced well-being in mice after unilateral knee joint CFA injection

CFA was injected into the left knee joint of female mice 7 days after FB injection to produce inflammation (Figure 4-2A). Accordingly, robust swelling was observed 24-hour after CFA injection in the ipsilateral knee (pre-CFA, 3.8 ± 0.07 mm vs. post-CFA, 4.6 ± 0.06 mm, $p < 0.0001$, $n = 17$, paired t-test), but not in the contralateral knee (pre-CFA, 3.7 ± 0.07 mm vs. post-CFA, 3.7 ± 0.06 mm, $n = 17$, $p > 0.9$, paired t-test, Figure 4-2 B, C).

Burrowing and digging are natural rodent behaviors and a decrease in burrowing behavior during inflammatory pain indicates reduced well-being in mice (Deacon, 2006b; Jirkof, 2014). Therefore, I hypothesized that in our digging paradigm, mice will dig less after knee inflammation suggestive of joint pain. During a 3 min test period (n = 7, Figure 4-2 A), neither the time spent digging (pre-FB, 45.8 ± 5.9 s vs. post-FB, 39.8 ± 4.7 s, ANOVA, Holm-Sidak's multiple comparison test, Figure 4-2D), nor the number of burrows dug (pre-FB, 3.8 ± 0.3 vs. post FB, 3.7 ± 0.2, ANOVA, Holm-Sidak's multiple comparison test, Figure 4-2E) was altered following FB injection. However, after CFA injection, we observed a decrease in digging time (pre-CFA, 52.7 ± 9.1 s vs. post-CFA, 17.9 ± 6.9 s, $p = 0.003$, ANOVA, Holm-Sidak's multiple comparison test, Figure 4-2D) and a decreased number of burrows dug (pre-CFA, 4.3 ± 0.2 vs. post-CFA, 2.1 ± 0.3, $p = 0.0003$, ANOVA, Holm-Sidak's multiple comparison test, Figure 4-2E). Comparison of post-FB and post-CFA time points also showed that CFA-injection produced a reduction in the time spent digging ($p = 0.003$ ANOVA, Holm-Sidak's multiple comparison test) and in the number of burrows dug ($p = 0.0003$, ANOVA, Holm-Sidak's multiple comparison test). This result indicates that CFA-induced knee inflammation decreases well-being in mice as indicated by the reduction in digging

behavior, which is similar to the reduced feeling of well-being experienced by arthritic patients largely due to spontaneous pain (Hawker et al., 2008; Treharne et al., 2005).

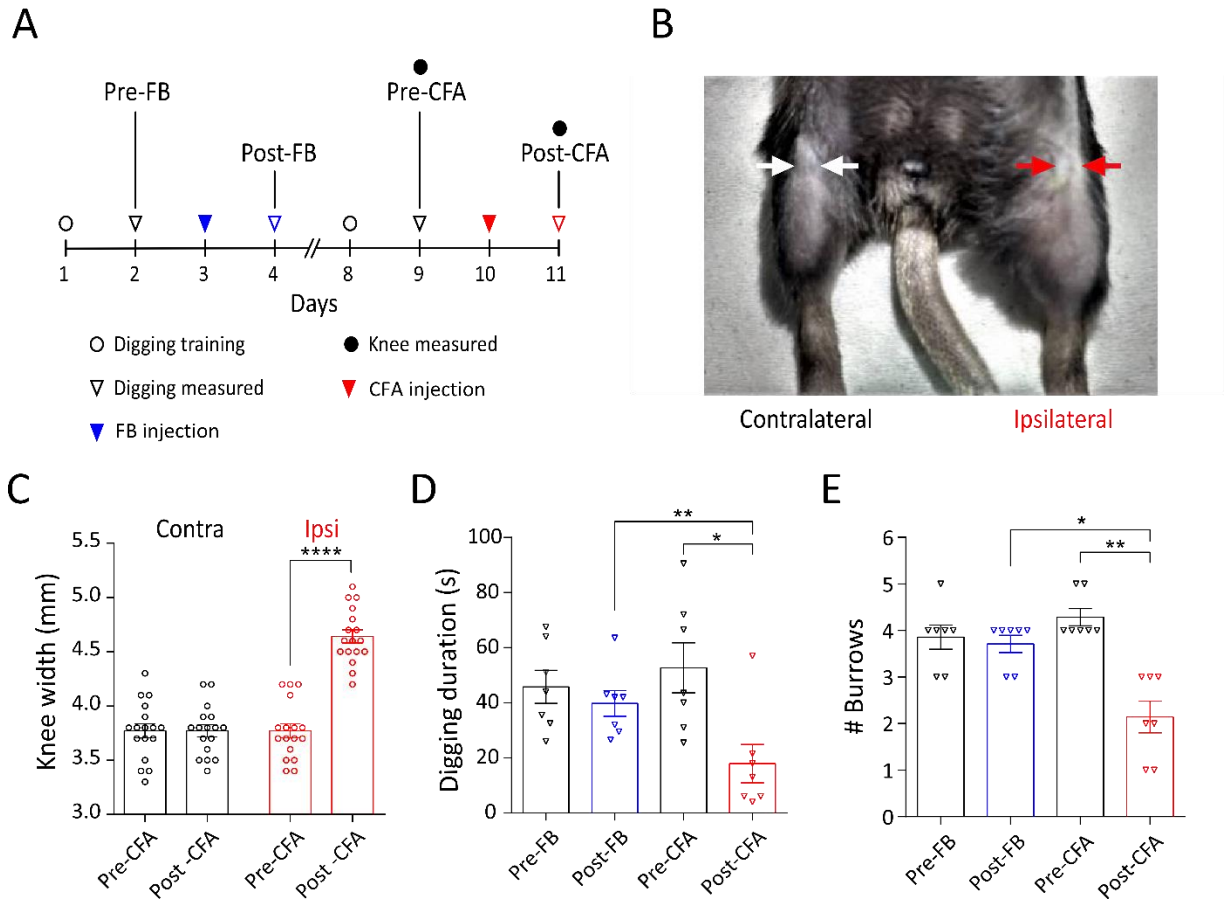

Figure 4-2: CFA model of acute knee inflammation in mice.
A) Experimental timeline indicating when intra-articular injections, behavioral training and measurements were conducted. B) Representative picture of CFA injected (ipsilateral) and non-injected (contralateral) knee (shaved before injections). Arrows indicate where knee width was measured. C) Knee width on the day of CFA injection (pre) and 24-hour after CFA injection (post) in the ipsilateral (red dots) and contralateral (black dots) knee (n = 17). **** indicates $p < 0.0001$, paired t-test. Plots of (D) time spent digging and (E) the number of visible burrows after a 3-min digging test (n = 7). * indicates $p < 0.05$, ** indicates $p < 0.01$, repeated measures ANOVA, Holm-Sidak's multiple comparison test. Error bars indicate SEM.

4.4.2 Action potential threshold of knee neurons decreases after intra-articular CFA injection

To understand the neural basis of the inflammation-induced reduction in digging behavior, I investigated the electrical properties of identified, dissociated knee-innervating DRG neurons. Properties of neurons harvested from the CFA injected side (CFA neurons) were compared to those of knee-innervating neurons isolated from the contralateral side (Cntrl neurons) served as control. Since excitability of neurons is a common feature of pain, I hypothesized that CFA neurons would be hyperexcitable.

Electrically-evoked action potentials (AP, Figure 4-3A) from CFA neurons (CFA, $n = 25$) and Cntrl neurons (Cntrl, $n = 27$) with similar diameters ($p = 0.6$, Figure 4-3B, Table 4-1) were recorded after 4-hour in culture. The AP threshold of CFA neurons was 30 % lower compared to Cntrl neurons ($p = 0.01$, unpaired t-test) (Figure 4-3C, Table 4-1), suggesting increased excitability and sensitization of CFA neurons. By contrast, there was no change in the half-peak duration (HPD, $p = 0.3$, unpaired t-test, Figure 4-3D), afterhyperpolarization (AHP) amplitude ($p = 0.06$, Figure 4-3E) or AP amplitude ($p = 0.7$, unpaired t-test, Table 4-1) of the electrically-evoked APs in CFA neurons compared to Cntrl neurons; however, the AHP duration increased ($p = 0.009$, unpaired t-test, Figure 4-3F).

Table 4-1: Properties of knee-innervating DRG neurons from the CFA injected (CFA) and contralateral (Cntrl) sides across time-in-culture.
* = significance test of CFA vs. Cntrl neurons in the same time group by unpaired t-test, # = significance test of CFA neurons amongst the three time points by ANOVA, ^ = significance test of Cntrl neurons amongst the three time points by ANOVA. */#/^ indicates $p < 0.05$, **/##/^^^ indicates $p < 0.01$, ***/###/^^^ indicates $p < 0.0001$.

	4-hour				24-hour				48-hour			
	CFA (n = 25)		Cntrl (n = 27)		CFA (n = 25)		Cntrl (n = 22)		CFA (n = 23)		Cntrl (n = 22)	
	Mean	SEM	Mean	SEM	Mean	SEM	Mean	SEM.	Mean	SEM	Mean	SEM
RMP (mV)	-55.7	2.1	-58.3	1.6	-55.3	1.3	-52.5	1.9	-55.6	1.3	-54.6	1.8
Diameter (mm)	31.5	0.7	31.9	0.5	31.6	0.8	32.6	0.9	29.2	0.8	29.1	1.1
Capacitance (pF)	45.7	4.2	58.2	4.2	53.8	5.6	52.9	8.2	36.2	4.6	48.5	6.4
Threshold (pA)	384.0	44.3	550.0*	48.3	473.6	42.9	682.7**	48.1	552.2	72.1	475.5	67.5
Half peak duration (HPD, ms)	1.3	0.2	1.0	0.1	1.0	0.2	1.7	0.3	2.1##	0.4	2.6^^^	0.4
Afterhypolarization (AHP, ms)	8.6**	1.0	4.9	0.8	10.8	2.0	7.9	1.5	10.9	1.9	14.3^^^	2.2
Afterhyperpolarization amplitude (AHP amplitude, mV)	16.1	0.8	13.8	0.9	16.5	0.9	14.2	0.9	14.1	1.0	16.8	1.4
Amplitude (mV)	88.2	4.8	86.2	4.6	79.3	5.1	68.3	6.4	82.7	4.6	83.1	5.5

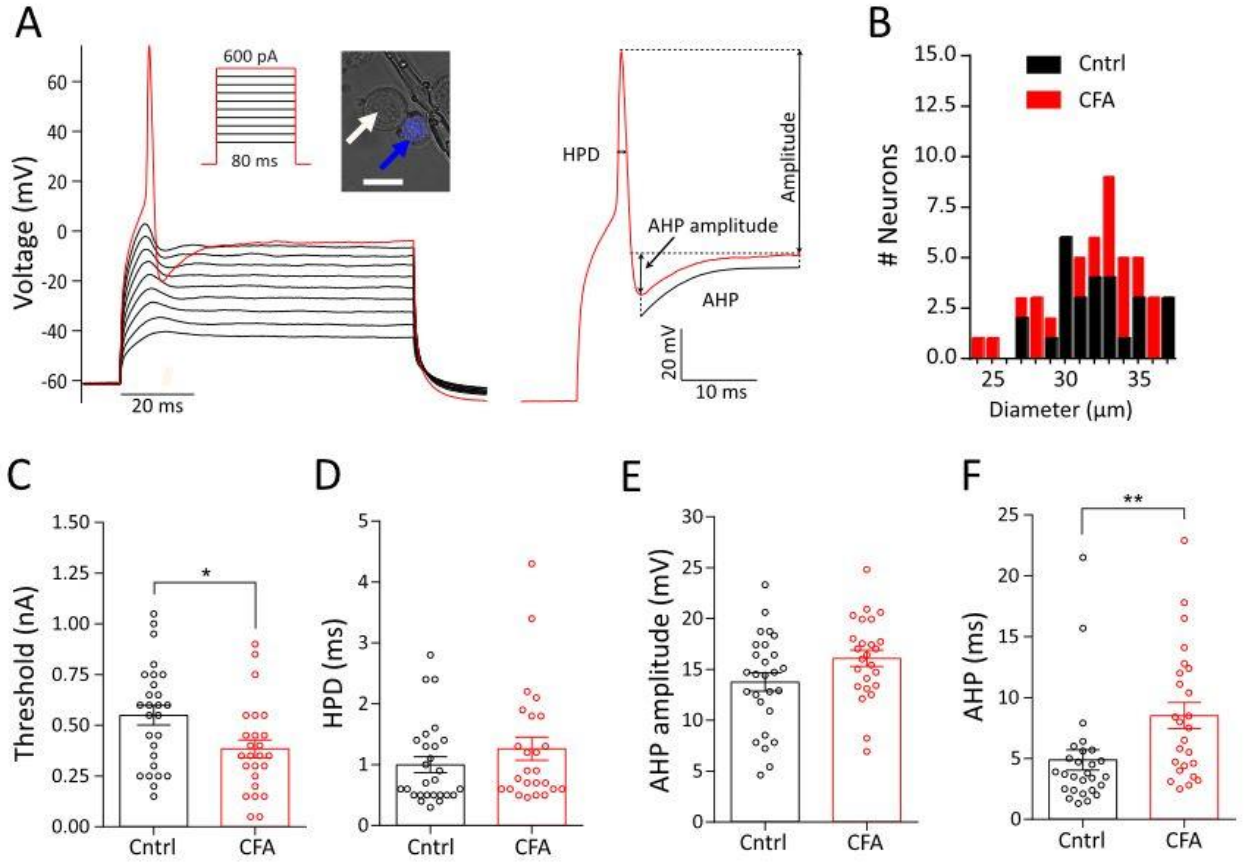

Figure 4-3: Action potential properties of knee neurons following acute knee inflammation.
A) Action potential generation protocol (inset) and response along with a close-up of an evoked AP from a knee neuron showing the different parameters measured. Example of a labeled knee neuron (blue arrow) and an unlabeled neuron (white arrow) shown in inset. Scale bar indicates 25 µm. B) Frequency distribution of neuronal diameter in µm of CFA (red, n = 25) and Cntrl (black, n = 27) neurons. C-F) Distribution of threshold (C), half peak duration (HPD) (D), afterhyperpolarization (AHP) (E) and AHP amplitude (F) after 4-hour in culture. Error bars indicate SEM, * indicates $p < 0.05$, ** indicates $p < 0.01$, unpaired t-test.

4.4.3 Acid-sensitivity does not change in knee neurons following inflammation

pH 5 to pH 7 solutions were used to determine if knee neuron acid sensitivity changes following knee CFA injection. Depending upon the pH stimulus used, virtually all neurons responded with an inward current (pH 7 = 80.6 ± 4.6%, pH 6 = 98.0 ± 2.0% and pH 5 = 100%, combined percentage from CFA and Cntrl groups). Inward currents were either rapidly inactivating followed by a sustained phase (transient + sustained, like those mediated by ASICs) or entirely sustained. The transient + sustained currents were only observed at pH 5 and pH 6 and their frequency was similar in CFA and Cntrl neurons (CFA, 16.3 ± 3.7%; Cntrl, 11.1 ± 3.7%, combined mean of pH 6 and pH 5) (Figure 4-4A and B). Sustained currents were the dominant response across the pH range tested (Figure 4-4A and C) and no difference was observed in the amplitude of response to any pH stimulus between CFA and Cntrl neurons (Figure 4-4D–F, Table 4-2). Furthermore, the magnitude of pH 5 evoked currents was the biggest followed by pH 6, and pH 7 in Cntrl neurons ($p < 0.0001$, ANOVA, Holm-Sidak multiple comparison test). However, no significant differences between the magnitudes of acid-evoked currents were observed in CFA neurons across this pH range.

Overall, this suggests that there was no overt change in acid sensitivity in knee neurons during acute inflammation.

Table 4-2: Sustained peak current densities of CFA and Cntrl DRG neurons in response to acid, TRP channel agonists and GABA across time-in-culture.
= significance test of CFA neurons amongst the three time points by ANOVA, ^ = significance test of Cntrl neurons amongst the three time points by ANOVA. #/^ indicates $p < 0.05$, ##/^^^ indicates $p < 0.01$, ###/^^^ indicates $p < 0.0001$.

Treatment	4-hour						24-hour						48-hour					
	CFA			Cntrl			CFA			Cntrl			CFA			Cntrl		
	Mean	SEM	n	Mean	SEM.	n	Mean	SEM	n	Mean	SEM	n	Mean	SEM	n	Mean	SEM	n
pH 7	1.0	0.2	19	0.6	0.08	23	4.0##	1.0	19	5.7^^^	1.5	17	1.5	0.5	14	1.5	2.7	15
pH 6	2.6	0.9	21	1.5	0.3	25	4.0	0.7	20	5.3	1.6	19	5.8	1.4	22	4.9	1.9	19
pH 5	5.3	2.3	20	2.3	0.3	23	14.9	4.3	21	14.5^^	4.2	19	7.4	1.4	19	7.9	2.9	15
Capsaicin	4.4	2.8	18	0.8	0.1	12	1.8	0.5	22	4.6	2.1	11	10.3	5.1	13	6.4	4.0	10
Cinnamaldehyde	0.8	0.2	10	0.7	0.09	18	2.2	0.4	19	2.3	0.7	14	0.9	0.3	8	2.5	2.0	5
Menthol	0.8	0.2	9	0.9	0.2	14	1.0	0.2	12	1.6	0.4	9	1.2	0.7	8	2.8	2.2	3
GABA	7.2	2.0	19	3.9	1.1	26	11.8*	2.6	22	4.3	0.9	19	8.3	2.7	18	4.3	1.7	16

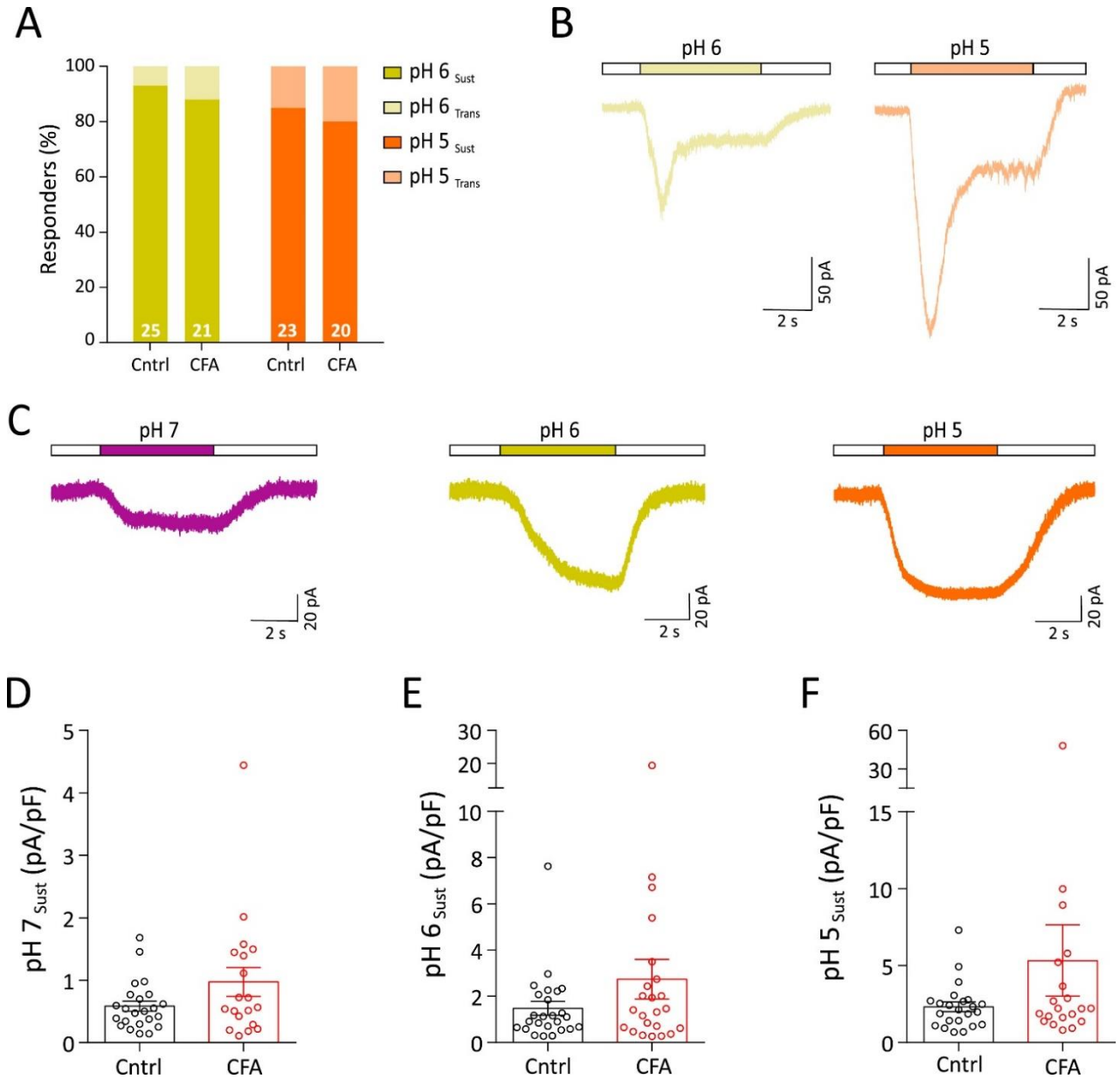

Figure 4-4: Acid sensitivity of knee neurons after acute inflammation.
A) Percentage frequency of transient + sustained vs. sustained only response to pH 6 (transient + sustained, light yellow; sustained, dark yellow) and pH 5 (transient + sustained, light orange; sustained, orange) B) Example traces of transient + sustained acid currents in response to pH 6 (light yellow) and pH 5 (light orange). C) Example traces of sustained response to pH 7 (purple), pH 6 (dark yellow) and pH 5 (orange). D-F) Peak current density of sustained pH 7, pH 6 and pH 5 responses (CFA: red dots, Cntrl: black dots).

4.4.4 Inflammation increases the proportion of TRPV1 expressing knee neurons

To determine if any change in TRP-mediated chemosensitivity occurs in knee neurons following exposure of distal nerve terminals to inflammatory mediators after CFA injection, I tested 10 μM capsaicin, 100 μM cinnamaldehyde and 100 μM menthol, agonists of TRPV1, TRPA1 and TRPM8 respectively.

The percentage of capsaicin-sensitive CFA neurons increased significantly compared to Cntrl neurons (CFA, 72% vs. Cntrl, 44%, $\chi2(1) = 4.0$, $p = 0.04$, chi-sq test, Figure 4-5A), but no change in the proportion of cinnamaldehyde-sensitive (CFA, 40%, Cntrl, 67%, $\chi2(1) = 3.7$, $p = 0.06$; chi-sq test, Figure 4-5B) or menthol-sensitive neurons (CFA, 35%, Cntrl, 51%, $\chi2(1) = 1.3$, $p = 0.2$, chi-sq test, Figure 4-5C) was observed. The magnitude of capsaicin ($p = 0.3$, unpaired t-test, Table 4-2), cinnamaldehyde and menthol-evoked currents (Table 4-2, cinnamaldehyde, $p = 0.5$; menthol, $p = 0.9$, unpaired t-test) also remained unchanged between the inflamed and non-inflamed condition.

Since an increased proportion of knee DRG neurons responding to capsaicin in inflammation suggests recruitment of a previously capsaicin "silent" population (Figure 4-5D), I expected an increased level of TRPV1 expression in knee neurons. To determine if this was the case, immunohistochemistry was conducted on whole DRG sections (L2-L5) from ipsilateral (CFA, $n = 1089$ neurons) and contralateral (Cntrl, $n = 1334$ neurons) sides of four mice (Figure 4-5Ei), and revealed that a significantly higher proportion of CFA neurons expressed TRPV1 (59.7%) compared to Cntrl neurons (44.6%, $\chi2(1) = 48.03$, $p < 0.0001$, chi-sq test, Figure 4-5Eii). One mechanism of TRPV1 upregulation is through binding of the inflammatory mediator NGF to its high affinity receptor tropomyosin receptor kinase A (TrkA) (Ji et al., 2002). In order to test whether NGF might be responsible for the observed upregulation of TRPV1 protein expression, we calculated the co-expression of TRPV1 and TrkA. Although, the proportion of knee neurons expressing TrkA (CFA, 39.3%, Cntrl, 42.6%) (Figure 4-5Eii) was no greater in CFA neurons than Cntrl neurons, there was a small, yet significant, increase in the proportion of CFA neurons co-expressing TRPV1 and TrkA compared to Cntrl neurons (CFA, 29.8%; Cntrl, 24.8%, $\chi2(1) = 5.6$, $p = 0.02$, chi-sq test, Figure 4-5Eii). Taken together, our data suggests that NGF-TrkA signaling might partially contribute to increased TRPV1 expression following CFA injection into the knee.

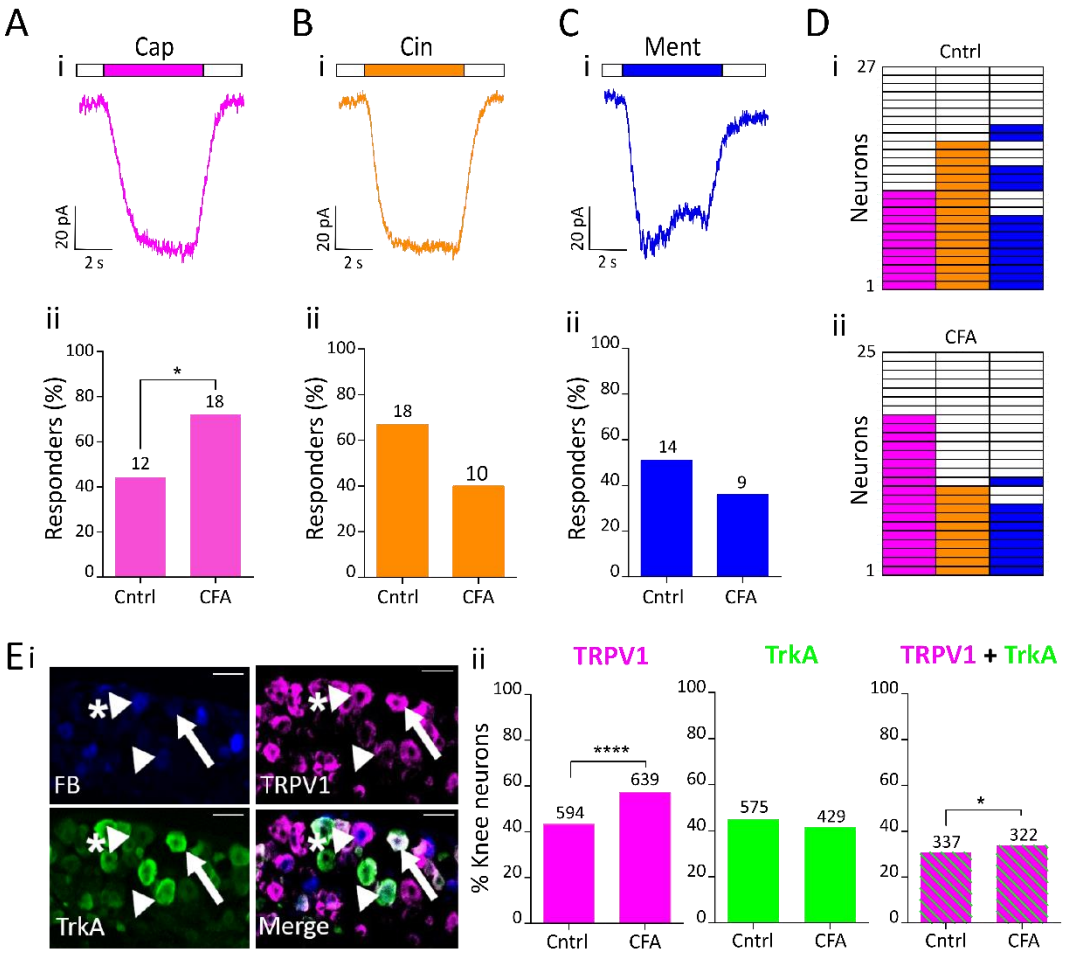

Figure 4-5: TRP agonist response profile of knee neurons following inflammation.
Representative traces of 10 μM capsaicin (pink, Ai), 100 μM cinnamaldehyde (orange, Bi) and 100 μM menthol (blue, Ci) response from a CFA neuron and their respective percentage frequency (Aii, Bii, Cii). D) Heat map of Cntrl (i, n = 27) and CFA (ii, n = 25) neurons responding to capsaicin, cinnamaldehyde and menthol. E (i) Representative images of a whole DRG section from L4 showing fast blue (FB) labeling from the knee (blue), TRPV1 expression (pink), TrkA expression (green) and a merged image; sections from an animal injected with CFA. White arrowhead shows a knee neuron that only expresses TrkA, white arrowhead with asterisk shows a knee neuron that expresses only TRPV1 and white arrow shows a knee neuron that co-expresses TRPV1 and TrkA. (ii) Proportion of knee neurons (L2-L5) that express TRPV1 (pink), TrkA (green) and both TRPV1 and TrkA (green and pink stripes) from Cntrl (n = 1334) and CFA (n = 1089) injected side. Numbers above the bars represent neurons stained positive with respective antibodies. * indicates $p < 0.05$, **** indicates $p < 0.0001$, chi-sq test.

4.4.5 Sustained $GABA_A$-evoked current magnitude increases in knee neurons following inflammation

Unlike in the central nervous system, GABA signaling can be excitatory in the peripheral nervous system and an inflammation-induced increase in amplitude of GABA-evoked currents has been reported in skin-labeled rat DRG neurons (Zhu et al., 2012). Based on this, I hypothesized that acute knee inflammation might also increase the magnitude of GABA-evoked currents in knee-innervating DRG neurons. Two types of GABA response were observed: i) the current reached a peak within 1.5 s of GABA application and was classified as transient + sustained (TS) (Figure 4-6Ai and Aii) and ii) the current did not reach its peak within the first 1.5 s, showed no desensitization and was classified as sustained (S, Figure 4-6Aiii). There were two further subtypes of TS responses: one showing a relatively monophasic desensitization throughout GABA application (Figure 4-6Ai) and a second showing a far slower desensitization with a more stable sustained phase (Figure 4-6Aii); I did not distinguish between these two categories due to the paucity of neurons in the first subgroup and since no response returned to baseline within 5 s.

There was no difference in the frequency of TS and S responses in CFA and Cntrl neurons (CFA: TS, 48%, S, 28% vs. Cntrl: TS, 52%, S, 44%, Figure 4-6Bi); although 100 μM GABA evoked a response in significantly fewer CFA (76%) than Cntrl (96%) neurons ($\chi 2(1) = 4.6$, $p = 0.03$, chi-sq test, Figure 4-6Bi). No difference in the GABA-evoked peak current density was observed overall between CFA and Cntrl neurons (Figure 4-6Bii, Table 4-2), however, GABA-evoked S type currents were of a significantly larger magnitude in CFA than Cntrl neurons (CFA, 8.0 ± 4.1 pA/pF, $n = 7$ vs. Cntrl, 1.7 ± 0.6 pA/pF, $n = 14$, $p = 0.04$, unpaired t-test). No such difference was observed for TS type currents (CFA, 6.7 ± 2.4 pA/pF, $n = 12$ vs. Cntrl, 6.5 ± 1.9, $n = 12$, $p = 0.9$, unpaired t-test) (Figure 4-6Biii).

I further investigated the subunit composition of the S-type GABA-evoked currents that showed a small, but significant increase in inflammation. All GABA-evoked currents were bicuculline (a $GABA_A$ antagonist) sensitive to some extent with bicuculline inhibiting more than 50% GABA responses in 6/7 CFA DRG and 8/12 Cntrl DRG (Figure 4-6Ci). These results replicate the previous observation in rat DRG neurons, that a fraction of the GABA-evoked current is bicuculline insensitive (Lee et al., 2012). The same study showed that S type $GABA_A$ currents can be mediated by δ subunit containing $GABA_A$ receptors and thus I tested the ability of the $GABA_A$

δ subunit agonist THIP to evoke currents in knee neurons. A sustained current in response to THIP was observed in 4/8 CFA and 6/11 Cntrl neurons, indicating similar expression of δ subunit containing $GABA_A$ receptors in knee neurons (Figure 4-6Ci, Cii). The peak current density of THIP-evoked currents was also similar ($p = 0.9$, unpaired t-test) in CFA (0.6 ± 0.2 pA/pF) and Cntrl (0.5 ± 0.1 pA/pF) neurons.

Surprisingly, not all neurons with S type GABA response showed THIP sensitivity; this combined with the presence of some bicuculline insensitive currents, suggests expression of either ρ subunit containing $GABA_A$ receptors, or perhaps $GABA_B$ receptors, both of which produce sustained currents in response to GABA and are not inhibited by bicuculline (Chebib and Johnston, 2001). Taken together, these data indicate the presence of diverse $GABA_A$ receptor subunits in CFA and Cntrl neurons and demonstrate an increase in GABA-mediated neuronal excitation following knee inflammation, although the detailed signaling and consequences of this excitation needs further investigation.

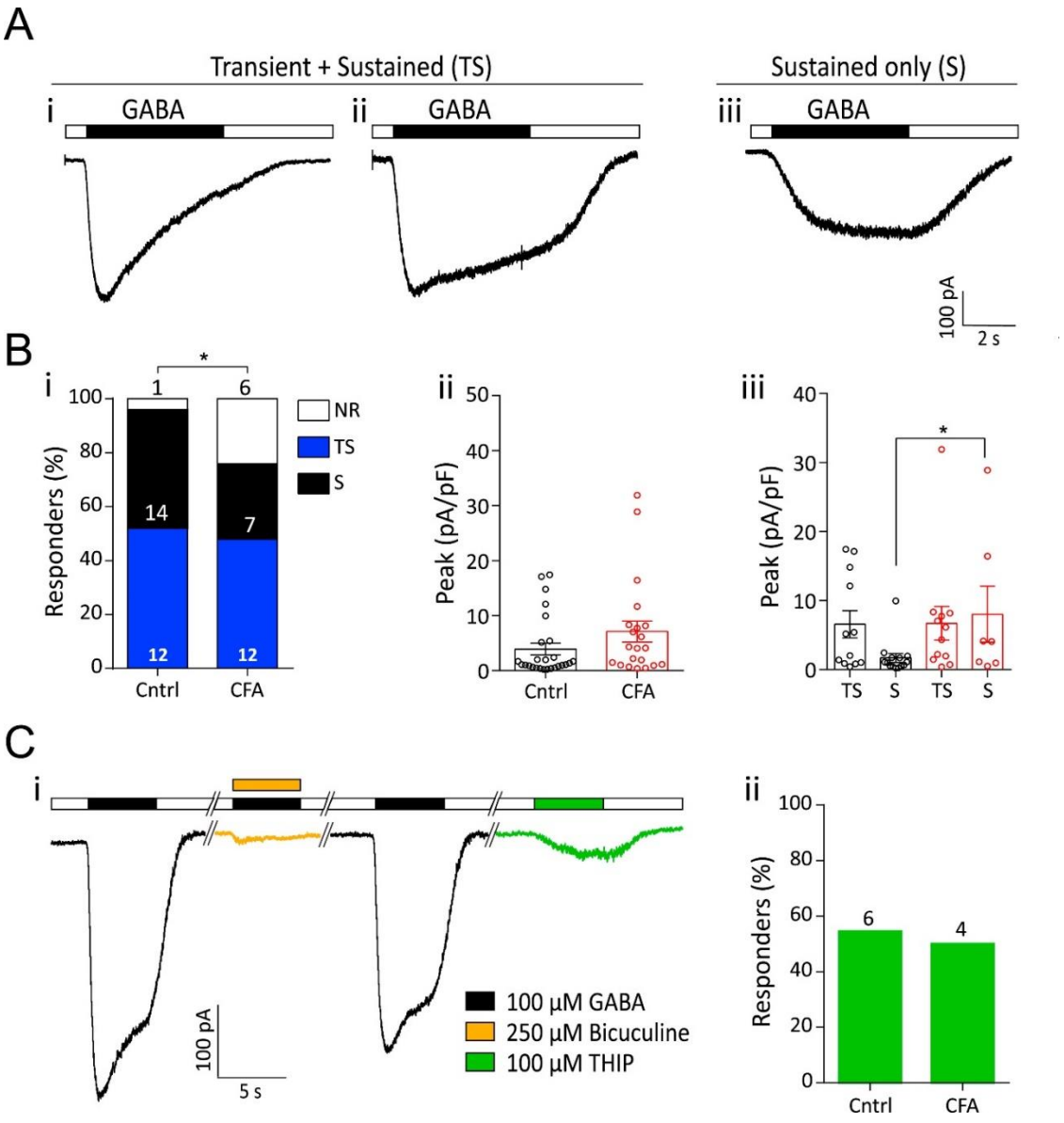

Figure 4-6: GABA-evoked currents in knee neurons after acute inflammation.
A) Representative traces of 100 µM GABA-evoked currents showing both transient and sustained phases (i, ii) and currents with only a sustained phase (iii). B (i) Percentage frequency of GABA-evoked transient + sustained currents (blue bars), sustained currents (black bars) and non-responders (white bars) in Cntrl and CFA neurons. (ii) Peak current density of all GABA-evoked currents (Cntrl: n = 26, CFA: 19) and (iii) GABA-evoked currents split into TS and S type (Cntrl: black dots; CFA: red dots). TS = transient + sustained currents, S = sustained only currents, error bars indicate SEM, * indicates $p < 0.05$, unpaired t-test. C) i - Example trace of bicuculline block (yellow) of GABA-evoked currents and THIP-evoked current (green) in a single neuron. ii – percentage frequency of Cntrl (n = 11) and CFA (n = 8) neurons with a GABA response that also responded to THIP. The numbers above the bars indicate the number of responsive neurons.

4.4.6 Time-in-culture leads to loss of inflammation-induced sensitization of knee neurons

Both the period of time that neurons cultured for prior to recordings (time-in-culture) and the constituents of the culture medium can greatly alter neuronal excitability (Scott and Edwards, 1980; Winter et al., 1988), and are thus both factors that can confound studying inflammation-induced changes in neuronal excitability, i.e. changes can occur *in vitro* in addition to those occurring *in vivo* prior to neuron isolation. To systematically characterize the effect of time-in-culture, I repeated the experiments described above on the CFA and Cntrl knee neurons after 24-hour (CFA, n = 25; Cntrl, n = 22) and 48-hour (CFA, n = 23; Cntrl, n = 22) in culture.

No change was observed in the resting membrane potential, capacitance or AP amplitude (Table 4-1) across the three time points. By contrast, whereas the AP threshold was similar across time points for CFA neurons ($p = 0.09$, ANOVA), it decreased for Cntrl neurons after 48-hour in culture compared to 24-hour ($p = 0.03$, ANOVA, Holm-Sidak multiple comparison test, Table 4-1). Interestingly, the inflammation-induced decrease in AP threshold of CFA neurons compared to Cntrl neurons that was observed at 4-hour (Figure 4-3C) and 24-hour ($p = 0.002$, unpaired t-test, Table 4-1) disappeared after 48-hour in culture (Table 4-1, $p = 0.44$, unpaired t-test), which suggests that time-in-culture leads to a loss of inflammation-induced hyperexcitability.

There was also a distinct AP widening, characterized by an increase in both HPD and AHP in the 48-hour group for Cntrl neurons, but just the HPD in CFA neurons. HPD increased by ~60% after 48-hour in both CFA ($p = 0.01$, ANOVA, Holm-Sidak multiple comparison test) and Cntrl ($p = 0.007$, ANOVA, Holm-Sidak multiple comparison test) neurons compared to the 4-hour group (Table 4-1). In Cntrl neurons, AHP increased by 191% in the 48-hour group compared to 4-hour and 81% compared to 24-hour group ($p = 0.0002$, ANOVA, Holm-Sidak multiple comparison test, Table 4-1). One CFA and one Cntrl neuron in the 48-hour culture group were excluded from this analysis because of a highly different AP waveform that could not be analyzed using the same measurements.

With regards to knee neuron acid sensitivity, the percentage of neurons with transient + sustained currents in response to pH 6 and pH 5 at 24-hour and 48-hour (Figure 4-7A) was similar to that at 4-hour (Figure 4-4A). Although a largely reversible increase in pH 7- (CFA and Cntrl) and pH 5-evoked (Cntrl) current amplitude was observed at 24-hour (pH 7: CFA, $p = 0.005$; Cntrl,

$p = 0.0003$; pH 6: CFA, $p = 0.06$; Cntrl, $p = 0.08$; and pH 5: CFA, $p = 0.06$; Cntrl, $p = 0.008$, ANOVA) (Table 4-2), there was no clear trend across different pH stimuli for either CFA or Cntrl neurons.

For knee neuron TRP-mediated chemosensitivity, the CFA-induced increase in the proportion of capsaicin-sensitive neurons observed at 4-hour was maintained at 24-hour (CFA, 88% vs. Cntrl, 50%, $\chi2(1) = 8.1$, $p = 0.004$, chi-sq test), but was absent in the 48-hour group (CFA, 54.2% vs. Cntrl, 43.5%, $\chi2(1) = 0.5$, $p = 0.5$, chi-sq test), a result that further confirms observations that after 48-hour in culture the inflammation-induced effects are lost. In addition, the proportion of cinnamaldehyde (CFA, 33.3%; Cntrl, 21.7%) and menthol-sensitive (CFA, 33.3%; Cntrl, 13.0%) neurons after 48-hour in culture decreased compared to the other two time points, although this decrease was only significant in Cntrl neurons (cinnamaldehyde, $\chi2(1) = 11.9$, $p = 0.0006$; menthol, $\chi2(1) = 7.8$, $p = 0.005$, chi-sq test) (Figure 4-7B). No significant difference in the peak current density of TRP agonist-evoked currents was observed across time-in-culture (Table 4-2).

When GABA-evoked currents were split into TS and S types, no changes in the peak current density were observed between CFA and Cntrl after 24-hour or 48-hour in culture. However, combining both TS and S currents, CFA neurons had larger amplitude GABA-evoked currents than Cntrl neurons after 24-hour in culture ($p = 0.01$, unpaired t-test, Table 4-2); an effect that was not seen in the 48-hour group ($p = 0.2$, unpaired t-test, Table 4-2). Previously, it has been shown in cultured rat DRG neurons that the proportion of S type GABA-evoked currents increased with time-in-culture (Lee et al., 2012), a result replicated here in mouse knee neurons (CFA, $\chi2(1) = 4.8$, $p = 0.03$, Cntrl, $\chi2(1) = 5.4$, $p = 0.02$, chi-sq test, Figure 4-7C). From this data, it could be recommended to avoid using DRG neurons for longer than 28-hour in culture to prevent loss of inflammation-induced sensitization events.

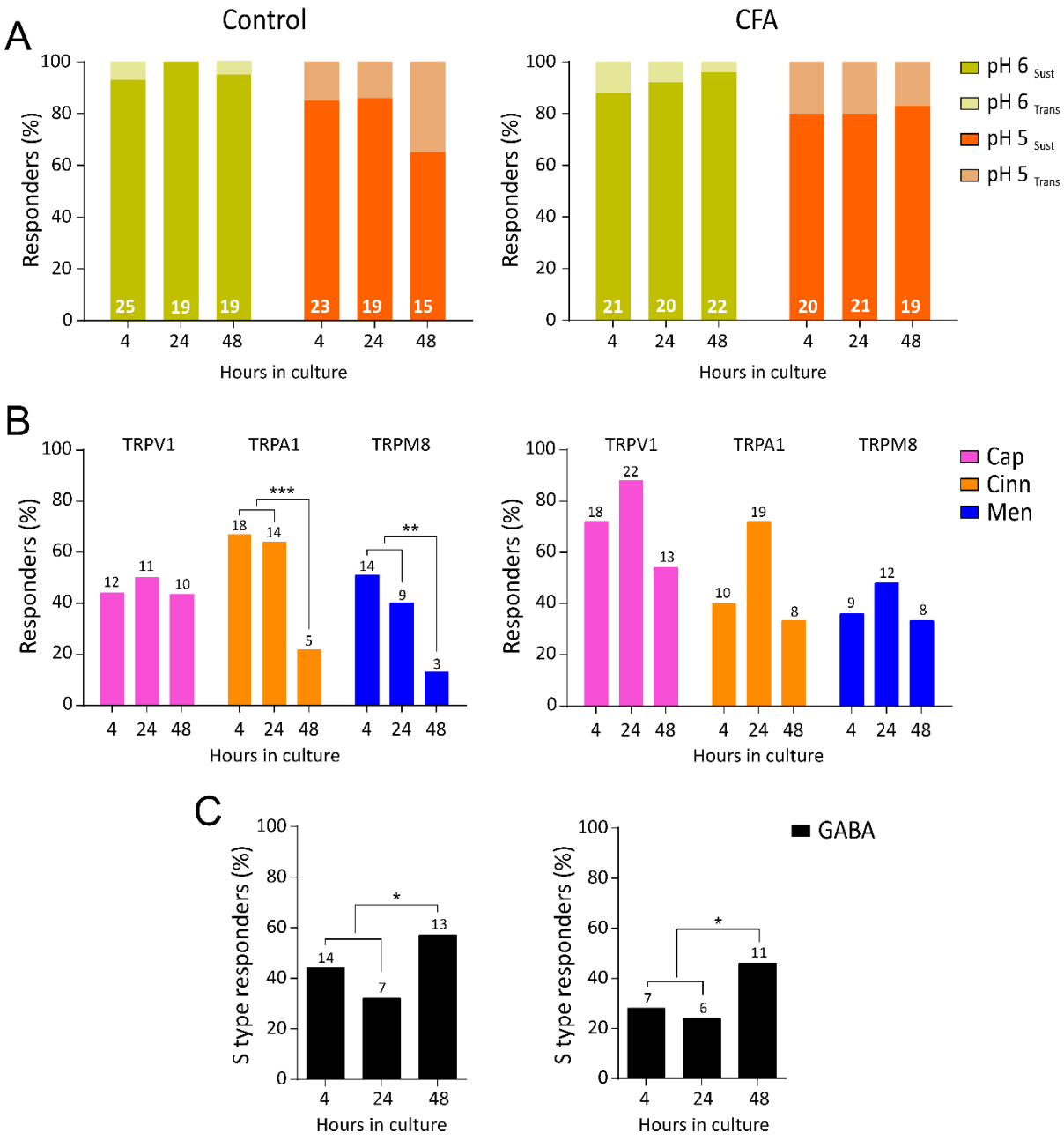

Figure 4-7: Time-in-culture effects on acid, TRP agonist and GABA sensitivity of knee neurons after inflammation.
A) Proportion of Cntrl (left) and CFA (right) neurons responding to pH 6 (yellow) and pH 5 (orange) with a transient + sustained type current (light shade) and sustained only type current (dark shade) across 4, 24 and 48-hour. B) Percentage frequency of Cntrl (left) and CFA (right) neurons sensitive to capsaicin (pink), cinnamaldehyde (orange) and menthol (blue) across 4, 24 and 48-hour in culture. C) Percentage of Cntrl (left) and CFA (right) neurons that had a sustained GABA-evoked current across 4, 24 and 48-hour in culture. * indicates $p < 0.05$, chi-sq test. The numbers above the bars indicate the number of responsive neurons.

4.4.7 TRPV1 inhibition reverses inflammation induced decrease in digging behavior

From characterization of CFA and Cntrl neurons, knee neuron TRPV1 expression emerged as an important target in CFA-induced knee inflammation due to is increased expression. Thus, I hypothesized that the decrease in digging behavior due to knee inflammation observed in mice can be reversed by the peripherally restricted TRPV1 antagonist A-425619.

On day 2 of the experimental timeline (Figure 4-8A), both the CFA group ($n = 10$) and saline group ($n = 7$) spent a similar amount of time digging (CFA, 31.1 ± 6.1 s; Saline, 33.8 ± 6.4 s) and produced a similar number of burrows (CFA, 4.3 ± 0.4; Saline, 3.4 ± 0.4) during a 3 min test in the digging cage. Following CFA/saline injection, the CFA group showed an expected decrease in digging duration (17.4 ± 5.2 s, $p = 0.001$, repeated measures ANOVA, Holm-Sidak multiple comparison test, Figure 4-8B). In agreement with my hypothesis, this reduction of digging behavior in the CFA group was reversed 30 min after the injection of A-425619 (36.4 ± 7.0 s, $p = 0.001$, ANOVA, Holm-Sidak multiple comparison test, Figure 4-8B). A similar result was also obtained with the number of burrows (post-CFA, 2.1 ± 0.3; post-Antag, 4.0 ± 0.2, $p < 0.0001$, repeated measures ANOVA, Holm-Sidak multiple comparison test, Figure 4-8C). By contrast, the saline group did not show a decrease in digging behavior 24-hour after saline injection into the knee (Digging duration, 33.1 ± 5.3 s, $p = 0.5$; # Burrows, 3.7 ± 0.5, $p = 0.7$, repeated measures ANOVA, Holm-Sidak multiple comparison test, Figure 4-8D and E), further confirming that intra-articular injections do not affect digging behavior. The TRPV1 antagonist A-425619 also produced no effect on digging behavior in the saline group (Digging duration, 25.9 ± 6.3 s, $p = 0.5$; # Burrows, 3.3 ± 0.4, $p = 0.7$, ANOVA, Figure 4-8D and E), i.e. inhibition of TRPV1 does not interfere with spontaneous digging activity of mice. These results suggest that TRPV1 is an important mediator of inflammatory knee pain and might contribute to the inflammation-induced decrease in digging behavior in mice.

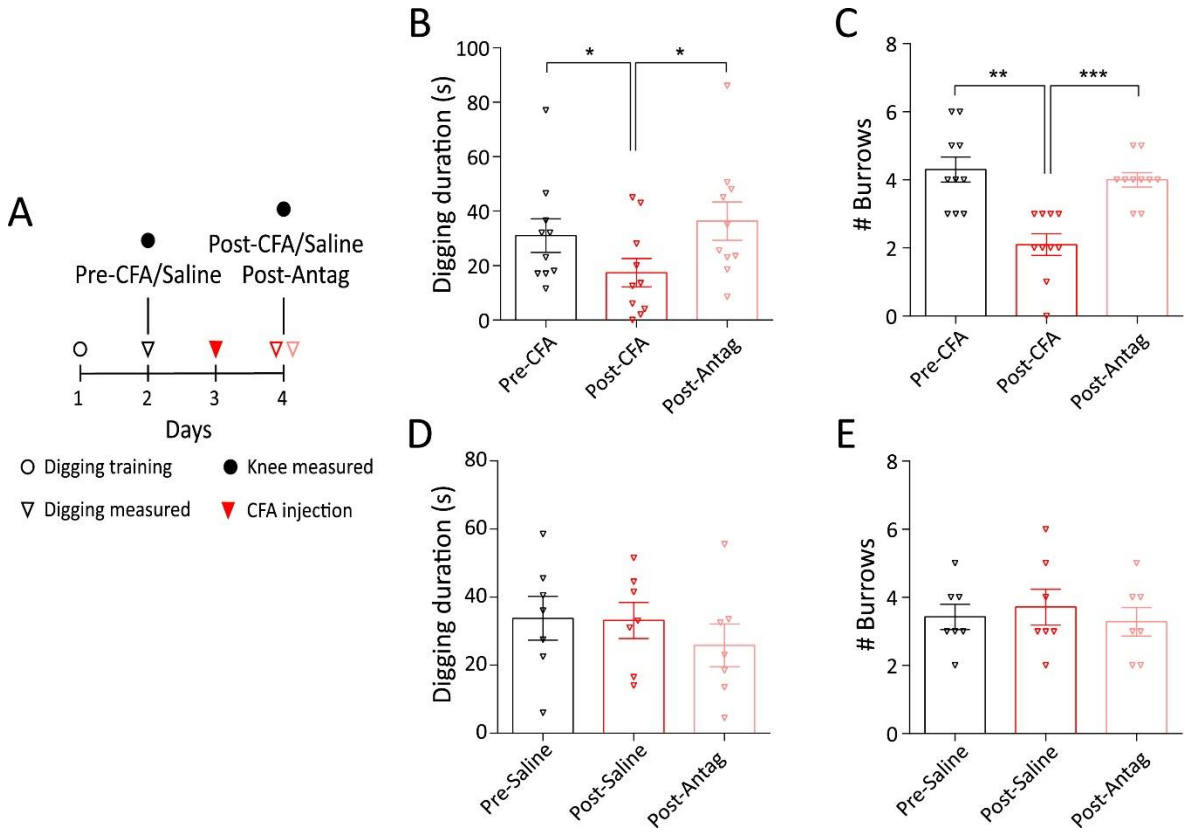

Figure 4-8: Digging behavior after injection of the TRPV1 antagonist A-425619.

A) Experimental timeline highlighting the days where behavioral testing and injection was performed. Distribution of time spent digging and the number of burrows in the CFA (B, C, n = 10) and saline group (D, E, n = 7). * indicates $p < 0.05$, ** indicates $p < 0.01$, *** indicates $p < 0.0001$. rmANOVA, Holm-Sidak multiple comparison test. Error bars indicate SEM.

4.5. Discussion

Innate rodent behaviors, such as burrowing, digging and nest-building are emerging assays of spontaneous pain that seek to mirror human activities of daily living (Deacon, 2006b; Jirkof, 2014). A decrease in burrowing behavior was observed in rats with CFA-induced knee inflammation (Rutten et al., 2014) and digging is a similar innate behavior that is quick and easy to test in a laboratory (Deacon, 2006b). Here we show that 24-hour after CFA-induced knee inflammation, mice spent significantly decreased time digging, suggesting that digging can be used as an ethologically relevant pain assay in mice; importantly, intra-articular injection of the retrograde tracer FB did not alter digging behavior.

Combining electrophysiology and retrograde labelling of the knee joints, I found enhanced excitability of knee neurons, manifested as decreased AP firing threshold. I also observed a contradictory increase in AHP relaxation time constant (but no change in AHP amplitude) because an increase in current mediated by hyperpolarization-activated cyclic nucleotide-gated ion channels (HCN), and thus a decrease in AHP, is associated with repetitive firing, as shown by one study in trigeminal ganglia neurons after CFA-induced inflammation (Flake and Gold, 2005). However, other studies using CFA-induced hind limb inflammation either observed no change in AHP (like our data at 24-hour in culture) (Djouhri and Lawson, 1999) or reported a decrease in AHP only in C-fibers (Weng et al., 2012). Therefore, our data possibly demonstrates the multifaceted nature of the molecular mechanisms regulating AHP, a suggestion supported by the wide range of AHP values reported (Djouhri et al., 1998; Lawson et al., 1996).

I also provide electrophysiological evidence that the number of capsaicin-sensitive (i.e. TRPV1 expressing) knee neurons increases during acute inflammation from ~50% to ~80%, suggesting recruitment of a previously silent neuronal population. This is an important finding because although it is known that inflammatory mediators released during joint pain can sensitize TRP channels, the role of TRPV1 and TRPA1 in acute inflammatory joint pain is unclear. Some studies report that TRPV1$^{-/-}$ mice do not develop CFA- (Keeble et al., 2005) or carrageenan- (Davis et al., 2000) induced hyperalgesia and others have shown that in DRG neurons TRPV1 protein expression increases in CFA-induced inflammation (Amaya et al., 2003; Ji et al., 2002; Yu et al., 2008). In direct contrast, other studies failed to show increased neuronal TRPV1 protein (Bär et al., 2004; Zhou et al., 2003) or mRNA expression (Ji et al., 2002) following CFA-induced

inflammation. Similarly, TRPA1$^{-/-}$ mice show normal development of CFA-induced hyperalgesia in some studies (Fernandes et al., 2011; Petrus et al., 2007), whereas others report attenuation of CFA- and carrageenan-induced hyperalgesia in TRPA1$^{-/-}$ mice (Garrison and Stucky, 2014; Moilanen et al., 2012) or following administration of a TRPA1 antagonist (Bonet et al., 2013; Eid et al., 2008). In agreement with our electrophysiological data, immunohistochemistry showed a similar magnitude increase in the proportion of TRPV1 expressing knee neurons.

The importance of increased TRPV1 function was demonstrated by reversal of the inflammation-induced reduction in digging behavior in mice by systemic administration of the TRPV1 antagonist, A-425619, which suggests that the increased TRPV1 expression observed at the cellular level drives the pain behaviors. Interestingly, it has recently been shown that intra-articular administration of a TRPV1 antagonist attenuated early osteoarthritic pain in a mono-sodium iodoacetate model of osteoarthritis (Haywood et al., 2018), thus suggesting a likely contribution of TRPV1 to arthritic pain in general. Historically in pre-clinical models, TRPV1 antagonists attenuated thermal hyperalgesia, but their efficacy in mechanical hyperalgesia and ongoing pain is unclear (Brandt et al., 2012). The peripherally restricted TRPV1 antagonist, A-425619, has been previously shown to reverse thermal and mechanical hypersensitivity in rat CFA models and also restore weight bearing ability in rat osteoarthritis models (Honore et al., 2005). Our data further establishes TRPV1 as an important drug target in inflammatory joint pain.

Multiple mechanisms may contribute to the increase in TRPV1 expression observed, for example, NGF released from a variety of cell types in arthritic joints may bind to TrkA and get retrogradely transported to DRG neurons to drive TRPV1 expression. Indeed, increased levels of NGF are found in rheumatic diseases and anti-NGF/TrkA therapy reduces arthritic pain in human and animal models (reviewed in (Seidel et al., 2013)). With regard to CFA-induced pain, it has been previously shown that the proportion of TrkA-expressing neurons innervating bone does not increase following CFA-induced bone pain (Nencini et al., 2017). We also observed no change in TrkA expression, but did observe a slight, yet significant, increase in TrkA-TRPV1 co-expression following knee inflammation which suggests that NGF-TrkA signaling may play a role in the increased TRPV1 expression observed here, but this requires further investigation, for example, repeating the study and administering an anti-NGF antibody to block NGF-TrkA signaling.

Protons are algogens detected by sensory neurons through a variety of means, including ASICs, TRPV1, background K^+ channels, Cl^- channels and proton-sensing G-protein coupled receptors (Pattison et al., 2019). I evaluated direct proton activation of knee neurons and found that acid-evoked currents are neither enhanced, nor is there any change in the proportion of ASIC-like currents, following CFA-induced knee inflammation. This result contradicts a previous report that showed decreased hyperalgesia of ASIC3$^{-/-}$, TDAG8$^{-/-}$ (T cell death associated gene, a proton-sensing GPCR) and TRPV1$^{-/-}$ mice after ankle inflammation (Hsieh et al., 2017) and another report that observed upregulation of ASIC3 immunoreactivity in knee-innervating DRG neurons after carrageenan-induced acute knee inflammation in mice (Ikeuchi et al., 2009). However, our findings agree with another study where ASIC1, ASIC2 and ASIC3 knockout mice did not display attenuated thermal or mechanical hyperalgesia after intraplantar CFA injection, suggesting that these ASIC subunits play no role in cutaneous CFA-induced hyperalgesia (Staniland and McMahon, 2009).

Information transfer from peripheral to central afferents is modulated by GABAergic signaling. $GABA_A$ receptors can modulate spinal pain processing by either post synaptic or pre synaptic inhibition. Pre-synaptic inhibition is produced by the afferent inputs from DRG neurons. Upon application of GABA, $GABA_A$ receptors are opened resulting in Cl^- efflux in DRG neurons because of the high intracellular Cl^- concentration (Batti et al., 2013; Kaneko et al., 2004). This phenomenon is called primary afferent depolarization (PAD). Under healthy conditions, PAD still produces pre-synaptic inhibition through inactivation of voltage gated Na^+ or Ca^{2+} channels, thus preventing AP generation/neurotransmitter release; and/or through a shunting mechanism which increases membrane conductance thus reducing neurotransmitter release (reviewed in (Guo and Hu, 2014)). During tissue/nerve damage (for example, inflammation), GABA-evoked PAD can switch from inhibitory to excitatory/dis-inhibitory by a depolarizing shift in E_{GABA} that increases PAD (which might result in direct action potential generation) (Cervero et al., 2003; Chen et al., 2014; Willis, 1999) and/or by a decrease in GABA-mediated conductance (Wei et al., 2013). Our data showing an increase in the magnitude of a subset GABA-evoked currents is consistent with a GABA-mediated disinhibitory effect in DRG neurons following acute knee inflammation.

Lastly, I show that time-in-culture does not affect inflammation-induced lowering of AP threshold up to 28-hour in culture, but that the lowered threshold is lost at 48-hour in culture. Furthermore I

show AP broadening, and a slight decrease in AP threshold in neurons from the contralateral side as reported before during a similar time course (Scott and Edwards, 1980). The present study also shows a decline in the frequency of response to capsaicin, cinnamaldehyde and menthol and the inflammation-induced increase in frequency of capsaicin-sensitive neurons, although maintained for up to 28-hour in culture is lost after 48-hour. Understanding how time-in-culture alters neuronal excitability is important for correctly designing studies, especially in such a widely used *in vitro* model as the acutely dissociated DRG neurons (Lee et al., 2012). Although this model has been extensively studied with patch clamp electrophysiology, the definition of "acute" remains relatively fluid – with some studies recording within 8-hour of dissection, while others make recordings after overnight incubation (18–28-hour). Based on this study, I conclude that electrophysiological properties in acutely dissociated DRG neurons remain relatively stable up to 28-hours.

In summary, we show that following unilateral acute inflammation of the knee, knee neurons have 1) a lower AP threshold 2) increased sensitivity to capsaicin and expression of TRPV1 and 3) an increasing trend in the magnitude of GABA-evoked currents up to 28-hours in culture. This specific sensitization signature of knee neurons highlights the importance of studying DRG neurons as a spatially heterogeneous group. Among these different modes of sensitization that likely contribute to the decreased mouse digging behavior following knee inflammation, an increase in TRPV1 function is perhaps most clinically relevant to inflammatory arthritis (reviewed in (Fernandes et al., 2013). This increase in TRPV1 function and expression is most likely mediated through inflammatory substances, such as NGF, being released into the joint environment by synoviocytes, therefore the next chapter will investigate the interaction between FLS and knee-innervating neurons.

Chapter 5. Sensitization of knee-innervating sensory neurons by TNF-α activated FLS: an *in vitro*, co-culture model of inflammatory pain.

This chapter is under peer-review and the pre-print can be accessed at (Chakrabarti et al., 2019b).

Authorship contributions in the published manuscript: I designed the studies, collected and analyzed data, and wrote the manuscript. Luke A. Pattison helped with FLS culture, conducted and analyzed semi-quantitative RT-PCR and revised the manuscript. Charity N. Bhebhe conducted and analyzed Ca^{2+} imaging experiments on dorsal root ganglion neurons using MIP-1γ and revised the manuscript. Dr Gerard Callejo helped with qPCR experimental design and revised the manuscript. Dr David C. Bulmer revised the manuscript. Dr Ewan St. John Smith was involved in the design of the study and writing of the manuscript.

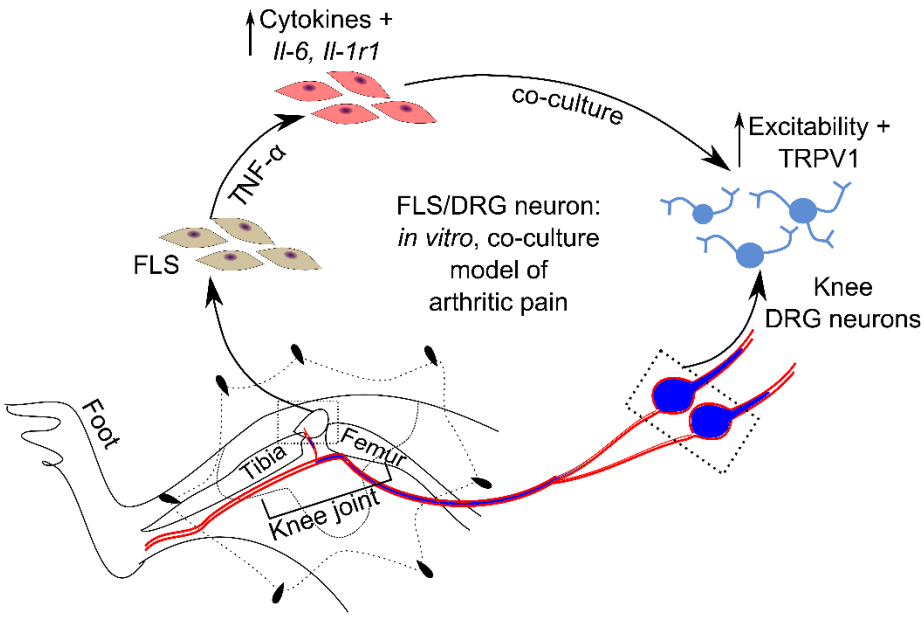

Figure 5-1: Graphical abstract for Chapter 5.

5.1.Key message

Peripheral sensitization manifested by hyperexcitability of DRG neurons underlies arthritic pain. In the knee joint, distal ends of DRG neurons (knee neurons) are in contact with a variety of non-neuronal cell types, including FLS and their secreted soluble inflammatory mediators. Therefore, I investigated the communication between knee neurons and FLS in a co-culture system to better understand the mechanisms involved in inflammatory arthritis. Results in this chapter show that after induction of inflammation via TNF-α (a cytokine that is upregulated in CFA mouse models) FLS (TNF-FLS) increased expression of inflammation-linked genes, as well as actively secreting pro-inflammatory cytokines. In co-culture with TNF-FLS, or mediators these cells secrete, knee neurons become hyperexcitable and show altered TRP channel function. Therefore, this Chapter establishes the contributions of non-neuronal FLS to pain in inflammatory arthritis.

5.2.Introduction

Inflammation is part of the body's immune response to tissue damage and involves multiple cell types, including lymphocytes and synoviocytes. These non-neuronal cells are either in direct contact with, or in close proximity to, the distal endings of DRG sensory neurons that innervate the joints. The physical interaction of sensory neurons with non-neuronal cells and the mediators they secrete, is thought to be involved in the development of peripheral sensitization of knee-innervating nerves, which is a key pathology in the development of inflammatory pain.

During inflammatory diseases such as RA, the joint undergoes hyperplasia due to T lymphocyte infiltration and FLS proliferation. FLS are key effector cells in RA as they become active upon stimulation by inflammatory cytokines (released by macrophage-like synoviocytes, MLS, and T cells) and secrete matrix metalloproteases (MMP) that cause joint destruction (Bottini and Firestein, 2013). In addition, FLS can also support and maintain the ongoing inflammation in arthritic joints by themselves secreting pro-inflammatory mediators (Bottini and Firestein, 2013). Building on this, recent single-cell transcriptional analysis of patient-derived RA-FLS, and their subsequent transfer into mouse knee joints, has identified distinct FLS subgroups: "destructive" and "inflammatory" (Croft et al., 2019). Furthermore, deletion of cadherin-11 (CDH-11), a key surface marker of FLS, causes hypoplasticity in murine joints and makes them resistant to

inflammatory arthritis (Lee et al., 2007), evidence further supporting a critical role of FLS in arthritic pathology.

FLS derived from rodent and human joints proliferate *in vitro*, unlike MLS, enabling their extensive characterization (Bartok and Firestein, 2010). Interestingly, human RA-FLS are shown to be "imprinted aggressors" that retain an inflammatory phenotype over several passages, although the effect of these activated FLS on sensory neurons remains largely unexplored (Bartok and Firestein, 2010; Hardy et al., 2013). In rodents, it has been reported that FLS derived from K/BxN mice (a spontaneous, chronic arthritis model) (Hardy et al., 2013) and supernatants from cultured FLS derived 3 days after induction of antigen-induced arthritis (AIA) in rats (von Banchet et al., 2007) have increased levels of secreted cytokines compared to control FLS. Several other studies have utilized interleukin 1β (IL-1β) or TNF-α stimulation to robustly induce an inflammatory phenotype in FLS (Chen et al., 2015; Guo et al., 2016; Hong et al., 2018; Llop-Guevara et al., 2015). In this study I tested two modes of FLS activation to understand their inflammatory phenotype. Firstly, I tested for a pro-inflammatory phenotype in FLS derived from mice 24-hours after CFA-induced knee inflammation which, as previously reported (Chapter 4) can produce robust knee inflammation, knee neuron hyperexcitability and a concomitant decrease in digging behavior (Chakrabarti et al., 2018). Secondly, I tested TNF-α (a cytokine that is upregulated in tissues derived CFA-injected mice (Woolf et al., 1997)) stimulated FLS derived from mouse knee, and determined their inflammatory phenotype to understand the potential of activated FLS to induce sensitization of sensory neurons.

Since arthritic FLS reside in a pro-inflammatory environment which is often (Andersson et al., 1999) (but not always (Wright et al., 2018)) acidic, it is perhaps unsurprising that they express algogen sensing ion channels including proton sensors (Christensen et al., 2005; Kolker et al., 2010) and various transient receptor potential (TRP) channels (Galindo et al., 2018), such as TRPV1 (transducer of noxious heat and low pH) and TRPA1 and TRPM8 (cold transducers). Experiments conducted on SW982 cells, a human tumor derived synoviocyte cell line, and primary FLS from an RA patient, have demonstrated that a Ca^{2+} influx occurs upon application of the TRPV1 agonist capsaicin in an acidic (pH 7.1) environment and upon application of the TRPA1 and TRPM8 agonist icilin (Kochukov et al., 2006). In addition to *Trpv1*, the human FLS cell lines SW982 and MH7A also express *Trpv4* (warmth and tonicity transducer), and both *Trpv1* and *Trpv4*

are upregulated by TNF-α stimulation (Itoh et al., 2009; Kochukov et al., 2009). Since most of these experiments were conducted on immortalized cell lines, which thus might not be physiologically relevant, there is a need to investigate TRP channel function in primary FLS. By contrast, acid sensors have been better studied in FLS derived from mouse joints, leading to the identification of ASIC3 as a major proton transducer. FLS from wild-type mice cultured in IL-1β show increased intracellular Ca^{2+} influx and cell death in response to acid compared to FLS derived from $ASIC3^{-/-}$ mice, suggesting a physiological role of ASIC3 and acid-sensing in general in FLS (Gong et al., 2014; Kolker et al., 2010; Sluka et al., 2013). Therefore, in this study I sought to compare the algogen sensitivity of FLS before and after inducing an inflammatory phenotype using Ca^{2+} imaging.

Given the complex interaction of cells in the joint environment, co-culture has proved to be an important tool for dissecting FLS biology. Co-culture of human RA-FLS with T cells (Bombara et al., 1993; Burger et al., 1998; Lebre et al., 2017; Yamamura et al., 2001) or macrophages/monocytes (Blue et al., 1993; Bondeson et al., 2006; Chomarat et al., 1995) increased the concentration of prostaglandin (PG) E_2, IL-6, IL-8, MMP-1 and MMP-3 in the culture medium, along with increased expression of adhesion molecules such as vascular cell-adhesion molecule (*Vcam-1*) on FLS in a cell-mediated and soluble-factor mediated manner. Furthermore, upregulation of these pro-inflammatory mediators in culture supernatants was inhibited by anti-TNF-α (Burger et al., 1998; Scott et al., 1997) and anti-IL-6 antibodies (Scott et al., 1997). Additionally, IL-15 secreted from human RA-FLS promotes survival of B cells (Benito-Miguel et al., 2012) and natural killer cells (Chan et al., 2008) in co-culture, further demonstrating the importance of FLS in maintaining the pro-inflammatory environment of arthritic joints. Although co-culture techniques have revealed multiple immune interactions within the joint environment, the communication between neurons and non-neuronal cells is less well understood in the context of knee inflammation. Culturing DRG neurons with FLS derived from chronic AIA rats increased expression of receptors associated with nociception, namely neurokinin 1 receptors, bradykinin 2 receptors and TRPV1 in neurons (von Banchet et al., 2007), validating the premise of co-culture studies to understand neuron-synoviocyte communication within the arthritic joint. However, these studies did not functionally assess modulation of DRG neuron excitability, which is a key mechanism of peripheral sensitization and hence pain. As reported recently (Chakrabarti et al., 2019a), human OA-SF (a fluid largely secreted by FLS (Bartok and Firestein, 2010)) can cause

hyperexcitability of murine sensory neurons and increase TRPV1 function (Chapter 3). Therefore, in this study, I hypothesized that after induction of inflammation, mouse knee-derived FLS will increase excitability and TRP function of knee-innervating DRG neurons (knee neurons) in an FLS-DRG neuron co-culture system. The specific aims of this Chapter are 1) to verify that FLS can be cultured from mouse patella using cell-outgrowth method 2) to identify upregulation of pro-inflammatory genes and secretion of pro-inflammatory cytokines from TNF-α stimulated FLS and FLS from mouse knees inflamed by CFA injection 3) to elucidate acid sensing capabilities of FLS before and after induction of inflammation 4) to understand whether TNF-FLS are able to excite and cause dysregulation of TRP channel function in knee neurons in co-culture.

5.3.Methods

See Materials and Methods Chapter for detailed description of isolation, culture 2.8.2, staining Section 2.10.2 and 2.10.3), measurement of gene expression levels (using qPCR and RT-PCR Section 2.11) and secreted cytokine assessment (mouse inflammatory antibody array blot, Section 2.12) of FLS. Mouse knee injections (Section 2.4), whole cell patch clamp electrophysiology (Section 2.13) and Ca^{2+} imaging (Section 2.14) on FLS/DRG neurons as well as the procedure for culture of Raw 267.4 (Section 2.9) has also been described in the Materials and Methods chapter. All animals used in this Chapter were females.

5.4.Results

5.4.1. Identification of adherent cells proliferated from mouse patellae as FLS

Key genes have been described that act as identifiers of cultured FLS isolated by enzymatic digestion of mouse joints (Hardy et al., 2013), as well as for establishing their inflammatory phenotype. In this study, RT-qPCR was performed on adherent cells (P2-P5) originating from the mouse patellae (from both CFA-injected, Ipsi, and contralateral, Contra, sides) that proliferated in culture (Figure 5-2A, B). From P2 to P3, the expression of the macrophage marker (Bartok and Firestein, 2010; Hardy et al., 2013) cluster of differentiation 68 (*Cd-68*, relative to the mouse macrophage cell line RAW 267.4) was significantly reduced (Figure 5-2C) while the expression

of FLS markers *Cdh-11* and *Cd-248* (Bartok and Firestein, 2010; Hardy et al., 2013) remained consistent from P2 to P5 (Figure 5-2Di, ii); the endothelial marker *Cd-31* was not detected (data not shown). These results suggest that from P3, cells cultured from mouse patellae were predominantly FLS and hence subsequent functional studies were conducted on FLS from P3-P6.

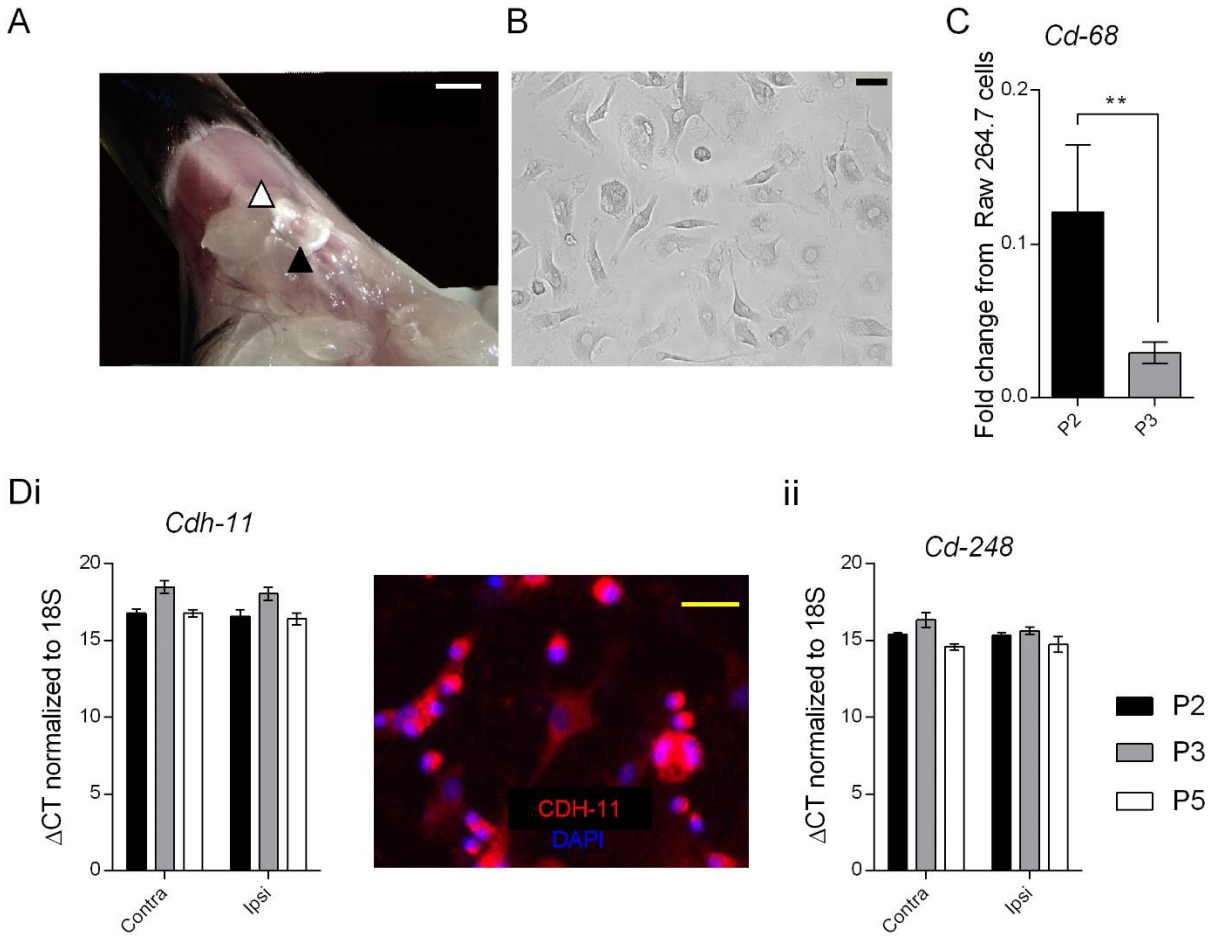

Figure 5-2: Characterization of FLS.

A) Representative picture showing exposed inside of the patella (black triangle) and the surrounding ligament and fat pad (white triangle) after midline resection and distal pull of the quadriceps muscles. Scale bar = 2 mm. B) Representative picture of FLS in culture. Scale bar = 50 µm. C) Bars show reduction in mRNA expression of the macrophage marker *Cd-68* from P2 to P3 expressed as fold change from macrophage cell line Raw 264.7 cells. ** p <0.01, ratio paired t-test. Di) Expression of FLS marker *Cdh-11* across P2-P5 in Ipsi and Contra FLS normalized to the housekeeping gene *18S* (left) and a representative image of CDH-11 (red) and DAPI (blue) stained FLS in culture. ii) Expression of FLS marker *Cd-248* across P2-P5 in Ipsi and Contra FLS normalized to the housekeeping gene *18S*. Error bars = SEM.

5.4.2. TNF-FLS, but not FLS derived from CFA injected inflamed knees, have a pro-inflammatory phenotype and secrete cytokines that activate DRG neurons.

To establish the inflammatory phenotype of FLS, I used RT-qPCR to determine the expression of the pro-inflammatory genes *Il-6, Il-1r1* and *Cox-2*, as well as the constitutively expressed gene *Cox-1*, from FLS derived from the inflamed knee (Ipsi, knee width, pre-CFA, 3.1 ± 0.09 mm vs. post-CFA, 4.1 ± 0.08 mm, n = 6, p = 0.0001, paired t-test, Figure 5-3A) of CFA injected mice and from FLS derived from the matched contralateral knee (Contra). No changes were found in expression levels of the genes between Contra and Ipsi FLS across P2-P5 (Figure 5-3A). However, when control FLS (P5, derived from knees of mice naïve to CFA) were stimulated with 10 ng/ml TNF-α for 48-hours, there was an upregulation of *Il-6* (fold change: Control, 1.5 ± 0.8 vs. TNF-FLS, 135.1 ± 31.1, n = 3, p = 0.006, unpaired t-test) and *Il-1r1* (fold change: Control, 1.1 ± 0.2 vs. TNF-FLS, 3.4 ± 1.0, n = 3, p = 0.04, unpaired t-test) expression levels, but not that of *Cox-1* (fold change: Control, 1.0 ± 0.2 vs. TNF-FLS, 0.8 ± 0.2, n = 3, p = 0.18, unpaired t-test) or *Cox-2* (fold change: Control, 1.0 ± 0.2 vs. TNF-FLS, 0.8 ± 0.2, n = 3, p = 0.2, unpaired t-test) (Figure 5-3B).

Next, the media (n = 3, each) isolated from control, Contra, Ipsi and TNF-FLS were tested against a mouse inflammation antibody array (Figure 5-3C) to determine the levels of different secreted pro-inflammatory mediators. The spot intensity values of inflammatory markers between Ipsi and Contra FLS were found to be similar (multiple t-tests with Holm-Sidak corrections, graph not shown), suggesting no difference in the levels of secreted cytokines. However, when spot intensities were normalized to control FLS, TNF-FLS media showed increased levels of secreted IL-6 ($p < 0.0001$, ANOVA followed by Tukey's multiple comparison test) and keratinocyte chemoattractant (KC, mouse homolog of IL-8, $p = 0.001$, ANOVA followed by Tukey's multiple comparison test) compared to Ipsi and Contra FLS (Figure 5-3Cii). When compared to control FLS media, only TNF-FLS media showed presence of regulated on activation, normal T-cell expressed and secreted (RANTES) and granulocyte-macrophage colony stimulating factor (GM-CSF). Additionally, TNF-FLS contained higher levels of IL-6 ($p < 0.0001$), KC ($p < 0.0001$), lipopolysaccharide induced chemokine (LIX, $p < 0.0001$), stromal cell derived factor 1 (SDF-1, $p < 0.0001$), fractalkine ($p < 0.0001$), monocyte chemoattractant protein 1 (MCP-1, $p < 0.0001$) and macrophage inhibitory protein 1γ (MIP-1γ, $p = 0.002$) and lower levels of macrophage colony stimulating factor (MCSF, $p = 0.003$) compared to control FLS media (multiple t-tests with Holm-

Sidak corrections, Figure 5-3Ciii). TNF-α was not detected in TNF-FLS media as has been previously observed in supernatant from TNF-α stimulated airway epithelial cells (Elizur et al., 2008).

Interestingly, MIP-1γ was elevated in both Ipsi and Contra FLS when compared to control and TNF-FLS (Figure 5-3Cii), perhaps indicating its role in acute, systemic inflammatory pathways. Indeed, MIP-1γ has been described as having a role in hyperalgesia induced by diabetic neuropathy in mice (Rojewska et al., 2018) and OA-related pain in rats (Dawes et al., 2013). Consistently, this study found that MIP-1γ directly activates mouse DRG neurons by producing a dose-dependent Ca^{2+} influx (Figure 5-3D), which thus might be a potential mechanism for the *in vivo* effects described above. However, because MIP-1γ does not have a human homolog (NCBI gene database entry #20308), and thus has limited clinical potential, I did not explore this further.

Taken together, these data suggest that TNF-α stimulation of FLS upregulates expression of canonical pro-inflammatory markers, whereas the *in vivo* pathology observed 24-hours after CFA-induced knee inflammation does not produce a sustained pro-inflammatory phenotype of FLS isolated from patellae of CFA mice. I also identified other soluble mediators secreted by TNF-FLS that might be involved in FLS-DRG neuron communication. Therefore, given the pro-inflammatory phenotype of TNF-FLS (and the lack of such phenotype in the CFA model), the rest of the study examining FLS/DRG neuron interactions focused solely on the TNF-FLS.

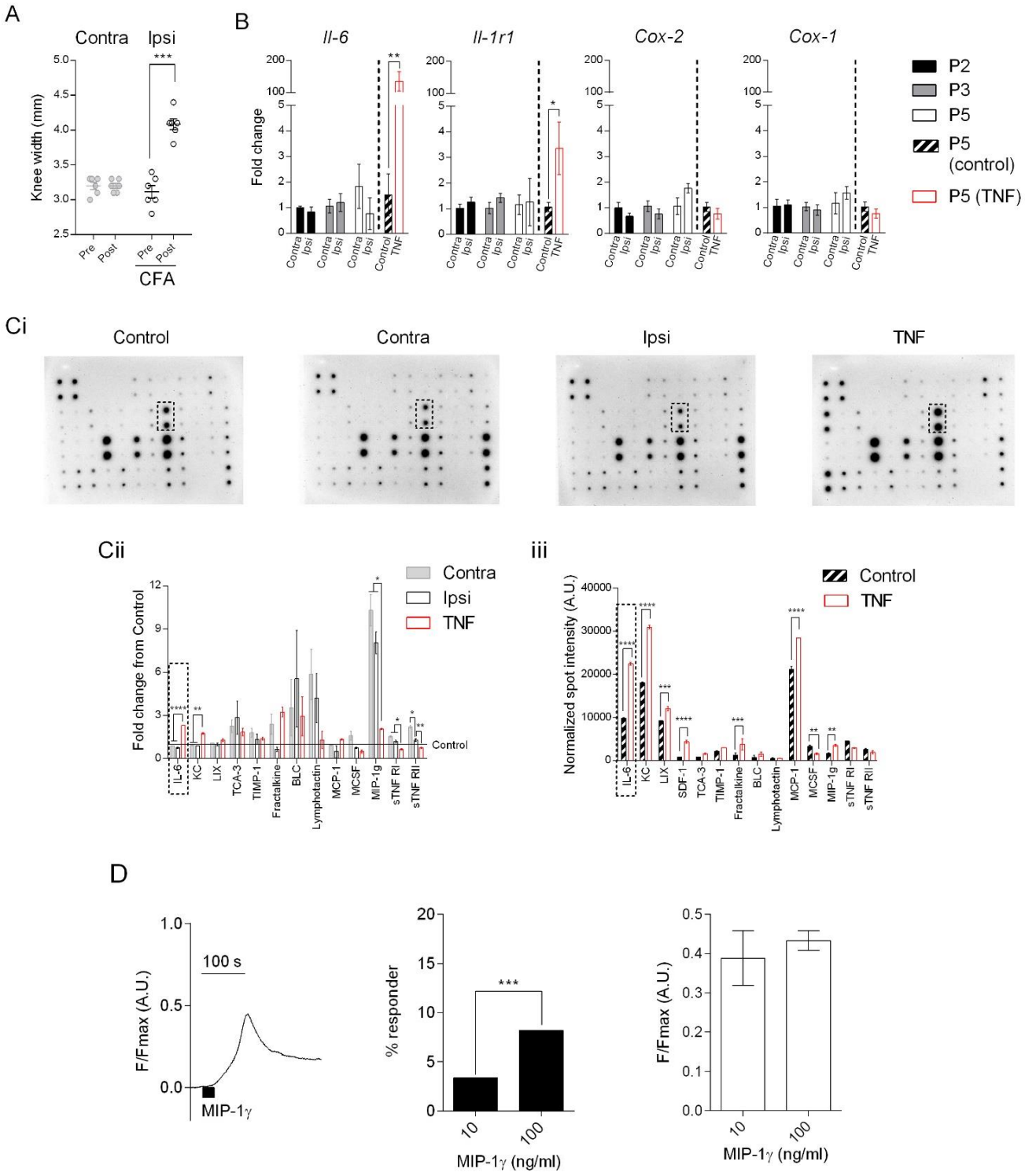
A
Contra
Ipsi
Knee width (mm)
Pre
Post
CFA
B
Il-6
Il-1r1
Cox-2
Cox-1
Fold change
P2
P3
P5
P5 (control)
P5 (TNF)
Ci
Control
Contra
Ipsi
TNF
Cii
Fold change from Control
Contra
Ipsi
TNF
IL-6
KC
LIX
TCA-3
TIMP-1
Fractalkine
BLC
Lymphotactin
MCP-1
MCSF
MIP-1g
sTNF RI
sTNF RII
iii
Normalized spot intensity (A.U.)
Control
TNF
SDF-1
D
F/Fmax (A.U.)
100 s
MIP-1γ
% responder
MIP-1γ (ng/ml)

Figure 5-3: Inflammatory phenotype of FLS.
A) Mouse knee width in Contra (grey circles) and Ipsi (black circles) limbs before and after injection of CFA (n = 6, paired t-test. B) Bars represent fold change of the genes *Il-6*, *Il1r1*, *Cox-2* and *Cox-1* from either Contra (vs. Ipsi) or control (vs. TNF). Black bars = P2, grey bars = P3, white bars = P5, black hatched bars = P5 control FLS, red bars = P5 TNF-FLS. C) Images of mouse inflammatory array membranes probed against FLS conditioned medium (i) which were quantified by densitometry and represented as bar graphs showing fold change of various cytokines in Contra, Ipsi and TNF from control FLS media (ii, ANOVA with Tukey's post-hoc test) and spot intensity differences between control and TNF-FLS only (iii, multiple t-test with Holm-Sidak correction). Dotted rectangles highlights IL-6 spots (Ci) and corresponding quantifications (Cii, iii). Only cytokines that were present in all of the compared groups are shown in graphs. D) Intracellular Ca^{2+} influx in lumbar DRG neurons in response to 20 s application of 100 ng/ml MIP-1γ, followed by percentage of neurons responding to 10 and 100 ng/ml of MIP-1γ and their respective peak response. > 500 neurons were imaged from three male mice. * $p < 0.05$, ** $p < 0.01$, *** $p < 0.001$ **** $p < 0.0001$. Error bars = SEM.

5.4.3. TNF-FLS have reduced sensitivity to mild acidosis, but enhanced sensitivity to more acidic pH.

During arthritis, FLS are located in an environment with abundant algogens, some of which have been shown to signal by modulating TRP channels (Bottini and Firestein, 2013). Therefore, FLS sensitivity was tested against to a range of acidic pH stimuli, as well as the prototypic TRP channel agonists, capsaicin (TRPV1), cinnamaldehyde (TRPA1) and menthol (TRPM8) using Ca^{2+}-imaging. Confirming results from other studies on acid sensing in FLS (Gong et al., 2014), I found that both control and TNF-FLS respond to a range of pH solutions (pH 4.0 – 7.0) with an increase in intracellular [Ca^{2+}] (Figure 5-4A, B). An increased percentage of control FLS (24.1 %) respond to pH 7.0 compared to TNF-FLS (11.0 %, $p = 0.0004$, chi-sq test), but in the more acidic range an increased percentage of TNF-FLS responded to acid than did control FLS, i.e. pH 6.0 (control, 7.2 % vs. TNF-FLS, 26.3 %, $p < 0.0001$, chi-sq test) and pH 5.0 (control, 14.4 % vs. TNF-FLS, 30.5 %, $p < 0.0001$, chi-sq test) (Figure 5-4Bi). At the very acidic pH of 4.0, ~40% ($p = 0.4$, chi-sq test, Figure 5-4Bi) of FLS responded in both groups, possibly due to a saturation, ceiling effect. Although the proportion of responding neurons varied, the magnitude of the peak normalized response was similar across the pH range in control (pH 7.0: 0.4 ± 0.04 F/Fmax (n = 50), pH 6.0: 0.4 ± 0.08 F/Fmax (n = 27), pH 5.0: 0.3 ± 0.03 F/Fmax (n = 46), pH 4.0: 0.3 ± 0.02 F/Fmax (n = 129)) and TNF-FLS (pH 7.0: 0.3 ± 0.06 F/Fmax (n = 21), pH 6.0: 0.4 ± 0.03 F/Fmax (n = 50), pH 5.0: 0.3 ± 0.02 F/Fmax (n = 58), pH 4.0: 0.3 ± 0.02 F/Fmax (n = 72), Figure 5-4Bii).

To identify the proton sensors expressed by FLS that likely mediate the responses measured, RT-PCR of control and TNF-FLS was conducted to determine the expression of proton-sensing GPCRs, ASICs and TRPV1. Our data show that FLS express the proton-sensing GPCRs – *Gpr4*, *Gpr65*, *Gpr68* and *Gpr132*, as well as *Asic1*, Asic*3* and *Trpv1* (Figure 5-4Ci). When relative expression was assessed compared to the housekeeping gene *18S*, *Gpr132* was found to be increased ($p = 0.005$, Figure 5-4Cii) in TNF-FLS implicating it as a potential contributor to the enhanced proportion of acid responders seen in TNF-FLS (Figure 5-4Bi). The pro-inflammatory phenotype of TNF-FLS was confirmed by the increased *Il-6* band intensity ($p < 0.0001$), as observed previously using qPCR (multiple t-tests with Holm-Sidak corrections, Figure 5-4Cii).

FLS sensitivity to TRP channel agonists was also tested, but only a few cells responded to each compound: capsaicin (control, 3/201, TNF-FLS, 13/252), cinnamaldehyde (control, 1/201, TNF-FLS, 11/252) and menthol (control, 0/201, TNF-FLS, 1/194) (data not shown). This led us to conclude that there are very few mouse primary FLS with functional TRPV1 (also corroborated by the observation of low *Trpv1* gene expression, Figure 5-4C), TRPA1 or TRPM8 ion channels and hence this was not explored further.

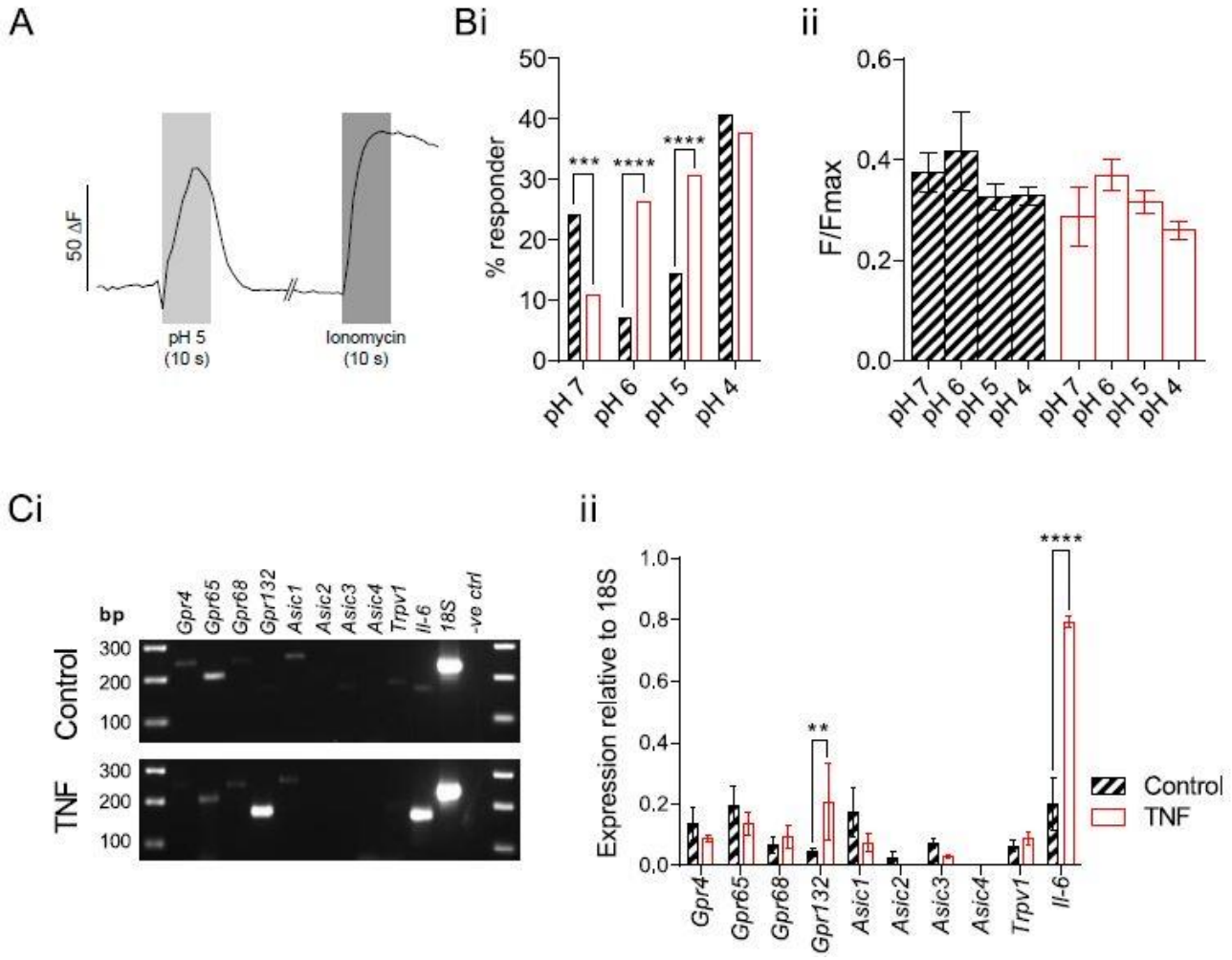

Figure 5-4: Acid sensitivity in FLS.

A) Representative Ca^{2+} imaging trace from an FLS responding to pH 5 and ionomycin. Bi) Bars representing proportions and magnitudes (ii) of control (black hatched) and TNF-FLS (red) responding to pH 7, 6, 5 and 4. Comparison between control vs. TNF-FLS made using chi-sq test. Data from three biological replicates in each category. Ci) Gel image of control and TNF-FLS expression of proton sensors along with the densitometry analysis of the relative band intensity compared to the 18S band (ii, multiple t-test with Holm-Sidak correction). ** $p < 0.01$, *** $p < 0.001$ and **** $p < 0.0001$. Error bars = SEM.

5.4.4. TNF-FLS increase knee-innervating DRG neuron excitability in co-culture.

Changes is primary sensory neuron excitability underlie peripheral sensitization which drives arthritic pain (Syx et al., 2018). Non-neuronal cells like FLS, which lie in close proximity to the distal terminals of knee neurons, could play instrumental roles in modulating sensory neuron excitability by direct cell contact and/or secretion of pro-inflammatory cytokines. To determine neuron/FLS communication in health and inflammation I compared the DRG neuronal excitability of four groups: 1) knee neuron mono-culture, 2) knee neurons co-cultured with control FLS (Figure 5-5A, B), 3) knee neurons with FLS that have been exposed to TNF media for 24-hour followed by DRG culture media for 24-hours and 4) knee neurons with conditioned media from FLS that have been exposed to TNF media for 48-hours to understand the role of soluble mediators in peripheral sensitization. In current-clamp mode, many spontaneously firing neurons were observed in groups 3 and 4. In order to statistically compare the proportions, the four group data were converted into binary categories: neuron mono-culture and neuron/control FLS co-culture were assigned to the class "healthy", and neuron/TNF-FLS and neuron/TNF-FLS media were assigned to the class "inflamed". 19.5% of inflamed neurons (neuron/TNF-FLS, 5/21; neuron/TNF-FLS media, 3/19) fired spontaneous AP compared to 2.7% (neuron mono-culture, 0/19; neuron/control FLS, 1/18) of healthy neurons ($p = 0.02$, chi-sq test) suggesting that there is a general increase in excitability of knee neurons when exposed to an FLS-mediated inflammatory environment (Figure 5-5C, D).

Upon measuring the AP properties (Figure 5-5D inset) I found that the resting membrane potential (RMP) was more depolarized in the neuron/TNF-FLS media group compared to both neuronal mono-culture ($p = 0.0004$) and neuron/control FLS co-culture ($p = 0.012$), which highlights that secreted pro-inflammatory factors from TNF-FLS likely act upon knee neurons to increase their excitability (ANOVA followed by Tukey's post hoc comparison, Figure 5-5Ei). The other measured properties were unchanged among the four groups (ANOVA followed by Tukey's post hoc comparison, Table 5-1, Figure 5-5Eii-iv).

Table 5-1: AP properties of knee neurons.
*** represents $p < 0.001$ when compared to knee neuron mono-culture, $ represents $p < 0.05$ when compared to neuron/control FLS co-culture.

	Knee neuron mono-culture (n = 19)		Knee neuron/control FLS (n = 18)		Knee neuron/TNF-FLS (n = 21)		Knee neuron/TNF-FLS media (n = 20)	
	Mean	SEM	Mean	SEM	Mean	SEM	Mean	SEM.
RMP (mV)	-46.6	2.0	-42.8	2.9	-39.7	2.3	-32.0***/$	2.3
Threshold (pA)	447.4	71.5	319.4	56.3	245.2	49.4	315.0	70.0
Half peak duration (HPD, ms)	2.2	0.4	2.3	0.2	2.4	0.5	2.4	0.6
Afterhyperpolarization amplitude (AHP peak, mV)	13.7	2.6	19.6	2.7	16.1	2.9	21.6	3.3

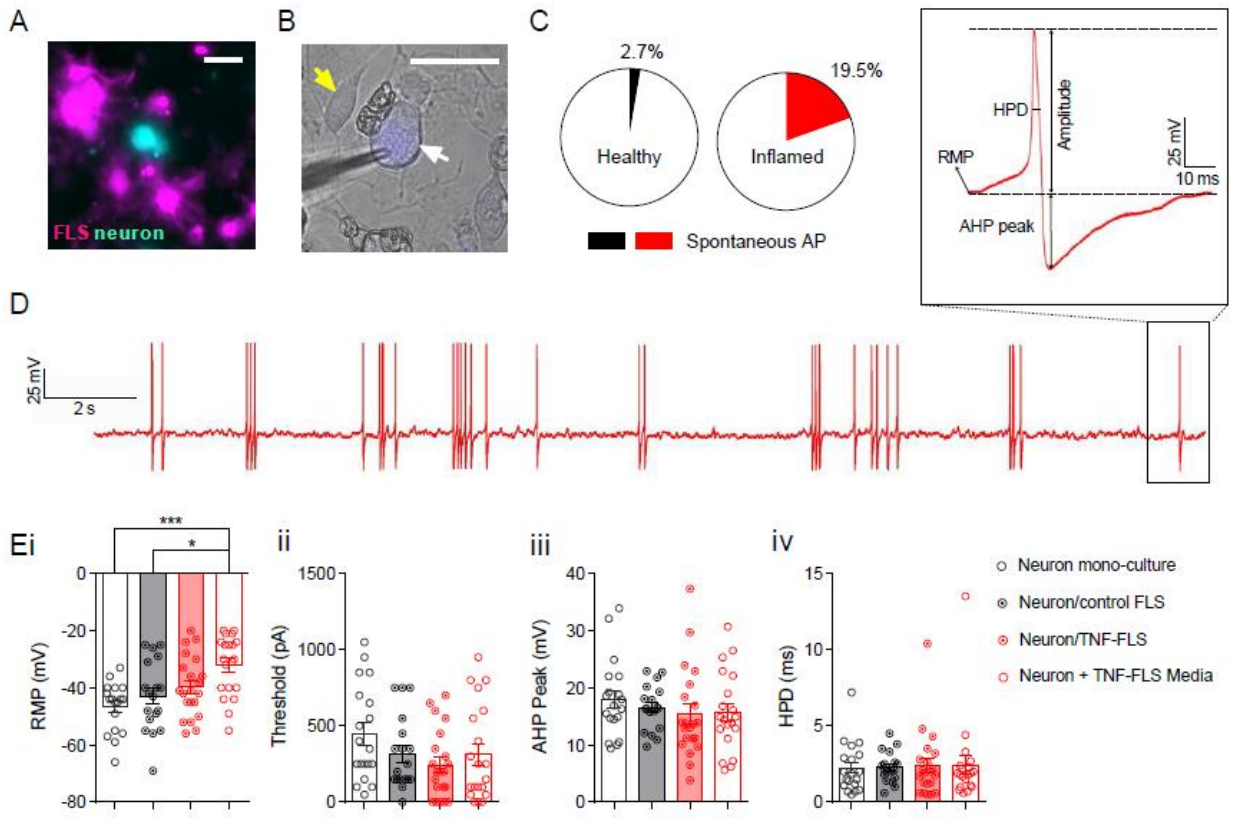

Figure 5-5: TNF-FLS induce an increase in knee neuron excitability.
A) Representative live-cell imaging picture showing FLS (magenta) and neuron (cyan) in co-culture. Scale bar = 50 µm. B) Representative FB labelled knee neuron (white arrow) being recorded using a patch pipette (triangular shadow), surrounded by FLS (yellow arrow). Scale bar = 50 µm. C) Pie-chart showing proportion of knee neurons that fired APs without current stimulation in healthy (neuron mono-culture + neuron/control FLS, n = 37, black) and inflamed (neuron/TNF-FLS + neuron/TNF-FLS media, n = 41, red) condition. D) Representative knee neuron incubated with TNF-FLS media firing spontaneous APs along with schematic diagram of the AP properties measured (inset). E) Bar graphs showing measured RMP (i), threshold (ii), AHP peak (iii) and HPD (iv) from knee neurons in mono-culture (n = 19, white bar/black open circle), in co-culture with control FLS (n = 18, grey bar/black dotted circle), in co-culture with TNF-FLS (n = 20, light red bar/red dotted circle) and incubated in TNF-FLS media (n = 21, white bar/red open circle). * $p < 0.05$ and *** $p < 0.001$, ANOVA followed by Tukey's post hoc test. Data from 4-5 female mice in each group. Error bars = SEM.

5.4.5. TNF-FLS increase TRPV1 function and decrease TRPA1/TRPM8 function of DRG neurons in co-culture.

DRG neurons in co-culture with inflamed FLS derived from AIA rats reportedly have increased expression of TRPV1 (von Banchet et al., 2007). Here I investigated whether FLS can modulate knee neuron responses to TRP channel agonists using whole cell patch clamp recordings. Knee neurons in mono-culture and when co-cultured with control FLS displayed very similar responses, i.e. a mean capsaicin peak current density response of 3.5 ± 1.0 pA/pF (n = 7) and 3.2 ± 0.9 pA/pF (n = 7) respectively. By contrast, knee neurons in neuron/TNF-FLS co-culture showed a trend for larger magnitude of capsaicin responses (27.7 ± 9.3 pA/pF, n = 8), and those cultured with TNF-FLS media had a capsaicin response of 65.8 ± 25.7 pA/pF (n = 7) which was significantly larger in magnitude than neuronal mono-culture (p = 0.02) and neuron/control FLS co-culture (p = 0.02) (ANOVA followed by Tukey's post-hoc comparison, Figure 5-6Ai,ii). However, no difference was observed between the percentage of capsaicin responders in healthy (40.5%) vs. inflamed groups (37.5%, p = 0.8, chi-sq test, Figure 5-6Aiii).

With regards to menthol (mono-culture, 2.4 ± 1.2 pA/pF, n = 7; neuron/healthy FLS, 4.8 ± 2.1 pA/pF, n = 6; neuron/TNF-FLS, 1.4 ± 1.2 pA/pF, n = 2; neuron/TNF-FLS conditioned media, 4.0 ± 1.9 pA/pF, n = 4; Figure 5-6Bi) and cinnamaldehyde (mono-culture, 1.9 ± 0.7 pA/pF, n = 10; neuron/healthy FLS, 2.8 ± 1.1 pA/pF, n = 4; neuron/TNF-FLS, 0.6 ± 0.3 pA/pF, n = 3, neuron/TNF-FLS conditioned media, 2.3 ± 1.5 pA/pF, n = 3; Figure 5-6Ci) responses, all four groups showed similar mean peak current density values (Figure 5-6Bii, Cii). However, in response to both the TRPA1 and TRPM8 agonists, the percentage of responding neurons was significantly less in the inflamed group compared to healthy (menthol: healthy vs. inflamed, 37.8% vs. 15%, p = 0.02, chi-sq test; cinnamaldehyde: healthy vs. inflamed, 43.2% vs. 15%, p = 0.006, chi-sq test, Figure 5-6Biii, Ciii). Taken together these data suggest that "inflamed" FLS can alter the TRP channel function of knee neurons in co-culture.

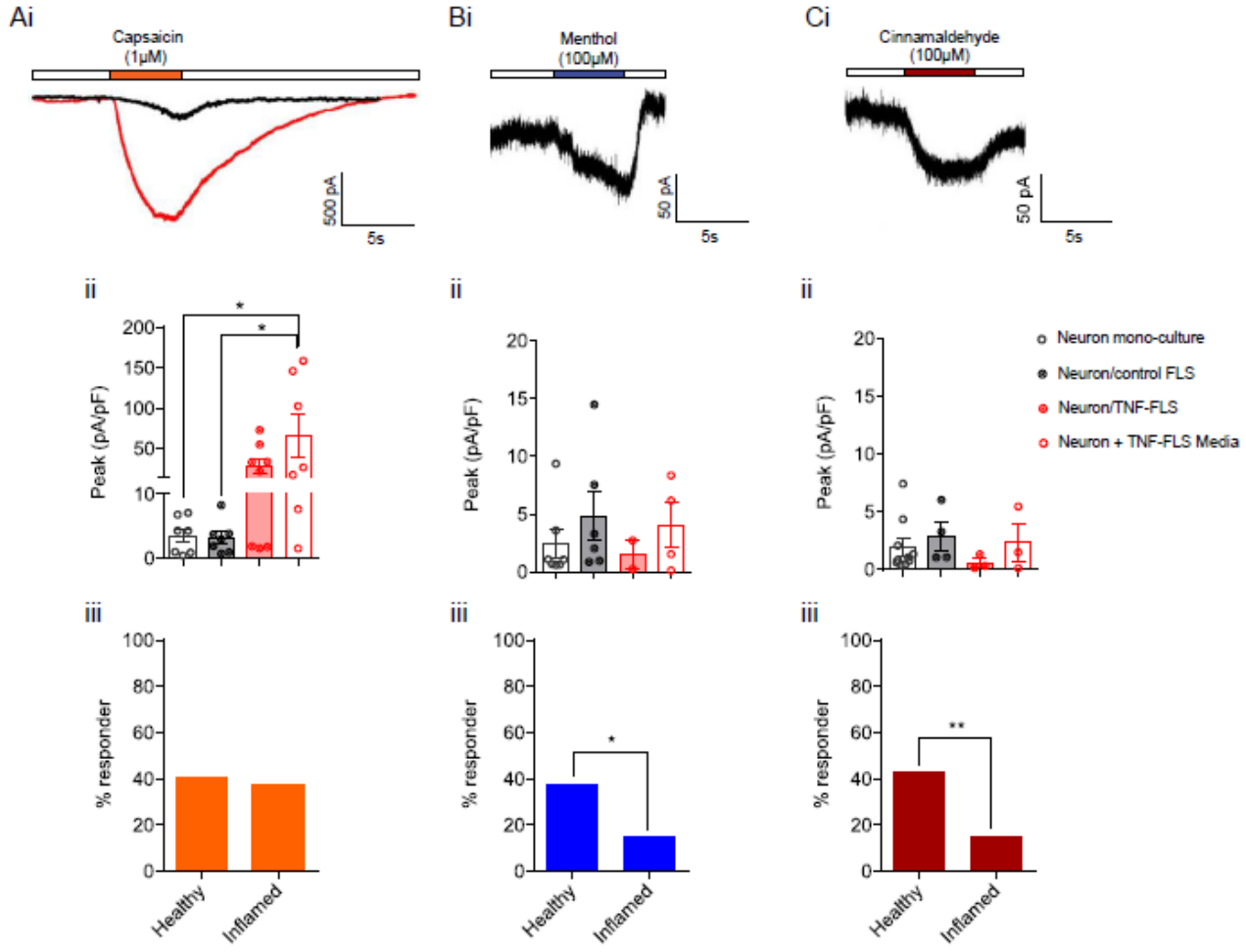

Figure 5-6: TNF-FLS mediated modulation of TRP agonist responses in knee neurons.
Representative traces showing capsaicin (TRPV1 agonist, Ai), cinnamaldehyde (TRPA1 agonist, Bi) and menthol- (TRPM8 agonist, Ci) evoked responses in knee neurons; black traces obtained from knee neurons in mono-culture, red trace obtained from a knee neuron incubated in TNF-FLS media. White boxes represent perfusion of extracellular solution. Bar graphs showing peak current densities of capsaicin- (Aii), cinnamaldehyde- (Bii) or menthol-evoked (Cii) currents from knee neurons in mono-culture (white bar/black open circle), in co-culture with control FLS (grey bar/black dotted circle), in co-culture with TNF-FLS (light red bar/red dotted circle) and when incubated in TNF-FLS media (white bar/red open circle); comparison between groups made using an ANOVA with Tukey's post hoc test. Bar graphs showing percent of knee neurons that responded to capsaicin (Aiii), cinnamaldehyde (Biii) and menthol (Ciii) in healthy (neuron mono-culture + neuron/control FLS) and inflamed (neuron/TNF-FLS + neuron/TNF-FLS media) condition. Comparison made using chi-sq test. * $p < 0.05$. Data from 4-5 female mice in each group. Error bars = SEM.

5.5.Discussion

In this study I have demonstrated that FLS can be obtained from mouse patellae via cell-outgrowth and maintained in culture. When stimulated with TNF-α, FLS show increased: pro-inflammatory gene expression, secretion of pro-inflammatory cytokines and acid sensitivity in the pH 6.0-5.0 range consistent with a pro-nociceptive, activated phenotype. Finally, I established a co-culture system, which shows that FLS and knee neurons can interact, specifically, factors secreted by TNF-FLS increase knee neuron excitability and the magnitude of the response to capsaicin, whereas the proportions of cinnamaldehyde and menthol responding neurons are diminished. The data in this Chapter thus demonstrate how FLS can regulate articular neurons and in turn arthritic pain.

FLS from mouse are generally cultured by enzymatically digesting and combining excised joints of fore- and hind-limbs (Gong et al., 2014; Hardy et al., 2013; Rosengren et al., 2007; Sluka et al., 2013), which assumes similarity of FLS derived from all joints. However, a genome-wide study on DNA-methylation has shown that important differences exist between knee and hip FLS, including differences in the genes involved in IL-6 signaling (Ai et al., 2016). By using a cell-outgrowth method to culture mouse FLS, as previously described in humans (Kawashima et al., 2013) and rats (von Banchet et al., 2007), I have avoided the biological ambiguity introduced by joint-to-joint variability. Using these FLS, I investigated the expression of inflammatory genes *Il-6*, *Il-1r1* and *Cox-2*, all of which have been linked to the inflammatory phenotype of FLS. In brief: stimulating human-derived FLS with IL-1β increases *Cox-2* and *Il-6* expression (Kawashima et al., 2013), increased *Il-6* expression is seen in FLS derived from K/BxN mice and following 24-hour stimulation of healthy mouse FLS with TNF-α (Hardy et al., 2013), and, lastly, supernatants from FLS derived 3 days into a rat AIA model show increased IL-6 and PGE_2 levels (von Banchet et al., 2007). Here, I observed that neither the expression level of *Il-6*, *Il-1r1*, *Cox-2*, nor the level of secreted cytokines were upregulated in FLS derived from CFA-injected knee. This is possibly because the model used here is too brief to influence FLS gene expression, there only being 24-hours between CFA administration and patellae removal. Indeed, evidence to support this is that FLS derived from rats with longer (3-28 days) AIA-induced knee inflammation did have higher PGE_2 and IL-6 concentrations in culture supernatants compared to control FLS (von Banchet et al., 2007). Alternatively, the affected area of the synovium might be too small for sufficient

proliferation of “inflamed” FLS within 24-hours and thus they are lost over time in culture. Overall, these results suggest a limited role of FLS in the acute CFA model of knee inflammation with regard to modulation of neuronal excitability.

I reasoned that FLS need more direct and prolonged exposure to inflammatory mediators to show a robust inflammatory phenotype. TNF-α is one such cytokine that is locally upregulated within 3-hours of intra-plantar CFA injection in mice (Woolf et al., 1997). It is also present in high concentrations in the synovial fluid (Larsson et al., 2015) and tissue of OA and RA patients (Parsonage et al., 2017; Tetta et al., 1990); along with anti-TNF-α agents being the leading treatment of RA (Taylor and Feldmann, 2009). In line with a key role for TNF-α in joint inflammation, I show that TNF-α stimulated FLS display increased expression of *Il-6* and *Il-1r1* mRNA, with a concomitant increase in secretion of many pro-inflammatory cytokines, including IL-6 as has been reported previously in human FLS (Jones et al., 2016). This observation is consistent with the “passive responder and imprinted aggressor model” of inflammatory FLS behavior (Bottini and Firestein, 2013), i.e. FLS can respond to a pro-inflammatory environment and then themselves become effectors to drive disease pathology. The functional repercussions of this model are not well-explored and here I investigated two such possibilities: change in FLS functionality after induction of inflammation and “inflamed” FLS-induced functional changes in nerves supplying the knee joint to drive pain.

Comparing the control and TNF-FLS response to acidic stimuli, I found a decreased percentage of TNF-FLS responding to pH 7.0, but in the pH 6.0-5.0 range the percentage of TNF-FLS responding to acidic stimulation increased. Multiple proton-sensors with sensitivity to varied pH range might underlie the apparent incongruity of TNF-FLS acid sensitivity in mild and strongly acidic environment (Pattison et al., 2019). For example, increased expression of proton sensors programmed to detect highly acidic environments can come at the cost of sensors active at mildly acidic range. This concept has been alluded to previously with mouse primary FLS showing increased *Asic3*, but decreased *Asic1*, expression after IL-1β stimulation (Gong et al., 2014). The present study shows that ASIC1 and 3 may underlie acid sensitivity in FLS, as has been shown previously (Gong et al., 2014; Sluka et al., 2013) and also shows that multiple proton-sensing GPCRs are expressed in FLS. Additionally, an increased level of *Gpr132* in TNF-FLS lends support to the hypothesized role of GPR132 (Christensen et al., 2005) in Ca^{2+} mobilization of FLS

in response to acidification. Furthermore, under control (i.e. non-sensitized conditions) TRPV1 is activated by pH ≤ 6.0, which can contribute to the enhanced acid response of TNF-FLS in that range. Although very few FLS responded to capsaicin at physiological pH of 7.4 (as has been shown before (Kochukov et al., 2006)), more cells responded following TNF-α stimulation compared to control.

In order to understand the effector role of FLS in driving nociception through peripheral sensitization, I set up a co-culture system combining FLS and knee neurons. Studying co-culture of rat FLS and DRG neurons, von Banchet *et al* showed using immunohistochemistry that bradykinin 2 receptor labelling (but not that of neurokinin 1 or TRPV1) was increased when DRG neurons were cultured with healthy rat FLS (von Banchet et al., 2007), i.e. co-culture of DRG neurons with FLS can alter expression of genes associated with nociception. Therefore, I first verified that knee neurons in co-culture with control FLS do not show dysregulation of excitability or TRP agonist response. Next I asked whether TNF-FLS modulate knee neuron function and found using whole cell patch clamp that 23% and 16% of knee neurons in neuron/TNF-FLS co-culture and neuron/TNF-FLS media (inflamed conditions) respectively evoked spontaneous AP compared to 6% in neuron/control FLS and 0% in neuron mono-culture (healthy conditions). This suggests that TNF-FLS increases excitability of knee neurons. von Banchet *et al* also showed that compared to mono-culture, FLS derived from acute and chronic AIA rats induced an increase in TRPV1 protein expression in DRG neurons (von Banchet et al., 2007). However, I did not see an increase in the proportion of neurons responding to capsaicin between healthy and inflamed conditions, which might reflect a species difference and/or difference in knee-specific neuronal population (unlike in this study, von Banchet *et al* did not discriminate between knee-innervating neurons and non-knee innervating neurons); however, I did observe that capsaicin responsive neurons produced larger magnitude responses when incubated with TNF-FLS medium, see below. I also observed that cinnamaldehyde and menthol-evoked responses were decreased in the inflamed condition, suggesting functional downregulation of TRPA1 and TRPM8. Functional downregulation of TRPA1 might be explained through desensitization via increased TRPV1 function (see below) (Akopian et al., 2007), or via an increase in intracellular Ca^{2+} (due to increased excitability in the inflamed condition) (Wang et al., 2008). The latter reason may also explain decrease of menthol-evoked responses (Sarria et al., 2011).

I also observed a tendency of a more depolarized RMP and an enhanced magnitude of capsaicin-evoked peak current density of knee neurons in inflamed conditions, albeit both only reached statistical significance in the TNF-FLS media incubated group when compared to mono-culture and neuron/control FLS. These results suggest that soluble mediators released by FLS are key players in modulating knee neuron excitability. I posit that because our experimental design involved a media change 24-hours after TNF incubation of FLS (so as not to directly stimulate neurons with residual TNF-α (Czeschik et al., 2008)) in the neuron/TNF-FLS co-culture condition, the accumulated soluble mediator concentrations were lower compared to when knee neurons were incubated in 48-hours TNF-FLS conditioned media (no remaining TNF-α was measured in the media at this point). Indeed, Chapter 3 has established the role of soluble mediators present in OA synovial fluid in increasing neuronal excitability and TRPV1 function (Chakrabarti et al., 2019a). These soluble mediators mainly consist of cytokines/chemokines which form complex signaling pathways with neurons (reviewed in (Miller et al., 2009; Schaible, 2014)). In this study, I have identified IL-6 (Fang et al., 2015), KC (Brandolini et al., 2017), RANTES (Oh et al., 2001), GM-CSF (Donatien et al., 2018), LIX (Merabova et al., 2012), SDF-1 (Oh et al., 2001), MCP-1 (Jung et al., 2008), MIP-1γ (present study) to be upregulated in TNF-FLS media which can also directly signal to neurons; and in the cases of IL-6, MCP-1 and GM-CSF increase TRPV1 function (Donatien et al., 2018; Fang et al., 2015; Jung et al., 2008). Although fractalkine does not directly stimulate neurons (Miller et al., 2009), a recent study showed a correlation between levels of this cytokine in protein extracted from human OA synovia and brain derived neurotrophic factor - tropomyosin receptor kinase B mediated signaling in joint nerves to induce mechanical hyperalgesia (Gowler et al., 2019). Therefore, I have established a direct inflammation-pain axis between FLS and DRG neurons. This system can also be adapted to investigate peripheral sensitization using FLS activated by other pro-inflammatory cytokines or arthritic synovial fluid.

As reported in other Chapters, this Chapter further demonstrates the importance of knee-neuron hyperexcitability in arthritic pain. Therefore, the next Chapter will investigate the use of viral tools to control neuronal excitation from the knee joint as a means of ameliorating arthritic pain.

Chapter 6. Intra-articular AAV-PHP.S mediated chemogenetic targeting of knee-innervating DRG neurons alleviates inflammatory pain in mice.

This Chapter is currently under peer-review.

Authorship contributions in the prepared manuscript: I designed experiments, collected and analyzed data and wrote the manuscript. Luke A. Pattison collected and analyzed behavioral data and revised the manuscript. Balint Doleschall helped with virus production. Rebecca H. Rickman generated the immunohistochemistry dataset. Dr Gerard Callejo helped with behavioral experiments and revised the manuscript. Drs Paul A. Heppenstall and Ewan St. J. Smith designed experiments and revised the manuscript. Packaging of viruses and some animal experiments in this Chapter were conducted at the European Molecular Biology Laboratory in Rome, Italy.

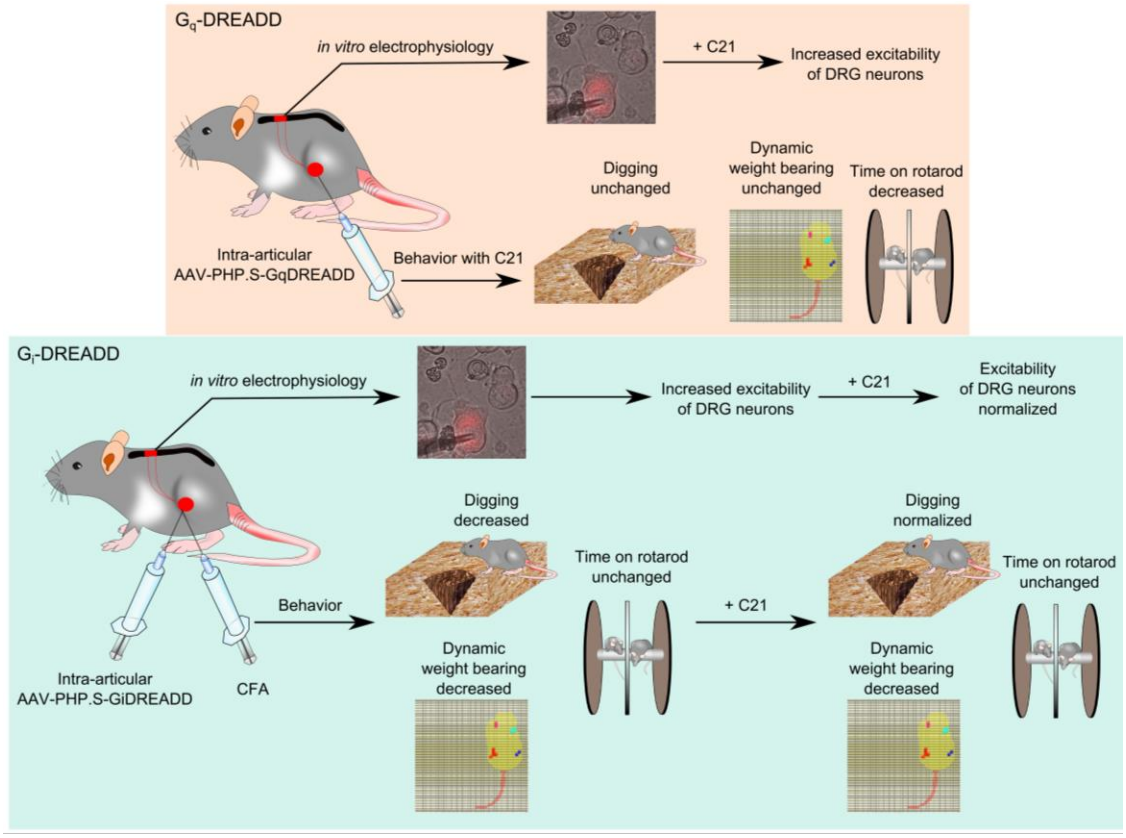

Figure 6-1: Graphical abstract for Chapter 6.

6.1.Key message

Joint pain is the major clinical symptom of arthritis that affects millions of people. Controlling the excitability of knee-innervating DRG neurons (knee neurons) by delivering excitatory or inhibitory genes could potentially provide pain relief. Gene delivery into DRG neurons by injection of adeno-associated virus (AAV) into peripheral organs has had limited success because of the large anatomical distances involved in the periphery. Here I show that the newly engineered serotype, AAV-PHP.S, can deliver functional excitatory (G_q) and inhibitory (G_i) designer receptors activated by designer drugs (DREADDs) into knee neurons to bidirectionally control excitability *in vitro*. *In vivo*, short-term G_q-DREADD activation caused a deficit in motor co-ordination while G_i-DREADD activation was able to alleviate knee inflammation-induced deficits in digging behavior, a measure of spontaneous pain associated with the clinical feeling of well-being. This approach may be utilized in translational pain research for peripheral organ specific pain relief.

6.2.Introduction

Peripheral sensitization, manifested by an increase in excitability of DRG neurons, underlies chronic pain in arthritis (Walsh and McWilliams, 2014). There is great heterogeneity of DRG neurons based upon gene expression (North et al., 2019; Zeisel et al., 2018) and functional attributes (Petruska et al., 2000), and this heterogeneity is further compounded by target innervation (Hockley et al., 2019; Immke and McCleskey, 2001). This variation in DRG neurons offers a unique opportunity to selectively tune the excitability of a distinct subset of DRG neuron in order to provide pain relief with reduced side-effects. For example, Chapter 3 and Chapter 4 show that the excitability of knee-innervating DRG neurons (identified by retrograde tracing) is increased after incubation with human OA synovial fluid samples (Chakrabarti et al., 2019a) and in a mouse model of inflammatory joint pain (Chakrabarti et al., 2018). These results suggest that modulation of the knee-innervating DRG neuron subset (knee neurons) can help control arthritic pain.

One way of specifically modulating neuronal excitability is through chemogenetics. This is a technology in which proteins can be engineered to interact with exogenous chemical activators that were previously unrecognized and which by themselves do not have any endogenous effects.

A variety of chemogenetic technologies exist that are based on engineered kinases, enzymes, G-protein coupled receptors (GPCRs) and ion channels (Roth, 2016). Recently, it was shown that a heteromeric glutamate-gated chloride ion channel (GluCl) modified to respond to exogenous ivermectin, but not to glutamate, when injected into the DRGs decreased hyperexcitability of sensory neurons and normalized mechanical and thermal nerve-injury induced hyperalgesia (Weir et al., 2017). However, this channel is too large to be completely packaged into AAVs and hence required co-transduction of α and β sub-units for expressing functional ion channels. By contrast, modified muscarinic receptor based designer receptors exclusively activated by designer drugs (DREADDs) are relatively small and effectively packaged into AAVs. DREADD technology has been shown to increase and decrease neuronal (mostly in the central nervous system, CNS) firing, which consequently affects a variety of behaviors (reviewed in (Roth, 2016; Wood et al., 2019a)), such as enhanced feeding (Krashes et al., 2011) or decreased wakefulness (Sasaki et al., 2011). In the peripheral nervous system (PNS), activation of the inhibitory DREADD $hM_4D(G_i)$ in Na_V 1.8 expressing DRG neurons decreased knee hyperalgesia and mechanical allodynia, along with a decrease in DRG neuron firing, in mice with early experimental OA pain induced by surgical destabilization of the medial meniscus (Miller et al., 2017). Similarly, activating G_i-DREADD in transient receptor potential vanilloid 1 (TRPV1) expressing DRG neurons (Saloman et al., 2016) increased heat pain threshold and reduced neuronal excitability in mice. Both of these studies used transgenic mice and therefore are less translatable across species due to the technical difficulties associated with targeting sensory neuron sub-populations in species without such transgenic tractability. In wild-type mice, G_i-DREADD delivered intraneurally to the sciatic nerve via AAV6 was able to increase both mechanical and thermal threshold (Iyer et al., 2016). Importantly however, none of these studies were specific to DRG neuron subsets innervating specific organs.

Delivery of transgenes from the periphery to the DRG neurons has been attempted for quite sometimes, with replication deficit herpes-simplex virus (HSV) tools showing some success in the PNS (reviewed in (Wolfe et al., 2012)). For example, HSV mediated neurotrophin-3 sub-cutaneous delivery into the footpad of chemically-induced diabetic mice protected against the progression of diabetic neuropathy (Chattopadhyay et al., 2007). However, HSVs have limited potential to be a clinically relevant gene therapy tool because of their cytotoxic effects (Johnson et al., 1992). By contrast, AAVs are useful tools for gene transfer that have been used for gene therapy in a variety of human diseases (Wang et al., 2019) and can be utilized in conjunction with DREADD

technology to selectively modulate neuronal activity of specific neuronal circuitry. Indeed, this has been achieved in the CNS (Aschauer et al., 2013), however, delivering genes by AAV injection into a peripheral organ to DRG neurons is challenging because of the low transduction capability of AAVs and the large anatomical distances involved in the PNS (Chan et al., 2017). A variety of AAV serotypes have shown little efficacy in transducing DRG neurons when injected subcutaneously, intra-muscularly or intra-plantarly in adult mice (Abdallah et al., 2018; Towne et al., 2009). To date, direct injection into DRG (Mason et al., 2010) or intrathecal injection (Storek et al., 2006; Weir et al., 2017) are the best ways for transducing DRG neurons, however, these routes of administration are invasive, technically complicated to perform and do not enable transduction of neurons innervating a defined target. The present study provides evidence that the PNS specific AAV serotype, AAV-PHP.S (Chan et al., 2017), discovered using targeted evolution, can infect DRG neurons with functional cargo following injected into the knee joint. Furthermore, using the inhibitory DREADD, $hM_4D(G_i)$, as a cargo, we show normalization of inflammatory pain induced deficit in digging behavior in mice, which is an ethologically relevant spontaneous pain measure indicating well-being (Jirkof, 2014). This study extends the use of AAV and DREADD technologies to study DRG neurons infected from a peripheral organ, which can have future applications in controlling pain pathologies.

The specific aims of this Chapter are 1) to identify an AAV serotype which when injected into the knee is able to transduce neurons in the DRG 2) to investigate whether AAV-PHP.S packaged with G_q-DREADD and G_i-DREADD are able to increase and decrease excitability of transduced neurons from the knee respectively 3) to investigate whether G_q-DREADD and G_i-DREADD mediated changes in knee neuron excitability can modulate mouse behavior.

6.3.Methods

See Materials and Methods chapter for detailed description of virus production (Section 2.3), mice injections (Section 2.4), whole cell patch clamp electrophysiology (Section 2.13) on DRG neurons and behavioral experiments (Sections 2.5, 2.6, 2.7). Both female and male animals were utilized in this Chapter, however the obtained results do not indicate any sex differences.

6.4.Results

6.4.1. Knee injected AAV-PHP.S, but not other serotypes tested, robustly transduces DRG neurons.

AAV-PHP.S is engineered to have a higher specificity towards peripheral neurons (Chan et al., 2017) and thus I hypothesized that this AAV serotype would be able to transduce DRG neurons when injected intra-articularly into the knee joint. In order to test this hypothesis, a non-systematic, semi-quantitative pilot study was first conducted to determine which, if any, of the AAV serotypes are able to transduce DRG neurons when injected into the knee joint. Approximately 360 neurons (3 dishes were imaged, and each dish typically contains ~120 neurons in our culture conditions) were imaged for the serotypes AAV1/2, AAV2, AAV9, AAV-retro and AAV-PHP.S packaged with EGFP or EYFP (n = 2 in each condition). I found that less than 1% of the neurons were transduced with each of the viral serotypes tested, except for AAV-PHP.S which transduced 12.5% of the neurons imaged (Figure 6-2A). Therefore, AAV-PHP.S was more systematically studied.

When AAV-PHP.S-CAG-dTomato and the commonly used retrograde tracer fast blue (FB) were co-injected unilaterally into one knee (n = 3, female), both FB and virus labelling was observed (Figure 6-2B). In agreement with previous reports using FB and other retrograde tracers (Chakrabarti et al., 2018; Cho and Valtschanoff, 2008; Ferreira-Gomes et al., 2010), I observed a similar proportion of labelling in the lumbar DRGs with FB and AAV-PHP.S-CAG-dTomato (FB %: L2: 6.6 ± 2.7, L3: 8.3 ± 1.4, L4: 6.6 ± 1.2, L5: 3.3 ± 1.6; AAV-PHP.S %: L2: 9.0 ± 2.8, L3: 7.3 ± 1.2, L4: 4.0 ± 0.5, L5: 3.3 ± 1.2, Figure 6-2C). Across L2-L5 DRG, there was ~ 40 % co-labelling of neurons with FB and AAV-PHP.S suggesting that both retrograde tracers label with a similar efficiency, but that neither is able to label the entire knee neuron population (Figure 6-2D, F). Furthermore, minimum was observed labelling in the contralateral side (Figure 6-2H). Previous reports suggest that ~40 % of knee neurons are TRPV1 expressing putative nociceptors (Chakrabarti et al., 2018; Cho and Valtschanoff, 2008). Similarly, using immunohistochemistry of DRG neurons, I found that ~30 % of both viral labelled and FB labelled neurons express TRPV1 (Figure 6-2E, G, I) suggesting that viral transduction did not substantially alter expression of the nociceptive gene TRPV1 and that AAV-PHP.S and FB are not preferentially tracing different populations of neurons. Taken together, the data suggest that intra-articular injection of AAV-

PHP.S in the knee joint transduces mouse DRG neurons in a similar manner to a routinely used retrograde tracer.

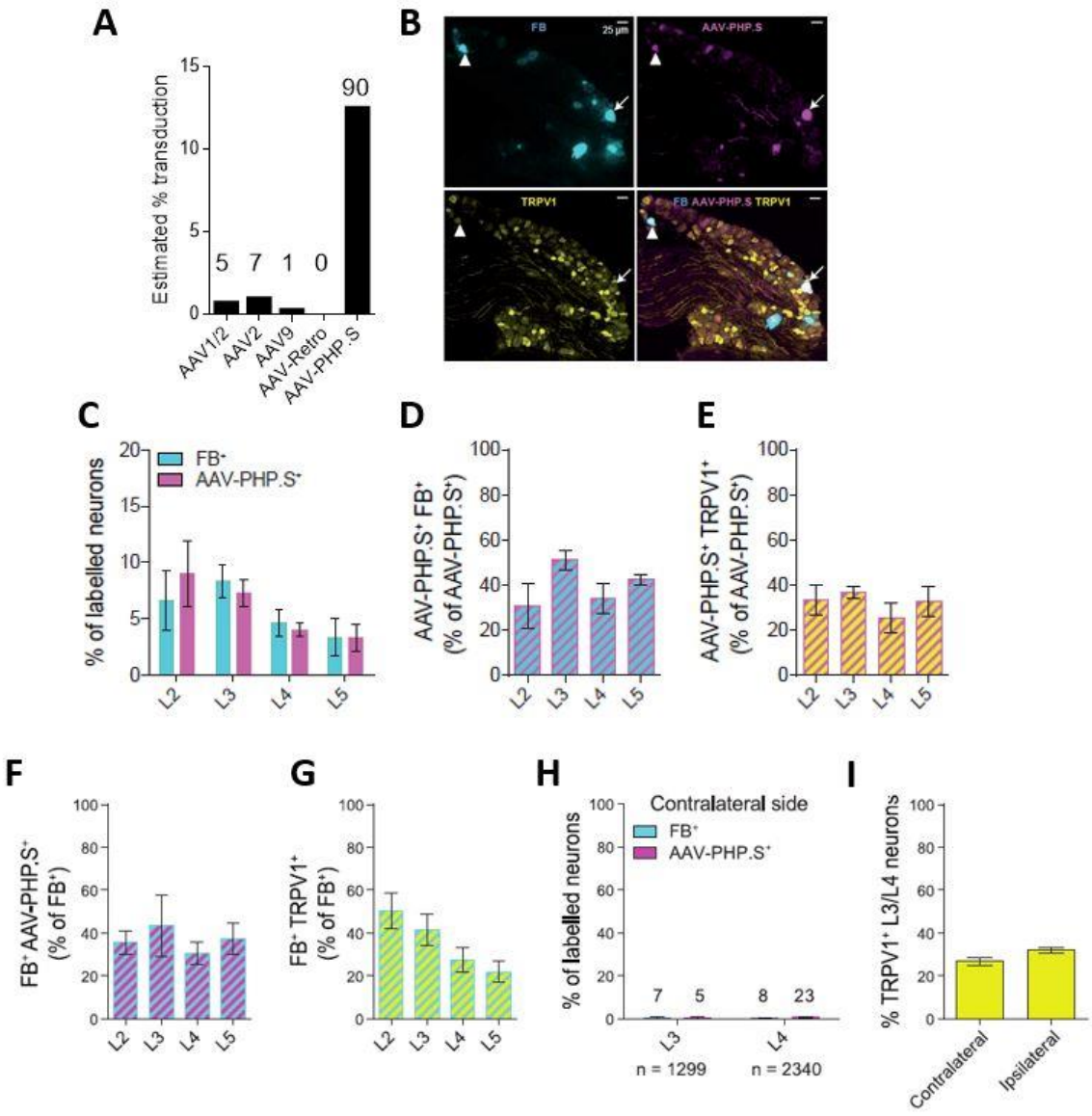

Figure 6-2: Retrograde tracing of knee-innervating DRG neurons using FB and AAV-PHP.S.

A) Bars showing estimated proportions of DRG neurons transduced with a variety of AAV serotypes. Data from 2 male mice in each group, B) Representative images of a whole DRG section showing knee neurons traced using FB (blue), AAV-PHP.S-CAG-dTomato (pink) and stained using an anti-TRPV1 antibody (yellow). C) Bar graphs showing percent of labelled neurons in L2-L5 DRG with FB and AAV. Percent of neurons showing co-localization of FB/AAV and TRPV1/AAV expressed as a percent of AAV^+ neurons (D, E) and of FB^+ neurons (F, G). Bar graphs showing percent of DRG neurons labelled with AAV-PHP.S and FB in the contralateral side (H) and a quantification of TRPV1 stained neurons in contralateral and injected side (I). Data obtained from 3 female mice. The numbers above the bars represent the total number of neurons counted positive for a particular reporter. Error bars = SEM.

6.4.2. The chemogenetic actuator, Compound 21, has no off-target effects in our behavioral paradigms.

Since the next part of the study relates to DREADDs, an important set of control experiment is to determine whether the chosen chemical actuator, Compound 21 (C21) has any off-target effects for the behavioral paradigms tested in the study. C21 was chosen as the DREADD activator since it has good bioavailability and is not converted into clozapine or clozapine-N-oxide (Jendryka et al., 2019). Naïve, wildtype mice (n = 8, 4 females and 4 males) were tested before and after C21 injection for digging behavior, dynamic weight bearing and rotarod. No difference in digging behavior was observed after C21 injection (Digging duration: Pre vs. Post C21, 27.5 ± 3.6 ms vs. 26.3 ± 6.7 ms; Number of burrows: Pre vs. Post C21, 4.1 ± 0.4 vs. 4.3 ± 0.5, Figure 6-3A). Similarly, dynamic weight bearing (Front/Rear paw weight ratio: Pre vs. Post C21, 0.4± 0.1 vs. 0.5 ± 0.1; % left paw weight: Pre vs. Post C21, 23.4 ± 1.2 vs. 21.5 ± 1.3, Figure 6-3B, C) and rotarod performance (Pre vs. Post-C21, 312.4 ± 17.8 s vs. 266.9 ± 25.4 s, Figure 6-3D) remained unchanged in these mice. Taken together, our data suggest that C21 does not produce changes in mice lacking DREADDs in the behavior paradigms tested in the following sections.

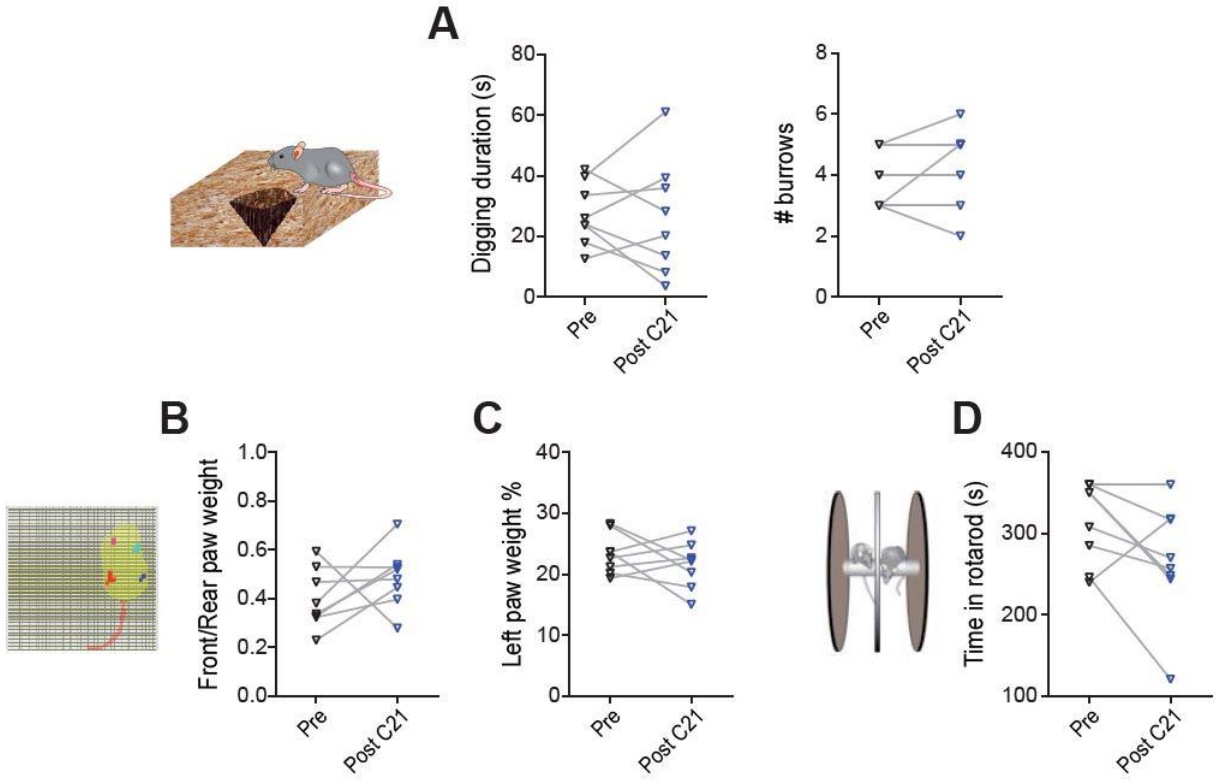

Figure 6-3: No off target behavioral effects of C21.
Digging duration and number of burrows (A), ratio of front and rear paw weight (B), rear left paw weight expressed as a percent of body weight (C), and time on rotarod (D) measured before (black) and after (blue) C21 administration in mice with no virus injections. Data obtained from 4 female and 4 male mice.

6.4.3. Excitatory G_q-DREADD delivered intra-articularly by AAV-PHP.S-hSyn-$hM_3D(G_q)$-mCherry does not change spontaneous pain behavior, but provokes a co-ordination deficit.

Next, I tested whether AAV-PHP.S can deliver functional $hM_3D(G_q)$ cargo into knee neurons via intra-articular injections, using whole cell patch clamp on acutely dissociated neurons isolated from mice with no previous exposure to C21. G_q-DREADDs couple to G_qPCR pathways and thus their activation causes neuronal excitation (Roth, 2016). Therefore, I hypothesized that when incubated with 10 nM C21, virally transduced neurons would be hyperexcitable compared to virally transduced neurons bathed in normal extracellular solution (ECS). In agreement with this hypothesis, I observed an increased number of neurons (Ctrl, 5.3% vs. C21, 27.8% $p = 0.03$, chi-sq test) spontaneously firing action potentials (AP) without injection of current in the C21 group (Figure 6-4A). Moreover, upon injection of increasing stepwise current injections, the threshold of AP generation was decreased (Table 6-1, $p = 0.02$, unpaired t-test) in the C21 group (Figure 6-4B); no change was observed in other electrical properties measured in these neurons (Table 6-1).

Based on previous studies (Chakrabarti et al., 2019a, 2018), I hypothesized that the measured increased excitability of knee-innervating neurons via G_q-DREADD system would cause pain-like behavior in mice, which was tested by measuring digging behavior (a measure of spontaneous pain as described previously (Chakrabarti et al., 2018; Deacon, 2006a)), dynamic weight bearing and rotarod behavior (a measure of motor co-ordination) (Tappe-Theodor et al., 2019) (Timeline in Figure 6-4C). Three weeks after virus injection into both knee joints, mice ($n = 8$, 4 males, 4 females in each group) injected with vehicle or C21 did not show changes in digging behavior (Digging duration: Pre vs. Post veh, 31.6 ± 3.7 ms vs. 21.3 ± 4.4 ms, Pre vs. Post C21, 25.2 ± 4.9 ms vs. 32.7 ± 4.7 ms; Number of burrows: Pre vs. Post veh, 4.6 ± 0.5 vs. 3.5 ± 0.4, Pre vs. Post C21, 3.9 ± 0.7 vs. 3.6 ± 0.5, Figure 6-4D, E) or weight bearing (Front/Rear paw weight ratio: Pre vs. Post veh, 0.5 ± 0.02 vs. 0.5 ± 0.04, Pre vs. Post C21, 0.4± 0.06 vs. 0.4 ± 0.03, Figure 6-4F,G). By contrast, after injection of C21, mice showed a marked decline in their ability to remain on the rotarod (Pre vs. Post veh, 273.5 ± 27.2 s vs. 243.9 ± 32.7 s, Pre vs. Post C21, 336.1 ± 12.9 s vs.

249.0 ± 18.9 s, p = 0.002, paired t-test) suggesting a deficit in their motor co-ordination (Figure 6-4H, I).

Taken together, the data suggest that AAV-PHP.S delivers functional G_q-DREADD into knee neurons and that when virally transduced knee neurons are activated, they do not cause overt pain-like behavior *in vivo*, but do cause a motor co-ordination deficit.

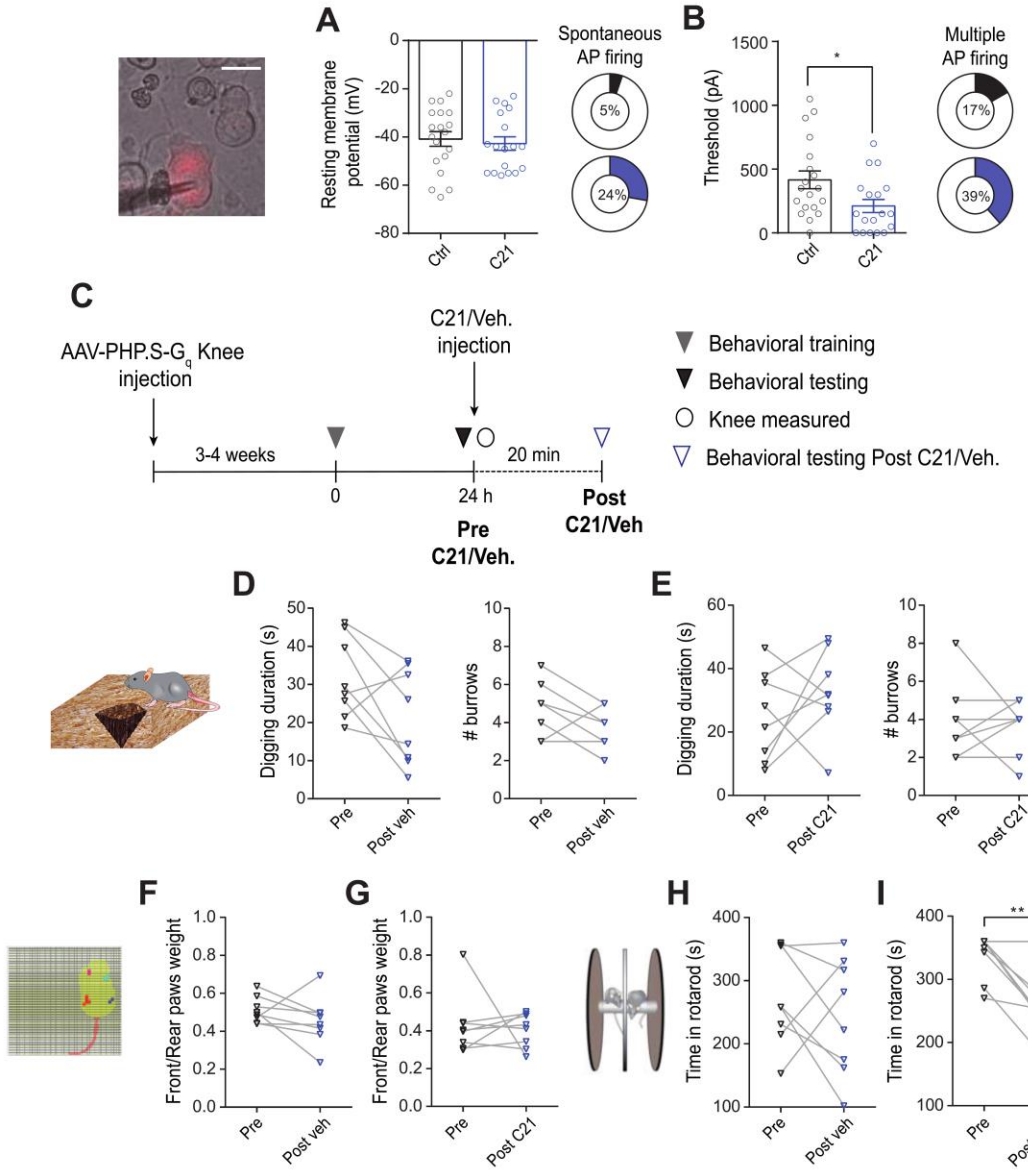

Figure 6-4: G_q-DREADD activation of knee neurons *in vitro* and *in vivo*.
A) Representative image of an AAV-PHP.S-hSyn-hM_3D(G_q)-mCherry transduced neuron (Scale bar = 25 µm, triangular shadow = recording electrode), bars showing resting membrane potential in Ctrl (black, n = 19) and C21 (blue, n = 18) conditions, pie-chart showing percent of neurons in each condition that fired spontaneous AP. B) Bars showing AP firing threshold in Ctrl (black, n = 19) and C21 (blue, n = 18) conditions, pie-chart showing percent of neurons in each condition that fired multiple AP upon current injection. *$p < 0.05$, unpaired t-test. Data obtained from 3 females and 2 male mice. C) Timeline showing when behaviors were conducted. Digging duration and burrows (along with schematic diagram), ratio of front and rear paw weight (along with schematic diagram) and rotarod behavior (along with schematic diagram) before and after vehicle (D, F, H) or C21 injection (E, G, I). ** $p < 0.01$, paired t-test. Data obtained from 4 female and 4 male mice. Error bars = SEM.

Table 6-1 Action potential properties of G_q-DREADD intra-articularly transduced knee neurons. RMP = Resting membrane potential, HPD = Half peak duration. * = $p < 0.05$ unpaired t-test.

	Ctrl (n = 19)		C21 (n = 18)	
	Mean	SEM	Mean	SEM
RMP (mV)	-40.8	3.0	-42.7	2.8
Threshold (pA)	415.8	69.7	211.1*	51.4
HPD (ms)	2.6	0.5	1.9	0.3
Afterhyperpolarization amplitude (AHP peak, mV)	14.7	2.1	16.8	2.8

6.4.4. Inhibitory G_i-DREADD delivered intra-articularly by AAV-PHP.S-hSyn-$hM_4D(G_i)$-mCherry reverses digging behavior deficits associated with inflammatory pain.

Intra-articular injection of complete Freund's adjuvant (CFA) induces robust knee inflammation in mice (Ctrl knee: pre CFA day, 3.1 ± 0.03 mm, post CFA day, 3.1 ± 0.03 mm; CFA knee: pre CFA day, 3.1 ± 0.02 mm, post CFA day, 4.0 ± 0.05 mm, n = 24, $p < 0.0001$, paired t-test, Figure 6-5A) and has been previously shown to increase the excitability of knee neurons innervating the inflamed knee compared to those innervating the contralateral side (Chakrabarti et al., 2018). I hypothesized that incubating the G_i-DREADD expressing knee neurons from the CFA side with C21 would reverse this increased neuronal excitability. Using whole cell electrophysiology of knee neurons, although there was no change in the RMP across any condition (Figure 6-5B, Table 6-2), the percent of CFA knee neurons firing spontaneous AP decreased after G_i-DREADD activation (CFA, 15% vs. CFA+ C21, 0%, $p = 0.02$, chi-sq test, Figure 6-5B). Moreover, in the absence of G_i-DREADD activation, CFA knee neurons had a decreased AP threshold compared to neurons from the control side, but the AP threshold of CFA knee neurons that were incubated in C21 was similar to that of neurons from the control side (Table 6-2, $p = 0.005$, ANOVA, Figure 6-5C). These results suggest that G_i-DREADD activation reverses the CFA-induced increase in neuronal excitability *in vitro*. Other electrical properties between groups were unchanged (Table 6-2).

The ability of G_i-DREADD when expressed in DRG neurons to modulate pain behavior is unclear. Whereas one study shows an increase in latency to both thermal and mechanical stimuli (Iyer et al., 2016), a second study shows only an increase in the paw withdrawal latency to thermal stimuli (Saloman et al., 2016). Nevertheless, based on the *in vitro* results in these studies, I hypothesized that activation of G_i-DREADDs in knee neurons post CFA would reverse spontaneous pain behavior in mice (Timeline in Figure 6-5D). In the control cohort of mice (n = 9, 5 males, 4 females) that received vehicle 24-hours after CFA injection, the CFA-induced decrease in digging behavior persisted compared to pre CFA (Digging duration: Pre CFA, 29.6 ± 2.7 ms, post CFA 16.6 ± 4.0 ms, post veh, 9.8 ± 2.8 ms, $p = 0.0005$, repeated measures ANOVA; Number of burrows: Pre CFA, 4.8 ± 0.3, post CFA 2.9 ± 0.3 ms, post veh, 2.3 ± 0.5 ms, n = 9, $p < 0.0001$, repeated measures ANOVA, Figure 6-5E). However, when C21 was administered to a separate cohort of

mice (n = 11, 7 males, 4 females) 24-hours after CFA injection, there was a marked recovery in digging behavior (Digging duration: Pre CFA, 29.7 ± 4.5 ms, post CFA 7.8 ± 1.9 ms, post C21, 19.0 ± 3.9 ms, p = 0.0002, repeated measures ANOVA; Number of burrows: Pre CFA, 4.5 ± 0.3, post CFA 2.4 ± 0.3 ms, post C21, 3.6 ± 1.4 ms, p = 0.0005, repeated measures ANOVA, Figure 6-5F) suggesting that decreasing the excitability of knee neurons via G_i-DREADD reduces inflammation induced spontaneous pain that is associated with an increase in the feeling of well-being and hence more digging. In contrast, acute chemogenetic inhibition of knee neurons was insufficient to reverse CFA-induced deficit in dynamic weight bearing (Rear left weight bearing as % of body weight: Pre CFA, 26.2 ± 2.0, post CFA, 10.6 ± 1.7, post veh, 11.6 ± 1.5, $p < 0.0001$; Pre CFA, 26.1 ± 1.1, post CFA, 12.4 ± 1.4, post C21, 13.3 ± 2.2, $p < 0.0001$, repeated measures ANOVA, Figure 6-5G, H) which might be because gait changes relating to weight bearing is more reflective of changes in joint biomechanics that is difficult to reverse by analgesics (Shepherd and Mohapatra, 2018). Furthermore, no change in rotarod behavior was observed following CFA-induced knee inflammation suggesting that this model does not cause an overt change in gross motor function and G_i-DREADD activation also had no effect (Pre CFA, 303.8 ± 18.3 s, post CFA, 315.9 ± 11.9 s, post veh, 306.6 ± 16.8 s; Pre CFA, 282.7 ± 17.3 s, post CFA, 286.4 ± 25.3 s, post C21, 317.4 ± 10.3 s, Figure 6-5I, J). Taken together, these results suggest that knee neuron specific inhibition of excitability can reverse inflammation induced deficit in digging behavior.

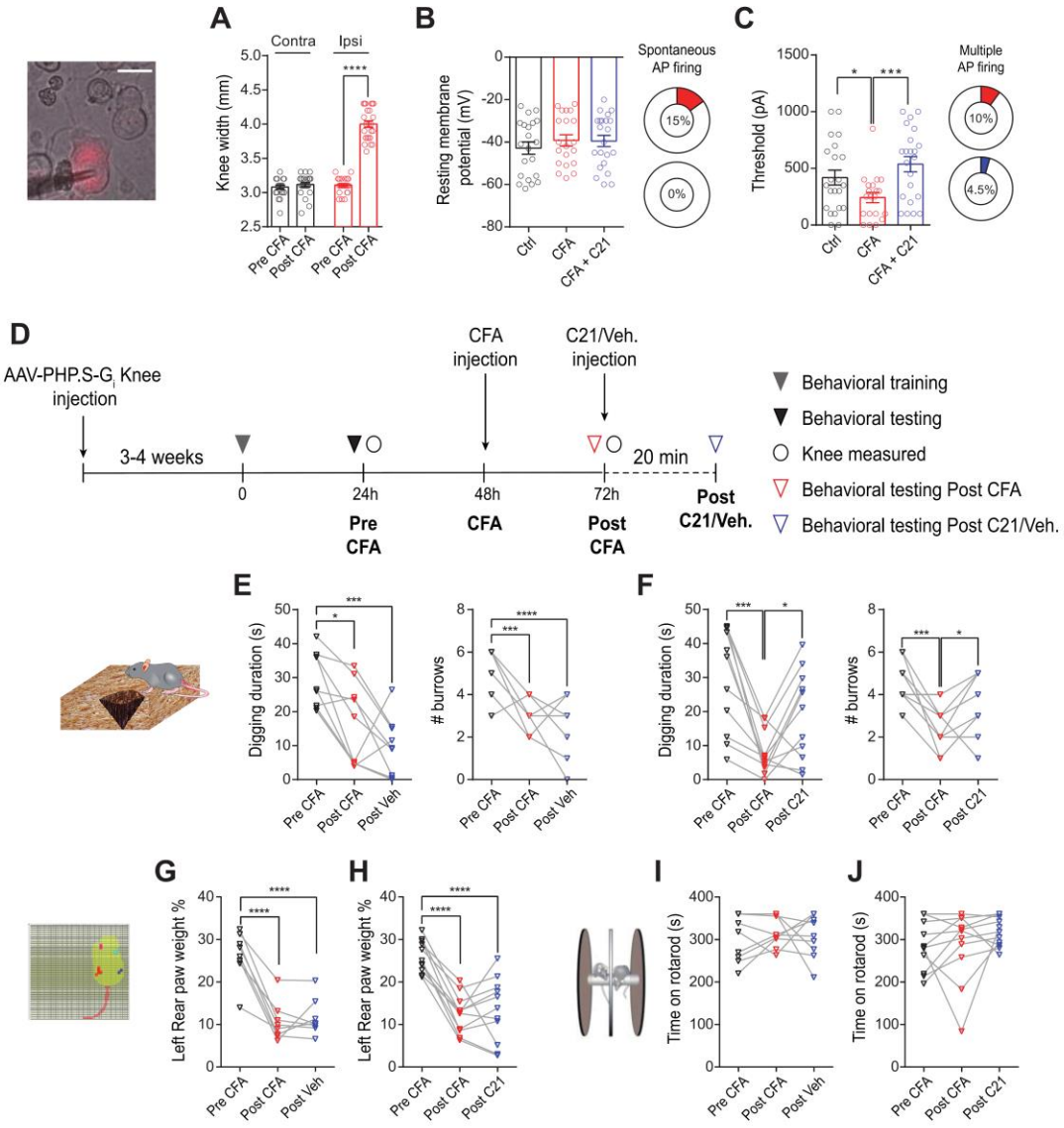

Figure 6-5: G_i-DREADD activation of knee neurons *in vitro* and *in vivo*.
Knee width before and after CFA injection in the non-injected (contra, black) and injected knee (ipsi, red), n = 20, paired t-test. B) RMP in Ctrl (black, n = 22), CFA (red, n = 20) and CFA+C21 (blue, n = 22) conditions, pie-chart of percentage of neurons in CFA and CFA+C21 condition that fired spontaneous AP. C) Bars showing AP threshold in Ctrl (black, n = 22), CFA (red, n = 20) and CFA+C21 (blue, n = 22) conditions, pie-chart of percent of neurons in CFA and CFA+C21 condition that fired multiple AP upon current injection. ANOVA and Holm-Sidak post hoc test. Data obtained from 2 female and 2 male mice. D) Timeline of behaviors conducted. Digging duration and number of burrows, rear left paw weight (% of body weight) and rotarod behavior pre and post-CFA and after vehicle (E, G, I, 4 females, 5 males mice) or C21 injection (F, H, J, 4 females, 7 males). *p < 0.05, ** p < 0.01, ***p < 0.001, **** p < 0.0001 repeated measures ANOVA and Holm-Sidak post hoc test. Error bars = SEM.

Table 6-2: Action potential properties of G_i-DREADD intra-articularly transduced knee neurons. RMP = resting membrane potential, HPD = Half peak duration. * = $p < 0.05$ CFA vs. Ctrl, $$ = $p < 0.01$ CFA vs. CFA+C21, unpaired t-test.

	Ctrl (n = 22)		CFA (n = 20)		CFA + C21 (n = 22)	
	Mean	SEM	Mean	SEM	Mean	SEM
RMP (mV)	-42.9	2.9	-39.2	2.7	-39.5	2.7
Threshold (pA)	418.2*	65.6	242.5	45.0	536.4$$	66.5
HPD (ms)	2.4	0.6	2.9	0.5	2.1	0.3
Afterhyperpolarization amplitude (AHP peak, mV)	12.9	1.3	16.5	1.3	13.8	1.6

6.5.Discussion

The findings in this study show that the AAV-PHP.S serotype can retrogradely deliver cargo to DRG neurons, in a peripheral tissue-specific manner, when injected into the knee joints without the need for invasive procedures or the requirement to generate transgenic mice. Moreover, the transduction efficiency of the virus is similar to the widely used retrograde tracer, FB. In-line with other co-labelling studies (Puigdellívol-Sánchez et al., 1998), the ~40% co-localization of AAV-PHP.S and FB fluorescence suggests that not all knee neurons are labeled by either tracer and the less than 100 % co-labeling is possibly due to their differing modes of retrograde transfer (Eisenman, 1985; Tervo et al., 2016).

Using this system, I show that it is possible to increase or decrease knee neuron excitability *in vitro* when G_q or G_i-DREADD cargoes were delivered by AAV-PHP.S. This result can be extended to study the role of anatomically-specific neuronal excitability when exposed to a variety of stimuli or pharmacological interventions. *In vivo*, chemogenetic activation was restricted to a short duration to reflect acute pain and within this timeframe we saw no spontaneous pain-like behavior with activation of G_q-DREADD in knee neurons. We surmise that G_q-mediated sub-threshold activation (Jaiswal and English, 2017) of the relatively low percentage of DRG neurons did not provide sufficient nociceptive input to drive change in ethologically relevant pain behaviors; whereas the observed decrease in co-ordination suggests that we have behaviorally engaged the virally transduced neurons. Notably, intra-articular injection would transduce DREADDs to both nociceptive and non-nociceptive population of knee neurons, therefore, a clear nocifensive behavior might not be apparent. Since a prior study has shown successful axon regeneration following peripheral nerve injury with repeated (but not after single) dosing of the DREADD activator CNO (Jaiswal et al., 2018), future studies using a repeated dosing strategy could be employed in this system for modelling chronic pain, being cautious of the potential risk of receptor desensitization (Roth, 2016).

Perhaps more relevant to future clinical applications is the ability of G_i-DREADDs to reverse pain behavior by decreasing neuronal excitability of knee neurons. Indeed, we show that G_i-DREADD activation restores a deficit in digging behavior induced by inflammatory knee pain. This strategy can be further refined to selectively inhibit genetically specific subpopulation of knee neurons by combining Cre-inducible viruses with their corresponding Cre-expressing transgenic mouse lines,

and hence provide insights into relative contributions of different knee neuron sub-populations in arthritic pain. Selectively exciting specific knee neuron sub-populations with G_q-DREADD might also produce pain-like behaviors that were not observed in this study. We also report that the CFA-induced deficit in weight bearing was not reversed following activation of G_i-DREADD in knee neurons, consistent with a previous report observing that reversal of deficits in gait changes are difficult to achieve with analgesics (Shepherd and Mohapatra, 2018).

Although findings from this study imply that modulating excitability of anatomically specific peripheral neurons can control arthritic pain, a number of challenges need to be addressed before their clinical translation. Since virus transduction and expression profile is different between non-human primates and rodents, the expression profile of AAV-PHP.S needs to be validated in non-human primates (Galvan et al., 2019). Additional work is also required to engineer more PNS specific AAVs and to optimize DREADDs (Magnus et al., 2011) and their corresponding ligands (Thompson et al., 2018) for increasing transduction efficiency and regulating dosing.

Overall, the present study provides initial proof-of-concept that peripheral tissue innervating DRG neurons can be specifically modulated by AAVs, opening the door to future studies on gene therapy in controlling pain.

Chapter 7. Conclusions and Future Directions

The major contribution of this thesis is the demonstration of the key role of knee-innervating DRG neuron (knee neuron) sensitization in arthritic pain, which was achieved by the development and utilization of several *in vitro* and *in vivo* models of inflammatory pain. The functional heterogeneity of DRG neurons based on target innervation (Petruska et al., 2000) has also been demonstrated, such that knee neurons have a lower threshold of AP generation compared to a randomly picked, acutely cultured neurons.

The findings of this thesis open up several avenues of investigation in the arthritic pain field. The following paragraphs will summarize the answers to the questions posed in Introduction, as well as discuss limitations of the findings and recommend future research that can further the field of arthritic pain research.

1) **Can clinical samples from human arthritis patients be used in combination with mouse tissue to create a translatable, *in vitro* model of arthritic pain?**

Chapter 3 shows that mediators present in SF derived from patients with painful OA can increase the excitability of knee neurons, implicating SF as an active nociceptive agent in arthritic pain. The major limitation of this study was that given the small number of OA-SF samples, I was neither able to correlate the pain scores of the individuals to the nociceptive potential changes observed through AP properties *in vitro*, nor was I able to determine sex-specific differences.

Therefore, a key future direction of these findings will be to replicate them with a larger pool of arthritic SF samples to correlate pain scores, identify differential effects of RA-SF vs. OA-SF and sex-specific changes in nociceptive potentials. Furthermore, this model can be adopted *in vivo* (as a clinically relevant mouse model) by intra-articular injection of acellularized SF and tested for pain measures established in this thesis (e.g., digging, dynamic weight bearing, rotarod) and in other studies (Gregory et al., 2013). To better understand the mechanism of action of SF, two major questions need to be answered: what are the mediators in arthritic SF that confer neuronal hyperexcitability and which neuronal genes are involved in SF-mediated hyperexcitablilty? To answer the first questions, omics techniques (Hasin et al., 2017) can be applied to identify lipids, proteins and metabolites present in SFs. The findings can then be clustered based on diagnosis and

pain scores before being ranked based on their differential abundance compared to control SF to identify the most promising hits. The best ranked molecules can then be tested on the SF/neuron *in vitro* system to measure their nociceptive potential via whole cell electrophysiology. In order to answer the second question, single-cell and bulk transcriptomics (North et al., 2019) can be performed on neurons incubated in whole SF and its components.

2) **Does the acute CFA-induced knee inflammation model sensitize knee neurons and therefore cause changes in spontaneous pain behavior?**

Chapter 4 reports that CFA-induced knee inflammation decreases digging behavior, which is a measure of spontaneous pain. Furthermore, after inflammation, there is increased knee neuron excitability and TRPV1 function, results suggesting sensitization of these sensory neurons. Consequently, blocking TRPV1 function systemically reverses inflammation induced decrease in digging. Although digging is useful for testing non-reflexive pain behavior, effectivity of this paradigm needs to be tested in chronic pain model, i.e., whether digging behavior remains suppressed throughout the chronic pain condition. The importance of TRPV1 in arthritic pain has been shown by multiple groups using multiple mouse models (Hsieh et al., 2017; Kelly et al., 2015; Zhang et al., 2013) and recently a study highlighted the differential contribution of TRPV1 in acute and chronic pain of a rodent OA model (Haywood et al., 2018). Therefore, future efforts can be directed at understanding TRPV1's relative importance in different DRG neuron subsets. Given that TRPV1 antagonists have had limited success for pain therapy because of their adverse effects (e.g., hyperthermia) (Galindo et al., 2018), another strategy would be to perform single cell transcriptomics on knee neurons in healthy and arthritic states to identify novel drug targets (a project currently underway in the Smith Lab). These targets can then be correlated with gene targets identified in the SF/neuron system (described above) to validate their clinical potential, after which antagonists of those targets can be administered in mice to test behavioral pain measures.

3) **Does communication exist between knee neurons and non-neuronal FLS that is relevant to arthritic pain?**

In Chapter 5, I found that murine knee-derived FLS when stimulated with the pro-inflammatory cytokine, TNF-α, can themselves secrete pro-inflammatory cytokines and that these released inflammatory factors increase excitability of knee neurons. This result suggests that direct

interaction of non-neuronal FLS and neurons is important in arthritic pain. A limitation of this approach is that I was only able to discern TNF-α related pro-inflammatory cascades in FLS and their effects on DRG neurons. However, multiple other pro- and anti-inflammatory mediators are present in an arthritic joint (Gobezie et al., 2007). Since I was not able to investigate the overall effect of these mediators on FLS with the acute CFA-induced knee inflammation model, future work can focus on testing the effects of FLS/neuron interactions in neuronal excitability with "inflamed" FLS derived from chronic mouse models of arthritis such as antigen induced arthritis (von Banchet et al., 2007) or K/BxN mice (Hardy et al., 2013).

Nevertheless, the results in Chapter 5 have translational potential given that human FLS contribute to SF, and soluble factors in OA-SF can excite knee neurons, as shown in Chapter 3. Additionally, TNF-α stimulated human FLS have been shown to secrete multiple cytokines in agreement with the murine data presented in this thesis (Jones et al., 2016), therefore, in the future, a human FLS/DRG neuron system can be established to directly study this link. Furthermore, given that I identify and emphasize the importance of soluble mediators in sensitizing nociceptors, direct application of these mediators on knee neurons could be conducted to reveal their specific sensitization capabilities.

Beyond the FLS/neuron interaction, the functional properties of FLS remains elusive. For example, further work is needed to extend the work presented in this thesis to identify the acid sensors in FLS. Furthermore, there is evidence of other ion channels being expressed by FLS which affects their membrane potential and hence depolarization induced secretions (Clark et al., 2017). Extending the knowledge of the ion channel expression by human FLS in health and disease can be used to help prevent arthritis progression and pain.

4) Can an AAV serotype be identified that can specifically deliver functional genes from the periphery (knee joint) to the DRG neurons to control neuronal excitability?

Chapter 6 identifies that a PNS-specific AAV serotype, AAV-PHP.S can transduce DRG neurons when injected intra-articularly in the knee joint. Given that I have shown excitability of knee neurons is important in controlling arthritic pain both *in vitro* and *in vivo*, this method provides an opportunity to specifically access these neurons which might limit side effects when adopted into clinics. For example, I have shown that TRPV1 function is increased in knee neurons, yet while

testing whether antagonizing TRPV1 alleviates arthritic pain phenotype I injected a systemic TRPV1 blocker. Using the viral technique, a TRPV1 aptamer (Xiang et al., 2017) could be packaged into AAV-PHP.S, which when delivered into the knee would allow us to investigate the effects of specifically blocking TRPV1 function in knee neurons. Beyond TRPV1, this technology can be utilized in the future to validate other drug targets identified by single cell transcriptomics in arthritic animals and SF/neuron systems.

Furthermore, I showed that excitatory or inhibitory DREADDs can be packaged into AAV-PHP.S to control knee neuron excitability; and that inhibitory DREADD activation ameliorates inflammatory knee pain behavior in mice. Although the results obtained suggest that G_q and G_i mediated excitation and inhibition respectively of AP firing are important in controlling arthritic pain, more direct neuronal controls can be tested in the future by combining this viral technique with optogenetics. In optogenetics a light gated ion channels (commonly channelrhodopsin for activation and halorhodopsin for inhibition) can be expressed in neurons which when activated cause direct neuronal activation/inhibition to modulate behavior (Yizhar et al., 2011). However the major barrier to widespread use of this technology is the inability of light to penetrate certain tissues such as the knee or the DRGs without an implant (Samineni et al., 2017). Recently, in a substantial technological advancement, machine learning tools have been used in the field of optogenetics to identify channelrhodopsins that show massively increased light sensitivity and can be stimulated transcranially (in mice) to activate neurons (Bedbrook et al., 2019). If these proteins are packaged into AAV-PHP.S and delivered intra-articularly, there is potential to control excitability of knee neurons by shining appropriate light through the skin.

Overall, efforts have been made in this thesis, in collaboration with clinicians and basic scientists with variety of skills, to identify and characterize peripheral mechanisms of sensitization in inflammatory knee pain with the overarching goal to improve the lives of others by administering safe and effective pain therapy in arthritis.

Chapter 8. References

Abdallah, K., Nadeau, F., Bergeron, F., Blouin, S., Blais, V., Bradbury, K.M., Lavoie, C.L., Parent, J.-L., Gendron, L., 2018. Adeno-associated virus 2/9 delivery of Cre recombinase in mouse primary afferents. Sci Rep 8, 7321–7321. https://doi.org/10.1038/s41598-018-25626-y

Abdo, H., Calvo-Enrique, L., Lopez, J.M., Song, J., Zhang, M.-D., Usoskin, D., El Manira, A., Adameyko, I., Hjerling-Leffler, J., Ernfors, P., 2019. Specialized cutaneous Schwann cells initiate pain sensation. Science 365, 695. https://doi.org/10.1126/science.aax6452

Abdus-Saboor, I., Fried, N.T., Lay, M., Burdge, J., Swanson, K., Fischer, R., Jones, J., Dong, P., Cai, W., Guo, X., Tao, Y.-X., Bethea, J., Ma, M., Dong, X., Ding, L., Luo, W., 2019. Development of a Mouse Pain Scale Using Sub-second Behavioral Mapping and Statistical Modeling. Cell Reports 28, 1623-1634.e4. https://doi.org/10.1016/j.celrep.2019.07.017

Abou-Raya, S., Abou-Raya, A., Helmii, M., 2012. Duloxetine for the management of pain in older adults with knee osteoarthritis: randomised placebo-controlled trial. Age and Ageing 41, 646–652. https://doi.org/10.1093/ageing/afs072

Agalave, N.M., Larsson, M., Abdelmoaty, S., Su, J., Baharpoor, A., Lundbäck, P., Palmblad, K., Andersson, U., Harris, H., Svensson, C.I., 2014. Spinal HMGB1 induces TLR4-mediated long-lasting hypersensitivity and glial activation and regulates pain-like behavior in experimental arthritis. PAIN® 155, 1802–1813. https://doi.org/10.1016/j.pain.2014.06.007

Ai, R., Hammaker, D., Boyle, D.L., Morgan, R., Walsh, A.M., Fan, S., Firestein, G.S., Wang, W., 2016. Joint-specific DNA methylation and transcriptome signatures in rheumatoid arthritis identify distinct pathogenic processes. Nat Commun 7, 11849–11849. https://doi.org/10.1038/ncomms11849

Akopian, A.N., Ruparel, N.B., Jeske, N.A., Hargreaves, K.M., 2007. Transient receptor potential TRPA1 channel desensitization in sensory neurons is agonist dependent and regulated by TRPV1-directed internalization. J Physiol 583, 175–193. https://doi.org/10.1113/jphysiol.2007.133231

Alarcó-Segovia, D., 1976. Pre-columbian representation of heberden's nodes. Arthritis & Rheumatism 19, 125–126. https://doi.org/10.1002/art.1780190127

Allchorne, A.J., Broom, D.C., Woolf, C.J., 2005. Detection of cold pain, cold allodynia and cold hyperalgesia in freely behaving rats. Mol Pain 1, 36–36. https://doi.org/10.1186/1744-8069-1-36

Amaya, F., Oh-hashi, K., Naruse, Y., Iijima, N., Ueda, M., Shimosato, G., Tominaga, M., Tanaka, Y., Tanaka, M., 2003. Local inflammation increases vanilloid receptor 1 expression within distinct subgroups of DRG neurons. Brain Research 963, 190–196. https://doi.org/10.1016/S0006-8993(02)03972-0

Anderson, M., Zheng, Q., Dong, X., 2018. Investigation of Pain Mechanisms by Calcium Imaging Approaches. Neurosci Bull 34, 194–199. https://doi.org/10.1007/s12264-017-0139-9

Andersson, D.A., Gentry, C., Alenmyr, L., Killander, D., Lewis, S.E., Andersson, A., Bucher, B., Galzi, J.-L., Sterner, O., Bevan, S., Högestätt, E.D., Zygmunt, P.M., 2011. TRPA1 mediates spinal antinociception induced by acetaminophen and the cannabinoid Δ9-tetrahydrocannabiorcol. Nature Communications 2, 551. https://doi.org/10.1038/ncomms1559

Andersson, S.E., Lexmuller, K., Johansson, A., Ekstrom, G.M., 1999. Tissue and intracellular pH in normal periarticular soft tissue and during different phases of antigen induced arthritis in the rat. J Rheumatol 26, 2018–2024.

Ängeby Möller, K., Berge, O.-G., Finn, A., Stenfors, C., Svensson, C.I., 2015. Using gait analysis to assess weight bearing in rats with Freund′s complete adjuvant-induced monoarthritis to improve predictivity: Interfering with the cyclooxygenase and nerve growth factor pathways. European Journal of Pharmacology 756, 75–84. https://doi.org/10.1016/j.ejphar.2015.02.050

Anné, J., Hedrick, B.P., Schein, J.P., 2016. First diagnosis of septic arthritis in a dinosaur. R Soc Open Sci 3, 160222–160222. https://doi.org/10.1098/rsos.160222

Annecchino, L.A., Schultz, S.R., 2018. Progress in automating patch clamp cellular physiology. Brain and Neuroscience Advances 2, 2398212818776561. https://doi.org/10.1177/2398212818776561
Araldi, D., Ferrari, L.F., Levine, J.D., 2015. Repeated Mu-Opioid Exposure Induces a Novel Form of the Hyperalgesic Priming Model for Transition to Chronic Pain. J Neurosci 35, 12502–12517. https://doi.org/10.1523/JNEUROSCI.1673-15.2015
Archer, B.H., 1936. Classification of Arthritis. Journal of the American Medical Association 107, 1069–1069. https://doi.org/10.1001/jama.1936.02770390061027
Arendt-Nielsen, L., 2017. Joint pain: more to it than just structural damage? PAIN 158.
Aschauer, D.F., Kreuz, S., Rumpel, S., 2013. Analysis of Transduction Efficiency, Tropism and Axonal Transport of AAV Serotypes 1, 2, 5, 6, 8 and 9 in the Mouse Brain. PLOS ONE 8, e76310. https://doi.org/10.1371/journal.pone.0076310
Atzeni, F., Masala, I.F., Sarzi-Puttini, P., 2018. A Review of Chronic Musculoskeletal Pain: Central and Peripheral Effects of Diclofenac. Pain Ther 7, 163–177. https://doi.org/10.1007/s40122-018-0100-2
Austin, A.E., 2017. The Cost of a Commute: A Multidisciplinary Approach to Osteoarthritis in New Kingdom Egypt. International Journal of Osteoarchaeology 27, 537–550. https://doi.org/10.1002/oa.2575
Ayala-Caminero, R., Pinzón-Herrera, L., Martinez, C.A.R., Almodovar, J., 2017. Polymeric scaffolds for three-dimensional culture of nerve cells: a model of peripheral nerve regeneration. MRS Commun 7, 391–415. https://doi.org/10.1557/mrc.2017.90
Balakrishnan, L., Bhattacharjee, M., Ahmad, S., Nirujogi, R.S., Renuse, S., Subbannayya, Y., Marimuthu, A., Srikanth, S.M., Raju, R., Dhillon, M., Kaur, N., Jois, R., Vasudev, V., Ramachandra, Y., Sahasrabuddhe, N.A., Prasad, T.K., Mohan, S., Gowda, H., Shankar, S., Pandey, A., 2014. Differential proteomic analysis of synovial fluid from rheumatoid arthritis and osteoarthritis patients. Clinical Proteomics 11, 1. https://doi.org/10.1186/1559-0275-11-1
Balazs, E.A., Watson, D., Duff, I.F., Roseman, S., 1967. Hyaluronic acid in synovial fluid. I. Molecular parameters of hyaluronic acid in normal and arthritis human fluids. Arthritis Rheum 10, 357–376.
Bando, Y., Grimm, C., Cornejo, V.H., Yuste, R., 2019a. Genetic voltage indicators. BMC Biology 17, 71. https://doi.org/10.1186/s12915-019-0682-0
Bando, Y., Sakamoto, M., Kim, S., Ayzenshtat, I., Yuste, R., 2019b. Comparative evaluation of genetically encoded voltage indicators. Cell reports 26, 802–813.
Bär, K.-J., Schaible, H.-G., Bräuer, R., Halbhuber, K.-J., von Banchet, G.S., 2004. The proportion of TRPV1 protein-positive lumbar DRG neurones does not increase in the course of acute and chronic antigen-induced arthritis in the knee joint of the rat. Neuroscience Letters 361, 172–175. https://doi.org/10.1016/j.neulet.2003.12.034
Bartok, B., Firestein, G.S., 2010. Fibroblast-like synoviocytes: key effector cells in rheumatoid arthritis. Immunological reviews 233, 233–255. https://doi.org/10.1111/j.0105-2896.2009.00859.x
Barton, N.J., McQueen, D.S., Thomson, D., Gauldie, S.D., Wilson, A.W., Salter, D.M., Chessell, I.P., 2006. Attenuation of experimental arthritis in TRPV1R knockout mice. Experimental and Molecular Pathology 81, 166–170. https://doi.org/10.1016/j.yexmp.2006.04.007
Basbaum, A.I., Bautista, D.M., Scherrer, G., Julius, D., 2009. Cellular and Molecular Mechanisms of Pain. Cell 139, 267–284. https://doi.org/10.1016/j.cell.2009.09.028
Batti, L., Mukhtarov, M., Audero, E., Ivanov, A., Paolicelli, R.C., Zurborg, S., Gross, C., Bregestovski, P., Heppenstall, P.A., 2013. Transgenic mouse lines for non-invasive ratiometric monitoring of intracellular chloride. Frontiers in Molecular Neuroscience 6, 11. https://doi.org/10.3389/fnmol.2013.00011
Becker, W.C., Sullivan, L.E., Tetrault, J.M., Desai, R.A., Fiellin, D.A., 2008. Non-medical use, abuse and dependence on prescription opioids among U.S. adults: Psychiatric, medical and substance use correlates. Drug and Alcohol Dependence 94, 38–47. https://doi.org/10.1016/j.drugalcdep.2007.09.018

Bedbrook, C.N., Yang, K.K., Robinson, J.E., Mackey, E.D., Gradinaru, V., Arnold, F.H., 2019. Machine learning-guided channelrhodopsin engineering enables minimally invasive optogenetics. Nature Methods 16, 1176–1184. https://doi.org/10.1038/s41592-019-0583-8

Bedson, J., Croft, P.R., 2008. The discordance between clinical and radiographic knee osteoarthritis: a systematic search and summary of the literature. BMC Musculoskelet Disord 9. https://doi.org/10.1186/1471-2474-9-116

Belkouch, M., Dansereau, M.-A., Tétreault, P., Biet, M., Beaudet, N., Dumaine, R., Chraibi, A., Mélik-Parsadaniantz, S., Sarret, P., 2014. Functional up-regulation of Nav1.8 sodium channel in Aβ afferent fibers subjected to chronic peripheral inflammation. J Neuroinflammation 11, 45–45. https://doi.org/10.1186/1742-2094-11-45

Benito-Miguel, M., García-Carmona, Y., Balsa, A., Bautista-Caro, M.-B., Arroyo-Villa, I., Cobo-Ibáñez, T., Bonilla-Hernán, M.G., de Ayala, C.P., Sánchez-Mateos, P., Martín-Mola, E., Miranda-Carús, M.-E., 2012. IL-15 Expression on RA Synovial Fibroblasts Promotes B Cell Survival. PLOS ONE 7, e40620. https://doi.org/10.1371/journal.pone.0040620

Bennell, K.L., Hinman, R.S., 2011. A review of the clinical evidence for exercise in osteoarthritis of the hip and knee. Journal of Science and Medicine in Sport 14, 4–9. https://doi.org/10.1016/j.jsams.2010.08.002

Bennett, D.L., Clark, A.J., Huang, J., Waxman, S.G., Dib-Hajj, S.D., 2019. The Role of Voltage-Gated Sodium Channels in Pain Signaling. Physiological Reviews 99, 1079–1151. https://doi.org/10.1152/physrev.00052.2017

Berkley, K.J., 1997. Sex differences in pain. Behavioral and Brain Sciences 20, 371–380.

Berridge, M.J., Bootman, M.D., Roderick, H.L., 2003. Calcium: calcium signalling: dynamics, homeostasis and remodelling. Nature reviews Molecular cell biology 4, 517.

Bhattacharjee, M., Balakrishnan, L., Renuse, S., Advani, J., Goel, R., Sathe, G., Keshava Prasad, T.S., Nair, B., Jois, R., Shankar, S., Pandey, A., 2016. Synovial fluid proteome in rheumatoid arthritis. Clinical Proteomics 13, 12. https://doi.org/10.1186/s12014-016-9113-1

Billiau, A., Matthys, P., 2001. Modes of action of Freund's adjuvants in experimental models of autoimmune diseases. Journal of Leukocyte Biology 70, 849–860. https://doi.org/10.1189/jlb.70.6.849

Birbara, C., Dabezies, E.J., Jr, Burr, A.M., Fountaine, R.J., Smith, M.D., Brown, M.T., West, C.R., Arends, R.H., Verburg, K.M., 2018. Safety and efficacy of subcutaneous tanezumab in patients with knee or hip osteoarthritis. J Pain Res 11, 151–164. https://doi.org/10.2147/JPR.S135257

Black, J.A., Liu, S., Tanaka, M., Cummins, T.R., Waxman, S.G., 2004. Changes in the expression of tetrodotoxin-sensitive sodium channels within dorsal root ganglia neurons in inflammatory pain. Pain 108. https://doi.org/10.1016/j.pain.2003.12.035

Blake, D.R., Robson, P., Ho, M., Jubb, R.W., McCabe, C.S., 2005. Preliminary assessment of the efficacy, tolerability and safety of a cannabis-based medicine (Sativex) in the treatment of pain caused by rheumatoid arthritis. Rheumatology 45, 50–52. https://doi.org/10.1093/rheumatology/kei183

Blue, M.L., Conrad, P., Webb, D.L., Sarr, T., Macaro, M., 1993. Interacting monocytes and synoviocytes induce adhesion molecules by a cytokine-regulated process. Lymphokine Cytokine Res 12, 213–218.

Blumberg, B.S., Bunim, J.J., Calmns, E., Pirani, C.L., Zvaifler, N.J., 1964. ARA nomenclature and classification of arthritis and rheumatism (tentative). Arthritis & Rheumatism 7, 93–97. https://doi.org/10.1002/art.1780070113

Blyth, F.M., Briggs, A.M., Schneider, C.H., Hoy, D.G., March, L.M., 2019. The Global Burden of Musculoskeletal Pain-Where to From Here? Am J Public Health 109, 35–40. https://doi.org/10.2105/AJPH.2018.304747

Boileau, C., Martel-Pelletier, J., Abram, F., Raynauld, J.-P., Troncy, É., D'Anjou, M.-A., Moreau, M., Pelletier, J.-P., 2008. Magnetic resonance imaging can accurately assess the long-term

progression of knee structural changes in experimental dog osteoarthritis. Ann Rheum Dis 67, 926. https://doi.org/10.1136/ard.2007.077297
Bombara, M.R., Webb, D.L., Conrad, P., Marior, C.W., Sarr, T., Ranges, G.E., Aune, T.M., Grave, J.M., Blue, M.-L., 1993. Cell contact between T cells and synovial fibroblasts causes induction of adhesion molecules and cytokines. Journal of Leukocyte Biology 54, 399–406. https://doi.org/10.1002/jlb.54.5.399
Bond, M., 2011. Pain education issues in developing countries and responses to them by the International Association for the Study of Pain. Pain Res Manag 16, 404–406. https://doi.org/10.1155/2011/654746
Bondeson, J., Wainwright, S.D., Lauder, S., Amos, N., Hughes, C.E., 2006. The role of synovial macrophages and macrophage-produced cytokines in driving aggrecanases, matrix metalloproteinases, and other destructive and inflammatory responses in osteoarthritis. Arthritis Research & Therapy 8, R187. https://doi.org/10.1186/ar2099
Bonet, I.J.M., Fischer, L., Parada, C.A., Tambeli, C.H., 2013. The role of transient receptor potential A 1 (TRPA1) in the development and maintenance of carrageenan-induced hyperalgesia. Neuropharmacology 65, 206–212. https://doi.org/10.1016/j.neuropharm.2012.09.020
Bottini, N., Firestein, G.S., 2013. Duality of fibroblast-like synoviocytes in RA: passive responders and imprinted aggressors. Nat Rev Rheumatol. 9. https://doi.org/10.1038/nrrheum.2012.190
Bourinet, E., Altier, C., Hildebrand, M.E., Trang, T., Salter, M.W., Zamponi, G.W., 2014. Calcium-Permeable Ion Channels in Pain Signaling. Physiological Reviews 94, 81–140. https://doi.org/10.1152/physrev.00023.2013
Bove, S., Laemont, K., Brooker, R., Osborn, M., Sanchez, B., Guzman, R., Hook, K., Juneau, P., Connor, J., Kilgore, K., 2006. Surgically induced osteoarthritis in the rat results in the development of both osteoarthritis-like joint pain and secondary hyperalgesia. Osteoarthritis and Cartilage 14, 1041–1048.
Brackertz, D., Mitchell, G.F., Mackay, I.R., 1977. Antigen-induced arthritis in mice. Arthritis & Rheumatism 20, 841–850. https://doi.org/10.1002/art.1780200314
Brand, D.D., Latham, K.A., Rosloniec, E.F., 2007. Collagen-induced arthritis. Nature Protocols 2, 1269–1275. https://doi.org/10.1038/nprot.2007.173
Brandolini, L., Benedetti, E., Ruffini, P.A., Russo, R., Cristiano, L., Antonosante, A., d'Angelo, M., Castelli, V., Giordano, A., Allegretti, M., Cimini, A., 2017. CXCR1/2 pathways in paclitaxel-induced neuropathic pain. Oncotarget 8, 23188–23201. https://doi.org/10.18632/oncotarget.15533
Brandt, M.R., Beyer, C.E., Stahl, S.M., 2012. TRPV1 Antagonists and Chronic Pain: Beyond Thermal Perception. Pharmaceuticals 5, 114–132. https://doi.org/10.3390/ph5020114
Breedveld, F.C., Dayer, J.M., 2000. Leflunomide: mode of action in the treatment of rheumatoid arthritis. Ann Rheum Dis 59, 841–849. https://doi.org/10.1136/ard.59.11.841
Brenn, D., Richter, F., Schaible, H.-G., 2007. Sensitization of unmyelinated sensory fibers of the joint nerve to mechanical stimuli by interleukin-6 in the rat: An inflammatory mechanism of joint pain. Arthritis & Rheumatism 56, 351–359. https://doi.org/10.1002/art.22282
Brennan-Olsen, S.L., Cook, S., Leech, M.T., Bowe, S.J., Kowal, P., Naidoo, N., Ackerman, I.N., Page, R.S., Hosking, S.M., Pasco, J.A., Mohebbi, M., 2017. Prevalence of arthritis according to age, sex and socioeconomic status in six low and middle income countries: analysis of data from the World Health Organization study on global AGEing and adult health (SAGE) Wave 1. BMC Musculoskelet Disord 18, 271–271. https://doi.org/10.1186/s12891-017-1624-z
Brenner, D.S., Golden, J.P., Gereau, R.W., 4th, 2012. A novel behavioral assay for measuring cold sensation in mice. PLoS One 7, e39765–e39765. https://doi.org/10.1371/journal.pone.0039765
Briggs, A.M., Cross, M.J., Hoy, D.G., Sànchez-Riera, L., Blyth, F.M., Woolf, A.D., March, L., 2016. Musculoskeletal Health Conditions Represent a Global Threat to Healthy Aging: A Report for the 2015 World Health Organization World Report on Ageing and Health. The Gerontologist 56, S243–S255. https://doi.org/10.1093/geront/gnw002

Burger, D., Rezzonico, R., Li, J.-M., Modoux, C., Pierce, R.A., Welgus, H.G., Dayer, J.-M., 1998. Imbalance between interstitial collagenase and tissue inhibitor of metalloproteinases 1 in synoviocytes and fibroblasts upon direct contact with stimulated T lymphocytes: Involvement of membrane-associated cytokines. Arthritis & Rheumatism 41, 1748–1759. https://doi.org/10.1002/1529-0131(199810)41:10<1748::AID-ART7>3.0.CO;2-3

Burston, J.J., Valdes, A.M., Woodhams, S.G., Mapp, P.I., Stocks, J., Watson, D.J.G., Gowler, P.R.W., Xu, L., Sagar, D.R., Fernandes, G., Frowd, N., Marshall, L., Zhang, W., Doherty, M., Walsh, D.A., Chapman, V., 2019. The impact of anxiety on chronic musculoskeletal pain and the role of astrocyte activation. Pain 160, 658–669. https://doi.org/10.1097/j.pain.0000000000001445

Caceres, A.I., Liu, B., Jabba, S.V., Achanta, S., Morris, J.B., Jordt, S., 2017. Transient Receptor Potential Cation Channel Subfamily M Member 8 channels mediate the anti-inflammatory effects of eucalyptol. British Journal of Pharmacology 174, 867–879. https://doi.org/10.1111/bph.13760

Caires, R., Luis, E., Taberner, F.J., Fernandez-Ballester, G., Ferrer-Montiel, A., Balazs, E.A., Gomis, A., Belmonte, C., de la Peña, E., 2015. Hyaluronan modulates TRPV1 channel opening, reducing peripheral nociceptor activity and pain. Nature Communications 6, 8095. https://doi.org/10.1038/ncomms9095

Calvino, B., Besson, J.M., Boehrer, A., Depaulis, A., 1996. Ultrasonic vocalization (22-28 kHz) in a model of chronic pain, the arthritic rat: effects of analgesic drugs. Neuroreport: An International Journal for the Rapid Communication of Research in Neuroscience.

Campenot, R.B., 1977. Local control of neurite development by nerve growth factor. Proc Natl Acad Sci U S A 74, 4516–4519. https://doi.org/10.1073/pnas.74.10.4516

Carlson, A.K., Rawle, R.A., Adams, E., Greenwood, M.C., Bothner, B., June, R.K., 2018. Application of global metabolomic profiling of synovial fluid for osteoarthritis biomarkers. Biochemical and Biophysical Research Communications 499, 182–188. https://doi.org/10.1016/j.bbrc.2018.03.117

Carlton, S.M., Lekan, H.A., Kim, S.H., Chung, J.M., 1994. Behavioral manifestations of an experimental model for peripheral neuropathy produced by spinal nerve ligation in the primate. Pain 56, 155–166. https://doi.org/10.1016/0304-3959(94)90090-6

Centers for Disease Control and Prevention, 2015. Arthritis-related statistics [WWW Document]. URL https://www.cdc.gov/arthritis/data_statistics/arthritis-related-stats.htm (accessed 11.30.19).

Cervero, F., Laird, J.M.A., García-Nicas, E., 2003. Secondary hyperalgesia and presynaptic inhibition: an update. European Journal of Pain 7, 345–351. https://doi.org/10.1016/S1090-3801(03)00047-8

Cesare, P., McNaughton, P., 1996. A novel heat-activated current in nociceptive neurons and its sensitization by bradykinin. Proc Natl Acad Sci U S A 93, 15435–15439. https://doi.org/10.1073/pnas.93.26.15435

Chakrabarti, S., Jadon, D.R., Bulmer, D.C., Smith, E.St.J., 2019a. Human osteoarthritic synovial fluid increases excitability of mouse dorsal root ganglion sensory neurons: an in-vitro translational model to study arthritic pain. Rheumatology. https://doi.org/10.1093/rheumatology/kez331

Chakrabarti, S., Pattison, L.A., Bhebhe, C.N., Callejo, G., Bulmer, D.C., Smith, E.St.J., 2019b. Sensitization of knee-innervating sensory neurons by tumor necrosis factor-α activated fibroblast-like synoviocytes: an in vitro, co-culture model of inflammatory pain. bioRxiv 791251. https://doi.org/10.1101/791251

Chakrabarti, S., Pattison, L.A., Singhal, K., Hockley, J.R.F., Callejo, G., Smith, E.St.J., 2018. Acute inflammation sensitizes knee-innervating sensory neurons and decreases mouse digging behavior in a TRPV1-dependent manner. Neuropharmacology 143, 49–62. https://doi.org/10.1016/j.neuropharm.2018.09.014

Challis, R.C., Ravindra Kumar, S., Chan, K.Y., Challis, C., Beadle, K., Jang, M.J., Kim, H.M., Rajendran, P.S., Tompkins, J.D., Shivkumar, K., Deverman, B.E., Gradinaru, V., 2019. Systemic AAV vectors for widespread and targeted gene delivery in rodents. Nature Protocols 14, 379–414. https://doi.org/10.1038/s41596-018-0097-3

Chalmers, P.N., Sherman, S.L., Raphael, B.S., Su, E.P., 2011. Rheumatoid synovectomy: does the surgical approach matter? Clin Orthop Relat Res 469, 2062–2071. https://doi.org/10.1007/s11999-010-1744-3

Chan, A., Filer, A., Parsonage, G., Kollnberger, S., Gundle, R., Buckley, C.D., Bowness, P., 2008. Mediation of the proinflammatory cytokine response in rheumatoid arthritis and spondylarthritis by interactions between fibroblast-like synoviocytes and natural killer cells. Arthritis & Rheumatism 58, 707–717. https://doi.org/10.1002/art.23264

Chan, K.Y., Jang, M.J., Yoo, B.B., Greenbaum, A., Ravi, N., Wu, W.-L., Sánchez-Guardado, L., Lois, C., Mazmanian, S.K., Deverman, B.E., Gradinaru, V., 2017. Engineered AAVs for efficient noninvasive gene delivery to the central and peripheral nervous systems. Nature neuroscience 20, 1172–1179. https://doi.org/10.1038/nn.4593

Changizi Ashtiyani, S., Golestanpour, A., Shamsi, M., Tabatabaei, S.M., Ramazani, M., 2012. Rhazes' prescriptions in treatment of gout. Iran Red Crescent Med J 14, 108–112.

Chaplan, S.R., Bach, F.W., Pogrel, J.W., Chung, J.M., Yaksh, T.L., 1994. Quantitative assessment of tactile allodynia in the rat paw. Journal of Neuroscience Methods 53, 55–63. https://doi.org/10.1016/0165-0270(94)90144-9

Chattopadhyay, M., Mata, M., Goss, J., Wolfe, D., Huang, S., Glorioso, J.C., Fink, D.J., 2007. Prolonged preservation of nerve function in diabetic neuropathy in mice by herpes simplex virus-mediated gene transfer. Diabetologia 50, 1550–1558. https://doi.org/10.1007/s00125-007-0702-4

Chebib, M., Johnston, G.A.R., 2001. The "ABC" of GABA receptors: a brief overview. Clinical and Experimental Pharmacology and Physiology 26, 937–940. https://doi.org/10.1046/j.1440-1681.1999.03151.x

Chen, C., Zhang, J., Sun, L., Zhang, Y., Gan, W.-B., Tang, P., Yang, G., 2019. Long-term imaging of dorsal root ganglia in awake behaving mice. Nature Communications 10, 3087. https://doi.org/10.1038/s41467-019-11158-0

Chen, C.-X., Chen, J.-Y., Kou, J.-Q., Xu, Y.-L., Wang, S.-Z., Zhu, Q., Yang, L., Qin, Z.-H., 2015. Suppression of Inflammation and Arthritis by Orally Administrated Cardiotoxin from Naja naja atra. Evid Based Complement Alternat Med 2015, 387094. https://doi.org/10.1155/2015/387094

Chen, J.T., Guo, D., Campanelli, D., Frattini, F., Mayer, F., Zhou, L., Kuner, R., Heppenstall, P.A., Knipper, M., Hu, J., 2014. Presynaptic GABAergic inhibition regulated by BDNF contributes to neuropathic pain induction. Nature Communications 5, 5331.

Chen, Y., Willcockson, H.H., Valtschanoff, J.G., 2009. Vanilloid receptor TRPV1-mediated phosphorylation of ERK in murine adjuvant arthritis. Osteoarthritis and Cartilage 17, 244–251. https://doi.org/10.1016/j.joca.2008.06.015

Cheng, Y., Macera, C.A., Davis, D.R., Ainsworth, B.E., Troped, P.J., Blair, S.N., 2000. Physical activity and self-reported, physician-diagnosed osteoarthritis: is physical activity a risk factor? Journal of Clinical Epidemiology 53, 315–322. https://doi.org/10.1016/S0895-4356(99)00168-7

Chisholm, K.I., Khovanov, N., Lopes, D.M., La Russa, F., McMahon, S.B., 2018. Large Scale In Vivo Recording of Sensory Neuron Activity with GCaMP6. eNeuro 5, ENEURO.0417-17.2018. https://doi.org/10.1523/ENEURO.0417-17.2018

Cho, W.G., Valtschanoff, J.G., 2008. Vanilloid receptor TRPV1-positive sensory afferents in the mouse ankle and knee joints. Brain Research 1219, 59–65. https://doi.org/10.1016/j.brainres.2008.04.043

Chomarat, P., Rissoan, M.C., Pin, J.J., Banchereau, J., Miossec, P., 1995. Contribution of IL-1, CD14, and CD13 in the increased IL-6 production induced by in vitro monocyte-synoviocyte interactions. J. Immunol. 155, 3645.

Chou, R., McDonagh, M.S., Nakamoto, E., Griffin, J., 2011. Analgesics for Osteoarthritis: An Update of the 2006 Comparative Effectiveness Review. Agency for Healthcare Research and Quality (US), Rockville (MD).

Christensen, A.D., Haase, C., Cook, A.D., Hamilton, J.A., 2016. K/BxN Serum-Transfer Arthritis as a Model for Human Inflammatory Arthritis. Frontiers in Immunology 7, 213. https://doi.org/10.3389/fimmu.2016.00213

Christensen, B.N., Kochukov, M., McNearney, T.A., Taglialatela, G., Westlund, K.N., 2005. Proton-sensing G protein-coupled receptor mobilizes calcium in human synovial cells. Am J Physiol Cell Physiol 289. https://doi.org/10.1152/ajpcell.00039.2005

Christiansen, B.A., Anderson, M.J., Lee, C.A., Williams, J.C., Yik, J.H.N., Haudenschild, D.R., 2012. Musculoskeletal changes following non-invasive knee injury using a novel mouse model of post-traumatic osteoarthritis. Osteoarthritis and Cartilage 20, 773–782. https://doi.org/10.1016/j.joca.2012.04.014

Chuang, H., Prescott, E.D., Kong, H., Shields, S., Jordt, S.-E., Basbaum, A.I., Chao, M.V., Julius, D., 2001. Bradykinin and nerve growth factor release the capsaicin receptor from PtdIns(4,5)P2-mediated inhibition. Nature 411, 957–962. https://doi.org/10.1038/35082088

Chuang, T.K., Killam, K.F., Chuang, L.F., Kung, H.F., Sheng, W.S., Chao, C.C., Yu, L., Chuang, R.Y., 1995. Mu Opioid Receptor Gene Expression in Immune Cells. Biochemical and Biophysical Research Communications 216, 922–930. https://doi.org/10.1006/bbrc.1995.2709

Ciurtin, C., Majeed, Y., Naylor, J., Sukumar, P., English, A.A., Emery, P., Beech, D.J., 2010. TRPM3 channel stimulated by pregnenolone sulphate in synovial fibroblasts and negatively coupled to hyaluronan. BMC Musculoskeletal Disorders 11, 111. https://doi.org/10.1186/1471-2474-11-111

Clark, A.K., Grist, J., Al-Kashi, A., Perretti, M., Malcangio, M., 2012. Spinal cathepsin S and fractalkine contribute to chronic pain in the collagen-induced arthritis model. Arthritis & Rheumatism 64, 2038–2047. https://doi.org/10.1002/art.34351

Clark, A.K., Yip, P.K., Malcangio, M., 2009. The liberation of fractalkine in the dorsal horn requires microglial cathepsin S. Journal of Neuroscience 29, 6945–6954.

Clark, R.B., Schmidt, T.A., Sachse, F.B., Boyle, D., Firestein, G.S., Giles, W.R., 2017. Cellular electrophysiological principles that modulate secretion from synovial fibroblasts. J Physiol 595, 635–645. https://doi.org/10.1113/JP270209

Cole, B.J., Karas, V., Hussey, K., Merkow, D.B., Pilz, K., Fortier, L.A., 2017. Hyaluronic acid versus platelet-rich plasma: a prospective, double-blind randomized controlled trial comparing clinical outcomes and effects on intra-articular biology for the treatment of knee osteoarthritis. The American journal of sports medicine 45, 339–346.

Combe, R., Bramwell, S., Field, M.J., 2004. The monosodium iodoacetate model of osteoarthritis: a model of chronic nociceptive pain in rats? Neuroscience Letters 370, 236–240. https://doi.org/10.1016/j.neulet.2004.08.023

Cook, A.D., Hamilton, J.A., 2018. Investigational therapies targeting the granulocyte macrophage colony-stimulating factor receptor-α in rheumatoid arthritis: focus on mavrilimumab. Ther Adv Musculoskelet Dis 10, 29–38. https://doi.org/10.1177/1759720X17752036

Corder, G., Castro, D.C., Bruchas, M.R., Scherrer, G., 2018. Endogenous and Exogenous Opioids in Pain. Annu Rev Neurosci 41, 453–473. https://doi.org/10.1146/annurev-neuro-080317-061522

Creamer, P., Hunt, M., Dieppe, P., 1996. Pain mechanisms in osteoarthritis of the knee: effect of intraarticular anesthetic. The Journal of rheumatology 23, 1031–1036.

Cregger, M., Berger, A.J., Rimm, D.L., 2006. Immunohistochemistry and Quantitative Analysis of Protein Expression. Archives of Pathology & Laboratory Medicine 130, 1026–1030. https://doi.org/10.1043/1543-2165(2006)130[1026:IAQAOP]2.0.CO;2

Crofford, L.J., 2010. Adverse effects of chronic opioid therapy for chronic musculoskeletal pain. Nature Reviews Rheumatology 6, 191–197. https://doi.org/10.1038/nrrheum.2010.24

Croft, A.P., Campos, J., Jansen, K., Turner, J.D., Marshall, J., Attar, M., Savary, L., Wehmeyer, C., Naylor, A.J., Kemble, S., Begum, J., Dürholz, K., Perlman, H., Barone, F., McGettrick, H.M., Fearon, D.T., Wei, K., Raychaudhuri, S., Korsunsky, I., Brenner, M.B., Coles, M., Sansom, S.N., Filer, A., Buckley, C.D., 2019. Distinct fibroblast subsets drive inflammation and damage in arthritis. Nature 570, 246–251. https://doi.org/10.1038/s41586-019-1263-7

Cutolo, M., Sulli, A., Pizzorini, C., Seriolo, B., Straub, R.H., 2001. Anti-inflammatory mechanisms of methotrexate in rheumatoid arthritis. Ann Rheum Dis 60, 729. https://doi.org/10.1136/ard.60.8.729

Czeschik, J.C., Hagenacker, T., Schäfers, M., Büsselberg, D., 2008. TNF-α differentially modulates ion channels of nociceptive neurons. Neuroscience Letters 434, 293–298. https://doi.org/10.1016/j.neulet.2008.01.070

da Silva Serra, I., Husson, Z., Bartlett, J.D., Smith, E.S.J., 2016. Characterization of cutaneous and articular sensory neurons. Molecular Pain 12. https://doi.org/10.1177/1744806916636387

Dahl, L.B., Dahl, I.M., Engström-Laurent, A., Granath, K., 1985. Concentration and molecular weight of sodium hyaluronate in synovial fluid from patients with rheumatoid arthritis and other arthropathies. Ann Rheum Dis 44, 817. https://doi.org/10.1136/ard.44.12.817

Dalla Costa, E., Minero, M., Lebelt, D., Stucke, D., Canali, E., Leach, M.C., 2014. Development of the Horse Grimace Scale (HGS) as a Pain Assessment Tool in Horses Undergoing Routine Castration. PLOS ONE 9, e92281. https://doi.org/10.1371/journal.pone.0092281

D'Amour, F.E., Smith, D.L., 1941. A method for determining loss of pain sensation. J Pharmacol Exp Ther 72, 74–9.

D'Anjou, M.-A., Moreau, M., Troncy, É., Martel-Pelletier, J., Abram, F., Raynauld, J.-P., Pelletier, J.-P., 2008. Osteophytosis, Subchondral Bone Sclerosis, Joint Effusion and Soft Tissue Thickening in Canine Experimental Stifle Osteoarthritis: Comparison Between 1.5 T Magnetic Resonance Imaging and Computed Radiography. Veterinary Surgery 37, 166–177. https://doi.org/10.1111/j.1532-950X.2007.00363.x

Davis, J.B., Gray, J., Gunthorpe, M.J., Hatcher, J.P., Davey, P.T., Overend, P., Harries, M.H., Latcham, J., Clapham, C., Atkinson, K., Hughes, S.A., Rance, K., Grau, E., Harper, A.J., Pugh, P.L., Rogers, D.C., Bingham, S., Randall, A., Sheardown, S.A., 2000. Vanilloid receptor-1 is essential for inflammatory thermal hyperalgesia. Nature 405, 183.

Dawes, J.M., Kiesewetter, H., Perkins, J.R., Bennett, D.L.H., McMahon, S.B., 2013. Chemokine expression in peripheral tissues from the monosodium iodoacetate model of chronic joint pain. Mol Pain 9, 57–57. https://doi.org/10.1186/1744-8069-9-57

Deacon, R.M.J., 2006a. Digging and marble burying in mice: simple methods for in vivo identification of biological impacts. Nature Protocols 1, 122.

Deacon, R.M.J., 2006b. Burrowing in rodents: a sensitive method for detecting behavioral dysfunction. Nat. Protocols 1, 118–121. https://doi.org/10.1038/nprot.2006.19

Deng, X., Wang, D., Wang, S., Wang, H., Zhou, H., 2018. Identification of key genes and pathways involved in response to pain in goat and sheep by transcriptome sequencing. Biological Research 51, 25. https://doi.org/10.1186/s40659-018-0174-7

Deng, Z., Zeng, C., Yang, Y., Li, Y., Wei, J., Yang, T., Li, H., Lei, G., 2016. Topical diclofenac therapy for osteoarthritis: a meta-analysis of randomized controlled trials. Clinical Rheumatology 35, 1253–1261. https://doi.org/10.1007/s10067-015-3021-z

Dequeker, J., 2006. What can a rheumatologist learn from paintings? Acta Reumatol Port 31, 11–13.

Dequeker, J., 2001. Benign familial hypermobility syndrome and Trendelenburg sign in a painting "The Three Graces" by Peter Paul Rubens (1577-1640). Ann Rheum Dis 60, 894–895.

Dequeker, J., Fabry, G., Vanopdenbosch, L., 2001. Hieronymus Bosch (1450-1516): paleopathology of the medieval disabled and its relation to the Bone and Joint Decade 2000-2010. Isr Med Assoc J 3, 864–871.

Deuis, J.R., Dvorakova, L.S., Vetter, I., 2017. Methods Used to Evaluate Pain Behaviors in Rodents. Front Mol Neurosci 10, 284–284. https://doi.org/10.3389/fnmol.2017.00284

Deuis, J.R., Vetter, I., 2016. The thermal probe test: A novel behavioral assay to quantify thermal paw withdrawal thresholds in mice. Temperature (Austin) 3, 199–207. https://doi.org/10.1080/23328940.2016.1157668

Deval, E., Noël, J., Lay, N., Alloui, A., Diochot, S., Friend, V., Jodar, M., Lazdunski, M., Lingueglia, E., 2008. ASIC3, a sensor of acidic and primary inflammatory pain. The EMBO Journal 27, 3047–3055. https://doi.org/10.1038/emboj.2008.213

Dittert, I., Benedikt, J., Vyklický, L., Zimmermann, K., Reeh, P.W., Vlachová, V., 2006. Improved superfusion technique for rapid cooling or heating of cultured cells under patch-clamp conditions. Journal of Neuroscience Methods 151, 178–185. https://doi.org/10.1016/j.jneumeth.2005.07.005

Djouhri, L., Bleazard, L., Lawson, S.N., 1998. Association of somatic action potential shape with sensory receptive properties in guinea-pig dorsal root ganglion neurones. The Journal of Physiology 513, 857–872. https://doi.org/10.1111/j.1469-7793.1998.857ba.x

Djouhri, L., Lawson, S.N., 1999. Changes in somatic action potential shape in guinea-pig nociceptive primary afferent neurones during inflammation in vivo. The Journal of Physiology 520, 565–576. https://doi.org/10.1111/j.1469-7793.1999.t01-1-00565.x

Donatien, P., Anand, U., Yiangou, Y., Sinisi, M., Fox, M., MacQuillan, A., Quick, T., Korchev, Y.E., Anand, P., 2018. Granulocyte-macrophage colony-stimulating factor receptor expression in clinical pain disorder tissues and role in neuronal sensitization. Pain Rep 3, e676–e676. https://doi.org/10.1097/PR9.0000000000000676

Doran, C., Chetrit, J., Holley, M.C., Grundy, D., Nassar, M.A., 2015. Mouse DRG Cell Line with Properties of Nociceptors. PLOS ONE 10, e0128670. https://doi.org/10.1371/journal.pone.0128670

Dustrude, E.T., Moutal, A., Yang, X., Wang, Y., Khanna, M., Khanna, R., 2016. Hierarchical CRMP2 posttranslational modifications control NaV1.7 function. Proc Natl Acad Sci U S A 113, E8443–E8452. https://doi.org/10.1073/pnas.1610531113

Eberwine, J., Sugimoto, Y., 2001. Northern Blotting, in: Brenner, S., Miller, J.H. (Eds.), Encyclopedia of Genetics. Academic Press, New York, pp. 1350–1352. https://doi.org/10.1006/rwgn.2001.0907

Edwards, R.R., Giles, J., Bingham, C.O., 3rd, Campbell, C., Haythornthwaite, J.A., Bathon, J., 2010. Moderators of the negative effects of catastrophizing in arthritis. Pain Med 11, 591–599. https://doi.org/10.1111/j.1526-4637.2010.00804.x

Eid, S.R., Crown, E.D., Moore, E.L., Liang, H.A., Choong, K.-C., Dima, S., Henze, D.A., Kane, S.A., Urban, M.O., 2008. HC-030031, a TRPA1 selective antagonist, attenuates inflammatory- and neuropathy-induced mechanical hypersensitivity. Mol Pain 4, 48–48. https://doi.org/10.1186/1744-8069-4-48

Eisenman, L.M., 1985. Uptake of the retrograde fluorescent tracer Fast blue from the cerebrospinal fluid of the rat. Neuroscience Letters 60, 241–246. https://doi.org/10.1016/0304-3940(85)90584-1

Elizur, A., Adair-Kirk, T.L., Kelley, D.G., Griffin, G.L., Demello, D.E., Senior, R.M., 2008. Tumor necrosis factor-alpha from macrophages enhances LPS-induced clara cell expression of keratinocyte-derived chemokine. Am J Respir Cell Mol Biol 38, 8–15. https://doi.org/10.1165/rcmb.2007-0203OC

Emery, E.C., Luiz, A.P., Sikandar, S., Magnúsdóttir, R., Dong, X., Wood, J.N., 2016. In vivo characterization of distinct modality-specific subsets of somatosensory neurons using GCaMP. Sci Adv 2, e1600990–e1600990. https://doi.org/10.1126/sciadv.1600990

Emery, E.C., Young, G.T., Berrocoso, E.M., Chen, L., McNaughton, P.A., 2011. HCN2 Ion Channels Play a Central Role in Inflammatory and Neuropathic Pain. Science 333, 1462. https://doi.org/10.1126/science.1206243

Engvall, E., 1980. Enzyme immunoassay ELISA and EMIT, in: Methods in Enzymology. Elsevier, pp. 419–439.

Entezami, P., Fox, D.A., Clapham, P.J., Chung, K.C., 2011. Historical perspective on the etiology of rheumatoid arthritis. Hand clinics 27, 1–10. https://doi.org/10.1016/j.hcl.2010.09.006

Erlanger, J., Gasser, H.S., 1937. Electrical signs of nervous activity.

Ethgen, O., Bruyere, O., Richy, F., Dardennes, C., Reginster, J.-Y., 2004. Health-related quality of life in total hip and total knee arthroplasty. A qualitative and systematic review of the literature. J Bone Joint Surg Am 86, 963–974. https://doi.org/10.2106/00004623-200405000-00012

Evans, C.H., Ghivizzani, S.C., Robbins, P.D., 2018. Arthritis gene therapy is becoming a reality. Nature Reviews Rheumatology 14, 381–382. https://doi.org/10.1038/s41584-018-0009-5
Evans, C.H., Ghivizzani, S.C., Robbins, P.D., 2017. Gene Delivery to Joints by Intra-Articular Injection. Human Gene Therapy 29, 2–14. https://doi.org/10.1089/hum.2017.181
Fang, D., Kong, L.-Y., Cai, J., Li, S., Liu, X.-D., Han, J.-S., Xing, G.-G., 2015. Interleukin-6-mediated functional upregulation of TRPV1 receptors in dorsal root ganglion neurons through the activation of JAK/PI3K signaling pathway: roles in the development of bone cancer pain in a rat model. Pain 156, 1124–1144. https://doi.org/10.1097/j.pain.0000000000000158
Farr, M., Garvey, K., Bold, A.M., Kendall, M.J., Bacon, P.A., 1985. Significance of the hydrogen ion concentration in synovial fluid in rheumatoid arthritis. Clin Exp Rheumatol 3, 99–104.
Ferland, C., Laverty, S., Beaudry, F., Vachon, P., 2011. Gait analysis and pain response of two rodent models of osteoarthritis. Pharmacology Biochemistry and Behavior 97, 603–610.
Fernandes, E.S., Russell, F.A., Alawi, K.M., Sand, C., Liang, L., Salamon, R., Bodkin, J.V., Aubdool, A.A., Arno, M., Gentry, C., Smillie, S.-J., Bevan, S., Keeble, J.E., Malcangio, M., Brain, S.D., 2016. Environmental cold exposure increases blood flow and affects pain sensitivity in the knee joints of CFA-induced arthritic mice in a TRPA1-dependent manner. Arthritis Research & Therapy 18, 7. https://doi.org/10.1186/s13075-015-0905-x
Fernandes, E.S., Russell, F.A., Spina, D., McDougall, J.J., Graepel, R., Gentry, C., Staniland, A.A., Mountford, D.M., Keeble, J.E., Malcangio, M., Bevan, S., Brain, S.D., 2011. A Distinct Role for Transient Receptor Potential Ankyrin 1, in Addition to Transient Receptor Potential Vanilloid 1, in Tumor Necrosis Factor alpha-Induced Inflammatory Hyperalgesia and Freund's Complete Adjuvant-Induced Monarthritis. Arthritis and Rheumatism 63, 819–829. https://doi.org/10.1002/art.30150
Fernandes, E.S., S, A., R, K., Brain, S., 2013. TRP Receptors in Arthritis, Gaining Knowledge for Translation from Experimental Models. https://doi.org/10.2174/1876386301306010050
Fernandez-Pena, C., 2013. Targeting TRPM8 for pain relief. The Open Pain Journal 6, 154–164. https://doi.org/10.2174/1876386301306010154
Ferreira-Gomes, J., Adães, S., Sarkander, J., Castro-Lopes, J.M., 2010. Phenotypic alterations of neurons that innervate osteoarthritic joints in rats. Arthritis & Rheumatism 62, 3677–3685. https://doi.org/10.1002/art.27713
Fink, D.J., Wechuck, J., Mata, M., Glorioso, J.C., Goss, J., Krisky, D., Wolfe, D., 2011. Gene therapy for pain: Results of a phase I clinical trial. Annals of Neurology 70, 207–212. https://doi.org/10.1002/ana.22446
Flake, N.M., Gold, M.S., 2005. Inflammation alters sodium currents and excitability of temporomandibular joint afferents. Neuroscience Letters 384, 294–299. https://doi.org/10.1016/j.neulet.2005.04.091
Flower, R., 2003. What are all the things that aspirin does? BMJ 327, 572–573. https://doi.org/10.1136/bmj.327.7415.572
French, H.P., Smart, K.M., Doyle, F., 2017. Prevalence of neuropathic pain in knee or hip osteoarthritis: a systematic review and meta-analysis. Presented at the Seminars in arthritis and rheumatism, Elsevier, pp. 1–8.
Fritsch, K.O., Hamoud, H., Allam, A.H., Grossmann, A., Nur El-Din, A.-H., Abdel-Maksoud, G., Soliman, M.A.-T., Badr, I., Sutherland, J.D., Sutherland, M.L., Akl, M., Finch, C.E., Thomas, G.S., Wann, L.S., Thompson, R.C., 2015. The orthopedic diseases of ancient Egypt. Anat Rec (Hoboken) 298, 1036–1046. https://doi.org/10.1002/ar.23136
Fu, J.Y., Masferrer, J.L., Seibert, K., Raz, A., Needleman, P., 1990. The induction and suppression of prostaglandin H2 synthase (cyclooxygenase) in human monocytes. Journal of Biological Chemistry 265, 16737–16740.
Fu, S., Cheuk, Y., Hung, L., Chan, K., 2012. Limb Idleness Index (LII): a novel measurement of pain in a rat model of osteoarthritis. Osteoarthritis and cartilage 20, 1409–1416.

Fujikado, N., Saijo, S., Iwakura, Y., 2006. Identification of arthritis-related gene clusters by microarray analysis of two independent mouse models for rheumatoid arthritis. Arthritis Res Ther 8, R100–R100. https://doi.org/10.1186/ar1985

Furman, B.D., Strand, J., Hembree, W.C., Ward, B.D., Guilak, F., Olson, S.A., 2007. Joint degeneration following closed intraarticular fracture in the mouse knee: A model of posttraumatic arthritis. Journal of Orthopaedic Research 25, 578–592. https://doi.org/10.1002/jor.20331

Futami, I., Ishijima, M., Kaneko, H., Tsuji, K., Ichikawa-Tomikawa, N., Sadatsuki, R., Muneta, T., Arikawa-Hirasawa, E., Sekiya, I., Kaneko, K., 2012. Isolation and Characterization of Multipotential Mesenchymal Cells from the Mouse Synovium. PLoS ONE 7, e45517. https://doi.org/10.1371/journal.pone.0045517

Galindo, T., Reyna, J., Weyer, A., 2018. Evidence for Transient Receptor Potential (TRP) Channel Contribution to Arthritis Pain and Pathogenesis. Pharmaceuticals (Basel, Switzerland) 11, 105. https://doi.org/10.3390/ph11040105

Galvan, A., Raper, J., Hu, X., Paré, J.-F., Bonaventura, J., Richie, C.T., Michaelides, M., Mueller, S.A.L., Roseboom, P.H., Oler, J.A., Kalin, N.H., Hall, R.A., Smith, Y., 2019. Ultrastructural localization of DREADDs in monkeys. European Journal of Neuroscience 50, 2801–2813. https://doi.org/10.1111/ejn.14429

Ganchingco, J.R.C., Fukuyama, T., Yoder, J.A., Bäumer, W., 2019. Calcium imaging of primary canine sensory neurons: Small-diameter neurons responsive to pruritogens and algogens. Brain and Behavior n/a, e01428. https://doi.org/10.1002/brb3.1428

Garrison, S.R., Stucky, C.L., 2014. Contribution of Transient Receptor Potential Ankyrin 1 to Chronic Pain in Aged Mice With Complete Freund's Adjuvant–Induced Arthritis. Arthritis & Rheumatology 66, 2380–2390. https://doi.org/10.1002/art.38724

Garrod, A.E., 1890. A treatise on rheumatism and rheumatoid arthritis. Griffin.

Gauldie, S.D., McQueen, D.S., Clarke, C.J., Chessell, I.P., 2004. A robust model of adjuvant-induced chronic unilateral arthritis in two mouse strains. J Neurosci Methods 139, 281–291. https://doi.org/10.1016/j.jneumeth.2004.05.003

Gee, K.R., Brown, K.A., Chen, W.-N.U., Bishop-Stewart, J., Gray, D., Johnson, I., 2000. Chemical and physiological characterization of fluo-4 Ca2+-indicator dyes. Cell Calcium 27, 97–106. https://doi.org/10.1054/ceca.1999.0095

Geenen, R., Overman, C.L., Christensen, R., Åsenlöf, P., Capela, S., Huisinga, K.L., Husebø, M.E.P., Köke, A.J.A., Paskins, Z., Pitsillidou, I.A., Savel, C., Austin, J., Hassett, A.L., Severijns, G., Stoffer-Marx, M., Vlaeyen, J.W.S., Fernández-de-las-Peñas, C., Ryan, S.J., Bergman, S., 2018. EULAR recommendations for the health professional's approach to pain management in inflammatory arthritis and osteoarthritis. Ann Rheum Dis 77, 797. https://doi.org/10.1136/annrheumdis-2017-212662

Geiler, T., Kriegsmann, Jöu., Keyszer, G.M., Gay, R.E., Gay, S., 1994. A new model for rheumatoid arthritis generated by engraftment of rheumatoid synovial tissue and normal human cartilage into SCID mice. Arthritis & Rheumatism: Official Journal of the American College of Rheumatology 37, 1664–1671.

Gibofsky, A., 2012. Overview of epidemiology, pathophysiology, and diagnosis of rheumatoid arthritis. Am J Manag Care 18.

Gilbert, S.J., Bonnet, C.S., Stadnik, P., Duance, V.C., Mason, D.J., Blain, E.J., 2018. Inflammatory and degenerative phases resulting from anterior cruciate rupture in a non-invasive murine model of post-traumatic osteoarthritis. J Orthop Res 36, 2118–2127. https://doi.org/10.1002/jor.23872

Glant, T.T., Mikecz, K., Arzoumanian, A., Poole, A.R., 1987. Proteoglycan-induced arthritis in balb/c mice. Arthritis & Rheumatism: Official Journal of the American College of Rheumatology 30, 201–212.

Gobezie, R., Kho, A., Krastins, B., Sarracino, D.A., Thornhill, T.S., Chase, M., Millett, P.J., Lee, D.M., 2007. High abundance synovial fluid proteome: distinct profiles in health and osteoarthritis. Arthritis research & therapy 9, R36–R36. https://doi.org/10.1186/ar2172

Goins, W.F., Cohen, J.B., Glorioso, J.C., 2012. Gene therapy for the treatment of chronic peripheral nervous system pain. Neurobiology of Disease 48, 255–270. https://doi.org/10.1016/j.nbd.2012.05.005
Goldring, M.B., Otero, M., 2011. Inflammation in osteoarthritis. Current opinion in rheumatology 23, 471–478. https://doi.org/10.1097/BOR.0b013e328349c2b1
Gong, K., Ohara, P.T., Jasmin, L., 2016. Patch Clamp Recordings on Intact Dorsal Root Ganglia from Adult Rats. J Vis Exp 54287. https://doi.org/10.3791/54287
Gong, W., Kolker, S.J., Usachev, Y., Walder, R.Y., Boyle, D.L., Firestein, G.S., Sluka, K.A., 2014. Acid-sensing ion channel 3 decreases phosphorylation of extracellular signal-regulated kinases and induces synoviocyte cell death by increasing intracellular calcium. Arthritis Research & Therapy 16, R121. https://doi.org/10.1186/ar4577
Gowler, P.R.W., Li, L., Woodhams, S.G., Bennett, A.J., Suzuki, R., Walsh, D.A., Chapman, V., 2019. Peripheral brain derived neurotrophic factor contributes to chronic osteoarthritis joint pain. PAIN Articles in Press.
Greenbaum, D., Colangelo, C., Williams, K., Gerstein, M., 2003. Comparing protein abundance and mRNA expression levels on a genomic scale. Genome Biology 4, 117. https://doi.org/10.1186/gb-2003-4-9-117
Gregory, M.H., Capito, N., Kuroki, K., Stoker, A.M., Cook, J.L., Sherman, S.L., 2012. A review of translational animal models for knee osteoarthritis. Arthritis 2012, 764621–764621. https://doi.org/10.1155/2012/764621
Gregory, N., Harris, A., Robinson, C., Dougherty, P., Fuchs, P., Sluka, K., 2013. An overview of animal models of pain: disease models and outcome measures. The journal of pain : official journal of the American Pain Society 14, 10.1016/j.jpain.2013.06.008. https://doi.org/10.1016/j.jpain.2013.06.008
Grienberger, C., Konnerth, A., 2012. Imaging Calcium in Neurons. Neuron 73, 862–885. https://doi.org/10.1016/j.neuron.2012.02.011
Grubb, B.D., Birrell, G.J., McQueen, D.S., Iggo, A., 1991. The role of PGE2 in the sensitization of mechanoreceptors in normal and inflamed ankle joints of the rat. Experimental Brain Research 84, 383–392. https://doi.org/10.1007/BF00231460
Guedes, V., Castro, J.P., Brito, I., 2018. Topical capsaicin for pain in osteoarthritis: A literature review. Reumatología Clínica (English Edition) 14, 40–45. https://doi.org/10.1016/j.reumae.2016.07.013
Guedj, D., Weinberger, A., 1990. Effect of weather conditions on rheumatic patients. Ann Rheum Dis 49, 158. https://doi.org/10.1136/ard.49.3.158
Guo, D., Hu, J., 2014. Spinal presynaptic inhibition in pain control. Neuroscience 283, 95–106. https://doi.org/10.1016/j.neuroscience.2014.09.032
Guo, W., Yu, D., Wang, X., Luo, C., Chen, Y., Lei, W., Wang, C., Ge, Y., Xue, W., Tian, Q., Gao, X., Yao, W., 2016. Anti-inflammatory effects of interleukin-23 receptor cytokine-binding homology region rebalance T cell distribution in rodent collagen-induced arthritis. Oncotarget 7, 31800–31813. https://doi.org/10.18632/oncotarget.9309
Gupta, R.C., Lall, R., Srivastava, A., Sinha, A., 2019. Hyaluronic Acid: Molecular Mechanisms and Therapeutic Trajectory. Frontiers in Veterinary Science 6, 192. https://doi.org/10.3389/fvets.2019.00192
Gureje, O., Von Korff, M., Simon, G.E., Gater, R., 1998. Persistent Pain and Well-beingA World Health Organization Study in Primary Care. JAMA 280, 147–151. https://doi.org/10.1001/jama.280.2.147
Gwilym, S.E., Filippini, N., Douaud, G., Carr, A.J., Tracey, I., 2010. Thalamic atrophy associated with painful osteoarthritis of the hip is reversible after arthroplasty: A longitudinal voxel-based morphometric study. Arthritis & Rheumatism 62, 2930–2940.
Gwilym, S.E., Keltner, J.R., Warnaby, C.E., Carr, A.J., Chizh, B., Chessell, I., Tracey, I., 2009. Psychophysical and functional imaging evidence supporting the presence of central sensitization in a cohort of osteoarthritis patients. Arthritis Rheum 61. https://doi.org/10.1002/art.24837

Haberberger, R.V., Barry, C., Dominguez, N., Matusica, D., 2019. Human Dorsal Root Ganglia. Front Cell Neurosci 13, 271–271. https://doi.org/10.3389/fncel.2019.00271
Hacein-Bey-Abina, S., Garrigue, A., Wang, G.P., Soulier, J., Lim, A., Morillon, E., Clappier, E., Caccavelli, L., Delabesse, E., Beldjord, K., Asnafi, V., MacIntyre, E., Dal Cortivo, L., Radford, I., Brousse, N., Sigaux, F., Moshous, D., Hauer, J., Borkhardt, A., Belohradsky, B.H., Wintergerst, U., Velez, M.C., Leiva, L., Sorensen, R., Wulffraat, N., Blanche, S., Bushman, F.D., Fischer, A., Cavazzana-Calvo, M., 2008. Insertional oncogenesis in 4 patients after retrovirus-mediated gene therapy of SCID-X1. J Clin Invest 118, 3132–3142. https://doi.org/10.1172/JCI35700
Hachisuka, J., Baumbauer, K.M., Omori, Y., Snyder, L.M., Koerber, H.R., Ross, S.E., 2016. Semi-intact ex vivo approach to investigate spinal somatosensory circuits. eLife 5, e22866. https://doi.org/10.7554/eLife.22866
Hall, B.E., Prochazkova, M., Sapio, M.R., Minetos, P., Kurochkina, N., Binukumar, B.K., Amin, N.D., Terse, A., Joseph, J., Raithel, S.J., Mannes, A.J., Pant, H.C., Chung, M.-K., Iadarola, M.J., Kulkarni, A.B., 2018. Phosphorylation of the Transient Receptor Potential Ankyrin 1 by Cyclin-dependent Kinase 5 affects Chemo-nociception. Sci Rep 8, 1177–1177. https://doi.org/10.1038/s41598-018-19532-6
Hampshire, V., Robertson, S., 2015. Using the facial grimace scale to evaluate rabbit wellness in post-procedural monitoring. Lab Animal 44, 259–260. https://doi.org/10.1038/laban.806
Hanack, C., Moroni, M., Lima, W.C., Wende, H., Kirchner, M., Adelfinger, L., Schrenk-Siemens, K., Tappe-Theodor, A., Wetzel, C., Kuich, P.H., Gassmann, M., Roggenkamp, D., Bettler, B., Lewin, G.R., Selbach, M., Siemens, J., 2015. GABA blocks pathological but not acute TRPV1 pain signals. Cell 160, 759–770. https://doi.org/10.1016/j.cell.2015.01.022
Hanesch, U., McDougall, J., Pawlak, M., 2000. Inhibitory effects of gabapentin on rat articular afferent mechanosensitivity. Regulatory Peptides 89, 63.
Hardy, R.S., Hülso, C., Liu, Y., Gasparini, S.J., Fong-Yee, C., Tu, J., Stoner, S., Stewart, P.M., Raza, K., Cooper, M.S., Seibel, M.J., Zhou, H., 2013. Characterisation of fibroblast-like synoviocytes from a murine model of joint inflammation. Arthritis Research & Therapy 15, R24–R24. https://doi.org/10.1186/ar4158
Hargreaves, K., Dubner, R., Brown, F., Flores, C., Joris, J., 1988. A new and sensitive method for measuring thermal nociception in cutaneous hyperalgesia. Pain 32, 77–88. https://doi.org/10.1016/0304-3959(88)90026-7
Harper, A.A., 1991. Similarities between some properties of the soma and sensory receptors of primary afferent neurones. Exp Physiol 76, 369–377. https://doi.org/10.1113/expphysiol.1991.sp003504
Harper, A.A., Lawson, S.N., 1985. Conduction velocity is related to morphological cell type in rat dorsal root ganglion neurones. J Physiol 359, 31–46. https://doi.org/10.1113/jphysiol.1985.sp015573
Harte, S.E., Harris, R.E., Clauw, D.J., 2018. The neurobiology of central sensitization. Journal of Applied Biobehavioral Research 23, e12137. https://doi.org/10.1111/jabr.12137
Hasin, Y., Seldin, M., Lusis, A., 2017. Multi-omics approaches to disease. Genome Biology 18, 83. https://doi.org/10.1186/s13059-017-1215-1
Hauck, B., Chen, L., Xiao, W., 2003. Generation and Characterization of Chimeric Recombinant AAV Vectors. Molecular therapy : the journal of the American Society of Gene Therapy 7, 419–425.
Hawker, G.A., Stewart, L., French, M.R., Cibere, J., Jordan, J.M., March, L., Suarez-Almazor, M., Gooberman-Hill, R., 2008. Understanding the pain experience in hip and knee osteoarthritis – an OARSI/OMERACT initiative. Osteoarthritis and Cartilage 16, 415–422. https://doi.org/10.1016/j.joca.2007.12.017
Hayar, A., Gu, C., Al-Chaer, E.D., 2008. An improved method for patch clamp recording and calcium imaging of neurons in the intact dorsal root ganglion in rats. J Neurosci Methods 173, 74–82. https://doi.org/10.1016/j.jneumeth.2008.05.023

Haywood, A.R., Hathway, G.J., Chapman, V., 2018. Differential contributions of peripheral and central mechanisms to pain in a rodent model of osteoarthritis. Scientific Reports 8, 7122. https://doi.org/10.1038/s41598-018-25581-8

He, B., Christin, M., Mouchbahani-Constance, S., Davidova, A., Sharif-Naeini, R., 2017. Mechanosensitive ion channels in articular nociceptors drive mechanical allodynia in osteoarthritis. Osteoarthritis and cartilage 25, 2091–2099.

Heimans, L., Boer, K.V.W., Koudijs, K.M., Visser, K., Goekoop-Ruiterman, Y.P., Harbers, J.B., Steup-Beekman, G.M., Lard, L.R., Grillet, B.A., Huizinga, T.W., Allaart, C.F., 2013. Health-related quality of life and functional ability in patients with early arthritis during remission steered treatment: results of the IMPROVED study. Arthritis Research & Therapy 15, R173. https://doi.org/10.1186/ar4361

Heppelmann, B., Pawlak, M., 1997. Sensitisation of articular afferents in normal and inflamed knee joints by substance P in the rat. Neuroscience letters 223, 97–100.

Hildebrand, C., Öqvist, G., Brax, L., Tuisku, F., 1991. Anatomy of the rat knee joint and fibre composition of a major articular nerve. The Anatomical Record 229, 545–555.

Hillery, C.A., Kerstein, P.C., Vilceanu, D., Barabas, M.E., Retherford, D., Brandow, A.M., Wandersee, N.J., Stucky, C.L., 2011. Transient receptor potential vanilloid 1 mediates pain in mice with severe sickle cell disease. Blood 118, 3376–3383. https://doi.org/10.1182/blood-2010-12-327429

Hines, A.E., Birn, H., Teglbjærg, P.S., Sinkjær, T., 1996. Fiber type composition of articular branches of the tibial nerve at the knee joint in man. The Anatomical Record: An Official Publication of the American Association of Anatomists 246, 573–578.

Hinojosa-Azaola, A., Alcocer-Varela, J., 2014. Art and rheumatology: the artist and the rheumatologist's perspective. Rheumatology 53, 1725–1731. https://doi.org/10.1093/rheumatology/ket459

Hochberg, M.C., Martel-Pelletier, J., Monfort, J., Möller, I., Castillo, J.R., Arden, N., Berenbaum, F., Blanco, F.J., Conaghan, P.G., Doménech, G., Henrotin, Y., Pap, T., Richette, P., Sawitzke, A., du Souich, P., Pelletier, J.-P., 2016. Combined chondroitin sulfate and glucosamine for painful knee osteoarthritis: a multicentre, randomised, double-blind, non-inferiority trial versus celecoxib. Ann Rheum Dis 75, 37. https://doi.org/10.1136/annrheumdis-2014-206792

Hockley, J.R.F., Taylor, T.S., Callejo, G., Wilbrey, A.L., Gutteridge, A., Bach, K., Winchester, W.J., Bulmer, D.C., McMurray, G., Smith, E.S.J., 2019. Single-cell RNAseq reveals seven classes of colonic sensory neuron. Gut 68, 633. https://doi.org/10.1136/gutjnl-2017-315631

Hockley, J.R.F., Taylor, T.S., Callejo, G., Wilbrey, A.L., Gutteridge, A., Bach, K., Winchester, W.J., Bulmer, D.C., McMurray, G., Smith, E.S.J., 2018. Single-cell RNAseq reveals seven classes of colonic sensory neuron. Gut. https://doi.org/10.1136/gutjnl-2017-315631

Hodgkin, A.L., Huxley, A.F., 1939. Action potentials recorded from inside a nerve fibre. Nature 144, 710.

Hong, R., Sur, B., Yeom, M., Lee, B., Kim, K.S., Rodriguez, J.P., Lee, S., Kang, K.S., Huh, C.-K., Lee, S.C., Hahm, D.-H., 2018. Anti-inflammatory and anti-arthritic effects of the ethanolic extract of Aralia continentalis Kitag. in IL-1β-stimulated human fibroblast-like synoviocytes and rodent models of polyarthritis and nociception. Phytomedicine 38, 45–56. https://doi.org/10.1016/j.phymed.2017.10.016

Honore, P., Wismer, C.T., Mikusa, J., Zhu, C.Z., Zhong, C., Gauvin, D.M., Gomtsyan, A., El Kouhen, R., Lee, C.-H., Marsh, K., Sullivan, J.P., Faltynek, C.R., Jarvis, M.F., 2005. A-425619 [1-Isoquinolin-5-yl-3-(4-trifluoromethyl-benzyl)-urea], a Novel Transient Receptor Potential Type V1 Receptor Antagonist, Relieves Pathophysiological Pain Associated with Inflammation and Tissue Injury in Rats. J Pharmacol Exp Ther 314, 410. https://doi.org/10.1124/jpet.105.083915

Hsieh, W.-S., Kung, C.-C., Huang, S.-L., Lin, S.-C., Sun, W.-H., 2017. TDAG8, TRPV1, and ASIC3 involved in establishing hyperalgesic priming in experimental rheumatoid arthritis. Scientific Reports 7, 8870. https://doi.org/10.1038/s41598-017-09200-6

Hu, G., Huang, K., Hu, Y., Du, G., Xue, Z., Zhu, X., Fan, G., 2016. Single-cell RNA-seq reveals distinct injury responses in different types of DRG sensory neurons. Scientific Reports 6, 31851. https://doi.org/10.1038/srep31851

Hu, K., Xu, L., Cao, L., Flahiff, C.M., Brussiau, J., Ho, K., Setton, L.A., Youn, I., Guilak, F., Olsen, B.R., Li, Y., 2006. Pathogenesis of osteoarthritis-like changes in the joints of mice deficient in type IX collagen. Arthritis & Rheumatism 54, 2891–2900. https://doi.org/10.1002/art.22040

Hua, B., O'Brien, K., 2010. Osteoarthritis and Chinese medicine: An overview of theories and evidence 94, 44–49.

Huggins, J.P., Smart, T.S., Langman, S., Taylor, L., Young, T., 2012. An efficient randomised, placebo-controlled clinical trial with the irreversible fatty acid amide hydrolase-1 inhibitor PF-04457845, which modulates endocannabinoids but fails to induce effective analgesia in patients with pain due to osteoarthritis of the knee. PAIN® 153, 1837–1846. https://doi.org/10.1016/j.pain.2012.04.020

Hugle, T., Kovacs, H., Heijnen, I.A.F.M., Daikeler, T., Baisch, U., Hicks, J.M., Valderrabano, V., 2012. Synovial fluid metabolomics in different forms of arthritis assessed by nuclear magnetic resonance spectroscopy. Clin Exp Rheumatol 30, 240–245.

Ikeuchi, M., Kolker, S.J., Sluka, K.A., 2009. Acid-sensing ion channel 3 expression in mouse knee joint afferents and effects of carrageenan-induced arthritis. J Pain 10. https://doi.org/10.1016/j.jpain.2008.10.010

Immke, D.C., McCleskey, E.W., 2001. Lactate enhances the acid-sensing Na+ channel on ischemia-sensing neurons. Nature Neuroscience 4, 869–870. https://doi.org/10.1038/nn0901-869

Itoh, Y., Hatano, N., Hayashi, H., Onozaki, K., Miyazawa, K., Muraki, K., 2009. An environmental sensor, TRPV4 is a novel regulator of intracellular Ca2+ in human synoviocytes. American Journal of Physiology-Cell Physiology 297, C1082–C1090. https://doi.org/10.1152/ajpcell.00204.2009

Iyer, S.M., Vesuna, S., Ramakrishnan, C., Huynh, K., Young, S., Berndt, A., Lee, S.Y., Gorini, C.J., Deisseroth, K., Delp, S.L., 2016. Optogenetic and chemogenetic strategies for sustained inhibition of pain. Sci Rep 6, 30570–30570. https://doi.org/10.1038/srep30570

Jackson, K.L., Dayton, R.D., Deverman, B.E., Klein, R.L., 2016. Better Targeting, Better Efficiency for Wide-Scale Neuronal Transduction with the Synapsin Promoter and AAV-PHP.B. Frontiers in Molecular Neuroscience 9, 116. https://doi.org/10.3389/fnmol.2016.00116

Jaffe, E.A., Weksler, B.B., 1979. Recovery of endothelial cell prostacyclin production after inhibition by low doses of aspirin. J Clin Invest 63, 532–535. https://doi.org/10.1172/JCI109332

Jaiswal, P.B., English, A.W., 2017. Chemogenetic enhancement of functional recovery after a sciatic nerve injury. Eur J Neurosci 45, 1252–1257. https://doi.org/10.1111/ejn.13550

Jaiswal, P.B., Mistretta, O.C., Ward, P.J., English, A.W., 2018. Chemogenetic Enhancement of Axon Regeneration Following Peripheral Nerve Injury in the SLICK-A Mouse. Brain Sci 8, 93. https://doi.org/10.3390/brainsci8050093

Jamieson, D.G., Moss, A., Kennedy, M., Jones, S., Nenadic, G., Robertson, D.L., Sidders, B., 2014. The pain interactome: connecting pain-specific protein interactions. Pain 155, 2243–2252. https://doi.org/10.1016/j.pain.2014.06.020

Jendryka, M., Palchaudhuri, M., Ursu, D., van der Veen, B., Liss, B., Kätzel, D., Nissen, W., Pekcec, A., 2019. Pharmacokinetic and pharmacodynamic actions of clozapine-N-oxide, clozapine, and compound 21 in DREADD-based chemogenetics in mice. Sci Rep 9, 4522–4522. https://doi.org/10.1038/s41598-019-41088-2

Ji, G., Neugebauer, V., 2011. Pain-related deactivation of medial prefrontal cortical neurons involves mGluR1 and GABA(A) receptors. J Neurophysiol 106, 2642–2652. https://doi.org/10.1152/jn.00461.2011

Ji, Q., Zheng, Y., Zhang, G., Hu, Y., Fan, X., Hou, Y., Wen, L., Li, L., Xu, Y., Wang, Y., Tang, F., 2019. Single-cell RNA-seq analysis reveals the progression of human osteoarthritis. Ann Rheum Dis 78, 100. https://doi.org/10.1136/annrheumdis-2017-212863

Ji, R.-R., Samad, T.A., Jin, S.-X., Schmoll, R., Woolf, C.J., 2002. p38 MAPK Activation by NGF in Primary Sensory Neurons after Inflammation Increases TRPV1 Levels and Maintains Heat Hyperalgesia. Neuron 36, 57–68. https://doi.org/10.1016/S0896-6273(02)00908-X

Jimenez-Vargas, N.N., Pattison, L.A., Zhao, P., Lieu, T., Latorre, R., Jensen, D.D., Castro, J., Aurelio, L., Le, G.T., Flynn, B., Herenbrink, C.K., Yeatman, H.R., Edgington-Mitchell, L., Porter, C.J.H., Halls, M.L., Canals, M., Veldhuis, N.A., Poole, D.P., McLean, P., Hicks, G.A., Scheff, N., Chen, E., Bhattacharya, A., Schmidt, B.L., Brierley, S.M., Vanner, S.J., Bunnett, N.W., 2018. Protease-activated receptor-2 in endosomes signals persistent pain of irritable bowel syndrome. Proc Natl Acad Sci USA 115, E7438. https://doi.org/10.1073/pnas.1721891115

Jirkof, P., 2014. Burrowing and nest building behavior as indicators of well-being in mice. Journal of Neuroscience Methods 234, 139–146. https://doi.org/10.1016/j.jneumeth.2014.02.001

Johansen, J.P., Fields, H.L., Manning, B.H., 2001. The affective component of pain in rodents: direct evidence for a contribution of the anterior cingulate cortex. Proceedings of the National Academy of Sciences 98, 8077–8082.

Johnson, C.I., Argyle, D.J., Clements, D.N., 2016. In vitro models for the study of osteoarthritis. The Veterinary Journal 209, 40–49. https://doi.org/10.1016/j.tvjl.2015.07.011

Johnson, P.A., Miyanohara, A., Levine, F., Cahill, T., Friedmann, T., 1992. Cytotoxicity of a replication-defective mutant of herpes simplex virus type 1. J Virol 66, 2952–2965.

Jones, D.S., Jenney, A.P., Swantek, J.L., Burke, J.M., Lauffenburger, D.A., Sorger, P.K., 2016. Profiling drugs for rheumatoid arthritis that inhibit synovial fibroblast activation. Nature Chemical Biology 13, 38.

Jozwiak-Bebenista, M., Nowak, J.Z., 2014. Paracetamol: mechanism of action, applications and safety concern. Acta Pol Pharm 71, 11–23.

Judge, A., Arden, N.K., Cooper, C., Kassim Javaid, M., Carr, A.J., Field, R.E., Dieppe, P.A., 2012. Predictors of outcomes of total knee replacement surgery. Rheumatology 51, 1804–1813. https://doi.org/10.1093/rheumatology/kes075

Jung, H., Toth, P.T., White, F.A., Miller, R.J., 2008. Monocyte chemoattractant protein-1 functions as a neuromodulator in dorsal root ganglia neurons. J Neurochem 104, 254–263. https://doi.org/10.1111/j.1471-4159.2007.04969.x

Kaiser, M.I., 2011. The limits of reductionism in the life sciences. Hist Philos Life Sci 33, 453–476.

Kaneko, H., Putzier, I., Frings, S., Kaupp, U.B., Gensch, T., 2004. Chloride Accumulation in Mammalian Olfactory Sensory Neurons. J. Neurosci. 24, 7931. https://doi.org/10.1523/JNEUROSCI.2115-04.2004

Kannan, M., Vasan, G., Huang, C., Haziza, S., Li, J.Z., Inan, H., Schnitzer, M.J., Pieribone, V.A., 2018. Fast, in vivo voltage imaging using a red fluorescent indicator. Nat Methods 15, 1108–1116. https://doi.org/10.1038/s41592-018-0188-7

Katz, J.N., Earp, B.E., Gomoll, A.H., 2010. Surgical management of osteoarthritis. Arthritis Care Res (Hoboken) 62, 1220–1228. https://doi.org/10.1002/acr.20231

Kawashima, M., Ogura, N., Akutsu, M., Ito, K., Kondoh, T., 2013. The anti-inflammatory effect of cyclooxygenase inhibitors in fibroblast-like synoviocytes from the human temporomandibular joint results from the suppression of PGE2 production. Journal of oral pathology & medicine : official publication of the International Association of Oral Pathologists and the American Academy of Oral Pathology 42, 499–506. https://doi.org/10.1111/jop.12045

Keeble, J., Russell, F., Curtis, B., Starr, A., Pinter, E., Brain, S.D., 2005. Involvement of transient receptor potential vanilloid 1 in the vascular and hyperalgesic components of joint inflammation. Arthritis and Rheumatism 52, 3248–3256. https://doi.org/10.1002/art.21297

Keffer, J., Probert, L., Cazlaris, H., Georgopoulos, S., Kaslaris, E., Kioussis, D., Kollias, G., 1991. Transgenic mice expressing human tumour necrosis factor: a predictive genetic model of arthritis. The EMBO journal 10, 4025–4031.

Kellaway, P., 1946. The part played by electric fish in the early history of bioelectricity and electrotherapy. Bulletin of the History of Medicine 20, 112–137.

Kelly, S., Chapman, R.J., Woodhams, S., Sagar, D.R., Turner, J., Burston, J.J., Bullock, C., Paton, K., Huang, J., Wong, A., McWilliams, D.F., Okine, B.N., Barrett, D.A., Hathway, G.J., Walsh, D.A., Chapman, V., 2015. Increased function of pronociceptive TRPV1 at the level of the joint in a rat

model of osteoarthritis pain. Ann Rheum Dis 74, 252. https://doi.org/10.1136/annrheumdis-2013-203413
Keystone, E.C., Kavanaugh, A.F., Sharp, J.T., Tannenbaum, H., Hua, Y., Teoh, L.S., Fischkoff, S.A., Chartash, E.K., 2004. Radiographic, clinical, and functional outcomes of treatment with adalimumab (a human anti–tumor necrosis factor monoclonal antibody) in patients with active rheumatoid arthritis receiving concomitant methotrexate therapy: A randomized, placebo-controlled, 52-week trial. Arthritis & Rheumatism 50, 1400–1411. https://doi.org/10.1002/art.20217
Khachigian, L.M., 2006. Collagen antibody-induced arthritis. Nature Protocols 1, 2512–2516. https://doi.org/10.1038/nprot.2006.393
Kienzler, J.L., Gold, M., Nollevaux, F., 2010. Systemic bioavailability of topical diclofenac sodium gel 1% versus oral diclofenac sodium in healthy volunteers. J Clin Pharmacol 50. https://doi.org/10.1177/0091270009336234
Kingsbury, S.R., Gross, H.J., Isherwood, G., Conaghan, P.G., 2014. Osteoarthritis in Europe: impact on health status, work productivity and use of pharmacotherapies in five European countries. Rheumatology 53, 937–947. https://doi.org/10.1093/rheumatology/ket463
Knowlton, W.M., Fisher, A., Bautista, D.M., McKemy, D.D., 2010. TRPM8, but not TRPA1, is required for neural and behavioral responses to acute noxious cold temperatures and cold-mimetics in vivo. Pain 150, 340–350. https://doi.org/10.1016/j.pain.2010.05.021
Kochukov, M.Y., McNearney, T.A., Fu, Y., Westlund, K.N., 2006. Thermosensitive TRP ion channels mediate cytosolic calcium response in human synoviocytes. Am J Physiol Cell Physiol 291. https://doi.org/10.1152/ajpcell.00553.2005
Kochukov, M.Y., McNearney, T.A., Yin, H., Zhang, L., Ma, F., Ponomareva, L., Abshire, S., Westlund, K.N., 2009. Tumor Necrosis Factor-Alpha (TNF-α) Enhances Functional Thermal and Chemical Responses of TRP Cation Channels in Human Synoviocytes. Mol Pain 5, 1744-8069-5–49. https://doi.org/10.1186/1744-8069-5-49
Kolker, S.J., Walder, R.Y., Usachev, Y., Hillman, J., Boyle, D.L., Firestein, G.S., Sluka, K.A., 2010. Acid-sensing ion channel 3 expressed in type B synoviocytes and chondrocytes modulates hyaluronan expression and release. ANNALS OF THE RHEUMATIC DISEASES 69, 903–909. https://doi.org/10.1136/ard.2009.117168
Kosinska, M.K., Liebisch, G., Lochnit, G., Wilhelm, J., Klein, H., Kaesser, U., Lasczkowski, G., Rickert, M., Schmitz, G., Steinmeyer, J., 2014. Sphingolipids in human synovial fluid--a lipidomic study. PLoS One 9, e91769–e91769. https://doi.org/10.1371/journal.pone.0091769
Kraemer, W., Ratamess, N., Maresh, C., Anderson, J., Volek, J., P. TIBERIO, D., E. JOYCE, M., N. MESSINGER, B., French, D., Sharman, M., R. RUBIN, M., Gomez, A., 2001. A Cetylated Fatty Acid Topical Cream with Menthol Reduces Pain and Improves Functional Performance in Patients with Arthritis.
Krashes, M.J., Koda, S., Ye, C., Rogan, S.C., Adams, A.C., Cusher, D.S., Maratos-Flier, E., Roth, B.L., Lowell, B.B., 2011. Rapid, reversible activation of AgRP neurons drives feeding behavior in mice. J Clin Invest 121, 1424–1428. https://doi.org/10.1172/JCI46229
Krug, H.E., Dorman, C., Blanshan, N., Frizelle, S., Mahowald, M., 2019. Spontaneous and Evoked Measures of Pain in Murine Models of Monoarticular Knee Pain. JoVE e59024. https://doi.org/10.3791/59024
Kunnumakkara, A.B., Banik, K., Bordoloi, D., Harsha, C., Sailo, B.L., Padmavathi, G., Roy, N.K., Gupta, S.C., Aggarwal, B.B., 2018. Googling the Guggul (Commiphora and Boswellia) for Prevention of Chronic Diseases. Frontiers in Pharmacology 9, 686. https://doi.org/10.3389/fphar.2018.00686
Kuyinu, E.L., Narayanan, G., Nair, L.S., Laurencin, C.T., 2016. Animal models of osteoarthritis: classification, update, and measurement of outcomes. J Orthop Surg Res 11, 19–19. https://doi.org/10.1186/s13018-016-0346-5
Kwiecinski, J., 2014. Reactive Arthritis in Ancient Egypt: A Possible Description in Medical Papyri. J Rheumatol 41, 556. https://doi.org/10.3899/jrheum.131099

Kyostio-Moore, S., Nambiar, B., Hutto, E., Ewing, P.J., Piraino, S., Berthelette, P., Sookdeo, C., Matthews, G., Armentano, D., 2011. STR/ort mice, a model for spontaneous osteoarthritis, exhibit elevated levels of both local and systemic inflammatory markers. Comp Med 61, 346–355.

Laedermann, C.J., Abriel, H., Decosterd, I., 2015. Post-translational modifications of voltage-gated sodium channels in chronic pain syndromes. Frontiers in Pharmacology 6, 263. https://doi.org/10.3389/fphar.2015.00263

Laird, J.M., Carter, A.J., Grauert, M., Cervero, F., 2001. Analgesic activity of a novel use-dependent sodium channel blocker, crobenetine, in mono-arthritic rats. Br J Pharmacol 134, 1742–1748. https://doi.org/10.1038/sj.bjp.0704428

Lampa, J., Westman, M., Kadetoff, D., Agréus, A.N., Le Maître, E., Gillis-Haegerstrand, C., Andersson, M., Khademi, M., Corr, M., Christianson, C.A., 2012. Peripheral inflammatory disease associated with centrally activated IL-1 system in humans and mice. Proceedings of the National Academy of Sciences 109, 12728–12733.

Lane, N.E., Schnitzer, T.J., Birbara, C.A., Mokhtarani, M., Shelton, D.L., Smith, M.D., Brown, M.T., 2010. Tanezumab for the Treatment of Pain from Osteoarthritis of the Knee. N Engl J Med 363, 1521–1531. https://doi.org/10.1056/NEJMoa0901510

Langford, D.J., Bailey, A.L., Chanda, M.L., Clarke, S.E., Drummond, T.E., Echols, S., Glick, S., Ingrao, J., Klassen-Ross, T., LaCroix-Fralish, M.L., Matsumiya, L., Sorge, R.E., Sotocinal, S.G., Tabaka, J.M., Wong, D., van den Maagdenberg, A.M.J.M., Ferrari, M.D., Craig, K.D., Mogil, J.S., 2010. Coding of facial expressions of pain in the laboratory mouse. Nature Methods 7, 447–449. https://doi.org/10.1038/nmeth.1455

Langford, L.A., 1983. Unmyelinated axon ratios in cat motor, cutaneous and articular nerves. Neuroscience letters 40, 19–22.

Larsson, S., Englund, M., Struglics, A., Lohmander, L.S., 2015. Interleukin-6 and tumor necrosis factor alpha in synovial fluid are associated with progression of radiographic knee osteoarthritis in subjects with previous meniscectomy. Osteoarthritis and Cartilage 23, 1906–1914. https://doi.org/10.1016/j.joca.2015.05.035

Lascaratos, J., 1995. "Arthritis" in Byzantium (AD 324-1453): unknown information from non-medical literary sources. Annals of the rheumatic diseases 54, 951–957.

Lawson, S.N., McCarthy, P.W., Prabhakar, E., 1996. Electrophysiological properties of neurones with CGRP-like immunoreactivity in rat dorsal root ganglia. Journal of Comparative Neurology 365, 355–366. https://doi.org/10.1002/(SICI)1096-9861(19960212)365:3<355::AID-CNE2>3.0.CO;2-3

Leardini, G., Salaffi, F., Caporali, R., Canesi, B., Rovati, L., Montanelli, R., 2004. Direct and indirect costs of osteoarthritis of the knee. Clin Exp Rheumatol 22, 699–706.

Lebre, M.C., Vieira, P.L., Tang, M.W., Aarrass, S., Helder, B., Newsom-Davis, T., Tak, P.P., Screaton, G.R., 2017. Synovial IL-21/TNF-producing CD4+ T cells induce joint destruction in rheumatoid arthritis by inducing matrix metalloproteinase production by fibroblast-like synoviocytes. Journal of Leukocyte Biology 101, 775–783. https://doi.org/10.1189/jlb.5A0516-217RR

Lechner, S.G., Lewin, G.R., 2009. Peripheral sensitisation of nociceptors via G-protein-dependent potentiation of mechanotransduction currents. J Physiol 587, 3493–3503. https://doi.org/10.1113/jphysiol.2009.175059

Lee, A.S., De Jesús-Cortés, H., Kabir, Z.D., Knobbe, W., Orr, M., Burgdorf, C., Huntington, P., McDaniel, L., Britt, J.K., Hoffmann, F., Brat, D.J., Rajadhyaksha, A.M., Pieper, A.A., 2016. The Neuropsychiatric Disease-Associated Gene cacna1c Mediates Survival of Young Hippocampal Neurons. eNeuro 3, ENEURO.0006-16.2016. https://doi.org/10.1523/ENEURO.0006-16.2016

Lee, D.M., Kiener, H.P., Agarwal, S.K., Noss, E.H., Watts, G.F.M., Chisaka, O., Takeichi, M., Brenner, M.B., 2007. Cadherin-11 in Synovial Lining Formation and Pathology in Arthritis. Science 315, 1006. https://doi.org/10.1126/science.1137306

Lee, J., Kim, Y., Yi, H., Diecke, S., Kim, J., Jung, H., Rim, Y.A., Jung, S.M., Kim, M., Kim, Y.G., Park, S.-H., Kim, H.-Y., Ju, J.H., 2014. Generation of disease-specific induced pluripotent stem cells from patients with rheumatoid arthritis and osteoarthritis. Arthritis Res Ther 16, R41–R41. https://doi.org/10.1186/ar4470

Lee, K.Y., Charbonnet, M., Gold, M.S., 2012. Upregulation of high affinity GABA(A) receptors in cultured rat dorsal root ganglion neurons. Neuroscience 208C, 133–142. https://doi.org/10.1016/j.neuroscience.2012.01.050

Lewis, T., 1938. Study of Somatic Pain. British Medical Journal 1, 321–325.

Li, X., Kim, J.-S., van Wijnen, A.J., Im, H.-J., 2011. Osteoarthritic tissues modulate functional properties of sensory neurons associated with symptomatic OA pain. Molecular Biology Reports 38, 5335–5339. https://doi.org/10.1007/s11033-011-0684-7

Lin, K.J., De Caterina, R., Garcia Rodriguez, L.A., 2014. Low-dose aspirin and upper gastrointestinal bleeding in primary versus secondary cardiovascular prevention: a population-based, nested case-control study. Circ Cardiovasc Qual Outcomes 7, 70–77. https://doi.org/10.1161/CIRCOUTCOMES.113.000494

Lindia, J.A., McGowan, E., Jochnowitz, N., Abbadie, C., 2005. Induction of CX3CL1 expression in astrocytes and CX3CR1 in microglia in the spinal cord of a rat model of neuropathic pain. The Journal of Pain 6, 434–438.

Livak, K.J., Schmittgen, T.D., 2001. Analysis of Relative Gene Expression Data Using Real-Time Quantitative PCR and the 2−ΔΔCT Method. Methods 25, 402–408. https://doi.org/10.1006/meth.2001.1262

Llop-Guevara, A., Porras, M., Cendón, C., Di Ceglie, I., Siracusa, F., Madarena, F., Rinotas, V., Gómez, L., van Lent, P.L., Douni, E., Chang, H.D., Kamradt, T., Román, J., 2015. Simultaneous inhibition of JAK and SYK kinases ameliorates chronic and destructive arthritis in mice. Arthritis Research & Therapy 17, 356. https://doi.org/10.1186/s13075-015-0866-0

Loeser, R.F., Goldring, S.R., Scanzello, C.R., Goldring, M.B., 2012. Osteoarthritis: a disease of the joint as an organ. Arthritis Rheum 64, 1697–1707. https://doi.org/10.1002/art.34453

Lories, R.J.U., Derese, I., De Bari, C., Luyten, F.P., 2003. In vitro growth rate of fibroblast-like synovial cells is reduced by methotrexate treatment. Ann Rheum Dis 62, 568. https://doi.org/10.1136/ard.62.6.568

Luesink, D., 2019. Anatomy. Brill, Leiden, The Netherlands.

Lundkvist, J., Kastäng, F., Kobelt, G., 2008. The burden of rheumatoid arthritis and access to treatment: health burden and costs. The European Journal of Health Economics 8, 49–60. https://doi.org/10.1007/s10198-007-0088-8

Lyons, M.R., West, A.E., 2011. Mechanisms of specificity in neuronal activity-regulated gene transcription. Progress in Neurobiology 94, 259–295. https://doi.org/10.1016/j.pneurobio.2011.05.003

Magnus, C.J., Lee, P.H., Atasoy, D., Su, H.H., Looger, L.L., Sternson, S.M., 2011. Chemical and genetic engineering of selective ion channel-ligand interactions. Science 333, 1292–1296. https://doi.org/10.1126/science.1206606

Majeed, M.H., Sherazi, S.A.A., Bacon, D., Bajwa, Z.H., 2018. Pharmacological Treatment of Pain in Osteoarthritis: A Descriptive Review. Current Rheumatology Reports 20, 88. https://doi.org/10.1007/s11926-018-0794-5

Malfait, A., Ritchie, J., Gil, A., Austin, J.-S., Hartke, J., Qin, W., Tortorella, M., Mogil, J., 2010. ADAMTS-5 deficient mice do not develop mechanical allodynia associated with osteoarthritis following medial meniscal destabilization. Osteoarthritis and cartilage 18, 572–580.

Malfait, A.M., Little, C.B., McDougall, J.J., 2013. A commentary on modelling osteoarthritis pain in small animals. Osteoarthritis and Cartilage 21, 1316–1326. https://doi.org/10.1016/j.joca.2013.06.003

Malfait, A.-M., Miller, R.J., 2016. Emerging Targets for the Management of Osteoarthritis Pain. Current osteoporosis reports 14, 260–268. https://doi.org/10.1007/s11914-016-0326-z

Malm, K., Bergman, S., Andersson, M.L., Bremander, A., Larsson, I., 2017. Quality of life in patients with established rheumatoid arthritis: A phenomenographic study. SAGE Open Med 5, 2050312117713647–2050312117713647. https://doi.org/10.1177/2050312117713647

Malmström, V., Ho, K., Lun, J., Tam, P., Cheah, K., Holmdahl, R., 1997. Arthritis susceptibility in mice expressing human type II collagen in cartilage. Scandinavian journal of immunology 45, 670–677.

Mandl, P., Alasti, F., Kerschbaumer, A., Kaltenberger, R., Krennert, T., Supp, G., Landesmann, U., Smolen, J., Aletaha, D., 2017. THU0633 Temperature sensitivity in patients with rheumatoid arthritis. Ann Rheum Dis 76, 445. https://doi.org/10.1136/annrheumdis-2017-eular.5134

Manitpisitkul, P., Flores, C.M., Moyer, J.A., Romano, G., Shalayda, K., Tatikola, K., Hutchison, J.S., Mayorga, 2018. A multiple-dose double-blind randomized study to evaluate the safety, pharmacokinetics, pharmacodynamics and analgesic efficacy of the TRPV1 antagonist JNJ-39439335 (mavatrep). sjpain 18, 151. https://doi.org/10.1515/sjpain-2017-0184

Marra, S., Ferru-Clément, R., Breuil, V., Delaunay, A., Christin, M., Friend, V., Sebille, S., Cognard, C., Ferreira, T., Roux, C., Euller-Ziegler, L., Noel, J., Lingueglia, E., Deval, E., 2016. Non-acidic activation of pain-related Acid-Sensing Ion Channel 3 by lipids. EMBO J 35, 414–428. https://doi.org/10.15252/embj.201592335

Mason, M.R.J., Ehlert, E.M.E., Eggers, R., Pool, C.W., Hermening, S., Huseinovic, A., Timmermans, E., Blits, B., Verhaagen, J., 2010. Comparison of AAV serotypes for gene delivery to dorsal root ganglion neurons. Mol Ther 18, 715–724. https://doi.org/10.1038/mt.2010.19

Massier, J., Eitner, A., Segond von Banchet, G., Schaible, H.-G., 2015. Effects of Differently Activated Rodent Macrophages on Sensory Neurons: Implications for Arthritis Pain. Arthritis & Rheumatology 67, 2263–2272. https://doi.org/10.1002/art.39134

Mauderli, A.P., Acosta-Rua, A., Vierck, C.J., 2000. An operant assay of thermal pain in conscious, unrestrained rats. Journal of neuroscience methods 97, 19–29.

Mauri, C., Williams, R.O., Walmsley, M., Feldmann, M., 1996. Relationship between Th1/Th2 cytokine patterns and the arthritogenic response in collagen-induced arthritis. European journal of immunology 26, 1511–1518.

McCall, M.N., McMurray, H.R., Land, H., Almudevar, A., 2014. On non-detects in qPCR data. Bioinformatics 30, 2310–2316. https://doi.org/10.1093/bioinformatics/btu239

McDougall, J.J., 2006. Arthritis and Pain. Neurogenic origin of joint pain. Arthritis Research & Therapy 8, 220–220. https://doi.org/10.1186/ar2069

McWilliams, L.A., Goodwin, R.D., Cox, B.J., 2004. Depression and anxiety associated with three pain conditions: results from a nationally representative sample. Pain 111, 77–83. https://doi.org/10.1016/j.pain.2004.06.002

Meek, I.L., Van de Laar, M.A.F.J., E Vonkeman, H., 2010. Non-Steroidal Anti-Inflammatory Drugs: An Overview of Cardiovascular Risks. Pharmaceuticals (Basel) 3, 2146–2162. https://doi.org/10.3390/ph3072146

Megat, S., Ray, P.R., Moy, J.K., Lou, T.-F., Barragán-Iglesias, P., Li, Y., Pradhan, G., Wanghzou, A., Ahmad, A., Burton, M.D., North, R.Y., Dougherty, P.M., Khoutorsky, A., Sonenberg, N., Webster, K.R., Dussor, G., Campbell, Z.T., Price, T.J., 2019. Nociceptor Translational Profiling Reveals the Ragulator-Rag GTPase Complex as a Critical Generator of Neuropathic Pain. J. Neurosci. 39, 393. https://doi.org/10.1523/JNEUROSCI.2661-18.2018

Melli, G., Höke, A., 2009. Dorsal Root Ganglia Sensory Neuronal Cultures: a tool for drug discovery for peripheral neuropathies. Expert Opin Drug Discov 4, 1035–1045. https://doi.org/10.1517/17460440903266829

Melville, K.M., Robling, A.G., van der Meulen, M.C.H., 2015. In vivo axial loading of the mouse tibia. Methods Mol Biol 1226, 99–115. https://doi.org/10.1007/978-1-4939-1619-1_9

Merabova, N., Kaminski, R., Krynska, B., Amini, S., Khalili, K., Darbinyan, A., 2012. JCV agnoprotein-induced reduction in CXCL5/LIX secretion by oligodendrocytes is associated with activation of apoptotic signaling in neurons. J Cell Physiol 227, 3119–3127. https://doi.org/10.1002/jcp.23065

Messier, S.P., Mihalko, S.L., Legault, C., Miller, G.D., Nicklas, B.J., DeVita, P., Beavers, D.P., Hunter, D.J., Lyles, M.F., Eckstein, F., Williamson, J.D., Carr, J.J., Guermazi, A., Loeser, R.F., 2013. Effects of Intensive Diet and Exercise on Knee Joint Loads, Inflammation, and Clinical Outcomes Among Overweight and Obese Adults With Knee Osteoarthritis: The IDEA Randomized Clinical Trial. JAMA 310, 1263–1273. https://doi.org/10.1001/jama.2013.277669

Miller, R.E., Ishihara, S., Bhattacharyya, B., Delaney, A., Menichella, D.M., Miller, R.J., Malfait, A.-M., 2017. Chemogenetic Inhibition of Pain Neurons in a Mouse Model of Osteoarthritis. Arthritis Rheumatol 69, 1429–1439. https://doi.org/10.1002/art.40118

Miller, R.J., Jung, H., Bhangoo, S.K., White, F.A., 2009. Cytokine and chemokine regulation of sensory neuron function. Handb Exp Pharmacol 417–449. https://doi.org/10.1007/978-3-540-79090-7_12

Mills, C., McMackin, M., Jaffe, R., Yu, J., Zininberg, E., Slee, D., Gogas, K., Bradbury, M., 2008. Effects of the transient receptor potential vanilloid 1 antagonist A-425619 on body temperature and thermoregulation in the rat. Neuroscience 156, 165–174. https://doi.org/10.1016/j.neuroscience.2008.06.069

Mis, M.A., Yang, Y., Tanaka, B.S., Gomis-Perez, C., Liu, S., Dib-Hajj, F., Adi, T., Garcia-Milian, R., Schulman, B.R., Dib-Hajj, S.D., Waxman, S.G., 2019. Resilience to Pain: A Peripheral Component Identified Using Induced Pluripotent Stem Cells and Dynamic Clamp. J. Neurosci. 39, 382. https://doi.org/10.1523/JNEUROSCI.2433-18.2018

Miyazawa, K., Mori, A., Okudaira, H., 1998. Establishment and Characterization of a Novel Human Rheumatoid Fibroblast-Like Synoviocyte Line, MH7A, Immortalized with SV40 T Antigen. Journal of Biochemistry 124, 1153–1162. https://doi.org/10.1093/oxfordjournals.jbchem.a022233

Mogil, J.S., 2012. Sex differences in pain and pain inhibition: multiple explanations of a controversial phenomenon. Nat Rev Neurosci 13, 859–866. https://doi.org/10.1038/nrn3360

Mogil, J.S., 2009. Animal models of pain: progress and challenges. Nature Reviews Neuroscience 10, 283–294. https://doi.org/10.1038/nrn2606

Moilanen, L.J., Laavola, M., Kukkonen, M., Korhonen, R., Leppänen, T., Högestätt, E.D., Zygmunt, P.M., Nieminen, R.M., Moilanen, E., 2012. TRPA1 Contributes to the Acute Inflammatory Response and Mediates Carrageenan-Induced Paw Edema in the Mouse. Scientific Reports 2, 380.

Mok, C.C., 2013. Rituximab for the treatment of rheumatoid arthritis: an update. Drug Des Devel Ther 8, 87–100. https://doi.org/10.2147/DDDT.S41645

Molliver, D.C., Radeke, M.J., Feinstein, S.C., Snider, W.D., 1995. Presence or absence of TrKA protein distinguishes subsets of small sensory neurons with unique cytochemical characteristics and dorsal horn projections. Journal of Comparative Neurology 361, 404–416. https://doi.org/10.1002/cne.903610305

Moore, C., Gupta, R., Jordt, S.-E., Chen, Y., Liedtke, W.B., 2018. Regulation of Pain and Itch by TRP Channels. Neuroscience Bulletin 34, 120–142. https://doi.org/10.1007/s12264-017-0200-8

Müller-Ladner, U., Kriegsmann, J., Franklin, B.N., Matsumoto, S., Geiler, T., Gay, R.E., Gay, S., 1996. Synovial fibroblasts of patients with rheumatoid arthritis attach to and invade normal human cartilage when engrafted into SCID mice. The American journal of pathology 149, 1607.

Murphy, L., Schwartz, T.A., Helmick, C.G., Renner, J.B., Tudor, G., Koch, G., Dragomir, A., Kalsbeek, W.D., Luta, G., Jordan, J.M., 2008. Lifetime risk of symptomatic knee osteoarthritis. Arthritis Rheum 59, 1207–1213. https://doi.org/10.1002/art.24021

Murphy, L.B., Helmick, C.G., Schwartz, T.A., Renner, J.B., Tudor, G., Koch, G.G., Dragomir, A.D., Kalsbeek, W.D., Luta, G., Jordan, J.M., 2010. One in four people may develop symptomatic hip osteoarthritis in his or her lifetime. Osteoarthritis Cartilage 18, 1372–1379. https://doi.org/10.1016/j.joca.2010.08.005

Neogi, T., 2013. The epidemiology and impact of pain in osteoarthritis. Osteoarthritis and Cartilage 21, 1145–1153. https://doi.org/10.1016/j.joca.2013.03.018

Neugebauer, V., Rümenapp, P., Schaible, H.-G., 1996. Calcitonin gene-related peptide is involved in the spinal processing of mechanosensory input from the rat's knee joint and in the generation and

maintenance of hyperexcitability of dorsal horn neurons during development of acute inflammation. Neuroscience 71, 1095–1109.
Neumann, E., Khawaja, K., Müller-Ladner, U., 2014. G protein-coupled receptors in rheumatology. Nature Reviews Rheumatology 10, 429.
Nieto, F.R., Clark, A.K., Grist, J., Chapman, V., Malcangio, M., 2015. Calcitonin Gene-Related Peptide–Expressing Sensory Neurons and Spinal Microglial Reactivity Contribute to Pain States in Collagen-Induced Arthritis. Arthritis & Rheumatology 67, 1668–1677. https://doi.org/10.1002/art.39082
Niki, Y., Yamada, H., Seki, S., Kikuchi, T., Takaishi, H., Toyama, Y., Fujikawa, K., Tada, N., 2001. Macrophage-and neutrophil-dominant arthritis in human IL-1α transgenic mice. The Journal of clinical investigation 107, 1127–1135.
Nissen, S.E., Yeomans, N.D., Solomon, D.H., Lüscher, T.F., Libby, P., Husni, M.E., Graham, D.Y., Borer, J.S., Wisniewski, L.M., Wolski, K.E., Wang, Q., Menon, V., Ruschitzka, F., Gaffney, M., Beckerman, B., Berger, M.F., Bao, W., Lincoff, A.M., 2016. Cardiovascular Safety of Celecoxib, Naproxen, or Ibuprofen for Arthritis. N Engl J Med 375, 2519–2529. https://doi.org/10.1056/NEJMoa1611593
North, R.Y., Li, Y., Ray, P., Rhines, L.D., Tatsui, C.E., Rao, G., Johansson, C.A., Zhang, H., Kim, Y.H., Zhang, B., Dussor, G., Kim, T.H., Price, T.J., Dougherty, P.M., 2019. Electrophysiological and transcriptomic correlates of neuropathic pain in human dorsal root ganglion neurons. Brain 142, 1215–1226. https://doi.org/10.1093/brain/awz063
Obeidat, A.M., Miller, R.E., Miller, R.J., Malfait, A.-M., 2019. The nociceptive innervation of the normal and osteoarthritic mouse knee. Osteoarthritis and Cartilage 27, 1669–1679. https://doi.org/10.1016/j.joca.2019.07.012
O'Brien, C., Woolf, C.J., Fitzgerald, M., Lindsay, R.M., Molander, C., 1989. Differences in the chemical expression of rat primary afferent neurons which innervate skin, muscle or joint. Neuroscience 32, 493–502. https://doi.org/10.1016/0306-4522(89)90096-1
O'Brien, M., McDougall, J.J., 2018. Cannabis and joints: scientific evidence for the alleviation of osteoarthritis pain by cannabinoids. Current Opinion in Pharmacology 40, 104–109. https://doi.org/10.1016/j.coph.2018.03.012
Oh, S.B., Tran, P.B., Gillard, S.E., Hurley, R.W., Hammond, D.L., Miller, R.J., 2001. Chemokines and Glycoprotein120 Produce Pain Hypersensitivity by Directly Exciting Primary Nociceptive Neurons. J. Neurosci. 21, 5027. https://doi.org/10.1523/JNEUROSCI.21-14-05027.2001
Okun, A., Liu, P., Davis, P., Ren, J., Remeniuk, B., Brion, T., Ossipov, M.H., Xie, J., Dussor, G.O., King, T., Porreca, F., 2012. Afferent drive elicits ongoing pain in a model of advanced osteoarthritis. Pain 153, 924–933. https://doi.org/10.1016/j.pain.2012.01.022
Old, E.A., Clark, A.K., Malcangio, M., 2015. The Role of Glia in the Spinal Cord in Neuropathic and Inflammatory Pain, in: Schaible, H.-G. (Ed.), Pain Control. Springer Berlin Heidelberg, Berlin, Heidelberg, pp. 145–170. https://doi.org/10.1007/978-3-662-46450-2_8
Paredes, R.M., Etzler, J.C., Watts, L.T., Zheng, W., Lechleiter, J.D., 2008. Chemical calcium indicators. Methods 46, 143–151. https://doi.org/10.1016/j.ymeth.2008.09.025
Parsonage, G., Falciani, F., Burman, A., Filer, A., Ross, E., Bofill, M., Martin, S., Salmon, M., Buckley, C.D., 2017. Global gene expression profiles in fibroblasts from synovial, skin and lymphoid tissue reveals distinct cytokine and chemokine expression patterns. Thromb Haemost 90, 688–697. https://doi.org/10.1160/TH03-04-0208
Pattison, L.A., Callejo, G., St John Smith, E., 2019. Evolution of acid nociception: ion channels and receptors for detecting acid. Philosophical Transactions of the Royal Society B: Biological Sciences 374, 20190291. https://doi.org/10.1098/rstb.2019.0291
Payne, C.E., Brown, A.R., Theile, J.W., Loucif, A.J.C., Alexandrou, A.J., Fuller, M.D., Mahoney, J.H., Antonio, B.M., Gerlach, A.C., Printzenhoff, D.M., Prime, R.L., Stockbridge, G., Kirkup, A.J., Bannon, A.W., England, S., Chapman, M.L., Bagal, S., Roeloffs, R., Anand, U., Anand, P., Bungay, P.J., Kemp, M., Butt, R.P., Stevens, E.B., 2015. A novel selective and orally

bioavailable Nav 1.8 channel blocker, PF-01247324, attenuates nociception and sensory neuron excitability. Br J Pharmacol 172, 2654–2670. https://doi.org/10.1111/bph.13092
Pearson, C.M., 1956. Development of Arthritis, Periarthritis and Periostitis in Rats Given Adjuvants. Proceedings of the Society for Experimental Biology and Medicine 91, 95–101. https://doi.org/10.3181/00379727-91-22179
Peiris, M., Hockley, J.R., Reed, D.E., Smith, E.S.J., Bulmer, D.C., Blackshaw, L.A., 2017. Peripheral K(V)7 channels regulate visceral sensory function in mouse and human colon. Mol Pain 13, 1744806917709371–1744806917709371. https://doi.org/10.1177/1744806917709371
Petrus, M., Peier, A.M., Bandell, M., Hwang, S.W., Huynh, T., Olney, N., Jegla, T., Patapoutian, A., 2007. A role of TRPA1 in mechanical hyperalgesia is revealed by pharmacological inhibition. Molecular Pain 3, 40–40. https://doi.org/10.1186/1744-8069-3-40
Petruska, J.C., Napaporn, J., Johnson, R.D., Gu, J.G., Cooper, B.Y., 2000. Subclassified Acutely Dissociated Cells of Rat DRG: Histochemistry and Patterns of Capsaicin-, Proton-, and ATP-Activated Currents. Journal of Neurophysiology 84, 2365–2379. https://doi.org/10.1152/jn.2000.84.5.2365
Platzer, A., Nussbaumer, T., Karonitsch, T., Smolen, J.S., Aletaha, D., 2019. Analysis of gene expression in rheumatoid arthritis and related conditions offers insights into sex-bias, gene biotypes and co-expression patterns. PLoS One 14, e0219698–e0219698. https://doi.org/10.1371/journal.pone.0219698
Prato, V., Taberner, F.J., Hockley, J.R.F., Callejo, G., Arcourt, A., Tazir, B., Hammer, L., Schad, P., Heppenstall, P.A., Smith, E.S., Lechner, S.G., 2017. Functional and Molecular Characterization of Mechanoinsensitive "Silent" Nociceptors. Cell Reports 21, 3102–3115. https://doi.org/10.1016/j.celrep.2017.11.066
Przewłocki, R., Przewłocka, B., 2001. Opioids in chronic pain. European Journal of Pharmacology 429, 79–91. https://doi.org/10.1016/S0014-2999(01)01308-5
Puigdellívol-Sánchez, A., Prats-Galino, A., Ruano-Gil, D., Molander, C., 1998. Efficacy of the fluorescent dyes Fast Blue, Fluoro-Gold, and Diamidino Yellow for retrograde tracing to dorsal root ganglia after subcutaneous injection. Journal of Neuroscience Methods 86, 7–16. https://doi.org/10.1016/S0165-0270(98)00137-X
Qu, L., Caterina, M.J., 2016. Enhanced excitability and suppression of A-type K+ currents in joint sensory neurons in a murine model of antigen-induced arthritis. Scientific Reports 6, 28899. https://doi.org/10.1038/srep28899
Randall, L.O., 1957. A method for measurement of analgesic activity on inflamed tissues. Arch Int Pharmacodyn. 111, 409–419.
Raphael, I., Nalawade, S., Eagar, T.N., Forsthuber, T.G., 2015. T cell subsets and their signature cytokines in autoimmune and inflammatory diseases. Cytokine 74, 5–17. https://doi.org/10.1016/j.cyto.2014.09.011
Ray, P., Torck, A., Quigley, L., Wangzhou, A., Neiman, M., Rao, C., Lam, T., Kim, J.-Y., Kim, T.H., Zhang, M.Q., Dussor, G., Price, T.J., 2018. Comparative transcriptome profiling of the human and mouse dorsal root ganglia: an RNA-seq-based resource for pain and sensory neuroscience research. Pain 159, 1325–1345. https://doi.org/10.1097/j.pain.0000000000001217
Rech, J., Hess, A., Finzel, S., Kreitz, S., Sergeeva, M., Englbrecht, M., Doerfler, A., Saake, M., Schett, G., 2013. Association of brain functional magnetic resonance activity with response to tumor necrosis factor inhibition in rheumatoid arthritis. Arthritis & Rheumatism 65, 325–333. https://doi.org/10.1002/art.37761
Rees, H., Sluka, K.A., Westlund, K., Willis, W.D., 1995. The role of glutamate and GABA receptors in the generation of dorsal root reflexes by acute arthritis in the anaesthetized rat. The Journal of physiology 484, 437–445.
Richardson, D., Pearson, R.G., Kurian, N., Latif, M.L., Garle, M.J., Barrett, D.A., Kendall, D.A., Scammell, B.E., Reeve, A.J., Chapman, V., 2008. Characterisation of the cannabinoid receptor

system in synovial tissue and fluid in patients with osteoarthritis and rheumatoid arthritis. Arthritis Research & Therapy 10, R43. https://doi.org/10.1186/ar2401
Ritter, A.M., Mendell, L.M., 1992. Somal membrane properties of physiologically identified sensory neurons in the rat: effects of nerve growth factor. Journal of Neurophysiology 68, 2033–2041. https://doi.org/10.1152/jn.1992.68.6.2033
Rojewska, E., Zychowska, M., Piotrowska, A., Kreiner, G., Nalepa, I., Mika, J., 2018. Involvement of Macrophage Inflammatory Protein-1 Family Members in the Development of Diabetic Neuropathy and Their Contribution to Effectiveness of Morphine. Front Immunol 9, 494–494. https://doi.org/10.3389/fimmu.2018.00494
Rosengren, S., Boyle, D.L., Firestein, G.S., 2007. Acquisition, culture, and phenotyping of synovial fibroblasts. Methods in molecular medicine 135, 365–375.
Roth, B.L., 2016. DREADDs for Neuroscientists. Neuron 89, 683–694. https://doi.org/10.1016/j.neuron.2016.01.040
Rothschild, B.M., Arriaza, B., Woods, R.J., Dutour, O., 1999. Spondyloarthropathy identified as the etiology of Nubian erosive arthritis. Am J Phys Anthropol 109, 259–267. https://doi.org/10.1002/(SICI)1096-8644(199906)109:2<259::AID-AJPA10>3.0.CO;2-3
Rouwette, T., Sondermann, J., Avenali, L., Varela, D., Schmidt, M., 2016. Standardized profiling of the membrane-enriched proteome of mouse dorsal root ganglia provides novel insights into chronic pain. Molecular & Cellular Proteomics 15, mcp.M116.058966. https://doi.org/10.1074/mcp.M116.058966
Rutten, K., Robens, A., Read, S.J., Christoph, T., 2014. Pharmacological validation of a refined burrowing paradigm for prediction of analgesic efficacy in a rat model of sub-chronic knee joint inflammation. European Journal of Pain 18, 213–222. https://doi.org/10.1002/j.1532-2149.2013.00359.x
Safiri, S., Kolahi, A.A., Hoy, D., Smith, E., Bettampadi, D., Mansournia, M.A., Almasi-Hashiani, A., Ashrafi-Asgarabad, A., Moradi-Lakeh, M., Qorbani, M., Collins, G., Woolf, A.D., March, L., Cross, M., 2019. Global, regional and national burden of rheumatoid arthritis 1990–2017: a systematic analysis of the Global Burden of Disease study 2017. Ann Rheum Dis 78, 1463. https://doi.org/10.1136/annrheumdis-2019-215920
Sakmann, B., Neher, E., 1984. Patch clamp techniques for studying ionic channels in excitable membranes. Annual review of physiology 46, 455–472.
Salaffi, F., Giacobazzi, G., Di Carlo, M., 2018. Chronic Pain in Inflammatory Arthritis: Mechanisms, Metrology, and Emerging Targets-A Focus on the JAK-STAT Pathway. Pain Res Manag 2018, 8564215–8564215. https://doi.org/10.1155/2018/8564215
Saloman, J.L., Scheff, N.N., Snyder, L.M., Ross, S.E., Davis, B.M., Gold, M.S., 2016. Gi-DREADD Expression in Peripheral Nerves Produces Ligand-Dependent Analgesia, as well as Ligand-Independent Functional Changes in Sensory Neurons. J Neurosci 36, 10769–10781. https://doi.org/10.1523/JNEUROSCI.3480-15.2016
Samineni, V.K., Mickle, A.D., Yoon, J., Grajales-Reyes, J.G., Pullen, M.Y., Crawford, K.E., Noh, K.N., Gereau, G.B., Vogt, S.K., Lai, H.H., Rogers, J.A., Gereau, R.W., 2017. Optogenetic silencing of nociceptive primary afferents reduces evoked and ongoing bladder pain. Scientific Reports 7, 15865. https://doi.org/10.1038/s41598-017-16129-3
Samuel, E., 1952. The autonomic and somatic innervation of the articular capsule. The Anatomical Record 113, 53–70.
Samulowitz, A., Gremyr, I., Eriksson, E., Hensing, G., 2018. “Brave Men” and “Emotional Women”: A Theory-Guided Literature Review on Gender Bias in Health Care and Gendered Norms towards Patients with Chronic Pain. Pain Res Manag 2018, 6358624–6358624. https://doi.org/10.1155/2018/6358624
San Segundo-Val, I., Sanz-Lozano, C.S., 2016. Introduction to the Gene Expression Analysis, in: Isidoro García, M. (Ed.), Molecular Genetics of Asthma. Springer New York, New York, NY, pp. 29–43. https://doi.org/10.1007/978-1-4939-3652-6_3

Sandercock, D.A., Barnett, M.W., Coe, J.E., Downing, A.C., Nirmal, A.J., Di Giminiani, P., Edwards, S.A., Freeman, T.C., 2019. Transcriptomics Analysis of Porcine Caudal Dorsal Root Ganglia in Tail Amputated Pigs Shows Long-Term Effects on Many Pain-Associated Genes. Front Vet Sci 6, 314–314. https://doi.org/10.3389/fvets.2019.00314

Sara Nencini, Mitchell Ringuet, Dong-Hyun Kim, Yu-Jen Chen, Claire Greenhill, Jason J Ivanusic, 2017. Mechanisms of nerve growth factor signaling in bone nociceptors and in an animal model of inflammatory bone pain. Mol Pain 13, 1744806917697011. https://doi.org/10.1177/1744806917697011

Sarria, I., Ling, J., Zhu, M.X., Gu, J.G., 2011. TRPM8 acute desensitization is mediated by calmodulin and requires PIP(2): distinction from tachyphylaxis. J Neurophysiol 106, 3056–3066. https://doi.org/10.1152/jn.00544.2011

Sarzi-Puttini, P., Batticciotto, A., Atzeni, F., Bazzichi, L., Di Franco, M., Salaffi, F., Marotto, D., Ceribelli, A., Ablin, J.N., Hauser, W., 2019. Medical cannabis and cannabinoids in rheumatology: where are we now? Expert Rev Clin Immunol 15, 1019–1032. https://doi.org/10.1080/1744666X.2019.1665997

Sasaki, K., Suzuki, M., Mieda, M., Tsujino, N., Roth, B., Sakurai, T., 2011. Pharmacogenetic modulation of orexin neurons alters sleep/wakefulness states in mice. PLoS One 6, e20360–e20360. https://doi.org/10.1371/journal.pone.0020360

Schaible, H.-G., 2014. Nociceptive neurons detect cytokines in arthritis. ARTHRITIS RESEARCH & THERAPY 16. https://doi.org/10.1186/s13075-014-0470-8

Schaible, H.-G., Ebersberger, A., von Banchet, G.S., 2002. Mechanisms of Pain in Arthritis. Annals of the New York Academy of Sciences 966, 343–354. https://doi.org/10.1111/j.1749-6632.2002.tb04234.x

Schaible, H.G., Schmidt, R.F., 1985. Effects of an experimental arthritis on the sensory properties of fine articular afferent units. Journal of Neurophysiology 54, 1109–1122. https://doi.org/10.1152/jn.1985.54.5.1109

Schaible, H.G., Schmidt, R.F., 1983. Responses of fine medial articular nerve afferents to passive movements of knee joints. Journal of Neurophysiology 49, 1118–1126. https://doi.org/10.1152/jn.1983.49.5.1118

Schinnerling, K., Rosas, C., Soto, L., Thomas, R., Aguillón, J.C., 2019. Humanized Mouse Models of Rheumatoid Arthritis for Studies on Immunopathogenesis and Preclinical Testing of Cell-Based Therapies. Frontiers in Immunology 10, 203. https://doi.org/10.3389/fimmu.2019.00203

Schnitzer, T.J., Easton, R., Pang, S., Levinson, D.J., Pixton, G., Viktrup, L., Davignon, I., Brown, M.T., West, C.R., Verburg, K.M., 2019. Effect of Tanezumab on Joint Pain, Physical Function, and Patient Global Assessment of Osteoarthritis Among Patients With Osteoarthritis of the Hip or Knee: A Randomized Clinical Trial. JAMA 322, 37–48. https://doi.org/10.1001/jama.2019.8044

Schnitzer, T.J., Ekman, E.F., Spierings, E.L., Greenberg, H.S., Smith, M.D., Brown, M.T., West, C.R., Verburg, K.M., 2015. Efficacy and safety of tanezumab monotherapy or combined with non-steroidal anti-inflammatory drugs in the treatment of knee or hip osteoarthritis pain. Annals of the rheumatic diseases 74, 1202–1211.

Schött, E., Berge, O.-G., Ängeby-Möller, K., Hammarström, G., Dalsgaard, C.-J., Brodin, E., 1994. Weight bearing as an objective measure of arthritic pain in the rat. Journal of Pharmacological and Toxicological Methods 31, 79–83. https://doi.org/10.1016/1056-8719(94)90046-9

Schuelert, N., Johnson, M.P., Oskins, J.L., Jassal, K., Chambers, M.G., McDougall, J.J., 2011. Local application of the endocannabinoid hydrolysis inhibitor URB597 reduces nociception in spontaneous and chemically induced models of osteoarthritis. PAIN 152, 975–981. https://doi.org/10.1016/j.pain.2010.11.025

Schuelert, N., McDougall, J.J., 2012. Involvement of Nav 1.8 sodium ion channels in the transduction of mechanical pain in a rodent model of osteoarthritis. Arthritis Research & Therapy 14, R5. https://doi.org/10.1186/ar3553

Scott, B.B., Weisbrot, L.M., Greenwood, J.D., Bogoch, E.R., Paige, C.J., Keystone, E.C., 1997. Rheumatoid arthritis synovial fibroblast and U937 macrophage/monocyte cell line interaction in cartilage degradation. Arthritis & Rheumatism 40, 490–498. https://doi.org/10.1002/art.1780400315
Scott, B.S., Edwards, B.A., 1980. Electric membrane properties of adult mouse DRG neurons and the effect of culture duration. J Neurobiol 11, 291–301. https://doi.org/10.1002/neu.480110307
Scott, L.J., 2017. Tocilizumab: A Review in Rheumatoid Arthritis. Drugs 77, 1865–1879. https://doi.org/10.1007/s40265-017-0829-7
Segond von Banchet, G., Kiehl, M., Schaible, H.-G., 2005. Acute and long-term effects of IL-6 on cultured dorsal root ganglion neurones from adult rat. Journal of Neurochemistry 94, 238–248. https://doi.org/10.1111/j.1471-4159.2005.03185.x
Seidel, M.F., Wise, B.L., Lane, N.E., 2013. Nerve growth factor: an update on the science and therapy. Osteoarthritis and Cartilage 21, 1223–1228. https://doi.org/10.1016/j.joca.2013.06.004
Serra, I. da S., Husson, Z., Bartlett, J.D., Smith, E.S., 2016. Characterization of cutaneous and articular sensory neurons.
Sharma, J.N., Arora, R., 1973. Arthritis in ancient Indian literature. Indian journal of history of science 8, 37.
Shepherd, A.J., Mohapatra, D.P., 2018. Pharmacological validation of voluntary gait and mechanical sensitivity assays associated with inflammatory and neuropathic pain in mice. Neuropharmacology 130, 18–29. https://doi.org/10.1016/j.neuropharm.2017.11.036
Shepherd, D.E.T., Seedhom, B.B., 1999. Thickness of human articular cartilage in joints of the lower limb. Ann Rheum Dis 58, 27. https://doi.org/10.1136/ard.58.1.27
Short, C.L., 1974. The antiquity of rheumatoid arthritis. Arthritis Rheum 17, 193–205. https://doi.org/10.1002/art.1780170302
Sluka, K.A., Frey-Law, L., Hoeger Bement, M., 2018. Exercise-induced pain and analgesia? Underlying mechanisms and clinical translation. Pain 159 Suppl 1, S91–S97. https://doi.org/10.1097/j.pain.0000000000001235
Sluka, K.A., Rasmussen, L.A., Edgar, M.M., O'Donnell, J.M., Walder, R.Y., Kolker, S.J., Boyle, D.L., Firestein, G.S., 2013. Acid-sensing ion channel 3 deficiency increases inflammation but decreases pain behavior in murine arthritis. https://doi.org/10.1002/art.37862
Smedegård, G., Björk, J., 1995. Sulphasalazine: Mechanism of Action in Rheumatoid Arthritis. Rheumatology XXXIV, 7–15. https://doi.org/10.1093/rheumatology/XXXIV.suppl_2.7
Smith, E.S., Cadiou, H., McNaughton, P.A., 2007. Arachidonic acid potentiates acid-sensing ion channels in rat sensory neurons by a direct action. Neuroscience 145. https://doi.org/10.1016/j.neuroscience.2006.12.024
Smith, E.St.J., Omerbašić, D., Lechner, S.G., Anirudhan, G., Lapatsina, L., Lewin, G.R., 2011. The Molecular Basis of Acid Insensitivity in the African Naked Mole-Rat. Science 334, 1557. https://doi.org/10.1126/science.1213760
Smolen, J.S., Steiner, G., 2003. Therapeutic strategies for rheumatoid arthritis. Nat Rev Drug Discov 2, 473–488. https://doi.org/10.1038/nrd1109
Sokolove, J., Lepus, C.M., 2013. Role of inflammation in the pathogenesis of osteoarthritis: latest findings and interpretations. Ther Adv Musculoskelet Dis 5, 77–94. https://doi.org/10.1177/1759720X12467868
Soni, A., Wanigasekera, V., Mezue, M., Cooper, C., Javaid, M.K., Price, A.J., Tracey, I., 2019. Central Sensitization in Knee Osteoarthritis: Relating Presurgical Brainstem Neuroimaging and PainDETECT-Based Patient Stratification to Arthroplasty Outcome. Arthritis Rheumatol 71, 550–560. https://doi.org/10.1002/art.40749
Srikanth, V.K., Fryer, J.L., Zhai, G., Winzenberg, T.M., Hosmer, D., Jones, G., 2005. A meta-analysis of sex differences prevalence, incidence and severity of osteoarthritis. Osteoarthritis and cartilage 13, 769–781.

St. John Smith, E., 2018. Advances in understanding nociception and neuropathic pain. Journal of Neurology 265, 231–238. https://doi.org/10.1007/s00415-017-8641-6
Staniland, A.A., McMahon, S.B., 2009. Mice lacking acid-sensing ion channels (ASIC) 1 or 2, but not ASIC3, show increased pain behaviour in the formalin test. European Journal of Pain 13, 554–563. https://doi.org/10.1016/j.ejpain.2008.07.001
Starobova, H., S W A, H., Lewis, R.J., Vetter, I., 2018. Transcriptomics in pain research: insights from new and old technologies. Mol Omics 14, 389–404. https://doi.org/10.1039/c8mo00181b
Staunton, C.A., Lewis, R., Barrett-Jolley, R., 2013. Ion Channels and Osteoarthritic Pain: Potential for Novel Analgesics. Current Pain and Headache Reports 17, 378. https://doi.org/10.1007/s11916-013-0378-z
Steen, K.H., Reeh, P.W., 1993. Sustained graded pain and hyperalgesia from harmless experimental tissue acidosis in human skin. Neuroscience Letters 154, 113–116. https://doi.org/10.1016/0304-3940(93)90184-M
Stefanini, M., Martino, C. de, Zamboni, L., 1967. Fixation of Ejaculated Spermatozoa for Electron Microscopy. Nature 216, 173–174. https://doi.org/10.1038/216173a0
Stoop, J.N., Tibbitt, C.A., van Eden, W., Robinson, J.H., Hilkens, C.M., 2013. The choice of adjuvant determines the cytokine profile of T cells in proteoglycan-induced arthritis but does not influence disease severity. Immunology 138, 68–75.
Storek, B., Harder, N.M., Banck, M.S., Wang, C., McCarty, D.M., Janssen, W.G., Morrison, J.H., Walsh, C.E., Beutler, A.S., 2006. Intrathecal long-term gene expression by self-complementary adeno-associated virus type 1 suitable for chronic pain studies in rats. Mol Pain 2, 4–4. https://doi.org/10.1186/1744-8069-2-4
Stucky, C.L., 2007. IB4-Positive Neurons, Role in Inflammatory Pain, in: Schmidt, R.F., Willis, W.D. (Eds.), Encyclopedia of Pain. Springer Berlin Heidelberg, Berlin, Heidelberg, pp. 952–955. https://doi.org/10.1007/978-3-540-29805-2_1855
Stucky, C.L., Lewin, G.R., 1999. Isolectin B_4-Positive and -Negative Nociceptors Are Functionally Distinct. J. Neurosci. 19, 6497.
Sturrock, R., Sharma, J., Buchanan, W., 1977. Evidence of rheumatoid arthritis in ancient India. Arthritis & Rheumatism: Official Journal of the American College of Rheumatology 20, 42–44.
Sugimoto, H., Kawakami, K., 2019. Low-cost Protocol of Footprint Analysis and Hanging Box Test for Mice Applied the Chronic Restraint Stress. JoVE e59027. https://doi.org/10.3791/59027
Sun, W., Meednu, N., Rosenberg, A., Rangel-Moreno, J., Wang, V., Glanzman, J., Owen, T., Zhou, X., Zhang, H., Boyce, B.F., Anolik, J.H., Xing, L., 2018. B cells inhibit bone formation in rheumatoid arthritis by suppressing osteoblast differentiation. Nature Communications 9, 5127. https://doi.org/10.1038/s41467-018-07626-8
Sundukova, M., Prifti, E., Bucci, A., Kirillova, K., Serrao, J., Reymond, L., Umebayashi, M., Hovius, R., Riezman, H., Johnsson, K., 2019. A Chemogenetic Approach for the Optical Monitoring of Voltage in Neurons. Angewandte Chemie 131, 2363–2366.
Sutherland, F.I., Bannatyne, B.A., Kerr, R., Riddell, J.S., Maxwell, D.J., 2002. Inhibitory amino acid transmitters associated with axons in presynaptic apposition to cutaneous primary afferent axons in the cat spinal cord. J Comp Neurol 452, 154–162. https://doi.org/10.1002/cne.10374
Swensen, A.M., Herrington, J., Bugianesi, R.M., Dai, G., Haedo, R.J., Ratliff, K.S., Smith, M.M., Warren, V.A., Arneric, S.P., Eduljee, C., Parker, D., Snutch, T.P., Hoyt, S.B., London, C., Duffy, J.L., Kaczorowski, G.J., McManus, O.B., 2012. Characterization of the Substituted N-Triazole Oxindole TROX-1, a Small-Molecule, State-Dependent Inhibitor of Ca_v2 Calcium Channels. Mol Pharmacol 81, 488. https://doi.org/10.1124/mol.111.075226
Sydenham, T., Swan, J., 1742. The Entire Works of Dr. Thomas Sydenham: Newly Made English from the Originals: Wherein the History of Acute and Chronic Diseases, and the Safest and Most Effectual Methods of Treating Them, are Faithfully, Clearly, and Accurately Delivered. To which are Added, Explanatory and Practical Notes, from the Best Medicinal Writers. Edward Cave.

Syx, D., Tran, P.B., Miller, R.E., Malfait, A.-M., 2018. Peripheral Mechanisms Contributing to Osteoarthritis Pain. Current Rheumatology Reports 20, 9. https://doi.org/10.1007/s11926-018-0716-6

Tamer Mahmoud Tamer, 2013. Hyaluronan and synovial joint: function, distribution and healing. Interdisciplinary Toxicology 6, 111–125. https://doi.org/10.2478/intox-2013-0019

Taneja, V., David, C.S., 2010. Role of HLA class II genes in susceptibility/resistance to inflammatory arthritis: studies with humanized mice. Immunological reviews 233, 62–78.

Tang, L., Jia, P., Zhao, L., Kang, D., Luo, Y., Liu, J., Li, L., Zheng, H., Li, Y., Li, N., Guyatt, G., Sun, X., 2018. Acupuncture treatment for knee osteoarthritis with sensitive points: protocol for a multicentre randomised controlled trial. BMJ Open 8, e023838. https://doi.org/10.1136/bmjopen-2018-023838

Tappe-Theodor, A., King, T., Morgan, M.M., 2019. Pros and Cons of Clinically Relevant Methods to Assess Pain in Rodents. Neuroscience & Biobehavioral Reviews 100, 335–343. https://doi.org/10.1016/j.neubiorev.2019.03.009

Taylor, C.W., Genazzani, A.A., Morris, S.A., 1999. Expression of inositol trisphosphate receptors. Cell Calcium 26, 237–251. https://doi.org/10.1054/ceca.1999.0090

Taylor, P.C., Feldmann, M., 2009. Anti-TNF biologic agents: still the therapy of choice for rheumatoid arthritis. Nature Reviews Rheumatology 5, 578.

Teichert, R.W., Smith, N.J., Raghuraman, S., Yoshikami, D., Light, A.R., Olivera, B.M., 2012. Functional profiling of neurons through cellular neuropharmacology. Proc Natl Acad Sci USA 109, 1388. https://doi.org/10.1073/pnas.1118833109

Tervo, D.G.R., Hwang, B.-Y., Viswanathan, S., Gaj, T., Lavzin, M., Ritola, K.D., Lindo, S., Michael, S., Kuleshova, E., Ojala, D., Huang, C.-C., Gerfen, C.R., Schiller, J., Dudman, J.T., Hantman, A.W., Looger, L.L., Schaffer, D.V., Karpova, A.Y., 2016. A Designer AAV Variant Permits Efficient Retrograde Access to Projection Neurons. Neuron 92, 372–382. https://doi.org/10.1016/j.neuron.2016.09.021

Tetta, C., Camussi, G., Modena, V., Di Vittorio, C., Baglioni, C., 1990. Tumour necrosis factor in serum and synovial fluid of patients with active and severe rheumatoid arthritis. Ann Rheum Dis 49, 665–667. https://doi.org/10.1136/ard.49.9.665

The Institute for Health Metrics and Evaluation, 2017. Global burden of disease compare tool [WWW Document]. URL https://vizhub.healthdata.org/gbd-compare/ (accessed 11.30.19).

Thompson, K.J., Khajehali, E., Bradley, S.J., Navarrete, J.S., Huang, X.P., Slocum, S., Jin, J., Liu, J., Xiong, Y., Olsen, R.H.J., Diberto, J.F., Boyt, K.M., Pina, M.M., Pati, D., Molloy, C., Bundgaard, C., Sexton, P.M., Kash, T.L., Krashes, M.J., Christopoulos, A., Roth, B.L., Tobin, A.B., 2018. DREADD Agonist 21 Is an Effective Agonist for Muscarinic-Based DREADDs in Vitro and in Vivo. ACS Pharmacol. Transl. Sci. 1, 61–72. https://doi.org/10.1021/acsptsci.8b00012

Tighe, H., Silverman, G.J., Kozin, F., Tucker, R., Gulizia, R., Peebles, C., Lotz, M., Rhodes, G., Machold, K., Mosier, D.E., 1990. Autoantibody production by severe combined immunodeficient mice reconstituted with synovial cells from rheumatoid arthritis patients. European journal of immunology 20, 1843–1848.

Topp, R., Brosky, J.A., Pieschel, D., 2013. The Effect of Either Topical Menthol or a Placebo on Functioning and Knee Pain Among Patients With Knee OA. Journal of Geriatric Physical Therapy 36.

Touska, F., Winter, Z., Mueller, A., Vlachova, V., Larsen, J., Zimmermann, K., 2016. Comprehensive thermal preference phenotyping in mice using a novel automated circular gradient assay. Temperature 3, 77–91.

Towne, C., Pertin, M., Beggah, A.T., Aebischer, P., Decosterd, I., 2009. Recombinant adeno-associated virus serotype 6 (rAAV2/6)-mediated gene transfer to nociceptive neurons through different routes of delivery. Mol Pain 5, 52–52. https://doi.org/10.1186/1744-8069-5-52

Treharne, G.J., Kitas, G.D., Lyons, A.C., Booth, D.A., 2005. Well-being in Rheumatoid Arthritis: The Effects of Disease Duration and Psychosocial Factors. J Health Psychol 10, 457–474. https://doi.org/10.1177/1359105305051416

Tsantoulas, C., Laínez, S., Wong, S., Mehta, I., Vilar, B., McNaughton, P.A., 2017. Hyperpolarization-activated cyclic nucleotide-gated 2 (HCN2) ion channels drive pain in mouse models of diabetic neuropathy. Sci Transl Med 9, eaam6072–eaam6072. https://doi.org/10.1126/scitranslmed.aam6072

Tsien, R.Y., 1980. New calcium indicators and buffers with high selectivity against magnesium and protons: design, synthesis, and properties of prototype structures. Biochemistry 19, 2396–2404.

United Nations, 2019. World population prospects: the 2019 revision. [WWW Document]. URL https://www.un.org/en/sections/issues-depth/ageing/ (accessed 11.30.19).

Urban, R., Scherrer, G., Goulding, E.H., Tecott, L.H., Basbaum, A.I., 2011. Behavioral indices of ongoing pain are largely unchanged in male mice with tissue or nerve injury-induced mechanical hypersensitivity. Pain 152, 990–1000. https://doi.org/10.1016/j.pain.2010.12.003

U.S. National library of medicine, 2019. Clinical Trials [WWW Document]. URL https://clinicaltrials.gov/ (accessed 1.12.19).

Usoskin, D., Furlan, A., Islam, S., Abdo, H., Lonnerberg, P., Lou, D., Hjerling-Leffler, J., Haeggstrom, J., Kharchenko, O., Kharchenko, P.V., Linnarsson, S., Ernfors, P., 2015. Unbiased classification of sensory neuron types by large-scale single-cell RNA sequencing. Nat Neurosci 18, 145–153.

van Vollenhoven, R.F., 2009. Sex differences in rheumatoid arthritis: more than meets the eye.. BMC Med 7, 12–12. https://doi.org/10.1186/1741-7015-7-12

Varani, K., De Mattei, M., Vincenzi, F., Tosi, A., Gessi, S., Merighi, S., Pellati, A., Masieri, F., Ongaro, A., Borea, P.A., 2008. Pharmacological characterization of P2X1 and P2X3 purinergic receptors in bovine chondrocytes. Osteoarthritis and cartilage 16, 1421–1429.

Vasilyev, D.V., Shan, Q.J., Lee, Y.T., Soloveva, V., Nawoschik, S.P., Kaftan, E.J., Dunlop, J., Mayer, S.C., Bowlby, M.R., 2009. A Novel High-Throughput Screening Assay for HCN Channel Blocker Using Membrane Potential-Sensitive Dye and FLIPR. J Biomol Screen 14, 1119–1128. https://doi.org/10.1177/1087057109345526

von Banchet, G.S., Petrow, P.K., Bräuer, R., Schaible, H.-G., 2000. Monoarticular antigen-induced arthritis leads to pronounced bilateral upregulation of the expression of neurokinin 1 and bradykinin 2 receptors in dorsal root ganglion neurons of rats. Arthritis Research & Therapy 2, 424. https://doi.org/10.1186/ar121

von Banchet, G.S., Richter, J., Hückel, M., Rose, C., Bräuer, R., Schaible, H.-G., 2007. Fibroblast-like synovial cells from normal and inflamed knee joints differently affect the expression of pain-related receptors in sensory neurones: a co-culture study. Arthritis Research & Therapy 9, R6–R6. https://doi.org/10.1186/ar2112

Von Korff, M., 2013. Opioids for chronic musculoskeletal pain: Putting patient safety first. PAIN 154.

Vonkeman, H.E., Brouwers, J.R.B.J., van de Laar, M.A.F.J., 2006. Understanding the NSAID related risk of vascular events. BMJ 332, 895. https://doi.org/10.1136/bmj.332.7546.895

Vos, T., Flaxman, A.D., Naghavi, M., Lozano, R., Michaud, C., Ezzati, M., Shibuya, K., Salomon, J.A., Abdalla, S., Aboyans, V., Abraham, J., Ackerman, I., Aggarwal, R., Ahn, S.Y., Ali, M.K., AlMazroa, M.A., Alvarado, M., Anderson, H.R., Anderson, L.M., Andrews, K.G., Atkinson, C., Baddour, L.M., Bahalim, A.N., Barker-Collo, S., Barrero, L.H., Bartels, D.H., Basáñez, M.-G., Baxter, A., Bell, M.L., Benjamin, E.J., Bennett, D., Bernabé, E., Bhalla, K., Bhandari, B., Bikbov, B., Abdulhak, A.B., Birbeck, G., Black, J.A., Blencowe, H., Blore, J.D., Blyth, F., Bolliger, I., Bonaventure, A., Boufous, S., Bourne, R., Boussinesq, M., Braithwaite, T., Brayne, C., Bridgett, L., Brooker, S., Brooks, P., Brugha, T.S., Bryan-Hancock, C., Bucello, C., Buchbinder, R., Buckle, G., Budke, C.M., Burch, M., Burney, P., Burstein, R., Calabria, B., Campbell, B., Canter, C.E., Carabin, H., Carapetis, J., Carmona, L., Cella, C., Charlson, F., Chen, H., Cheng, A.T.-A., Chou, D., Chugh, S.S., Coffeng, L.E., Colan, S.D., Colquhoun, S., Colson, K.E., Condon, J., Connor, M.D., Cooper, L.T., Corriere, M., Cortinovis, M., de Vaccaro, K.C.,

Couser, W., Cowie, B.C., Criqui, M.H., Cross, M., Dabhadkar, K.C., Dahiya, M., Dahodwala, N., Damsere-Derry, J., Danaei, G., Davis, A., De Leo, D., Degenhardt, L., Dellavalle, R., Delossantos, A., Denenberg, J., Derrett, S., Des Jarlais, D.C., Dharmaratne, S.D., Dherani, M., Diaz-Torne, C., Dolk, H., Dorsey, E.R., Driscoll, T., Duber, H., Ebel, B., Edmond, K., Elbaz, A., Ali, S.E., Erskine, H., Erwin, P.J., Espindola, P., Ewoigbokhan, S.E., Farzadfar, F., Feigin, V., Felson, D.T., Ferrari, A., Ferri, C.P., Fèvre, E.M., Finucane, M.M., Flaxman, S., Flood, L., Foreman, K., Forouzanfar, M.H., Fowkes, F.G.R., Franklin, R., Fransen, M., Freeman, M.K., Gabbe, B.J., Gabriel, S.E., Gakidou, E., Ganatra, H.A., Garcia, B., Gaspari, F., Gillum, R.F., Gmel, G., Gosselin, R., Grainger, R., Groeger, J., Guillemin, F., Gunnell, D., Gupta, R., Haagsma, J., Hagan, H., Halasa, Y.A., Hall, W., Haring, D., Haro, J.M., Harrison, J.E., Havmoeller, R., Hay, R.J., Higashi, H., Hill, C., Hoen, B., Hoffman, H., Hotez, P.J., Hoy, D., Huang, J.J., Ibeanusi, S.E., Jacobsen, K.H., James, S.L., Jarvis, D., Jasrasaria, R., Jayaraman, S., Johns, N., Jonas, J.B., Karthikeyan, G., Kassebaum, N., Kawakami, N., Keren, A., Khoo, J.-P., King, C.H., Knowlton, L.M., Kobusingye, O., Koranteng, A., Krishnamurthi, R., Lalloo, R., Laslett, L.L., Lathlean, T., Leasher, J.L., Lee, Y.Y., Leigh, J., Lim, S.S., Limb, E., Lin, J.K., Lipnick, M., Lipshultz, S.E., Liu, W., Loane, M., Ohno, S.L., Lyons, R., Ma, J., Mabweijano, J., MacIntyre, M.F., Malekzadeh, R., Mallinger, L., Manivannan, S., Marcenes, W., March, L., Margolis, D.J., Marks, G.B., Marks, R., Matsumori, A., Matzopoulos, R., Mayosi, B.M., McAnulty, J.H., McDermott, M.M., McGill, N., McGrath, J., Medina-Mora, M.E., Meltzer, M., Memish, Z.A., Mensah, G.A., Merriman, T.R., Meyer, A.-C., Miglioli, V., Miller, M., Miller, T.R., Mitchell, P.B., Mocumbi, A.O., Moffitt, T.E., Mokdad, A.A., Monasta, L., Montico, M., Moradi-Lakeh, M., Moran, A., Morawska, L., Mori, R., Murdoch, M.E., Mwaniki, M.K., Naidoo, K., Nair, M.N., Naldi, L., Narayan, K.V., Nelson, P.K., Nelson, R.G., Nevitt, M.C., Newton, C.R., Nolte, S., Norman, P., Norman, R., O'Donnell, M., O'Hanlon, S., Olives, C., Omer, S.B., Ortblad, K., Osborne, R., Ozgediz, D., Page, A., Pahari, B., Pandian, J.D., Rivero, A.P., Patten, S.B., Pearce, N., Padilla, R.P., Perez-Ruiz, F., Perico, N., Pesudovs, K., Phillips, D., Phillips, M.R., Pierce, K., Pion, S., Polanczyk, G.V., Polinder, S., Pope, C.A., Popova, S., Porrini, E., Pourmalek, F., Prince, M., Pullan, R.L., Ramaiah, K.D., Ranganathan, D., Razavi, H., Regan, M., Rehm, J.T., Rein, D.B., Remuzzi, G., Richardson, K., Rivara, F.P., Roberts, T., Robinson, C., De Leòn, F.R., Ronfani, L., Room, R., Rosenfeld, L.C., Rushton, L., Sacco, R.L., Saha, S., Sampson, U., Sanchez-Riera, L., Sanman, E., Schwebel, D.C., Scott, J.G., Segui-Gomez, M., Shahraz, S., Shepard, D.S., Shin, H., Shivakoti, R., Silberberg, D., Singh, D., Singh, G.M., Singh, J.A., Singleton, J., Sleet, D.A., Sliwa, K., Smith, E., Smith, J.L., Stapelberg, N.J., Steer, A., Steiner, T., Stolk, W.A., Stovner, L.J., Sudfeld, C., Syed, S., Tamburlini, G., Tavakkoli, M., Taylor, H.R., Taylor, J.A., Taylor, W.J., Thomas, B., Thomson, W.M., Thurston, G.D., Tleyjeh, I.M., Tonelli, M., Towbin, J.A., Truelsen, T., Tsilimbaris, M.K., Ubeda, C., Undurraga, E.A., van der Werf, M.J., van Os, J., Vavilala, M.S., Venketasubramanian, N., Wang, M., Wang, W., Watt, K., Weatherall, D.J., Weinstock, M.A., Weintraub, R., Weisskopf, M.G., Weissman, M.M., White, R.A., Whiteford, H., Wiersma, S.T., Wilkinson, J.D., Williams, H.C., Williams, S.R., Witt, E., Wolfe, F., Woolf, A.D., Wulf, S., Yeh, P.-H., Zaidi, A.K., Zheng, Z.-J., Zonies, D., Lopez, A.D., Murray, C.J., 2012. Years lived with disability (YLDs) for 1160 sequelae of 289 diseases and injuries 1990–2010: a systematic analysis for the Global Burden of Disease Study 2010. The Lancet 380, 2163–2196. https://doi.org/10.1016/S0140-6736(12)61729-2

Vriens, J., Owsianik, G., Hofmann, T., Philipp, S.E., Stab, J., Chen, X., Benoit, M., Xue, F., Janssens, A., Kerselaers, S., Oberwinkler, J., Vennekens, R., Gudermann, T., Nilius, B., Voets, T., 2011. TRPM3 Is a Nociceptor Channel Involved in the Detection of Noxious Heat. Neuron 70, 482–494. https://doi.org/10.1016/j.neuron.2011.02.051

Vrontou, S., Wong, A.M., Rau, K.K., Koerber, H.R., Anderson, D.J., 2013. Genetic identification of C fibres that detect massage-like stroking of hairy skin in vivo. Nature 493, 669–673. https://doi.org/10.1038/nature11810

Vysokov, N., McMahon, S.B., Raouf, R., 2019. The role of NaV channels in synaptic transmission after axotomy in a microfluidic culture platform. Scientific Reports 9, 12915. https://doi.org/10.1038/s41598-019-49214-w

Wainger, B.J., Buttermore, E.D., Oliveira, J.T., Mellin, C., Lee, S., Saber, W.A., Wang, A.J., Ichida, J.K., Chiu, I.M., Barrett, L., Huebner, E.A., Bilgin, C., Tsujimoto, N., Brenneis, C., Kapur, K., Rubin, L.L., Eggan, K., Woolf, C.J., 2015. Modeling pain in vitro using nociceptor neurons reprogrammed from fibroblasts. Nat Neurosci 18, 17–24. https://doi.org/10.1038/nn.3886

Wall, P.D., Woolf, C.J., 1984. Muscle but not cutaneous C-afferent input produces prolonged increases in the excitability of the flexion reflex in the rat. The Journal of physiology 356, 443–458.

Wallace, I.J., Worthington, S., Felson, D.T., Jurmain, R.D., Wren, K.T., Maijanen, H., Woods, R.J., Lieberman, D.E., 2017. Knee osteoarthritis has doubled in prevalence since the mid-20th century. Proceedings of the National Academy of Sciences of the United States of America 114, 9332–9336. https://doi.org/10.1073/pnas.1703856114

Walsh, D.A., McWilliams, D.F., 2014. Mechanisms, impact and management of pain in rheumatoid arthritis. Nature Reviews Rheumatology 10, 581–592. https://doi.org/10.1038/nrrheum.2014.64

Wang, C., Li, G.-W., Huang, L.-Y.M., 2007. Prostaglandin E2 potentiation of P2X3 receptor mediated currents in dorsal root ganglion neurons. Molecular pain 3, 22.

Wang, D., Tai, P.W.L., Gao, G., 2019. Adeno-associated virus vector as a platform for gene therapy delivery. Nature Reviews Drug Discovery 18, 358–378. https://doi.org/10.1038/s41573-019-0012-9

Wang, H., Rivero-Melián, C., Robertson, B., Grant, G., 1994. transganglionic transport and binding of the isolectin B4 from Griffonia simplicifolia I in rat primary sensory neurons. Neuroscience 62, 539–551. https://doi.org/10.1016/0306-4522(94)90387-5

Wang, Y.Y., Chang, R.B., Waters, H.N., McKemy, D.D., Liman, E.R., 2008. The nociceptor ion channel TRPA1 is potentiated and inactivated by permeating calcium ions. J Biol Chem 283, 32691–32703. https://doi.org/10.1074/jbc.M803568200

Webster, B.S., Verma, S.K., Gatchel, R.J., 2007. Relationship between early opioid prescribing for acute occupational low back pain and disability duration, medical costs, subsequent surgery and late opioid use. Spine (Phila Pa 1976) 32, 2127–2132. https://doi.org/10.1097/BRS.0b013e318145a731

Wege, A.K., 2018. Humanized mouse models for the preclinical assessment of Cancer immunotherapy. BioDrugs 32, 245–266.

Wehling, P., Reinecke, J., Baltzer, A.W.A., Granrath, M., Schulitz, K.P., Schultz, C., Krauspe, R., Whiteside, T.W., Elder, E., Ghivizzani, S.C., Robbins, P.D., Evans, C.H., 2009. Clinical responses to gene therapy in joints of two subjects with rheumatoid arthritis. Hum Gene Ther 20, 97–101. https://doi.org/10.1089/hum.2008.075

Wei, B., Kumada, T., Furukawa, T., Inoue, K., Watanabe, M., Sato, K., Fukuda, A., 2013. Pre- and post-synaptic switches of GABA actions associated with Cl− homeostatic changes are induced in the spinal nucleus of the trigeminal nerve in a rat model of trigeminal neuropathic pain. Neuroscience 228, 334–348. https://doi.org/10.1016/j.neuroscience.2012.10.043

Weinberger, A., 1998. The Arthritis of Vincent van Gogh's Model, Augustine Roulin. J Clin Rheumatol 4, 39–41. https://doi.org/10.1097/00124743-199802000-00009

Weir, G.A., Middleton, S.J., Clark, A.J., Daniel, T., Khovanov, N., McMahon, S.B., Bennett, D.L., 2017. Using an engineered glutamate-gated chloride channel to silence sensory neurons and treat neuropathic pain at the source. Brain 140, 2570–2585. https://doi.org/10.1093/brain/awx201

Weng, X., Smith, T., Sathish, J., Djouhri, L., 2012. Chronic inflammatory pain is associated with increased excitability and hyperpolarization-activated current (Ih) in C- but not Aδ-nociceptors. PAIN® 153, 900–914. https://doi.org/10.1016/j.pain.2012.01.019

Wilder, F.V., Hall, B.J., Barrett, J.P., 2003. Osteoarthritis pain and weather. Rheumatology 42, 955–958. https://doi.org/10.1093/rheumatology/keg264

Willis, W.D.J., 1999. Dorsal root potentials and dorsal root reflexes: a double-edged sword. Exp Brain Res 124, 395–421.
Winter, J., Alistair Forbes, C., Sternberg, J., Lindsay, R.M., 1988. Nerve growth factor (NGF) regulates adult rat cultured dorsal root ganglion neuron responses to the excitotoxin capsaicin. Neuron 1, 973–981. https://doi.org/10.1016/0896-6273(88)90154-7
Wittert, G., Hope, P., Pyle, D., 1996. Tissue Distribution of Opioid Receptor Gene Expression in the Rat. Biochemical and Biophysical Research Communications 218, 877–881. https://doi.org/10.1006/bbrc.1996.0156
Wolfe, D., Mata, M., Fink, D.J., 2012. Targeted drug delivery to the peripheral nervous system using gene therapy. Neurosci Lett 527, 85–89. https://doi.org/10.1016/j.neulet.2012.04.047
Wood, J.N., Alles, S.R.A., Malfait, A.-M., Miller, R.J., 2019a. Chemo- and Optogenetic Strategies for the Elucidation of Pain Pathways. Oxford University Press.
Wood, J.N., Emery, E.C., Ernfors, P., 2018a. Dorsal Root Ganglion Neuron Types and Their Functional Specialization. https://doi.org/10.1093/oxfordhb/9780190860509.013.4
Wood, J.N., Gomez-Varela, D., Schmidt, M., 2018b. The Proteomics and Metabolomics of Pain—Opportunities for Systems Medicine. https://doi.org/10.1093/oxfordhb/9780190860509.013.15
Wood, J.N., Sun, W.-H., Su, Y.-S., Chen, C.-C., 2019b. The Transition from Acute to Chronic Pain. https://doi.org/10.1093/oxfordhb/9780190860509.013.28
Woodcock, J., 2009. A Difficult Balance — Pain Management, Drug Safety, and the FDA. N Engl J Med 361, 2105–2107. https://doi.org/10.1056/NEJMp0908913
Woolf, C.J., 2011. Central sensitization: implications for the diagnosis and treatment of pain. Pain 152, S2–S15. https://doi.org/10.1016/j.pain.2010.09.030
Woolf, C.J., Allchorne, A., Safieh-Garabedian, B., Poole, S., 1997. Cytokines, nerve growth factor and inflammatory hyperalgesia: the contribution of tumour necrosis factor α. British Journal of Pharmacology 121, 417–424. https://doi.org/10.1038/sj.bjp.0701148
Woolfe, G., MacDonald, A., 1944. The evaluation of the analgesic action of pethidine hydrochloride (Demerol). Journal of Pharmacology and Experimental Therapeutics 80, 300–307.
Wright, A.J., Husson, Z.M.A., Hu, D.-E., Callejo, G., Brindle, K.M., Smith, E.St.J., 2018. Increased hyperpolarized [1-13C] lactate production in a model of joint inflammation is not accompanied by tissue acidosis as assessed using hyperpolarized 13C-labelled bicarbonate. NMR in Biomedicine e3892-n/a. https://doi.org/10.1002/nbm.3892
Xiang, H., Liu, Z., Wang, F., Xu, H., Roberts, C., Fischer, G., Stucky, C., Caron, D., Pan, B., Hogan, Q., Yu, H., 2017. Primary sensory neuron-specific interference of TRPV1 signaling by AAV-encoded TRPV1 peptide aptamer attenuates neuropathic pain. Mol Pain 13, 1744806917717040–1744806917717040. https://doi.org/10.1177/1744806917717040
Xu, G.Y., Huang, L.Y., Zhao, Z.Q., 2000. Activation of silent mechanoreceptive cat C and Adelta sensory neurons and their substance P expression following peripheral inflammation. J Physiol 528 Pt 2, 339–348. https://doi.org/10.1111/j.1469-7793.2000.00339.x
Xu, S.-Z., Sukumar, P., Zeng, F., Li, J., Jairaman, A., English, A., Naylor, J., Ciurtin, C., Majeed, Y., Milligan, C.J., Bahnasi, Y.M., Al-Shawaf, E., Porter, K.E., Jiang, L.-H., Emery, P., Sivaprasadarao, A., Beech, D.J., 2008. TRPC channel activation by extracellular thioredoxin. Nature 451, 69–72. https://doi.org/10.1038/nature06414
Yamamura, Y., Gupta, R., Morita, Y., He, X., Pai, R., Endres, J., Freiberg, A., Chung, K., Fox, D.A., 2001. Effector Function of Resting T Cells: Activation of Synovial Fibroblasts. J. Immunol. 166, 2270. https://doi.org/10.4049/jimmunol.166.4.2270
Yizhar, O., Fenno, L.E., Davidson, T.J., Mogri, M., Deisseroth, K., 2011. Optogenetics in Neural Systems. Neuron 71, 9–34. https://doi.org/10.1016/j.neuron.2011.06.004
Yoshitomi, H., Sakaguchi, N., Kobayashi, K., Brown, G.D., Tagami, T., Sakihama, T., Hirota, K., Tanaka, S., Nomura, T., Miki, I., 2005. A role for fungal β-glucans and their receptor Dectin-1 in the induction of autoimmune arthritis in genetically susceptible mice. Journal of Experimental medicine 201, 949–960.

Young, G.T., Gutteridge, A., Fox, H.D., Wilbrey, A.L., Cao, L., Cho, L.T., Brown, A.R., Benn, C.L., Kammonen, L.R., Friedman, J.H., Bictash, M., Whiting, P., Bilsland, J.G., Stevens, E.B., 2014. Characterizing human stem cell-derived sensory neurons at the single-cell level reveals their ion channel expression and utility in pain research. Mol Ther 22, 1530–1543. https://doi.org/10.1038/mt.2014.86

Yu, L., Yang, F., Luo, H., Liu, F.Y., Han, J.S., Xing, G.G., Wan, Y., 2008. The role of TRPV1 in different subtypes of dorsal root ganglion neurons in rat chronic inflammatory nociception induced by complete Freund's adjuvant. Mol Pain 4. https://doi.org/10.1186/1744-8069-4-61

Zautra, A.J., Davis, M.C., Reich, J.W., Nicassario, P., Tennen, H., Finan, P., Kratz, A., Parrish, B., Irwin, M.R., 2008. Comparison of cognitive behavioral and mindfulness meditation interventions on adaptation to rheumatoid arthritis for patients with and without history of recurrent depression. Journal of Consulting and Clinical Psychology 76, 408–421. https://doi.org/10.1037/0022-006X.76.3.408

Zeisel, A., Hochgerner, H., Lönnerberg, P., Johnsson, A., Memic, F., van der Zwan, J., Häring, M., Braun, E., Borm, L.E., La Manno, G., Codeluppi, S., Furlan, A., Lee, K., Skene, N., Harris, K.D., Hjerling-Leffler, J., Arenas, E., Ernfors, P., Marklund, U., Linnarsson, S., 2018. Molecular Architecture of the Mouse Nervous System. Cell 174, 999-1014.e22. https://doi.org/10.1016/j.cell.2018.06.021

Zhang, H., Merrett, D.C., Jing, Z., Tang, J., He, Y., Yue, H., Yue, Z., Yang, D.Y., 2017. Osteoarthritis, labour division, and occupational specialization of the Late Shang China - insights from Yinxu (ca. 1250 - 1046 B.C.). PLOS ONE 12, e0176329. https://doi.org/10.1371/journal.pone.0176329

Zhang, R.-X., Ren, K., Dubner, R., 2013. Osteoarthritis pain mechanisms: Basic studies in animal models. Osteoarthritis and cartilage / OARS, Osteoarthritis Research Society 21, 1308–1315. https://doi.org/10.1016/j.joca.2013.06.013

Zhang, X., Lee, K.-Y., Priest, B.T., Belfer, I., Gold, M.S., 2015. Inflammatory mediator-induced modulation of GABA(A) currents in human sensory neurons. Neuroscience 310, 401–409. https://doi.org/10.1016/j.neuroscience.2015.09.048

Zhang, X., Priest, B.T., Belfer, I., Gold, M.S., 2017. Voltage-gated Na(+) currents in human dorsal root ganglion neurons. Elife 6, e23235. https://doi.org/10.7554/eLife.23235

Zhou, Y., Li, G.-D., Zhao, Z.-Q., 2003. State-dependent phosphorylation of ε-isozyme of protein kinase C in adult rat dorsal root ganglia after inflammation and nerve injury. Journal of Neurochemistry 85, 571–580. https://doi.org/10.1046/j.1471-4159.2003.01675.x

Zhu, Y., Lu, S., Gold, M.S., 2012. Persistent inflammation increases GABA-induced depolarization of rat cutaneous dorsal root ganglion neurons in vitro. Neuroscience 220, 330–340. https://doi.org/10.1016/j.neuroscience.2012.06.025